



PHD

Impact of calcitic aggregates on air lime mortar properties

Scannell, Sarah

Award date:
2017

Awarding institution:
University of Bath

[Link to publication](#)

Alternative formats

If you require this document in an alternative format, please contact:
openaccess@bath.ac.uk

Copyright of this thesis rests with the author. Access is subject to the above licence, if given. If no licence is specified above, original content in this thesis is licensed under the terms of the Creative Commons Attribution-NonCommercial 4.0 International (CC BY-NC-ND 4.0) Licence (<https://creativecommons.org/licenses/by-nc-nd/4.0/>). Any third-party copyright material present remains the property of its respective owner(s) and is licensed under its existing terms.

Take down policy

If you consider content within Bath's Research Portal to be in breach of UK law, please contact: openaccess@bath.ac.uk with the details. Your claim will be investigated and, where appropriate, the item will be removed from public view as soon as possible.

Impact of calcitic aggregates on air lime mortar properties

submitted by

Sarah Scannell

for the degree of Doctor of Philosophy

of the

University of Bath

Department of Architecture & Civil Engineering

February 2017

COPYRIGHT

Attention is drawn to the fact that copyright of this thesis rests with the author. A copy of this thesis has been supplied on condition that anyone who consults it is understood to recognise that its copyright rests with the author and that they must not copy it or use material from it except as permitted by law or with the consent of the author.

This thesis may be made available for consultation within the University Library and may be photocopied

or lent to other libraries for the purposes of consultation with effect from
.....

Signed on behalf of the Faculty of Engineering & Design

Acknowledgments

The following work was undertaken at the University of Bath in the Department of Architecture and Civil Engineering. The author would firstly like to thank Dr. Mike Lawrence and Professor Pete Walker, who both supervised this research and have provided invaluable insight and support throughout the preparation, lab testing and writing of this thesis.

Further thanks are due to the lab technicians in Architecture and Civil Engineering, who have assisted in undertaking numerous tests, as well as making themselves available to support any lab work when required. Additionally, thanks go to Fernando in Chemical Engineering, as well as Ursula and John in the Physics department.

The author also wishes to thank colleagues in the department, who have provided valuable thoughts and opinions as well as creating an enjoyable atmosphere in which to work. Thanks also go to Yunhong for undertaking some of the SEM imaging.

None of this work could have taken place without the joint funding provided by the EPSRC and Lhoist, to whom the author is incredibly grateful.

Finally the author would like to thank her husband, Ryan; without his support, the relocation to Bath to undertake the PhD would never have taken place.

Abstract

In recent years, the importance of aggregate type on the properties of mortars has become increasingly recognised. In the context of restoration, it is particularly important to achieve the optimum properties that provide the best compatibility between the repair mortar and the existing masonry. With that in mind, the properties of the aggregate, in addition to binder type, should be given priority when designing the repair mortar mix. A critical analysis of the current state of the art is presented, identifying the areas of research that have not yet been explored thoroughly. The role of calcitic aggregates in mortar is one such area, and the research presented here examines the notion that calcitic aggregates cause an increase in the strength of lime mortar. Little is known about the reason for the higher strengths observed, and therefore this research aimed to establish possible causes. This research analysed flexural/compressive strengths of a range of mortar mixes containing different types of aggregate, and confirms previous studies that use of limestone aggregates rather than silicate can lead to higher strengths in air lime mortar. Furthermore, the depth of carbonation in the samples was measured by phenolphthalein staining and is not found to relate directly to the mechanical strength of the mortars. A range of samples were subsequently analysed using TGA, MIP and SEM. TGA has shown that the quantity of $CaCO_3$ varies with the different aggregates used, with Ham Hill having around half as much mass loss as Portland and Stoke Ground respectively. It was found that the pore structure of the limestone mortars varied somewhat from the silicate sand mortars; aggregate pore structure was also found to differ significantly. The porosity of silicate sand was 5.81% while Portland was 49.9%. Detailed examination of the SEM images shows significant micro-structural differences between the different mortar mixes, with calcite crystals appearing on the surface of the limestone aggregates, and evidence of a more cohesive bond between binder and aggregate evident in the limestone aggregate mortars than the silicate sand mortars.

Contents

List of Figures	V
List of Tables	IX
1 Introduction	1
1.1 Thesis structure	1
1.2 Background	1
1.3 Lime	2
1.3.1 Background	2
1.3.2 Non-hydraulic lime	3
1.3.3 Hydraulic lime	4
1.3.4 Lime putty	5
1.3.5 Pozzolans	5
1.4 Types of aggregate	6
1.4.1 Silica sand	6
1.4.2 Calcitic aggregate	6
1.4.3 Dolomitic aggregate	7
1.5 Aims and objectives	8
2 A review of literature	9
2.1 Introduction	9
2.2 Fresh mortar properties	10
2.2.1 Introduction	10
2.2.2 Workability	10
2.2.3 Plasticity	13
2.2.4 Water retentivity	14
2.2.5 Yield stress	15
2.3 Aggregate characteristics	17
2.3.1 Introduction	17
2.3.2 Binder/aggregate ratio	17
2.3.3 Particle size distribution	18
2.3.4 Aggregate type	20
2.3.5 Aggregate shape	22
2.4 Chemistry	23
2.4.1 Introduction	23

2.4.2	Carbonation	24
2.4.3	Pozzolans	26
2.5	Hardened mortar characteristics	28
2.5.1	Introduction	28
2.5.2	Pore structure	28
2.5.3	Water absorption	30
2.5.4	Elastic modulus	31
2.5.5	Durability	32
2.5.6	Flexural and compressive strength	33
2.6	Overall conclusions	35
3	Research design	36
3.1	Introduction	36
3.2	Materials	37
3.3	Sample codes	38
3.3.1	Preliminary testing phase	39
3.3.2	Secondary testing phase	40
3.4	Materials and mix design	40
3.4.1	Preliminary testing phase	40
3.4.2	Secondary testing phase	44
3.4.3	Physical and chemical characterisation of aggregates	48
3.4.3.1	Pore structure of aggregates using mercury intrusion porosimetry	48
3.4.3.2	Chemical composition of aggregates using thermogravimetric analysis	52
3.4.3.3	SEM	53
3.5	Mass change in mortar specimens during curing	54
3.6	Tests and procedures	56
3.6.1	Abrams' Law	56
3.6.2	Batching	57
3.6.3	Flexural/compressive strength	57
3.6.4	Phenolphthalein staining	59
3.6.5	Thermogravimetric analysis	59
3.6.6	Scanning electron microscopy	61
3.6.7	Mercury intrusion porosimetry	62
4	Preliminary testing phase	64
4.1	Flexural/compressive testing results	64
4.2	Carbonation depth using phenolphthalein indicator	72
4.3	Scanning electron microscopy	73
4.4	Conclusions	76
5	Secondary testing phase	77

5.1	Flexural/compressive strength results	77
5.1.1	Introduction	77
5.1.2	Specimens with 1:2 B/Ag ratio	77
5.1.3	Specimens with 1:3 B/Ag ratio	81
5.1.4	Chemical indicators	95
5.1.5	TGA analysis	97
5.2	Pore structure	101
5.2.1	MIP	101
5.2.2	Effects of carbonation on sample density	113
5.3	Micro-structure and binder/aggregate interface using scanning electron microscopy	116
6	Analysis and discussion of findings	128
6.1	Introduction	128
6.2	Preliminary testing phase	128
6.2.1	Flexural and compressive strength testing	128
6.2.2	Qualitative analysis of carbonation	130
6.2.3	Scanning electron microscopy images	130
6.3	Secondary testing phase	137
6.3.1	Materials and mix design	137
6.3.2	Pore structure of aggregates	137
6.3.3	Chemical composition of aggregates using TGA	137
6.3.4	Micro-structure of aggregates using SEM	138
6.3.5	Mass loss of samples due to curing	138
6.3.6	Flexural and compressive strengths	140
6.3.7	Carbonation measured by phenolphthalein indicator and TGA	149
6.3.8	Pore structure of mortars measured using MIP	152
6.3.9	Mortar micro-structure using SEM	153
7	Conclusions	154
8	Recommendations for further work	157
9	References	158
A.0	Conference and journal papers	169
A.0.1	International Congress on Materials & Structural Stability	169
A.0.2	International Conference on Sustainability in Energy and Buildings	175
A.0.3	9th International Masonry Conference 2014	186
A.0.4	Journal of Civil Engineering and Architecture	197
A.0.5	The Journal of the Building Limes Forum	207

List of Figures

1.1	The Lime Cycle	3
3.1	Particle size distribution as per Standard sand, with additional 2mm fraction .	42
3.2	'as supplied' particle size distribution	46
3.3	Mean pore diameter versus incremental intrusion volume for Ham Hill aggregate	49
3.4	Mean pore diameter versus incremental intrusion volume for Portland aggregate	49
3.5	Mean pore diameter versus incremental intrusion volume for Stoke Ground aggregate	50
3.6	Mean pore diameter versus incremental intrusion volume for Standard sand . .	50
3.7	Mean pore diameter versus incremental intrusion volume for all aggregates . . .	51
3.8	Temperature versus TG for all aggregates (Ham Hill, Portland, Stoke Ground, Standard sand)	52
3.9	SEM images of each aggregate used	53
3.10	Average mass loss of samples at each curing period from the 7 day mass	56
3.11	Typical setup for 3 point flexural bending	58
4.1	Average flexural strengths for 1:2 mixes at 14 days curing	65
4.2	Average compressive strengths for 1:2 mixes at 14 days curing	65
4.3	Average flexural strengths for 1:2 mixes at 28 days curing	66
4.4	Average compressive strengths for 1:2 mixes at 28 days curing	66
4.5	Average flexural strengths for 1:3 mixes at 14 days curing	67
4.6	Average compressive strengths for 1:3 mixes at 14 days curing	68
4.7	Average flexural strengths for 1:3 mixes at 28 days curing	68
4.8	Average compressive strengths for 1:3 mixes at 28 days curing	69
4.9	Average flexural strengths for 1:4 mixes at 14 days curing	69
4.10	Average compressive strengths for 1:4 mixes at 14 days curing	70
4.11	Average flexural strengths for 1:4 mixes at 28 days curing	71
4.12	Average compressive strengths for 1:4 mixes at 28 days curing	72
4.13	Phenolphthalein staining (left) Ham Hill, (right) Standard sand	73
4.14	Standard sand sample at 430x magnification	74
4.15	Stoke Ground sample at 400x magnification	74
4.16	Portland sample at 430x magnification	75
4.17	Bath stone sample at 450x magnification	75
5.1	Average flexural strength for 1-2 'as supplied' samples	79
5.2	Average flexural strength for 1-2 'standard' samples	79

5.3	Average compressive strength for 1-2 'as supplied' samples	80
5.4	Average compressive strength for 1-2 'standard' samples	81
5.5	Average flexural strength for 1-3 'as supplied' samples	83
5.6	Average compressive strength for 1-3 'as supplied' samples	83
5.7	Average flexural strength at 14 days for 1:2 mixes	84
5.8	Average flexural strength at 14 days for 1:3 mixes	84
5.9	Average flexural strength at 28 days for 1:2 mixes	85
5.10	Average flexural strength at 28 days for 1:3 mixes	85
5.11	Average flexural strength at 90 days for 1:3 mixes	86
5.12	Average flexural strength at 180 days for 1:2 mixes	87
5.13	Average flexural strength at 180 days for 1:3 mixes	87
5.14	Average flexural strength at 360 days for 1:2 mixes	88
5.15	Average flexural strength at 360 days for 1:3 mixes	89
5.16	Average compressive strength at 14 days for 1:2 mixes	90
5.17	Average compressive strength at 14 days for 1:3 mixes	91
5.18	Average compressive strength at 28 days for 1:2 mixes	91
5.19	Average compressive strength at 28 days for 1:3 mixes	92
5.20	Average compressive strength at 90 days for 1:2 mixes	93
5.21	Average compressive strength at 90 days for 1:3 mixes	93
5.22	Average compressive strength at 180 days for 1:2 mixes	94
5.23	Average compressive strength at 180 days for 1:3 mixes	94
5.24	Average compressive strength at 360 days for 1:2 mixes	95
5.25	Average compressive strength at 360 days for 1:3 mixes	96
5.26	SG-3 'as supplied' mortars (left to right) 14, 28, 90, 180 and 360 days curing .	97
5.27	SS-3 'standard' mortars (left to right) 14, 28, 90, 180 and 360 days curing . . .	97
5.28	TG curve for H28-3, P28-3, SS28-3 - samples taken from the carbonated edge of the prism	98
5.29	TG curve for H28-3 a.s, P28-3 a.s, SG28-3 a.s, SS28-3 - samples taken from the carbonated edge of the prism	99
5.30	TG curve for P180-2 a.s, SG180-2 a.s, SS180-2 - samples taken from the carbonated edge of the prism	99
5.31	Temperature versus dTG for - samples were taken from the carbonated edge of the prism	100
5.32	Mean pore diameter versus incremental intrusion volume for H0-3 a.s and H360-3 a.s - H360 a.s sample was taken from the carbonated edge of the prism	101
5.33	Mean pore diameter versus incremental intrusion volume for H14-2 and H360-2 - samples taken from the carbonated edge of the prism	102
5.34	Mean pore diameter versus incremental intrusion volume for SG14-2, SG180-2 and SG360-2 - samples were taken from the carbonated edge of the prism . . .	103
5.35	Mean pore diameter versus incremental intrusion volume for SG0-3 a.s and SG360-3 a.s - samples were taken from the carbonated edge of the prism	103

5.36	Mean pore diameter versus incremental intrusion volume for SS28-3, SS360-3 and SG28-3 - samples were taken from the carbonated edge of the prism	104
5.37	Comparison of intrusion/extrusion curves for H360-2 according to the Washburn equation, Washburn equation with modified contact angle for extrusion (98°), and modified Washburn equation (Lawrence et al., 2007)	107
5.38	Comparison of intrusion/extrusion curves for H360-3 a.s according to the Washburn equation, Washburn equation with modified contact angle for extrusion (98°), and modified Washburn equation (Lawrence et al., 2007)	108
5.39	Comparison of intrusion/extrusion curves for P360-2 a.s according to the Washburn equation, Washburn equation with modified contact angle for extrusion (98°), and modified Washburn equation (Lawrence et al., 2007)	109
5.40	Comparison of intrusion/extrusion curves for SG360-2 a.s according to the Washburn equation, Washburn equation with modified contact angle for extrusion (98°), and modified Washburn equation (Lawrence et al., 2007)	110
5.41	Comparison of intrusion/extrusion curves for SS360-2 according to the Washburn equation, Washburn equation with modified contact angle for extrusion (98°), and modified Washburn equation (Lawrence et al., 2007)	111
5.42	Comparison of intrusion/extrusion curves for SS360-3 according to the Washburn equation, Washburn equation with modified contact angle for extrusion (98°), and modified Washburn equation (Lawrence et al., 2007)	112
5.43	Density vs. strength for samples in Table 5.9	113
5.44	Density vs. strength for Stoke Ground samples ('as supplied')	114
5.45	Density vs. strength for Ham Hill samples ('as supplied')	115
5.46	SEM image of carbonated Ham Hill aggregate mortar at 800x magnification . .	116
5.47	SEM image of carbonated Portland aggregate mortar at 800x magnification . .	117
5.48	SEM image of carbonated Stoke Ground aggregate mortar at 800x magnification	117
5.49	SEM image of carbonated Standard sand mortar at 800x magnification	118
5.50	SEM image of carbonated Standard sand mortar at 800x magnification	118
5.51	SEM image of Ham Hill aggregate mortar at 1:3 B/Ag ratio with 'standard' grading after 28 days curing - 400x magnification	119
5.52	SEM image of Portland aggregate mortar at 1:3 B/Ag ratio with 'standard' grading after 28 days curing - 400x magnification	120
5.53	SEM image of Stoke Ground aggregate mortar at 1:3 B/Ag ratio with 'standard' grading after 28 days curing - 100x magnification	120
5.54	SEM image of Standard sand mortar at 1:3 B/Ag ratio with 'standard' grading after 28 days curing - 800x magnification	121
5.55	SEM image of Ham Hill aggregate mortar at 1:2 B/Ag ratio with 'as supplied' grading after 90 days curing - 430x magnification	121
5.56	SEM image of Portland aggregate mortar at 1:2 B/Ag ratio with 'as supplied' grading after 90 days curing - 430x magnification	122

5.57	SEM image of Stoke Ground aggregate mortar at 1:2 B/Ag ratio with 'as supplied' grading after 90 days curing - 200x magnification	122
5.58	SEM image of Portland aggregate mortar at 1:2 B/Ag ratio with 'as supplied' grading after 180 days curing - 800x magnification	123
5.59	SEM image of Stoke Ground aggregate mortar at 1:2 B/Ag ratio with 'as supplied' grading after 180 days curing - 75x magnification	123
5.60	SEM image of Standard sand mortar at 1:2 B/Ag ratio with 'standard' grading after 180 days curing - 75x magnification	124
5.61	SEM image of Ham Hill aggregate mortar at 1:3 B/Ag ratio with 'as supplied' grading after 360 days curing - 430x magnification	124
5.62	SEM image of Portland aggregate mortar at 1:3 B/Ag ratio with 'as supplied' grading after 360 days curing - 100x magnification	125
5.63	SEM image of Stoke Ground aggregate mortar at 1:3 B/Ag ratio with 'as supplied' grading after 360 days curing - 200x magnification	125
5.64	SEM image of Standard sand mortar at 1:3 B/Ag ratio with 'standard' grading after 360 days curing - 200x magnification	126
5.65	SEM image of Standard sand mortar at 1:3 B/Ag ratio with 'standard' grading after 14 days curing - 50x magnification	126
5.66	SEM image of Standard sand mortar at 1:3 B/Ag ratio with 'standard' grading after 14 days curing - 50x magnification	127

List of Tables

1	Notations	XII
1.1	Description and 28 day compressive strength of NHL mortars	5
1.2	Types of limestone and their features	7
2.1	Summary of factors affecting workability	13
2.2	Summary of factors affecting plasticity	14
2.3	Summary of factors affecting water retentivity	15
2.4	Summary of factors affecting yield stress	16
2.5	Summary of the effect of B/Ag ratio	18
2.6	Summary of the effect of particle size distribution	20
2.7	Summary of the effect of aggregate type	22
2.8	Summary of the effect of aggregate shape	23
2.9	Summary of the effect of carbonation	26
2.10	Summary of the effect of pozzolans	27
2.11	Summary of factors affecting pore structure	30
2.12	Summary of factors affecting water absorption	31
2.13	Summary of factors affecting elastic modulus	32
2.14	Summary of factors affecting durability	33
2.15	Reproduction of part of a table of strengths (in MPa) using dry hydrated lime binder from Lawrence (2006)	34
2.16	Summary of factors affecting compressive/flexural strength	35
3.1	Description of the lithology of the limestone aggregates used in the research . .	38
3.2	Sample codes *note that '14' refers to the number of days the sample was cured for. Samples were also tested at 28 days of curing	39
3.3	Sample codes *note that '14' refers to the number of days the sample was cured for. Samples were also tested at 28, 90, 180 and 360 days of curing	40
3.4	Aggregate grading as per Standard sand, with additional 2mm fraction	41
3.5	Bulk densities of the dry hydrated lime and aggregates	43
3.6	Mortar mix design for 1:2 B/Ag ratio (by volume)	43
3.7	Mortar mix design for 1:3 B/Ag ratio (by volume)	43
3.8	Mortar mix design for 1:4 B/Ag ratio (by volume)	44
3.9	Particle sizes for 'as supplied' and 'standard' grading	45
3.10	Mix design for 1:2 'as supplied' mix	47

3.11	Mix design for 1:2 'standard' mix	47
3.12	Mix design for 1:3 'as supplied' mix	47
3.13	Mix design for 1:3 'standard' mix	47
3.14	Aggregate accessible porosity as measured by MIP	51
3.15	Average mass loss percentage of samples between 7 days and the date of test .	55
3.16	Common chemical indicators	59
4.1	Average carbonation depth of samples after 28 days curing with 1:2 B/Ag, 'standard' grading	73
5.1	Flexural strength for 1:2 mixes	78
5.2	Compressive strength for 1:2 mixes	78
5.3	Flexural strength for 1:3 mixes	82
5.4	Compressive strength for 1:3 mixes	82
5.5	Average depth of carbonation (mm)	96
5.6	Critical pore diameter	105
5.7	Accessible porosity for samples subject to MIP	106
5.8	Constants used in modified Washburn equation	106
5.9	Density comparison of Ham Hill and Standard sand mortars	113
6.1	Flexural and compressive strength results at 14 days with 1:2 B/Ag and 'standard' grading, confidence that results are significantly different from reference (SS14-2) at 95%, standard deviation about the mean shown as % error.	131
6.2	Flexural and compressive strength results at 28 days with 1:2 B/Ag and 'standard' grading, confidence that results are significantly different from reference (SS28-2) at 95%, standard deviation about the mean shown as % error.	132
6.3	Flexural and compressive strength results at 14 days with 1:3 B/Ag and 'standard' grading, confidence that results are significantly different from reference (SS14-3) at 95%, standard deviation about the mean shown as % error.	133
6.4	Flexural and compressive strength results at 28 days with 1:3 B/Ag and 'standard' grading, confidence that results are significantly different from reference (SS28-3) at 95%, standard deviation about the mean shown as % error.	134
6.5	Flexural and compressive strength results at 14 days with 1:4 B/Ag and 'standard' grading, confidence that results are significantly different from reference (SS14-4) at 95%, standard deviation about the mean shown as % error.	135
6.6	Flexural and compressive strength results at 28 days with 1:4 B/Ag and 'standard' grading, confidence that results are significantly different from reference (SS28-4) at 95%, standard deviation about the mean shown as % error.	136
6.7	Initial sample mass and final sample mass, including theoretical mass gain due to carbonation and mass loss due to drying	139

6.8	Flexural and compressive strength results at 14 days, confidence that results are significantly different from reference (SS14) at 95%, standard deviation about the mean shown as % error.	143
6.9	Flexural and compressive strength results at 28 days, confidence that results are significantly different from reference (SS28) at 95%, standard deviation about the mean shown as % error.	144
6.10	Flexural and compressive strength results at 90 days, confidence that results are significantly different from reference (SS90) at 95%, standard deviation about the mean shown as % error.	145
6.11	Flexural and compressive strength results at 180 days, confidence that results are significantly different from reference (SS180) at 95%, standard deviation about the mean shown as % error.	146
6.12	Flexural and compressive strength results at 360 days with 1: 2 B/Ag, confidence that results are significantly different from reference (SS360) at 95%, standard deviation about the mean shown as % error.	147
6.13	Flexural and compressive strength results at 360 days with 1:3 B/Ag, confidence that results are significantly different from reference (SS360) at 95%, standard deviation about the mean shown as % error.	148
6.14	Theoretical mass of $CaCO_3$ in specimens based on samples tested using TGA .	150
6.15	Theoretical mass of $CaCO_3$ in specimens based on samples tested using TGA .	151

Notations

Table 1: Notations

Notation	Description
CaO	Calcium oxide
$Ca(OH)_2$	Calcium hydroxide
$Mg(OH)_2$	Magnesium hydroxide
$CaCO_3$	Calcium carbonate
CO_2	Carbon dioxide
CSH	Calcium silicate hydrate
CAH	Calcium aluminate hydrate
MPa	MegaPascals (or N/mm^2)
SEM	Scanning electron microscopy
MIP	Mercury intrusion porosimetry
XRD	X-Ray diffraction
TGA	Thermogravimetric analysis
DTA	Differential thermal analysis
B/Ag	Binder/Aggregate
w/b	water/binder

1 Introduction

1.1 Thesis structure

The first chapter in this thesis introduces the need for the research and provides information on the different types of lime and types of aggregate. Furthermore, aims and objectives are detailed. In Chapter 2, a comprehensive literature review has been undertaken, discussing important mortar properties (both fresh and hardened states), with particular focus on how they impact compressive strength. Chapter 3 outlines the research design, including materials used, tests and procedures that were undertaken and the separation of the research in to two phases of work. Following this, Chapter 4 focuses on the primary testing phase, with information on materials and mix design, as well as test results. In Chapter 5, the secondary testing phase materials and mix design, test results are laid out. Chapter 6 moves on to a discussion of the findings in both phases, with speculation as to why the observed results might have occurred. The conclusions from the research are outlined in Chapter 7, before Chapter 8 suggests some recommendations for further work that might be beneficial. Following this, there is a comprehensive list of references. Finally, appendices contain conference papers and journal papers that have been produced throughout this research.

1.2 Background

Lime mortar has been used for centuries in masonry construction. The past few decades have seen an increase in restoration work on old structures, where the compatibility of old and new materials is of paramount importance. This means that cement-based materials are inappropriate as a repair material due to the significantly higher strengths they achieve over lime-based materials; a mortar with a higher strength than the original masonry would lead to more damage due to having less ability to accommodate movement. As a result, a build-up of stresses would cause the masonry to fail (Mosquera et al., 2002).

Lime mortars are inherently weak in compression, and research has shown that higher strengths can be obtained with use of limestone aggregate over silicate aggregate (Lawrence (2006), Lanas and Alvarez (2003), Arizzi and Cultrone (2012a)). Since low strengths are synonymous with poor durability, higher strengths could lead to longer-lasting mortars. The higher strengths obtained are still much lower than cement mortar strengths so should not have a detrimental effect on existing masonry. Aggregates are primarily used to provide structure to a mortar

(Farey et al., 2003) and their role in mortar strength has been largely underestimated. Despite various studies concluding that limestone aggregates can produce higher strength air lime mortars (Lawrence (2006), Lanas and Alvarez (2003), Arizzi and Cultrone (2012a)), little is known about the reasons why. Additionally, while adequate strength is required for durability of a mortar, it is also vital to ensure other characteristics are sufficient; porosity, water retentivity and plasticity are just a few of the important properties.

In the current climate, it is becoming increasingly recognized that carbon emissions need to be reduced; as the construction industry is responsible for around 50% of the UK's emissions (BIS, 2010), the use of low energy materials can contribute to this reduction. The current research is therefore being undertaken at a critical time, where the use of low energy materials have an opportunity to gain more recognition in industry. Air lime is a low energy binder due to the fact that during curing, almost all of the CO_2 that was emitted during the manufacturing process is reabsorbed during carbonation (Limetec, 2015). Carbonation gives a mortar strength through the transformation of $Ca(OH)_2$ into $CaCO_3$. It is the primary chemical reaction that occurs during setting of air lime mortar, and is a self-limiting process. This is due to the formation of calcite crystals around the calcium hydroxide particles, which block CO_2 penetration and subsequently some portlandite ($Ca(OH)_2$) always remains uncarbonated (Houst and Wittmann, 2002).

This research originated as a result of findings that with the use of limestone (calcitic) aggregate in air lime mortars, higher strength mortars can be achieved over mortars containing the more commonly used silicate aggregate. Little is known about the mechanisms involved, but further research is required in order to improve the buildability and potentially optimise the design of low energy mortars.

Consequently, the current research compares the impact of several limestone aggregates against a silicate aggregate on air lime mortar with a variety of mix specifications and curing times.

1.3 Lime

1.3.1 Background

Lime binders can be hydraulic, non-hydraulic (air lime) or lime putty. The different binders have varying impacts on the properties of the mortar. Lime has been used for thousands of years and is currently used extensively in conservation/repair work, due to the need for similar properties of existing and new material (Maravelaki-Kalaitzaki et al. (2005), Bromblet (1999), Moropoulou et al. (2005)). Figure 1.1 shows the lime cycle is a continuous process.

When calcium carbonate is burned at around 900° , heat is generated, and calcium oxide formed. The calcium oxide is then slaked with water to produce calcium hydroxide which

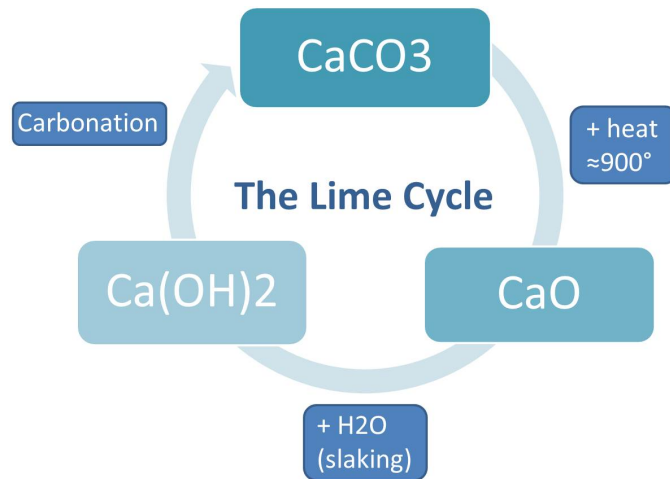


Figure 1.1: The Lime Cycle

subsequently carbonates in the presence of carbon dioxide and water, thus forming calcium carbonate. Equations 1.1-1.3 describe the reactions that occur in the lime cycle.



1.3.2 Non-hydraulic lime

In order to form non-hydraulic lime, chalk/limestone is burned at around 900°C to form calcium oxide (CaO), also known as quicklime, and is subsequently slaked with water to form calcium hydroxide (Ca(OH)_2). The amount of water used during slaking affects the final product that is formed. If the quantity of water is just enough to convert the quicklime, then the hydrate formed is a dry powder. When an excess of water is used, lime putty is formed.

Also referred to as air lime or hydrated lime, non-hydraulic lime will only set in the presence of CO_2 through the carbonation process. Carbonation is split up into several phases. Initially, CO_2 penetrates into the pores of the sample, where it is then dissolved in the moisture that is present in the sample to form carbonic acid. The carbonic acid subsequently reacts with the

calcium hydroxide to form calcium carbonate.

Once the calcium hydroxide is mixed with water and aggregate to form mortar, curing in air takes place in order for carbonation to occur and harden the mortar. The rate of carbonation is impacted by the relative humidity during curing, as well as the amount of moisture present in the sample. No clay should be present, and <1% unreacted water. Hydration of high calcium limes occurs at a quicker rate than dolomitic limes as the latter can easily be over-burnt.

Compressive strengths in non-hydraulic lime mortar are around 0.5-2MPa, which is significantly lower than the 2-15MPa range of hydraulic lime mortars. This makes non-hydraulic lime mortar best suited to conservation/repair work of old buildings, as the low strength of the mortar is weaker than the strength of the masonry; the mortar will fail before the masonry.

1.3.3 Hydraulic lime

Hydraulic lime binder sets by reaction with water and can therefore harden both in air and under water. The initial phase in the manufacturing process involves burning argillaceous or siliceous limestone at 950 – 1200 °C. Subsequently, the limestone is slaked; Equations 1.1-1.3 show the chemical reactions that take place.

When higher proportions of clay are present in the limestone, stronger mortars are produced. Where there is <12% clay content, the binder creates mortars with strengths closer to those of non-hydraulic lime. Hydraulic limes contain calcium silicates, calcium aluminates and calcium hydroxide. Belite (calcium disilicate) contributes to a larger proportion, with smaller occurrences of alite (calcium trisilicate). Lanas et al. (2004) say that for hydraulic lime, C_2S is the main hydraulic phase, with its hydration being responsible for later age strength, whereas C_3S is responsible for early age strength.

Hydraulic lime can be further categorised into two further types; (Artificial) Hydraulic Lime and Natural Hydraulic Lime. The former requires the addition of hydraulic and/or pozzolanic materials to the lime being burned in the kiln. On the other hand, Natural Hydraulic Lime (NHL) is formed from limestone containing impurities, and is split into 3 types defined by their 28 day compressive strengths (although there is some overlap), the specifications of which can be found in BS EN 459-1: 2015. A summary is presented below in Table 1.1.

NHL 2 is slow setting with properties similar to non-hydraulic lime. It is suitable for minimal exposure applications such as internal work, as well as conservation work as a result of its relatively low compressive strength. NHL 3.5 is used for general building work such as pointing. The strongest of the NHLs is NHL 5, which has a rapid set so is consequently ideal for extreme exposure conditions such as roofing, dams and harbours.

Table 1.1: Description and 28 day compressive strength of NHL mortars

Type	Classification	Compressive strength (MPa)
NHL 2	Feebly hydraulic	2-7
NHL 3.5	Moderately hydraulic	3.5-10
NHL 5	Eminently hydraulic	5-15

1.3.4 Lime putty

Lime putty is the saturated form of non-hydraulic lime; it is a suspension of lime in water. Burning/calcination of limestone converts it into calcium oxide, after which water is added in order to achieve hydrated lime. During slaking of lime putty, an excess of water is used and the putty is left for months to mature under water in an air tight container; it is the purest form of non-hydraulic lime. Over time larger crystals break down into smaller crystals. Conversely, Ostwald ripening is a phenomenon whereby small crystals dissolve and are then redeposited onto larger crystals which are more stable. Therefore the process occurring with the storage of lime putty is seen as a reverse Ostwald ripening, which continues to occur over time, creating smaller and smaller particles. There are several benefits to having smaller crystal size; since the particles have a larger surface area, plasticity, water retention and carbonation are all improved.

Ashurst and Dimes (1998) say that lime putty must be stored for a minimum of 2 weeks, but preferably for 2 months or more, and there is no upper limit to the storage time. Research by Cazalla et al. (2000) has shown that when putty is stored for longer (14 years rather than 1 year), a faster and higher degree of carbonation of mortar is achieved. It is thought that this is due to the higher amount of sub-micrometer portlandite crystals that were observed, which have a higher surface area and consequently a higher reactivity. Furthermore, plasticity, workability and water retention are all increased with a longer storage time.

1.3.5 Pozzolans

Pozzolans have been used since Roman times, where crushed pumice from Pozzuoli was added to lime putty, leading to the creation of artificial hydraulic lime.

The term 'pozzolan' defines a siliceous/ siliceous and aluminous material that is added to mortar/concrete to improve its properties, and reacts chemically with $Ca(OH)_2$. Pozzolans have different origins, composition and properties and can be natural or artificial. Some commonly used pozzolans are by-products from industrial processes, such as fly ash, silica

fume and metakaolin. Natural pozzolans can be found in certain areas, an example of which is volcanic ash. Consisting of pulverised rock, minerals and volcanic glass, volcanic ash particles are smaller than $2mm$ in diameter. Chemical composition includes silicon dioxide, iron and magnesium.

Sánchez-Moral et al. (2005) found that in Roman mortars, the high content of volcanic glass and other unstable materials in the aggregates assisted chemical reactions around the grains. As a result of their findings, the question is raised in this research as to whether calcitic aggregates are exhibiting pozzolanic behaviour leading to strength gains in the mortar. Since pozzolanic reactions rely not only on the chemical composition of the mortar, but also on the particle size, it would be beneficial to investigate use of more than one aggregate particle size distribution in this research in order to determine whether finer particles could have a pozzolanic effect.

1.4 Types of aggregate

Aggregate is primarily used as a filler in mortar and concrete. It is not often thought that the aggregate type has a significant impact on the mortar as a whole, although the effect of other factors such as shape, surface roughness and particle size distribution have been frequently studied. Siliceous sand is the most commonly used aggregate type, and is widely available throughout the construction industry. Limestone aggregates, whether calcitic or dolomitic, are used much less frequently but recent research is proving that further investigations are needed; calcitic aggregates can produce stronger mortars than those made using siliceous aggregates.

1.4.1 Silica sand

Silica sand is a naturally occurring granular material often in the form of quartz (a silica mineral) and has the chemical composition SiO_2 (silicon dioxide). It is a hard, chemically inert material which is resistant to weathering in part due to its low porosity. Silica sand contains low levels of impurities such as clay and iron oxide.

1.4.2 Calcitic aggregate

Calcitic aggregate can be either composed of angular or rounded grains, and has the chemical composition $CaCO_3$ (calcite). There are many different forms of calcitic aggregate; for example Bath Stone is an oolitic variety. Oolitic grains are round in shape and are $0.25-2mm$ in diameter. Table 1.2 shows a number of types of limestone and their features.

Lawrence (2006) found that mortars made from crushed oolitic stone were four times as strong as those made using silicate aggregates. This could be due to the similar pore structure that

Table 1.2: Types of limestone and their features

Type	Features
Chalk	Fine textured, mainly calcareous shells
Coquina	Mainly broken shell debris
Fossiliferous	Contains many fossils from sea creatures
Lithographic	Fine, uniform grain size, dense limestone
Oolitic	Mainly calcium carbonate oolites
Travertine	Formed by evaporative precipitation, such as stalactites
Tufa	Precipitation of calcium-laden waters at a hot spring for example

exists between the aggregate and mortar respectively (Lanas and Alvarez, 2003).

It is possible that if both aggregate and mortar have a similar porosity, CO_2 movement through the sample would be more constant, potentially leading to a faster and more complete carbonation.

1.4.3 Dolomitic aggregate

Dolomitic rock is sedimentary and composed mostly of the mineral dolomite, which has the chemical composition $CaMg(CO_3)_2$ (calcium magnesium carbonate). Similar to limestone, dolomite recrystallizes when subjected to increased heat and pressure; crystal size increases and the rock becomes crystalline in appearance. Dolomitic rock can be crushed to form aggregate, or calcined to form lime. Dolomitisation describes the process of a pre-existing limestone being replaced by dolomite. There are a number of impurities in dolomite, including silica, sulphur, iron dioxides and alumina.

Naik et al. (2006) determined that the use of dolomitic limestone in concrete helped to reduce both autogenous shrinkage and drying shrinkage at early ages. The research does not state what the impact of this was on the concrete, but reduced drying shrinkage would usually lead to fewer cracks in the concrete.

1.5 Aims and objectives

Previous studies have reported differences in mortar compressive strength (Lawrence, 2006; Lanas and Alvarez, 2003; Arizzi and Cultrone, 2012b), but there has been no systematic study prior to this. The primary aim of this research was to investigate the impact of calcitic aggregates on air lime mortars. Furthermore it was important to ascertain whether there is an ideal mix design to achieve the most preferable characteristics. Air lime mortar is an important material with preferential properties for use in restoration and conservation work. Similarities exist between air lime mortars and the original mortars used, meaning the original structure and new mortar are quite compatible. Consequently, there is less chance of damage occurring to the structure.

The main objective was to understand why calcitic aggregates have the capacity to produce air lime mortars with higher compressive strengths than their silicate aggregate counterparts. This was achieved by analysing data obtained from undertaking the following tests:

- Flexural and compressive strength testing on a number of mortar samples with several different mix specifications, in order to compare silicate aggregates' and calcitic aggregates' effect on strength. For the most part, limestone aggregates create mortars which perform better in compression but not necessarily flexure. Statistical analysis was used to validate the results.
- Chemical analysis and examination of levels of carbonation product in the samples using thermogravimetric analysis with a view to finding presence of a link between carbonation and the higher strengths observed with the calcitic aggregates. Furthermore, depth of carbonation will be established through use of a chemical indicator (phenolphthalein). It was found that whilst the carbonation depth varies throughout the specimens, it does not necessarily relate to compressive strength. TGA analysis showed that the specimens have different levels of carbonation, with Ham Hill aggregate appearing to create mortars with a greater quantity of $CaCO_3$.
- Pore size distribution and porosity using mercury intrusion porosimetry (MIP) in order to establish whether differences exist between mortars with each aggregate type. As expected, limestone aggregate mortars had greater porosity than the Standard sand samples. Additionally, the pore size distribution varied greatly, with limestone aggregate mortars having one distinct peak for mean pore diameter, whilst Standard sand mortars had multiple peaks.
- Image analysis using scanning electron microscopy (SEM) on specimens so as to determine whether the binder/aggregate bond differs between the calcitic aggregate mortars and the silicate aggregate mortars. The SEM will also determine differences in the presence of portlandite and calcite crystals. Differences were evident in the interfacial area of the binder/aggregate bond.

2 A review of literature

2.1 Introduction

There are three primary constituents of mortar; binder, aggregate (usually siliceous) and water. Aggregates have been found to have an effect on the properties of mortar, which could be attributed to the mineralogy, shape, surface roughness and porosity.

In the past few years, the similarities/differences between the aggregate and mortar composition have been thought to impact the mortars properties. Lanas and Alvarez (2003) make reference to this regarding the use of calcitic aggregate in air lime mortar, stating that the similarities between binder matrix and aggregate structure could be responsible for the higher strengths observed with the calcitic aggregate.

Based on current findings from the literature, it is clear that a gap exists in the knowledge surrounding the impact of calcitic aggregates on the performance of air lime mortars. It has been found that the use of calcitic aggregate in air lime mortars results in greater strengths than was to be expected (Lanas and Alvarez (2003), Lawrence et al. (2006) and Arizzi and Cultrone (2012a)), and this is worth exploring further as it may have a positive impact on the use of air lime mortars in the construction industry. Since higher strengths are associated with improved durability, use of air lime mortars may increase as a result. Despite these findings, there has been no investigation into the mechanisms. In fact, the findings raise a number of questions worth exploring, such as: How does calcitic aggregate impact mortar porosity/pore size distribution?; What impact is there on carbonation of mortars (both in terms of depth of carbonation and quantity of $CaCO_3$ produced)?

The literature review is split up into fresh mortar properties and hardened mortar characteristics, with sub-sections covering the most important aspects governing how mortars behave under different circumstances. The review looks at properties of mortars that impact performance (particularly compressive strength), in addition to fresh mortar properties that impact the ease of use by masons.

2.2 Fresh mortar properties

2.2.1 Introduction

Fresh mortar properties can give an indication of the final mortar strength; workability, plasticity, water retentivity, yield stress all contribute to the characteristics exhibited by fresh mortar. This section looks at the way in which fresh mortar properties influence a mortar's final properties.

2.2.2 Workability

Levin et al. (1956) demonstrate that workability in lime mortars is an exceptionally important property, in particular from the point of view of the mason and suggest that this is a result of workability defining the ease at which mortar can be applied. Workability influences strength, water resistance and workmanship of masonry construction (Levin et al., 1956). The research suggests that measuring workability is not straightforward, due to the substrate sucking water out of the wet mix once it has been applied, but this is not replicated during testing. In the work undertaken by Levin et al. (1956), high-calcium, dolomitic and magnesian hydrated limes are used, alongside natural silica sand. They were tested for plasticity (using the Emley plasticimeter) and water retentivity (using Rogers apparatus) and had a specific flow of 100-115mm. A relationship was found between plasticity and water retentivity; mortars with low water retentivity also exhibited low plasticity, however some limes that had low plasticity had high water retentivity. The research might have benefited from using more than one particle size distribution for the sand, as this will have impacted both plasticity and water retentivity.

Gunn (2005) noted that if the workability was insufficient, the mason would have a tendency to adjust the mortar, commonly by adding more water, leading to a detrimental effect on its properties. The author states that mortar can be classed as a tool, and implies that if you give the mason a better mortar, you will see a better result. It was found that Type S cement was not as workable as Type N, which has a higher lime content. No testing was undertaken in the work by Gunn (2005) but the author discusses what makes a good mortar, as well as the relationship between the mortar and masonry compressive strengths, and seeks to refute the common idea that a stronger mortar is synonymous with better masonry.

It was suggested by de Vekey (2005) that mortar should be able to flow freely, whilst still maintaining an adequate viscosity. Additionally, workability should remain for a few minutes after being applied to the stones, before starting to stiffen.

While it is unclear the exact parameters defining the measurement of workability, Levin et al. (1956) and Pavia and Hanley (2010) concur that water retentivity is a key factor, the former adding that water content is also a priority. Pavia and Hanley (2010) suggest that the internal friction of the mortar also plays a part. Internal friction is dependent on aggregate properties,

hydraulic strength of the binder, and mix proportions. Their investigations looked at NHL 2, 3.5 and 5, using mortar flows of 165, 185 and 195mm respectively. They found that NHL 2 had the best workability as well as the highest water retention. For NHL 2, the mortar with the lowest initial flow was found to have the best workability. This was not the case with either NHL 3.5 or 5. The research provides a good representation of workability in mortars since all three types of NHL were used, in addition to three different mortar flows, however it may also have been useful to compare these mortars against a non-hydraulic lime mortar.

Abell and Nichols (2002) proposed that the influence of the increase in surface area of lime hydration products is of paramount importance, and more so than the crystal morphology of the mortar. Their research measured flow and viscosity, but not water retention or plasticity. Both of these properties would have made a valuable addition to the research. Furthermore, the study only looked at Type S hydrated lime with the addition of Type I Portland Cement. A comparison between different types of lime mortar could have proved useful.

Additionally, air content and density are also thought to be important aspects affecting workability, as found by Hendrickx et al. (2008a) who also suggest that workability is evaluated better by the mason's feeling. This research also looked at two types of sand but no mention was found as to their impact on workability, which would have been beneficial. Hendrickx et al. (2008a) used a number of binders (CL90S, NHL 5 and Portland cement) totaling 7 different mixes. Two types of sand were also used; standardised (EN196-1) sand and a siliceous quarry sand. Importantly, the water/binder ratio was left free for the mason to decide by adding water to the mix themselves. This emphasises the significance of water content on a mortar's workability and suggests that imposing a set water/binder ratio over different mixes would not necessarily yield mortars of similar workability. Consequently, the current study does not have a set water/binder ratio, but instead aims for a specific flow for all the mixes. The main problem occurring as a result is that in practice, if it were left to the mason to define workability by adding their idea of the correct amount of water, there would be no adherence to standards and ultimately, the mechanical properties of each mortar would be unknown.

Workability can also be measured qualitatively through assessing the consistency of the fresh mortar by use of a flow table (BS EN 1015-3:1999). This method is ideal, as it is the consistency that the mason will focus on during application of the mortar. It is worth noting that Pavia and Hanley (2010) state that only certain flows have good workability, due to the need to still retain some consistency. Lime mortar is also frequently knocked up in order to reintroduce consistency, in particular with putties. Stone Tech (Accessed 12/02/13) asserts that this does not necessarily require water addition, but a lot of kneading and chopping of the material. Water may be necessary if knocking up a second time.

In terms of type of lime, Hendrickx et al. (2008a) found that hydrated lime is more workable than hydraulic lime. The author defined workability as measured by rheology and water retention. Given that water retention is a key influence on workability, it is likely that the lower water retention capacity of the NHL (in comparison to hydrated lime) found by Hendrickx et al.

(2008a) could be a contributing factor. Moncada and Godbey (2005) developed a lime-pozzoan mortar for use instead of Portland cement-admixture mortars which have very high compressive strength. It has been noted by Moncada and Godbey (2005) that cement mortar observes an increase in workability with an increase in the proportion of lime into the mix. Additionally, it was found that the high lime-pozzolan mortar had a superior workability than the high lime mortar. A particular benefit of this study is that it looked at both field testing and laboratory testing, and the results were concurrent with each other.

It has been found that various additives also affect the workability of mortar. Martinez-Ramirez et al. (1995) concluded that the addition of sepiolite to the mortar mix increased the viscosity of the mortar, thus decreasing its workability. Additionally, Tsimas and Raikos (1995) found that the addition of lime to cement mortars improves workability and water retentivity. Lime also has a higher degree of plasticity than cement.

Levin et al. (1956) found that workability has an impact on strength, water resistance and workmanship of masonry construction. Pavia and Hanley (2010) agree that workability impacts strength, with particular mention of bond strength, which the research claims is improved by the complete contact between mortar and brick, helped by the ease of spread of the mortar.

The general conclusions from the literature are that workability is an important aspect to consider when designing a mortar mix, and there are numerous tests that govern whether a mortar can be classed as workable or not.

One of the main concerns that has arisen from the review of the literature is the lack of clarity as to which properties should be taken into consideration in order to assess the workability of the fresh mortar. This uncertainty leads to a question of whether workability results from one paper can be comparable to another, as each piece of research may have a different interpretation of the parameters defining workability. In this research, workability will be determined by the feel of the wet mix before being tested for flow. A summary of findings can be seen in Table 2.1.

Table 2.1: Summary of factors affecting workability

	Aspect	Key characteristics
Workability	Practicality	Mortar needs to be easy to work so the mason won't add more water
	Controlling factors	Water retentivity, water content, internal friction, surface area, air content, density, consistency
	Knocking-up	Consistency reintroduced without need for extra water
	Type of lime	Hydrated lime more workable than hydraulic
	Impacts	Strength (particularly bond strength), water resistance and workmanship

2.2.3 Plasticity

It has been suggested by Tsimas and Raikos (1995) that properties for achieving a good plasticity in mortar should include: small crystals of the correct shape, adequate film of liquid surrounding each crystal, and a low surface tension of the lubricating liquid. Consequently, the platelet-like $Ca(OH)_2$ and $Mg(OH)_2$ have been classed as ideal. Walker (1982) suggests that it is the particle size (over shape) that contributes to plasticity of a mortar, and argues that $Mg(OH)_2$ has a high level of plasticity due to having tiny crystals of around $0.08\mu m$. The research attributes this to the fact that if each small particle were coated in water there would be a greater amount of water to lubricate larger particles.

Thomson (1999) and Arizzi et al. (2012a) agree that dolomitic lime hydrate and putty have a higher plasticity than calcium hydrate and putty. However, their reasons for this are different to the view expressed by Walker (1982). Arizzi et al. (2012a) suggest that there are more particle collisions in dolomitic lime, which could be partly responsible for this, in addition to the magnesium ions having a higher charge density. In contrast to Pavia and Hanley (2010) and Levin et al. (1956), it has been stated that viscosity does not correlate well with plasticity; this is evident for the four different mortars tested (Thomson, 1999). Furthermore, dolomitic lime mortar has been categorized as plastic, with calcitic lime being defined as pseudo-plastic by Arizzi et al. (2012a).

It has been suggested by Levin et al. (1956) that since highly plastic limes have a high water retentivity, plasticity should be the governing factor regarding requirements in the specification for mason's lime. Table 2.2 shows a summary of the findings.

Table 2.2: Summary of factors affecting plasticity

	Aspect	Key characteristics
Plasticity	Crystal morphology	Platelet-like crystals achieve good plasticity
	Type of lime	Dolomitic lime has higher plasticity than calcitic
	Water retentivity	Correlates well with plasticity

2.2.4 Water retentivity

Sebaibi et al. (2003) demonstrated that water retentivity varies from lime to lime; calcitic lime for example, has been found in some cases to be more water retentive than dolomitic lime. It is worth noting, however, that this paper used a variety of limes in a cement-lime mix rather than lime-only mixes, therefore no conclusions can be drawn about the performance of individual lime mortars.

In contrast to Sebaibi et al. (2003), research by Thomson (1999) found that dolomitic hydrated lime and putty exhibit significantly higher water retention values than the calcium hydrated lime and putty. Levin et al. (1956) found highly hydrated dolomitic lime to be more water retentive than both regularly hydrated dolomitic and regularly hydrated calcitic lime; they both showed similar values.

There is also a noticeable difference between the values obtained with a lime/sand mortar and a cement/lime/sand mortar, the former of which has been shown to be more water retentive, for the same B/Ag, (Green et al., 1999). Their work showed that with only a small addition of cement to lime mortar, there was a vast reduction in water retentivity. Additionally cement/lime mortars have a higher water retentivity than cement/lime-replacement mortars, as shown in work by Schuller et al. (1999). However, the paper does not specify exactly what is in the lime-replacement mortars, except to say that one is a pozzolanic material, another is proprietary, and the final one is composed of proprietary resin compounds, so it is difficult to establish any significance.

It has been noted by Schuller et al. (1999) that a lower water retentivity leads to reduced contact of the mortar with the stone/brickwork, potentially resulting in insufficient bond strength. Furthermore, Marie-Victoire and Bromblet (1999) demonstrated that a high water retentivity means that extreme drying is avoided early on, thus cracking is reduced. A comparison by Hansen et al. (1999) between a 2 year old lime putty and a 16 year old lime putty showed that the former exhibited a lower water retentivity, but it was suggested that ageing may not have been the only factor here.

Hendrickx et al. (2008b) pointed out that the main cause of bleeding, inhomogeneity and water loss is a low water retention value. Their research found that a lower water retentivity resulted in more bleeding for non-air entrained mortars.

Based on the conflicting findings regarding the water retentivity of calcitic and dolomitic limes respectively, it becomes vital to ascertain possible reasons for the discrepancies. It is possible that the differences arise from the aggregates that were used in each study.

During the literature search, no mention has been found as to whether different types/composition of the aggregates used have an effect on water retention, which seems like an important oversight given the porous nature of most aggregates.

It is clear, however, that water retentivity is a key aspect governing functionality of mortar. Since it is evident that lime mortar has a high water retentivity (and is higher than cement mortars), this is also ideal for conservation purposes. A summary of findings can be seen in Table 2.3.

Table 2.3: Summary of factors affecting water retentivity

	Aspect	Key characteristics
Water retentivity	Type of lime	Conflicting findings over dolomitic/calcitic
	Cement addition	More water retentive than lime only mixes
	Bond strength	Lower water retention means reduced contact/lower bond
	Cracking	Higher water retention leads to less cracking
	Bleeding	Lower water retention increases bleeding and inhomogeneity

2.2.5 Yield stress

A common method of measuring the yield stress of mortar is the vane test (Bauer et al., 2007; Hendrickx et al., 2009), which is traditionally used for clayey soil, and involves inserting a vane into a wet sample of material and applying torque until shear failure occurs. Bauer et al. (2007) tested several mortars using this method and concluded that the results from the vane test correlate well with cone penetration test, but they suggest that viscosity would also need to be measured to aid in defining workability.

Equation 2.1 shows the relationship between the maximum torque applied to the sample, and the yield stress.

$$T_m = \frac{\pi D^3}{2} \left(\frac{H}{D} + \frac{1}{3} \right) \tau_o \quad (2.1)$$

where T_m is the maximum torque, τ_o is the yield stress, and H & D are vane dimensions.

Westerholm et al. (2008) looked at the impact of aggregate fines on the rheological properties of cement mortar, and found that with a higher quantity of fines, a higher yield stress was observed. The study used a w/c ratio of 0.57.

Seabra et al. (2007) suggest that the yield stress of a hydraulic lime mortar decreases with the addition of an air entraining agent and super-plasticizer respectively. Hendrickx et al. (2008b) state that with use of calcic lime, which has a high desorptivity, bleeding occurs and the subsequent increase of yield stress is likely due to an increase of the solid fraction.

It has been suggested that if the yield stress is too high, the mortar will be consequently less workable (Hendrickx et al., 2009). In contrast to this, Hendrickx et al. (2008b) state that if the mortar binder has a higher SSA, the mortar will remain workable despite having a higher yield stress.

Hendrickx et al. (2009) also found that air lime mortar has almost 3x higher yield stress than cement mortar.

No mention has been made, to the author's knowledge, of a relationship between yield stress and aggregate type. This could be a useful piece of research, since more porous aggregates would absorb more water from the mortar mix and would consequently impact yield stress. Table 2.4 shows a summary of findings.

Table 2.4: Summary of factors affecting yield stress

	Aspect	Key characteristics
Yield stress	Workability	Decreases if yield stress is too high, unless binder has a higher SSA
	Binder type	Air lime mortar has higher yield stress than cement mortar
	Aggregate	An increase in fines leads to a higher yield stress

2.3 Aggregate characteristics

2.3.1 Introduction

Aggregates play a vital role in a mortar's matrix, and have a significant impact on both flexural and compressive strength. This section discusses the impact aggregates have on a number of mortar properties.

2.3.2 Binder/aggregate ratio

The binder/aggregate ratio has been identified as one of the most important characteristics of a mortar (Casadio et al., 2005). Their research evaluated methods of determining B/Ag ratio of archaeological lime mortars.

Stefanidou and Papayianni (2005) looked at the influence of aggregate properties on 14 hydrated lime mortars with B/Ag ratio ranging from 1:1.5 - 1:6, and state that for sand grading between 0-4mm, a high B/Ag ratio (1:1.5, 1:2.5, 1:3) means that a higher strength is achieved in lime mortars. This is supported by Lanas et al. (2004), who claim that using a higher proportion of binder leads to higher flexural/compressive strengths. However, at the time of writing, the 90 day strength results had not been obtained.

Hayen et al. (2001) assert that the B/Ag ratio has a marked effect on the depth of carbonation of hydrated lime mortars, at a certain curing age. It has also been noted by Hayen et al. (2001) that a higher B/Ag ratio leads to a greater total pore volume, with the suggestion that B/Ag ratio has the most significant impact on the pore structure of hydrated lime mortar. Additionally, a higher sand content has been suggested to result in coarser pore structures. Lanas et al. (2004) made apparent that making a lime mortar with high proportions of aggregate can have a negative effect on mortar cohesion, subsequently leading to an increased amount of superficial decay.

Cazalla et al. (2000) looked at the impact of lime putty at various ages on the impact of carbonation, and found that fastest and highest degree of carbonation occurred in the 14-year-old lime putty mortar, more specifically also having a B/Ag ratio of 1:4. Although the study did not test flexural/compressive strength, a faster and higher degree of carbonation would also point to a stronger mortar which would be in disagreement with Stefanidou and Papayianni (2005), however the latter used hydrated lime rather than lime putty. Table 2.5 shows a summary of findings.

Table 2.5: Summary of the effect of B/Ag ratio

	Aspect	Key characteristics
B/Ag ratio	Strength	Low B/Ag gives higher strength
	Carbonation	B/Ag affects depth of carbonation
	Pore volume	Higher B/Ag gives greater total pore volume
	Superficial decay	More superficial decay with higher proportions of aggregate

2.3.3 Particle size distribution

Research undertaken by Stefanidou and Papayianni (2005) showed that with the addition of coarse aggregates into lime mortars, stronger compaction is required in order to reduce the voids. Since volume change is lower in this case, long term strength is affected. Lanas and Alvarez (2003) state that the grain size distribution is the most important aggregate characteristic affecting the mechanical properties of lime mortar. This is backed up by their results showing that mortars with adequate grain size results in higher strengths being obtained. The authors found that using a B/Ag ratio of 1:1 led to compressive strengths 4-5MPa higher than using 1:2 B/Ag. However, this is not necessarily positive in terms of conservation work, since mortars should not be stronger than the masonry being repaired.

Winnefeld and Böttger (2006) noted that the addition of clayey fines has a significant impact on many properties of lime mortars. As a result of their addition to mortar, there is an increase in w/b ratio, which results in improved workability. The drying time is also increased as a result of the water retaining properties of the clay aggregate. Total porosity and capillary porosity also see an increase, with the addition of clayey fines, due to the increased w/b ratio. CL90 saw an increase in capillary porosity from around 15% when no clay was added, to 21% with the addition of 8% (by mass) clayey fines. LPC also saw an increase of 6% (from 18 – 24%) with addition of 8% clayey fines. All the mortars saw an increase in porosity with the addition of clay, with the biggest increase being with CL90. Total porosity with no clay was 24.48%, increasing to 30.28% with the addition of 8% (by mass) clayey fines. LPC saw a similar increase, from 25.10% to 30.65%. Isebaert et al. looked at pore-related properties of NHL 5 mortars and agree that with an increase in fines, porosity increases, possibly due to the increased water demand. It was also found that the quantity of smaller pores increased.

Hayen et al. (2001) confirm that pore volume increases with a higher proportion of finer sand. Mechanical strength is observed to decrease, as well as hygral properties and durability. It

was found that compressive and flexural strengths can be reduced by up to 50%. This is not necessarily a negative point in terms of restoration work where a low strength is desired, however, low strength is associated with low durability (Hayen et al., 2001).

Fragata and Veiga (2010) show that the addition of fines to mortar leads to substantially higher compressive/flexural strengths, and also an increase in bulk density. Calcitic aggregates were used in this study.

Kalagri et al. (2014) looked at the effect of various aggregate properties on NHL mortars and came to various conclusions. The research shows that with a lack of coarse aggregate, there is an increase in porosity of the mortar which then leads to degradation of mechanical properties as a result of the mortar requiring a higher water demand in order to achieve the same flow. Additionally, with the addition of coarse aggregates, both strength and packing density were seen to increase, as well as a decrease in total porosity of the mortar. It was also found that dynamic modulus of elasticity was affected by the presence of coarse aggregates similarly to compressive strength.

Winnefeld and Böttger (2006) also state that there is a decrease in the resistance to water vapour diffusion, which can also be seen as positive, as water egress is important in ancient masonry. Due to the higher capillary pore content that was observed by Winnefeld and Böttger (2006) however, freeze-thaw resistance was lowered. Ettringite was found to form primarily on the surface of the clay minerals, thus leading to a lower resistance to sulphate attack. The paper suggests that quartz/limestone should be used as fines.

Pavia and Toomey (2008) looked at a number of different aggregate characteristics and their impact on feebly hydraulic lime mortars. The research investigated the impact of aggregate grading, grain size and grain composition on flexural/compressive strength, water absorption, porosity, bulk density and capillary suction and note that if the aggregate is well graded, porosity, water absorption and capillary suction are all reduced. This is also true of angular grains and mortars with aggregates containing small average particle size. Their research also showed that the most angular grains had the highest flexural/compressive strength. Pavia and Toomey (2008) also show that flexural strength increases as average particle size decreases. It is important to note here that unlike Gonçalves et al. (2006), Pavia and Toomey (2008) were not using clayey fines, but sandstone, granite and limestone respectively. The research would have benefited from also looking at B/Ag ratio, as this would have provided a more holistic impression of the impacts of aggregates.

It has been suggested by Kazmierczak et al. (2010) that an increase in the proportion of fines in mortar renders results in more significant cracking, but that workability is favourable. It was also observed that higher size sands have a higher modulus of elasticity. A higher number of fines leads to greater water consumption and therefore is more plastic.

Binici et al. (2007) found that with the addition of high ratios of marble and limestone dusts respectively, concrete achieves a greater resistance to sodium sulphate attack. However, with

15% fine sand replacement, the lowest abrasion resistance was observed, and in the case of marble dust, an increase in resistance to water ingress occurs.

It is evident that the introduction of fines into the mortar mix has various impacts on its properties, some which are dependent on the composition of the aggregate as well. Furthermore, it is clear that the presence of coarse aggregates also play an important role. A summary of findings can be seen in Table 2.6.

Table 2.6: Summary of the effect of particle size distribution

	Aspect	Key characteristics
Particle size distribution	Strength	Adequate grain size leads to higher strengths
	Workability	Increases with an increase in finer sand
	Pore volume	Increases as average particle size decreases
	Flexural strength	Increases as average particle size decreases
	Porosity, capillary suction, water absorption	Reduced when sand is well graded
	Modulus of elasticity	Higher with use of higher size sands
	Sulphate attack	Addition of limestone and marble dusts provides greater resistance

2.3.4 Aggregate type

It has been found by Lanas and Alvarez (2003) and Arizzi and Cultrone (2012b) that pure limestone aggregates yield mortars with higher strengths than those containing siliceous aggregates. Lanas and Alvarez (2003) suggest that this is due to the limestone aggregate structure being similar to the calcitic binder matrix, which results in a lack of discontinuity. The compressive strengths they obtained ranged between $0.5MPa$ and $5.5MPa$; this was dependent on the B/Ag ratio and which lime binder was used. The highest value was at 360 days curing with lime containing $> 90\%CaCO_3$. The work by Arizzi and Cultrone (2012b) recorded significantly higher compressive strengths for calcitic aggregate mortars than silicate aggregate mortars at 28 days; the former achieved strengths of $1.03MPa \pm 0.03$ whilst the latter had strengths

of 0.05MPa . The authors suggest the strength differences were due to textural properties; the cohesion between the aggregate surface and the binder matrix was better in calcareous aggregate mortars due to the rough, porous surface of the aggregate. This was backed up by the SEM images, though no investigation as to why was undertaken, leaving a distinct gap in knowledge. Fragata and Veiga (2010) agree, but do not suggest reasons for this. Lanas and Alvarez (2003) suggest that silicate aggregates have small radius pores, while limestone aggregates have medium and large radius pores, demonstrating that limestone aggregates allow carbonation of the mortar to take place more readily.

Conversely, Pavia and Toomey (2008) state that the two sands containing the highest amount of calcite actually produced the weakest mortars. The limestone aggregate mortars (where the aggregate contained 84% CaCO_3) had compressive strengths from $0.8 - 1\text{MPa}$, whereas the mortars containing quartz and silicate aggregate respectively had strengths of $1.1 - 5\text{MPa}$. It has been suggested that the reason for this could be due to the use of chalk, which itself has a low mechanical strength. It was found that the highly siliceous aggregate produced the strongest mortar.

Carlos et al. (2010) studied the impact of increasing the proportion of limestone fines in concrete, while simultaneously lowering sand content. The paper looked at concretes with three different water/cement (w/c) ratios. The largest difference was observed with the 55% w/c ratio; compressive strength was 32N/mm^2 with 0% limestone fines (100% sand), increasing to 36N/mm^2 with 100% limestone fines (0% sand). It is unclear at what age of curing the specimens were tested for compressive strength but the comparison is still valid. While the impact of the limestone fines on concrete strength is less than limestone mortars (Lanas and Alvarez (2003), Arizzi and Cultrone (2012b)), this could be attributed to the fact that in this study, only fines were used, rather than a well graded aggregate which is known to produce higher strength mortars.

It was also noted by Carlos et al. (2010) that fine limestone aggregate can reduce shrinkage in concrete. With the addition of 100% limestone fines to the concrete, shrinkage was 15% less than the concrete containing 100% sand. This may also be applicable to lime mortar.

The largest differences in mortar strength due to aggregate type were found by Lawrence (2006) in his doctoral research into carbonation in non-hydraulic lime mortars. The research found that with use of oolitic aggregate (a calcitic variety) in a 4 month old lime putty, compressive strength at 28 days was around 3.5MPa whilst the silicate sand counterpart was just 0.75MPa . After 360 days of curing, the impact was even greater, with the silicate sand mortar achieving just 1.1MPa while the oolitic aggregate mortar was 6.2MPa . The higher strengths achieved here over those of Lanas and Alvarez (2003) at the same curing period might be a result of the use of lime putty over dry lime hydrate.

Naik et al. (2006) compared the use of crushed dolomitic limestone against crushed quartzite in concrete and found that at early ages, the limestone was weaker but at later stages, it was

either a similar strength or higher than the quartzite. Dolomitic limestone was also observed to yield the lowest autogeneous shrinkage and lowest resistance to chloride ion penetration.

The addition of marble dust to concrete has been found to improve compressive strength (Binici et al., 2007). After 12 months, concrete that contained limestone dust had compressive strengths of $44 - 48\text{MPa}$, whilst the concrete without limestone dust obtained a strength of 35MPa . Conversely, Menadi et al. (2009) found that the addition of limestone fines to concrete had no impact on strength up to 15% addition, while at 15% the concrete compressive strength actually saw a decrease, which the research states is due to higher gas permeability.

There is limited research concerning the effect of aggregate type on the properties of lime mortars, and based on the fact that calcitic aggregates seem to be showing better results than siliceous aggregates, with only guesses as to the mechanisms involved, it is clear there is a need for further investigations into possible reasons; methods could include microscopy to look at aggregate shape and binder/aggregate interface of the mortar, pore analysis to determine porosity and pore size distribution in the mortar, chemical analysis of the mortar to establish proportion of CaCO_3 and measurement of carbonation depth of the mortar sample. A summary of findings can be seen in Table 2.7.

Table 2.7: Summary of the effect of aggregate type

	Aspect	Key characteristics
Aggregate type	Strength	Pure limestone aggregates produce mortars with higher strengths than siliceous aggregate. Chalk has the opposite effect.
	Shrinkage	Limestone aggregate in concrete can reduce shrinkage. Dolomitic limestone yields lowest autogeneous shrinkage
	Carbonation	Limestone aggregates allow a higher level of carbonation due to having pores with larger radii than silicate aggregate

2.3.5 Aggregate shape

The geometrical properties of aggregate have a significant impact on mortars. Lanas and Alvarez (2003) and Lanas et al. (2004) point out that rounded grains have less adhesion to the binder and consequently the mechanical strength of the mortar is lower, whereas angular grains have a higher packing density, leading to improved mechanical strength. Pavia and Toomey

(2008) concur that angular aggregates have mortars with a higher mechanical strength (both flexural and compressive).

Stefanidou and Papayianni (2005) ascertained that when lime mortar contained coarse pebbles, voids occurred at the binder/aggregate interface. They suggested that a higher compaction of the mortar is required in order to improve the bond and reduce voids. The rounded shape of the pebbles is responsible for the poor bond.

Additionally, it was found that the angular shape of aggregates led to an increase in mortar cohesion (Isebaert et al.), resulting in improved resistance to compression forces. Although this study used NHL 5 mortars, this is a positive finding that may also help to improve the buildability of non-hydraulic lime mortars. Table 2.8 shows a summary of findings.

Table 2.8: Summary of the effect of aggregate shape

	Aspect	Key characteristics
Aggregate shape	Strength	Angular grains have higher mechanical strength due to better packing density than rounded grains
	Binder/aggregate bond	Rounded grains have more voids at the binder/aggregate interface
	Cohesion	Angular grains lead to an increase in mortar cohesion

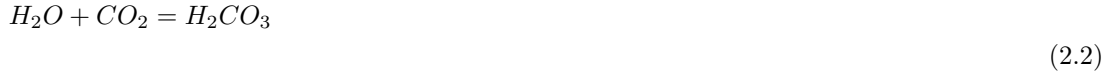
2.4 Chemistry

2.4.1 Introduction

Air lime mortar relies on chemical reactions in order to harden and gain strength; consequently, a significant amount of research has been undertaken, in particular on the carbonation process and how changes in curing conditions impact mortar carbonation. The addition of pozzolans has also been extensively researched, with studies into different types of pozzolans and how they react with lime to alter mortar properties.

2.4.2 Carbonation

Carbonation is the primary chemical reaction that occurs during the setting of air lime mortar, and is influenced by several factors; water content of a sample, relative humidity of curing, temperature, and the porosity of the material. The carbonation process describes the evolution of a mortar through chemical hardening, and can be split into two stages. In the first stage, CO_2 diffuses into the pores of the mortar where it reacts with moisture on the surface of the pores or in the air to form carbonic acid. This can be summarized in Equation 2.2.



Following this, the carbonic acid reacts with the portlandite ($Ca(OH)_2$), transforming it into calcite ($CaCO_3$) as seen in Equation 2.3.



During this process, samples see a weight gain upon transformation of calcium hydroxide to calcium carbonate. Furthermore, the pore structure changes over the carbonation period as a result of the chemical changes; a decrease in total pore volume can be seen (Van Balen and Van Gemert, 1994).

Ficks first law of diffusion can be used to describe the process of CO_2 penetrating the pores in mortar, shown in Equation 2.4.

$$J = -D \left(\frac{\delta\phi}{\delta x} \right) \quad (2.4)$$

Where J is diffusion flux, D is the diffusion coefficient, ϕ is the concentration and x is length. If carbonation occurs predominantly due to kinetic factors, $CaCO_3$ will subsequently precipitate in the form of aragonite/vaterite which will, at some point, be converted to calcite. However, if carbonation transpires mainly as a result of thermodynamic factors, then the $CaCO_3$ precipitates in the form of calcite, which is more stable.

Arandigoyen and Alvarez (2006) demonstrated the part carbonation plays in the porosity of mortar. Hydrated lime/cement mortars were used here, and a porosity decrease of around 10% was observed as a result of carbonation; it was found that fewer pores of $1\mu m$ can be found. Cizer et al. (2006) suggested that with an increase in open porosity of the mortar, a subsequent increase in carbonation depth was noticed. Lawrence et al. (2007) stated that the volume of $0.1\mu m$ pores increases as a result of carbonation in air lime mortars. Furthermore, Lawrence

et al. (2006) assert that the pore size distribution is likely to have an influence on the rate of the carbonation reaction.

Cultrone et al. (2005b) exposed mortar samples, made with aged lime putty, to a CO_2 rich atmosphere and concluded that 90% (weight) portlandite-calcite transformation occurred in just over a week. The paper also highlighted the fact that CO_2 concentration seemed to be independent of the rate of carbonation reaction. This was confirmed by Van Balen (2005) who tested in the range of 15-50% CO_2 concentration at a temperature of 20. Conversely, Dheilly et al. (2002) state that CO_2 concentration is in fact related to carbonation. It is important to mention that Cultrone et al. (2005b) point out that the micro-structure of new mineral phases can be destroyed by rapid carbonation; subsequently, calcium-silicate phases may not be detected.

It has been found by Cazalla et al. (2000) that differences exist in carbonation evolution depending on the ageing time of the hydrated lime; the fastest and highest level of carbonation is achieved with the long-term aged putty, especially when it a low B/Ag ratio is used. It has been suggested that this could be a result of this particular putty having small high-surface-area crystals (plate-like portlandite) which are known to be very reactive, hence rapid carbonation.

Lawrence et al. (2006) say that even when the carbonation process is thought to have ended, a substantial amount of lime remains uncarbonated.

Freedland and Gerns (2005) exposed mortar cubes to freezing temperatures during the first week of curing and noted that carbonation had not penetrated as deeply as the samples that were not exposed to freezing conditions. It was also observed that this could no longer be seen after 3 weeks.

Dheilly et al. (2002) undertook research on the carbonation of $Ca(OH)_2$ powder and revealed that the carbonation process speeds up when the atmospheric temperature is at $10^\circ C$ as opposed to both $20^\circ C$ and $40^\circ C$ respectively, regardless of CO_2 concentration. A high relative humidity has been observed by Lanas et al. (2005) to allow higher carbonation in both aerial and hydraulic lime mortars. This is due to the CO_2 reaction being improved given the greater amount of water in the atmosphere.

It has been found that with the exception of Lawrence et al. (2007) and Lanas et al. (2005), silicate sand is primarily used as aggregate. It would therefore be beneficial to look further at calcitic aggregates, in order to explore their effects on carbonation in more depth. A summary of findings can be seen in Table 2.9.

Table 2.9: Summary of the effect of carbonation

	Aspect	Key characteristics
Carbonation	Kinetic factors	$CaCO_3$ precipitates as aragonite/vaterite
	Thermodynamic factors	$CaCO_3$ precipitates as calcite
	Porosity	Decrease around 10% in cement/hydrated lime mortar
	Open porosity	Increased open porosity leads to increased carbonation depth
	Pore size	Increases in volume of 0.1 micrometre pores with increase in carbonation
	CO_2 concentration	Conflicting findings regarding effect on rate of carbonation
	Temperature	Samples exposed to freezing temperatures have less depth of carbonation
	Relative humidity (RH)	High RH allows higher level of carbonation

2.4.3 Pozzolans

Pozzolans are commonly used in mortar and concrete to enhance properties. They are silicate based and react with $Ca(OH)_2$ to form additional cementitious material. Equation 2.5 shows the reaction that occurs.



The pozzolan reacts with portlandite to form calcium silicate hydrate (C-S-H), which is the compound that chemically binds concrete. Consequently, more C-S-H leads to higher strengths in concrete. Cement is replaced with a pozzolan, rather than the pozzolan being an addition to the concrete. Lime mortar strength can also be increased by the addition of pozzolans, as well as having a more rapid setting time.

Research has shown that the addition of pozzolans can lead to refinement of a mortar's pore structure (Middendorf et al., 2005c; Khatib and Wild, 1998). Middendorf et al. (2005c) investigated the impact of partial replacement of cement with metakaolin on the sulphate resistance of mortars. They suggest that the reduction of calcium hydroxide as a result of cement replacement leads to a refinement of pore structure and consequently increased resistance to sulphate attack.

Shao et al. (2000) investigated the use of ground waste glass ($< 38\mu m$) as a partial replacement for cement in concrete. The research showed that the addition of the glass led to a strength increase at both early and late ages, and the authors suggested this could be due to the high alkali content of the glass. It was found that concrete with a 30% addition of $38\mu m$ glass, there was a 120% increase in strength between 3 and 90 days, a much higher increase than the use of 30% fly ash which saw a strength increase of 102% over the same time frame. The authors conclude that the smaller particle size of the glass ($38\mu m$) results in a higher reactivity with lime, and consequently higher compressive strength, as opposed to the glass with $75\mu m$ and $150\mu m$ respectively. The difference is more pronounced at 90 days.

Moncada and Godbey (2005) developed a high lime-pozzolan masonry mortar in view of replacing the high compressive strength Portland cement-admixture mortars in Mexico, which are incompatible with the soft masonry that is used. The high lime-pozzolan mortar achieved compressive strength results in the range of 1.6-2MPa, as opposed to the cement mortars which had ranges of around 11-14MPa. It was also found that the lime-pozzolan mortar had a higher yield and longer board-life, although the paper failed to mention the quantity or type of pozzolan that was used, which is vital if the research were to be reproduced.

Middendorf et al. (2005b) compared mortars with both washed and unwashed sands respectively, in order to determine any differences. They found that the use of unwashed sands led to mortars with higher compressive strengths, since there was a higher amount of SiO_2 in comparison with the washed sands. Table 2.10 shows a summary of findings.

Table 2.10: Summary of the effect of pozzolans

	Aspect	Key characteristics
Pozzolans	Pore structure	Increase in number of smaller pores
	Strength	Increase in strength with addition of pozzolans

2.5 Hardened mortar characteristics

2.5.1 Introduction

Although mortar hardens within a matter of days, the characteristics of the mortar continue to change over time. For air lime mortars, this is largely due to the fact that the carbonation process continues to change the pore structure and crystal sizes, which ultimately impacts total porosity and both flexural and compressive strength.

2.5.2 Pore structure

An appropriate repair mortar must have sufficient porosity to allow moisture transport through the mortar, and masonry to which it is applied. This is one of the reasons why Portland cement mortar is incompatible with ancient masonry; its low porosity hinders moisture transport, which can lead to damage of the masonry through a build up of moisture as well as deposition of soluble salts which also destroy the masonry.

It has been suggested by Lanas and Alvarez (2003) and Schäfer and Hilsdorf (1993) that the pore structure of the mortar is characterized by open porosity and pore size distribution. Elsen (2006) also indicates that specific surface is a key factor to consider when looking at the pore structure.

Air lime mortars set through carbonation alone; this changes the pore structure of the mortar. Moorehead (1986) details the way in which the conversion of $Ca(OH)_2$ to $CaCO_3$ impacts pore structure. The author states that for each g *mol* of $Ca(OH)_2$ converted, the volume of solid matter sees an increase of 11.8%. This increase in volume begins to fill up the internal pores, reducing their size. As a result, the mortar becomes less permeable to CO_2 with increasing conversion of $Ca(OH)_2$ to $CaCO_3$. Hence, carbonation is a self-limiting process. Furthermore, Arandigoyen et al. (2006) say that with carbonation of a mortar sample, a weight increase is observed due to the higher molar volume of $CaCO_3$ over $Ca(OH)_2$. They go on to quantify this, noting that pastes gain 26g per *mol* of carbonated $Ca(OH)_2$ as a result of the absorption of CO_2 and desorption of H_2O . Additionally, the authors concur with Moorehead (1986) that carbonation leads to a decrease in porosity.

Arandigoyen et al. (2006) found in their research that w/b ratio had an effect on the extent to which carbonation impacts porosity, claiming that with lower w/b ratio, there was a higher decrease in porosity due to a lower porosity and greater quantity of $Ca(OH)_2$ available to be carbonated per volume.

In cement only mortars, Mosquera et al. (2006) and Arandigoyen and Alvarez (2006) claim a reduction in binder leads to an increase in total porosity (and vice versa). On the other hand,

Lanas and Alvarez (2003) and Lanas et al. (2006) note that with lime mortars, higher binder proportions lead to an increase in porosity. Both papers state that this consequently means that the mortar is subjected to a quicker and more complete carbonation.

Additionally, Lanas and Alvarez (2003) have suggested that a porosity decrease is observed as a result of an increase in aggregate content. Elsen (2006) makes light of the difficulties encountered when interpreting porosity values of historic mortars, consequently suggesting that the complexity of the pore structure is the reason for this, due to the differences in pore structure between the stone aggregates and lime lumps. Elsen (2006) has also made the distinction between the pore shape of entrained and entrapped air, stating that the former consists of round, well distributed voids; the entrapped air, on the other hand, is characterised by voids that are both irregular in shape and distribution.

Izaguirre et al. (2011) investigated the use of polypropylene fibres in the mortar mix and found that they had the effect of blocking larger pores, and filling some smaller pores. Consequently, this meant there was a more uniform pore size distribution, and lower pore diameter.

It has been suggested by Arizzi and Cultrone (2012a) and Izaguirre et al. (2011) that if there is a higher amount of kneading water, then there will be corresponding higher porosity values. The former also looked at the effect of the addition of metakaolin to the mortar mix and found that in proportions greater than 10%, porosity values increased. The pores that subsequently developed were found to be similar to those usually formed by hydrated calcium silicates.

Abell et al. (1999) found that for cement mortar, the majority of pores were concentrated at around $0.05\mu m$ diameter (over 50%), with an almost linear decrease in concentration of pores from $0.1 - 5\mu m$. Lawrence et al. (2007) state that for carbonating mortars, the typical pore size range is $0.01 - 100\mu m$. The study found that the highest concentration of pores were $0.01\mu m$ in diameter (approximately $0.3mg/g$), while there was $0.15 - 0.2mg/g$ mercury intruded into pores of $0.1\mu m$. Fewer pores of $1\mu m$ were present, with the lowest concentration of pores at $10\mu m$ in diameter. Comparing these values with the findings from Abell et al. (1999), it is evident that the non-hydraulic lime mortar used by Lawrence et al. (2007) does not have as fine pore structure as the cement mortar; it should be noted that the non-hydraulic lime mortar had a higher water content. Interestingly, Arandigoyen et al. (2006) showed that cement mortar with 50% lime addition had the highest concentration of pores at $0.003\mu m$.

Table 2.11 shows a summary of findings.

Table 2.11: Summary of factors affecting pore structure

	Aspect	Key characteristics
Pore structure	Measurement	Open porosity and pore size distribution
	Total porosity	Increases with reduction in binder in cement only mortars, and with an increase in binder in lime mortars
	Complexity of structure	Difficulties interpreting porosity values of ancient mortars
	Air voids	Difference between shape of voids from entrapped/entrained air
	Kneading water	Higher amount leads to higher porosity values

2.5.3 Water absorption

Water absorption has been defined as the ratio of the mass of water a mortar can retain, to the dry mass of the mortar (BSI, 2002).

It has been suggested by Pavia and Toomey (2008) that aggregate properties can have an impact on the water absorption of the mortar, although not a substantial effect. The highest water absorption occurred in mortars that contained coarser, more rounded aggregate, with inferior grading. In contrast, the minimum water absorption occurred in mortars with the best grading, sharpest particle size and finest average particle size. Pavia and Toomey (2008) also noted that calcite content did not affect water absorption.

The type of lime used also seems to have an effect on water absorption, according to Chever et al. (2010), who suggest that in magnesium-lime mortars, an increase in magnesium-lime in the binder corresponds to an increase in water absorption. Furthermore, Pavia and Treacy (2006) compare the water absorption of OPC, fat lime and feebly hydraulic lime respectively, concluding that the former has the lowest water absorption. This is followed by the fat lime then the feebly hydraulic, although the whole range only covers 5%.

Pavia et al. (2005) also state that the hydraulic lime has a higher water absorption than the non-hydraulic, despite their assertion that the opposite is widely accepted. Although water absorption is an important property, the focus of this research was on the nature of the binder/aggregate interface, therefore testing that would enable an understanding of this were given priority. A summary of findings can be seen in Table 2.12.

Table 2.12: Summary of factors affecting water absorption

	Aspect	Key characteristics
Water absorption	Aggregate	Coarser, more rounded aggregate gave highest value of water absorption
	Lime type	Increase in amount of magnesium leads to increase in water absorption. Feebly hydraulic lime has higher water absorption than fat lime

2.5.4 Elastic modulus

It is known that a mortar with a high modulus of elasticity is not appropriate for conservation; the modulus of elasticity of cement mortar is almost 3x that of stone (Maravelaki-Kalaitzaki, 2007). On the other hand, lime mortars also have a plastic zone that is not present in cement-only mortars (Arandigoyen and Alvarez, 2007)). As a result, they are much more capable of accommodating movements of ancient masonry. Cement mortar, on the other hand, does not allow sufficient movement in the masonry and consequently, stresses build up and cause failure of the original structure.

Furthermore, aggregates can have an impact on the modulus of elasticity. Winnefeld and Böttger (2006) note that when a higher proportion of clayey fines is incorporated, the elastic modulus is reduced by up to 50%. It has been suggested that this may be attributed to the increase in w/b ratio required.

Limestone aggregates were also found to have an impact on modulus of elasticity; a higher percentage in concrete leads to a higher elastic modulus Carlos et al. (2010). Table 2.13 shows a summary of findings.

Table 2.13: Summary of factors affecting elastic modulus

	Aspect	Key characteristics
Elastic modulus	Cement mortar	Modulus almost 3x that of stone
	Clayey fines	Up to 50% reduction in elastic modulus
	Limestone aggregates	Higher percentage leads to higher elastic modulus
	Filler	Higher proportions means higher elastic modulus
	Sand type	Higher elastic modulus with use of calcareous sand over siliceous

2.5.5 Durability

Izaguirre et al. (2010) suggest that there are 5 main categories to take into account when assessing durability: wet & dry cycles, rain exposure, freezing & thawing cycles, exposure to pollutants, and the sun's rays. They go on to say that durability is dependent on various aspects of the mortar, including, but not limited to, characteristics of the binder and aggregate, B/Ag ratio, mortar permeability and water absorption, presence of admixtures, and curing conditions. Izaguirre et al. (2010) looked at the impact of the use of additives in lime mortar on durability, and found that adding a high dose of sodium oleate improves durability. Additionally, the research shows that the presence of air voids improves durability since water has more room for expansion during freezing cycles.

Nunes and Slizkova (2014) added linseed oil to lime and lime-metakaolin mortars and found that water transport by capillarity was consequently restricted, leading to an increase in resistance to *NaCl*.

Duran et al. (2014) also investigated the use of an additive to improve durability; nanosilica was added to air lime mortar (CL90-S with calcitic sand - 1:1 by volume). The study subjected the samples to different exposure conditions in a climatic chamber (temperature, relative humidity, rain and UV light), freeze-thaw cycles and sulphate attack. For each of the durability tests, it was found that the incorporation of nanosilica improved durability, delaying the advancement of decay.

Pavia and Treacy (2006) subjected samples to thermal and salt crystallization cycles, comparing lime putty, feebly hydraulic lime and Portland cement. It was found that non-hydraulic lime had a greater resistance to salt attack than feebly hydraulic lime, but both were significantly

less resistance than the Portland cement mortar. A summary of findings can be seen in Table 2.14.

Table 2.14: Summary of factors affecting durability

Aspect	Key characteristics
Additives	Additives to mortar mixes have proved to improve durability
Mortar type	Cement mortar is the most durable, while non-hydraulic lime is more durable than feebly hydraulic lime

2.5.6 Flexural and compressive strength

For the purpose of conservation of ancient masonry, lime mortar is the preferred choice over cement mortar, as it has lower compressive and flexural strengths; subsequently, the ancient masonry is not damaged after restoration. Due the high strength of cement mortar, there is a lack of movement allowed in the masonry it is applied to, which contributes to a build up of stresses. As a result, the weaker masonry will fail over the mortar. However, strength is synonymous with durability so an increase in the low compressive strengths of air lime mortars could be beneficial.

In research by Stewart et al. (2001), it was found that mortar using high calcium lime binder and sand aggregate achieved strengths of $0.3MPa$ after 60 days curing, rising to just $0.4MPa$ after 120 days curing. Lanas and Alvarez (2003) achieved higher strength non-hydraulic lime mortars than Stewart et al. (2001). For example, with use of a silicate sand, the lowest strength observed was $0.45MPa$ after 14 days curing, with the highest strength being achieved after 180 days curing, at $1.1MPa$. Interestingly, at 360 days, the strength was just $1MPa$; lower than the 180 day strength. The research also found that with use of calcitic aggregate, the 14 day strength was $0.6MPa$ rising to $2.3MPa$ at 180 days and again dropping at 360 days, where the strength was $2MPa$. Table 2.15 is a reproduction of part of a table from Lawrence (2006), showing strengths (in MPa) recorded with a variety of aggregates with dry hydrated lime binder.

Table 2.15: Reproduction of part of a table of strengths (in MPa) using dry hydrated lime binder from Lawrence (2006)

Aggregate type (B/Ag)	14 days	28 days	90 days	180 days	360 days
Bioclastic (1:3)	1.14	1.37	1.57	2.53	2.60
Bioclastic (1:1)	1.08	1.45	1.68	2.40	3.49
Oolitic (1:3)	2.03	2.33	2.57	3.51	4.39
Oolitic (1:2)	1.74	2.23	2.56	4.31	4.53
Oolitic (1:1)	2.21	2.86	3.65	4.93	5.03
Silicate (1:3)	0.28	0.38	0.54	0.59	0.55

It is in general agreement that the compressive strength of air lime mortar increases more than double after the first 28 days up to a year of curing (Moropoulou et al., 2005) and (Lanas and Alvarez, 2003). The latter also noted that an increase in binder content of air lime mortars improves the strength up to a point. Anything higher than a 2:1 ratio sees a significant strength reduction.

Arizzi and Cultrone (2012a) observe that with the addition of pozzolanas and other additives, higher mechanical strengths can be obtained. The addition of the pozzolana (metakaolin) resulted in the development of hydrated phases such as calcium silicate hydrate (CSH) and calcium aluminium silicate hydrate (CASH). Tuncoku and Caner-Saltik (2006) Cerny et al. (2006) and Izaguirre et al. (2011) are also in agreement.

Chever et al. (2010) found that magnesium lime mortar was 2.4x stronger than calcium lime mortar, sometimes developing strengths approaching those of feebly hydraulic lime mortars. Furthermore, Pavia et al. (2005) claim that feebly hydraulic lime was found to be 4x stronger than magnesium lime. When adding high proportions of lime putty to hydraulic lime/sand mortar, Teutonico and Yates (2000) noticed that there was a significant reduction in compressive strength at 60 days.

Fragata and Veiga (2010) compared the use of calcareous and siliceous sand in air lime mortar and found that compressive and flexural strength increased both with fines addition ratio and with age. This is also agreed on by Benachour et al. (2008) who state that compressive/flexural performance is either similar to or better than the reference. The research looked at the addition to cement of up to 45% (by mass) calcareous filler, and found that water demand also increased. The authors conclude that 0-25% (by mass) calcareous filler addition is the optimum quantity to replace normalised sand (EN 196-1). A constant workability and cement content were used.

In contrast, with the addition of clayey fines, a strength reduction (up to 50%) is observed (Winnefeld and Böttger, 2006). Their investigations looked at numerous mortars with cement, NHL and non-hydraulic lime binders respectively. The lower compressive strengths and lower

modulus of elasticity have been attributed to the increase in the water/binder ratio, although Lawrence and Walker (2008) concluded that the water/binder ratio has no impact on the compressive strength of non-hydraulic lime. The lower strengths are more likely a result of the lack of hydraulic phases in non-hydraulic lime mortar.

Since cement mortar has higher compressive/flexural strength than lime mortar, it is not surprising that the addition of cement to lime mortar increases the mechanical strength. Veiga et al. (2009) noted that with the addition of cement to air lime mortar, the highest flexural and compressive strengths were obtained over air lime combined with hydraulic lime, pozzolana, silica fume and metakaolin respectively. Table 2.16 shows a summary of findings.

Table 2.16: Summary of factors affecting compressive/flexural strength

	Aspect	Key characteristics
Compressive/ flexural	Mortar type	Lime mortar has lower strengths than cement mortar
	Pozzolanas	Higher mechanical strengths can be obtained
	Lime type	Magnesium lime mortar 2.4x stronger than calcium lime mortar
	Fines (calcareous/siliceous)	Higher proportion leads to higher strengths
	Clayey fines	More fines leads to a reduction in strength

2.6 Overall conclusions

Despite the extensive amount of literature found on the use of mortars in both conservation and new build, surprisingly little has been mentioned about the impact aggregates have; they are often seen as inert. Although silicate-based aggregates are in most common use, there is evidence to suggest that limestone aggregates can produce higher strength mortars, specifically when using an air-lime binder. Not much is known about the reasons for this, which identifies a need for further knowledge. If higher strength lime mortars could be confirmed, and mechanisms understood, their use could be applied to modern construction in addition to restoration thus leading to a lower carbon footprint in the construction industry.

3 Research design

3.1 Introduction

After extensively reviewing literature surrounding aggregates in lime mortars, it is evident that there is a need for an in-depth investigation of possible reasons why limestone aggregates have been found to produce stronger mortars (with non-hydraulic lime binder) than those made with silicate sand. Several sources concur that this is the case (Lanas and Alvarez, 2003; Arizzi and Cultrone, 2012b; Lawrence, 2006), but possible reasons for this have not been thoroughly explored. Consequently, it is difficult to say conclusively that the results will be consistent in future tests.

In the current climate, the need for reducing carbon emissions is of vital importance. Government targets aim to reduce emissions by 80% by 2050. Since the construction industry is responsible for around 50% of the UK's carbon emissions (BIS, 2010), there is increasing pressure to take action. The use of low energy materials (such as lime mortar) can be particularly helpful here. One of the aspects that makes lime mortar a low energy binder is that a certain amount of the CO_2 that was emitted during the manufacturing process is reabsorbed during curing (Limetec, 2015). Air lime mortar reabsorbs almost all of the CO_2 and this is reduced the more hydraulic a mortar becomes.

The main focus of the research was to investigate the impact calcitic aggregates have on air lime mortar, in relation to mortar containing silicate aggregate; more specifically, the reasons behind the higher mortar strengths observed in previous work. With this in mind, the first step was to select a number of aggregates that would be used in the study, as well as an appropriate binder. For Phase 1 of the research, 5 different limestone aggregates were used, and one silicate aggregate in the reference mortar. Mixes were made with 3 different B/Ag ratios (1:2, 1:3, 1:4) for each aggregate type. Flexural and compressive strength tests were then undertaken after curing for 28 days, at which time the samples were also stained with phenolphthalein in order to assess the depth of carbonation. Subsequently, samples were analysed using SEM in order to gain insight into why the different aggregate types affect mortar strength.

Phase 1 involved the preliminary investigations into air lime mortar. Six limestone aggregates were used, as well as a silicate aggregate as the reference material. B/Ag ratios used were 1:2, 1:3 and 1:4 by volume. Flexural and compressive strength tests were undertaken at 28 days to determine whether the limestone aggregates produced air lime mortars with higher compressive strengths than the silicate aggregate. Phenolphthalein staining was used to ascertain the

carbonation depth of the samples. Finally, SEM analysis primarily looked at the binder/aggregate interface in order to establish whether anything of significance was occurring.

Phase 2 built upon Phase 1 by concentrating on the 3 limestone aggregates producing consistently high strength mortars (throughout the different mix designs) whilst also reducing the B/Ag ratios used to just 1:2 and 1:3. Furthermore, samples were tested at a greater number of time periods (14, 28, 90, 180 and 360 days). Phenolphthalein staining was again used to determine depth of carbonation, but TGA was also utilised to provide quantifiable $CaCO_3$ proportions in the respective samples. SEM analysis looked at differences in binder/aggregate interface over time, whilst MIP data provided much needed detail on pore size distribution and sample porosity.

3.2 Materials

The materials used in Phase 1 of the research were non-hydraulic lime (CL90), and the following aggregates: Ham Hill limestone, Stoke Ground limestone, Doultling limestone, Blue Lias limestone and Standard sand (silicate, CEN-196). For Phase 2, Ham Hill, Portland and Stoke Ground limestones were used as well as the reference Standard sand. Table 3.1 shows the aggregates used in the research.

Table 3.1: Description of the lithology of the limestone aggregates used in the research

Limestone	Lithology
Doultong	Inferioir oolite of the middle Jurassic age. Crystalline, coarsely granular. Creamy brown/grey.
Ham Hill	From the lower Jurassic series. Well cemented mass of shells, crystalline calcite and iron minerals. Coarse grained with some fine grained areas.
Portland	From the Portlandian formation (Jurassic). Ranges from fine grained to open textured. Creamy white in colour. Consists of ooliths in a micrite matrix.
Stoke Ground	Oolitic limestone from the middle Jurassic period.
Bath Stone	Oolitic stone from the Jurassic period. Buff, shelly limestone.
Blue Lias	Late Triassic/early Jurassic period. Agriliceous limestone and mud-stone rich in fossil remains. Blue-grey in colour.

3.3 Sample codes

Figures 3.2 and 3.3 show the codes used for samples in both Phase 1 and Phase 2 of the research.

3.3.1 Preliminary testing phase

Table 3.2: Sample codes *note that '14' refers to the number of days the sample was cured for. Samples were also tested at 28 days of curing

Sample code	Description
BL14*-2	Blue Lias aggregate with 'standard' grading and 1:2 B/Ag ratio
BS14*-2	Bath stone aggregate with 'standard' grading and 1:2 B/Ag ratio
D14*-2	Doultong aggregate with 'standard' grading and 1:2 B/Ag ratio
H14*-2	Ham Hill aggregate with 'standard' grading and 1:2 B/Ag ratio
P14*-2	Portland aggregate with 'standard' grading and 1:2 B/Ag ratio
SG14*-2	Stoke Ground aggregate with 'standard' grading and 1:2 B/Ag ratio
SS14*-2	Standard sand aggregate with 'standard' grading and 1:2 B/Ag ratio
BL14*-3	Blue Lias aggregate with 'standard' grading and 1:3 B/Ag ratio
BS14*-3	Bath stone aggregate with 'standard' grading and 1:3 B/Ag ratio
D14*-3	Doultong aggregate with 'standard' grading and 1:3 B/Ag ratio
H14*-3	Ham Hill aggregate with 'standard' grading and 1:3 B/Ag ratio
P14*-3	Portland aggregate with 'standard' grading and 1:3 B/Ag ratio
SG14*-3	Stoke Ground aggregate with 'standard' grading and 1:3 B/Ag ratio
SS14*-3	Standard sand aggregate with 'standard' grading and 1:3 B/Ag ratio
BL14*-4	Blue Lias aggregate with 'standard' grading and 1:4 B/Ag ratio
BS14*-4	Bath stone aggregate with 'standard' grading and 1:4 B/Ag ratio
D14*-4	Doultong aggregate with 'standard' grading and 1:4 B/Ag ratio
H14*-4	Ham Hill aggregate with 'standard' grading and 1:4 B/Ag ratio
P14*-4	Portland aggregate with 'standard' grading and 1:4 B/Ag ratio
SG14*-4	Stoke Ground aggregate with 'standard' grading and 1:4 B/Ag ratio
SS14*-4	Standard sand aggregate with 'standard' grading and 1:4 B/Ag ratio

3.3.2 Secondary testing phase

Table 3.3: Sample codes *note that '14' refers to the number of days the sample was cured for. Samples were also tested at 28, 90, 180 and 360 days of curing

Sample code	Description
H14*-2	Ham Hill aggregate with 'standard' grading and 1:2 B/Ag ratio
H14*-2 a.s	Ham Hill aggregate with 'as supplied' grading and 1:2 B/Ag ratio
H14*-3	Ham Hill aggregate with 'standard' grading and 1:3 B/Ag ratio
H14*-3 a.s	Ham Hill aggregate with 'as supplied' grading and 1:3 B/Ag ratio
P14*-2	Portland aggregate with 'standard' grading and 1:2 B/Ag ratio
P14*-2 a.s	Portland aggregate with 'as supplied' grading and 1:2 B/Ag ratio
P14*-3	Portland aggregate with 'standard' grading and 1:3 B/Ag ratio
P14*-3 a.s	Portland aggregate with 'as supplied' grading and 1:3 B/Ag ratio
SG14*-2	Stoke Ground aggregate with 'standard' grading and 1:2 B/Ag ratio
SG14*-2 a.s	Stoke Ground aggregate with 'as supplied' grading and 1:2 B/Ag ratio
SG14*-3	Stoke Ground aggregate with 'standard' grading and 1:3 B/Ag ratio
SG14*-3 a.s	Stoke Ground aggregate with 'as supplied' grading and 1:3 B/Ag ratio
SS14*-2	Standard sand aggregate with 'standard' grading and 1:3 B/Ag ratio
SS14*-3	Standard sand aggregate with 'as supplied' grading and 1:3 B/Ag ratio

3.4 Materials and mix design

3.4.1 Preliminary testing phase

The limestones used in the preliminary testing phase were supplied by local quarries in the form of large chunks. The stones were broken up into smaller pieces in the lab, in order to be subsequently crushed into aggregates of the necessary sizes; the aggregate crusher allows approximate particle sizes to be selected. Following this, the aggregate was sieved into the required individual particle sizes, as seen in Figure 3.4 and Table 3.1, before being combined together in the correct proportions (Table 3.1). Prior to sieving, the aggregates were first dried in an oven set to 100°C for 24 hours in order to improve the ease of sieving and to prevent the particles from clumping together as this may lead to inaccuracies in the aggregate grading. The chosen particle size distribution for the limestones was selected to match that of the reference aggregate (Standard sand CEN 196-1). This was done so that the particle size distribution (which is known to impact mortar strength) could be ruled out as a cause of

strength differences.

The maximum particle size of the Standard sand was 1.6mm, so the decision was made to add a 2mm fraction to all aggregates. For the Standard sand, this fraction came from builders sand which was passed through a 4mm sieve and was retained in the 2mm sieve. This was done in order to reduce the risk of mortar shrinkage. Table 3.1 shows the percentage of aggregates passing through each sieve, with the particle size distribution shown in Figure 3.4.

It can be seen in Figure 3.1 that the aggregate grading follows a similar curve to the minimum percentage passing for Type S mortars, as defined in BS1200:1976, although with a higher proportion of fines. Importantly, the proportion of fines is less than the maximum passing for Type S mortars. Too high a proportion of fines can negatively impact mortar strength.

Table 3.4: Aggregate grading as per Standard sand, with additional 2mm fraction

Sieve size	Passing (%)
4mm	100
2mm	88
1.6mm	81.84
1mm	58.96
500 μm	29.04
160 μm	11.44
80 μm	0

Table 3.5 shows the bulk densities of the dry hydrate lime and the aggregates.

The mix design was created to try and find the optimum quantities that would achieve the highest mortar strength. For each aggregate type, three different B/Ag ratios were used. B/Ag ratio was by volume; density of the material was calculated and used to work out mass. The mix proportions for each B/Ag ratio can be seen in Tables 3.6-3.8.

Due to the importance of workability of a mortar, it was decided that rather than having a constant water/binder (w/b) ratio, the flow would be kept constant at 13cm +/- 0.5cm. The main reason behind this was due to findings that if a mortar wasnt deemed workable by the mason, more water would be added to the mix, thus altering the properties (Gunn, 2005).

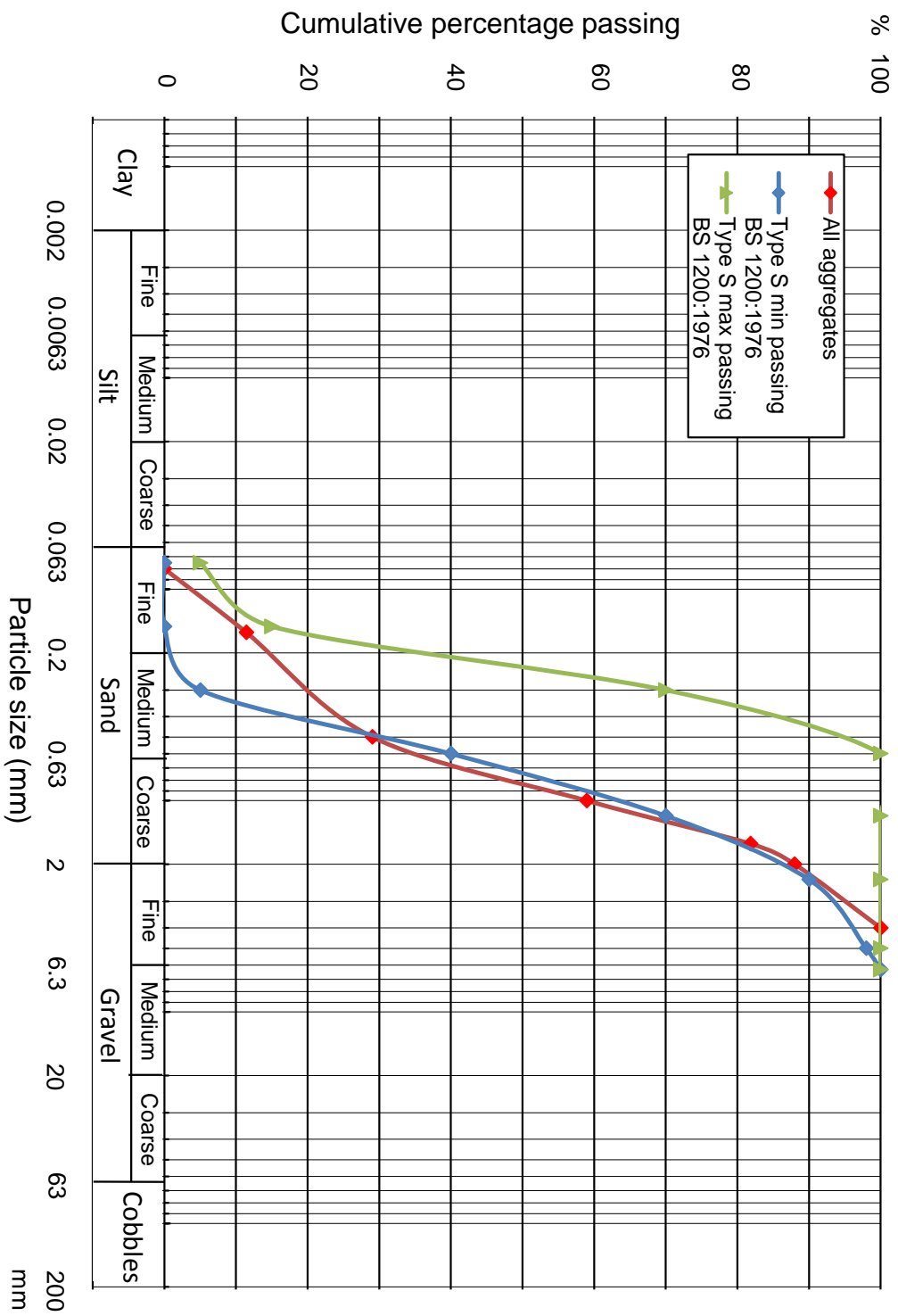


Figure 3.1: Particle size distribution as per Standard sand, with additional 2mm fraction

Table 3.5: Bulk densities of the dry hydrated lime and aggregates

Material	Bulk density (kg/m^3)
Dry hydrate (CL90)	490
Bath stone	2000
Blue Lias	2650
Doulting	2091
Ham Hill	2442
Portland	2596
Stoke Ground	2126
Standard	1500

Table 3.6: Mortar mix design for 1:2 B/Ag ratio (by volume)

1:2	Lime (g)	Aggregate (g)	Water (g)	w/b
Ham Hill	250	2500	487	1.95
Bath stone	250	2050	539	2.16
Blue Lias	250	2834	530	2.12
Doulting	250	2238	513	2.05
Portland	250	2781	493	1.97
Stoke Ground	250	2279	535	2.14
Standard sand	250	1536	250	1.00

Table 3.7: Mortar mix design for 1:3 B/Ag ratio (by volume)

1:3	Lime (g)	Aggregate (g)	Water (g)	w/b
Ham Hill	220	3282	649	1.95
Bath stone	220	2688	553	2.52
Blue Lias	220	3562	483	2.20
Stoke Ground	220	2857	482	2.19
Doulting	220	2810	544	2.47
Portland	220	3489	546	2.48
Standard sand	220	2016	289	1.31

Table 3.8: Mortar mix design for 1:4 B/Ag ratio (by volume)

1:4	Lime (g)	Aggregate (g)	Water (g)	w/b
Ham Hill	176	3501	672	3.82
Bath stone	176	2867	595	3.38
Blue Lias	176	3799	612	3.48
Stoke Ground	176	3647	633	3.60
Doultong	176	2998	581	3.30
Portland	176	3722	647	3.68
Standard sand	176	2150	288	1.64

The flow table test measures the consistence of a mortar; mortar was tamped down into a truncated cone in two layers, with 20 tamps per layer. The cone was subsequently removed and 15 drops of the table were made, at a rate of 1 drop per second. The diameter of the mortar spread was then measured in two directions with the average value being calculated for flow.

3.4.2 Secondary testing phase

For Phase 2, the materials sourced were provided by the quarries as 'dust' left behind from the cutting process. Some of the material (for all aggregates) was graded as per Phase 1, whilst some material was used 'as supplied'. The latter was sieved in order to determine particle size distribution which could then be compared against the particle size distribution of the Standard sand (modified with the addition of 2mm fraction). 1kg of material for each of the limestones was sieved, and percentages passing each sieve can be seen in Table 3.9.

In Table 3.9, it can be seen that each of the limestones have quite a different particle size distribution. Of the limestone aggregates, Ham Hill has a much higher proportion of grains below $0.125mm$ (more than twice that of Portland and Stoke Ground respectively), inclusive of the aggregate that was retained in the pan (i.e. smaller than $0.063mm$). Portland and Stoke Ground aggregates were found to have similar proportions of fines smaller than $0.25mm$, while Portland had more than twice the number of particles retained in the $0.25mm$ sieve than Ham Hill and Stoke Ground. Portland aggregate had the majority of particles concentrated in the $0.25mm$ and $0.5mm$ sieve sizes, while both Ham Hill and Stoke Ground had a much more even spread over the particle sizes. Whilst it is not possible to make a direct comparison of the limestone aggregates due the use of different sieve sizes, it is clear that the concentration of Standard sand particles is toward the larger sizes ($1mm$ and $1.6mm$), in contrast to the limestone aggregates. Furthermore, the proportion of fines seen in the Standard sand is similar to Portland and Stoke Ground; however, the minimum Standard sand size is $0.08mm$ whereas

Table 3.9: Particle sizes for 'as supplied' and 'standard' grading

Sieve size (mm)	Portland (% retained)	Ham Hill (% retained)	Stoke Ground (% retained)	Sieve size (mm)	Standard sand (% retained)
4	0	10	7	4	0
2	3	15	14	2	6
1	8	15	17	1.6	23
0.5	19	5	19	1	30
0.25	39	13	17	0.5	18
0.125	17	11	12	0.16	10
0.063	10	16	10	0.08	13
Pan	3	15	4	-	-

*Columns show percentage retained in each sieve. For the Standard sand, the percentages for the supplied packet have been adjusted to account for the addition of the 2mm fraction.

Portland and Stoke Ground have particles smaller than $0.063mm$.

Figure 3.2 shows how the limestones that were graded 'as supplied' compare against the grading of the Standard sand with the additional 2mm fraction that was also used in the preliminary testing phase.

In Tables 3.10 to 3.13, the specifications for the 4 mixes are displayed.

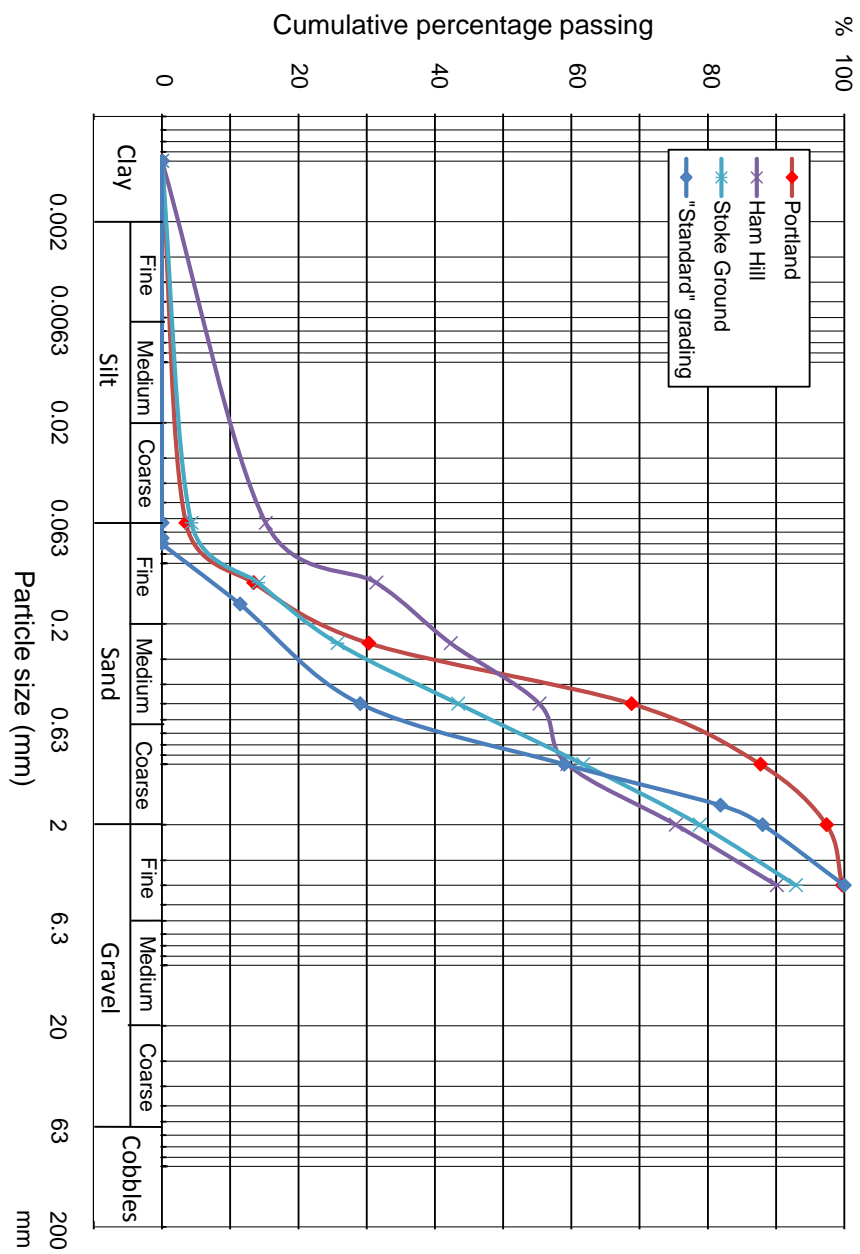


Figure 3.2: 'as supplied' particle size distribution

Table 3.10: Mix design for 1:2 'as supplied' mix

	Lime (g)	Aggregate (g)	Water (g)	w/b
Ham Hill	150	1495	525	3.50
Portland	150	1791	389	2.59
Stoke Ground	150	1468	405	2.70
Standard sand	150	1048	150	1.00

Table 3.11: Mix design for 1:2 'standard' mix

	Lime (g)	Aggregate (g)	Water (g)	w/b
Ham Hill	150	1495	400	2.67
Portland	150	1791	358	2.39
Stoke Ground	150	1468	374	2.49
Standard sand	150	1048	150	1.00

Table 3.12: Mix design for 1:3 'as supplied' mix

	Lime (g)	Aggregate (g)	Water (g)	w/b
Ham Hill	150	2243	579	3.86
Portland	150	2687	542	3.61
Stoke Ground	150	2202	390	2.60
Standard sand	150	1571	150	1.00

Table 3.13: Mix design for 1:3 'standard' mix

	Lime (g)	Aggregate (g)	Water (g)	w/b
Ham Hill	150	2243	458	3.05
Portland	150	2687	455	3.03
Stoke Ground	150	2202	351	2.34
Standard sand	150	1571	150	1.00

3.4.3 Physical and chemical characterisation of aggregates

The aggregates used in Phase 2 were characterised using MIP, TGA and SEM, in order to determine initial data such as porosity and chemical composition that could later be compared against values obtained from samples containing each aggregate respectively.

MIP is a useful tool for looking at the pore structure of a material. Pore size distribution, porosity and pore connectivity are all aspects of an aggregate that may influence mortar strength. Therefore, it is important to compare the aggregates individually rather than in the mortar matrix, to establish differences that may exist.

The use of TGA enables quantitative analysis of the chemical composition of a material. As a result, comparing the aggregates enables determination of whether aggregate composition influences mortar strength. It is also vital to know the $CaCO_3$ content in the limestones, so as to establish what proportion of a mortar specimen's $CaCO_3$ is attributable to the aggregate and how much is the result of carbonation of the specimen.

There are a number of benefits of using scanning electron microscopy to view aggregates. Firstly, aggregate shape can be examined in detail; one of the aggregate properties with the potential to influence strength is its shape. Secondly, surface texture of the aggregate can be seen, which can indicate whether a particular aggregate may have a better bond with the binder. However, if the bond is strong, it may not be possible to see the surface of the aggregate due to the presence of binder on the surface. Finally, since there will be more than one aggregate particle under the microscope (due to size), it will be possible to see whether the particles clump together or remain separate. If they clump together, this may influence the final strength of a mortar specimen.

3.4.3.1 Pore structure of aggregates using mercury intrusion porosimetry

Figure 3.3 shows the relationship between the mean pore diameter and the incremental intrusion volume. The peak shows the pore diameter at which the pore volume is most concentrated. Here, it can be seen that the greatest intruded volume ($0.019mL/g$) at a given point occurs at a pore diameter of $1.882\mu m$, with the majority of the pores ranging between approximately $0.2 - 3.5\mu m$.

In Figure 3.4, the differences with the Ham Hill aggregate are clearly evident. Two unmistakable peaks are visible; at $100\mu m$ the highest volume of pores was intruded ($0.018mL/g$) and at approximately $1.5\mu m$ the intruded volume was $0.011mL/g$. There are two distinct ranges where the majority of pores lie: $0.1 - 3\mu m$ and $20 - 100\mu m$. This first range does not differ significantly with that noted for the Ham Hill aggregate.

It can be seen in Figure 3.5 that the majority of pores have a diameter of approximately $1\mu m$, and that most of the pores lie between $0.1 - 3.5\mu m$.

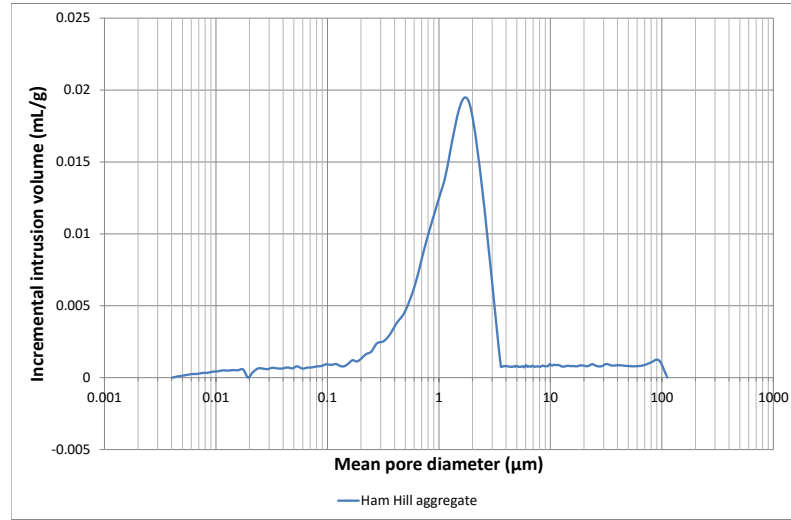


Figure 3.3: Mean pore diameter versus incremental intrusion volume for Ham Hill aggregate

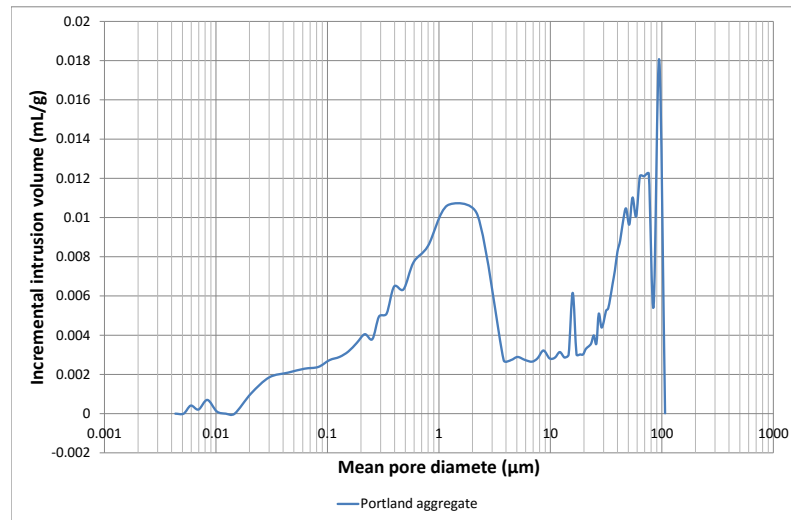


Figure 3.4: Mean pore diameter versus incremental intrusion volume for Portland aggregate

The three limestones all show a very similar trend, with the exception of the additional peak observed with the Portland aggregate. However, the Standard sand was markedly different, as expected. The most noticeable difference in Figure 3.6 is the location of the peak intrusion volume, which occurs at $100\mu m$, with $0.003mL/g$ intruded volume. While there is a gradual increase in the volume of pores with a diameter between $0.01 - 13\mu m$, the range with the highest volume of intruded pores is $13 - 100\mu m$.

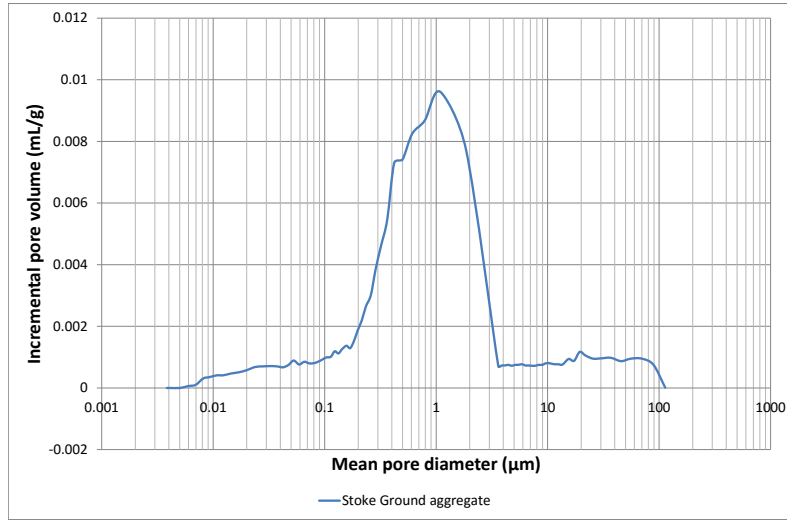


Figure 3.5: Mean pore diameter versus incremental intrusion volume for Stoke Ground aggregate

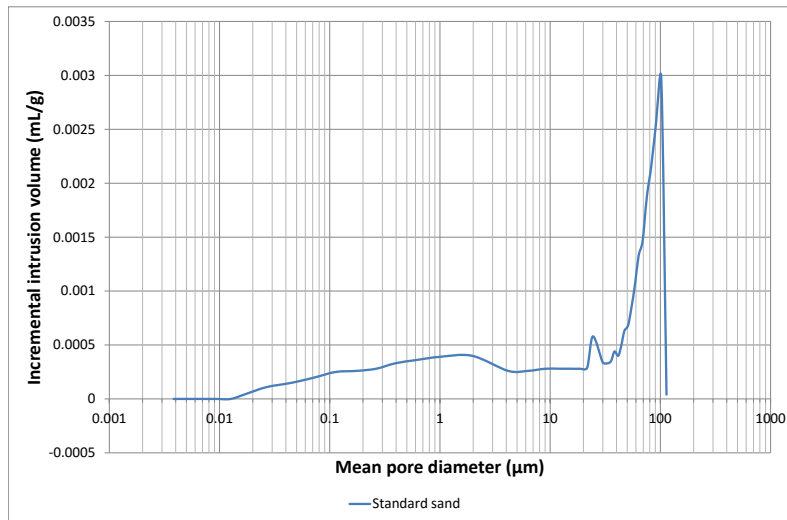


Figure 3.6: Mean pore diameter versus incremental intrusion volume for Standard sand

A comparison of the aggregates shows the marked difference between the limestones and the silicate sand, but also similarities and differences between the limestone aggregates. A distinct peak can be observed in Figure 3.7 which shows that at around $2\mu m$, Ham Hill aggregate had a much greater volume of pores than the other aggregates. The 3 limestones all have their peak between pore diameters of $1-2\mu m$, whereas Standard sand has the maximum volume of pores at around $100\mu m$. As silica (Standard sand) is significantly less porous than limestone (see Table

3.14), it is not surprising to see a much lower volume of pores than the limestones at most pore diameters. Of particular interest, is the Portland aggregate curve; there are several peaks as opposed to the individual peak evident on the curves for the other aggregates respectively. Portland aggregate has peaks at pore diameters of around $15\mu m$ and $100\mu m$ in addition to the peak mentioned earlier that falls between pore diameters of $1 - 2\mu m$. The most distinguished and interesting observation is the significantly larger volume of $100\mu m$ pores that the Portland aggregate has in comparison to Ham Hill and Stoke Ground aggregate. Both the Portland and Stoke Ground aggregates are oolitic

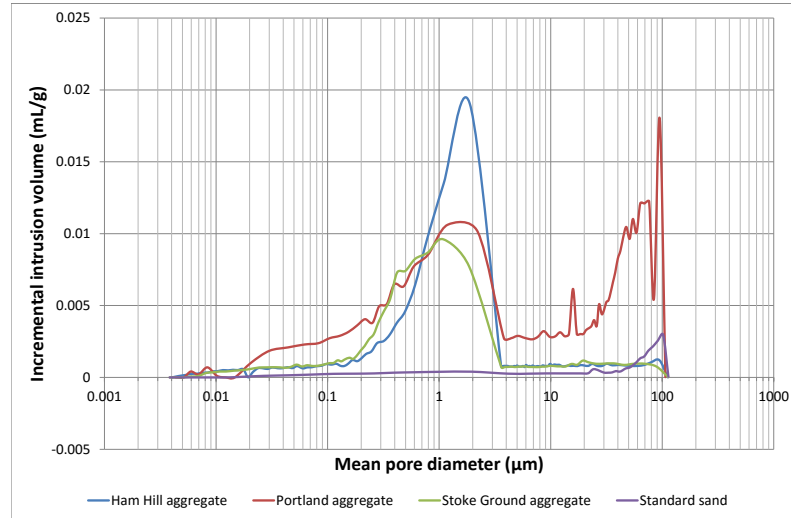


Figure 3.7: Mean pore diameter versus incremental intrusion volume for all aggregates

Table 3.14 shows the significant difference in porosity between the limestone aggregates and the silicate sand; the least porous limestone (Stoke Ground) is still more than 4x more porous than Standard sand (silicate). This will of course have an impact on CO_2 penetration throughout a mortar sample, as well as lessening the ability of binder to enter the pores of the aggregate. This, in turn, negatively impacts the binder/aggregate bond.

Table 3.14: Aggregate accessible porosity as measured by MIP

Aggregate type	Porosity (%)
Ham Hill	28.33
Portland	49.90
Stoke Ground	24.84
Standard sand	5.81

3.4.3.2 Chemical composition of aggregates using thermogravimetric analysis

The use of thermogravimetric analysis has enabled a comparison of the $CaCO_3$ content of each of the aggregates. Figure 3.8 shows a similar trend for the three limestone aggregates, with Portland and Stoke Ground having a very similar mass loss (close to 40%), while Ham Hill has lost approximately half the mass of the former two (around 22%). The temperature range where mass loss occurred was between 650 – 800°C.

The Standard sand exhibits no mass loss in this temperature range, as expected for SiO_2 , but nor is there any mass loss at other temperatures. Standard sand in fact sees an increase in mass of around 8%.

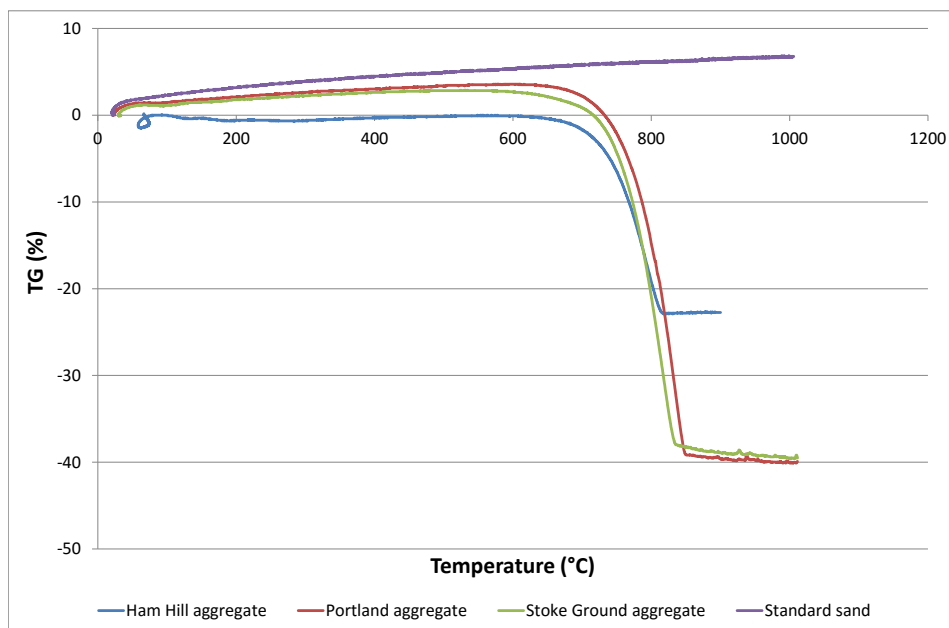


Figure 3.8: Temperature versus TG for all aggregates (Ham Hill, Portland, Stoke Ground, Standard sand)

3.4.3.3 SEM

It can clearly be seen from Figure 3.9 that there are significant differences in the aggregates. The surface of the Standard sand is much smoother than the limestone aggregates; Ham Hill, Stoke Ground and Portland all have finer particles of aggregate on the surface of the larger aggregate. This could lead to a greater proportion of finer particles in a given mix than expected from the sieve analysis, as they are sticking to larger particles.

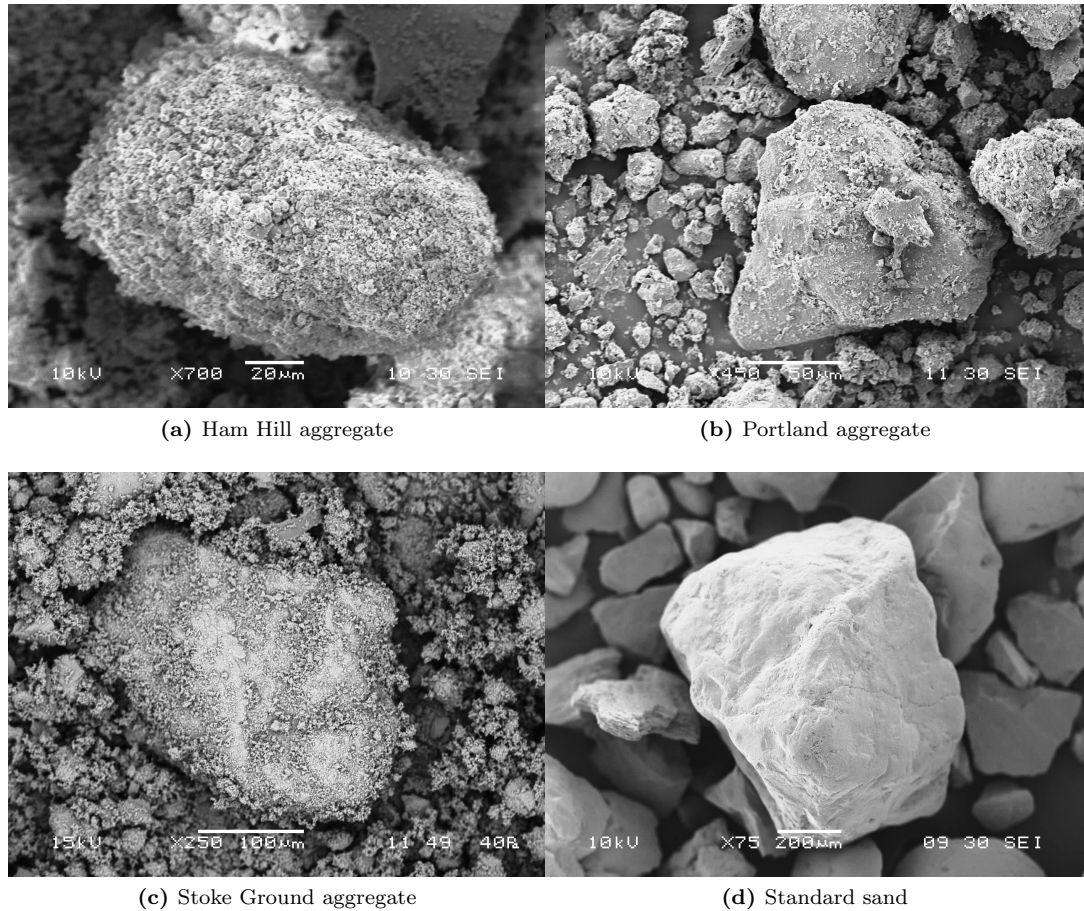


Figure 3.9: SEM images of each aggregate used

3.5 Mass change in mortar specimens during curing

During the curing period, air lime mortar undergoes a complex mass change; a decrease in mass occurs due to drying of the mortar, while conversion of $Ca(OH)_2$ to $CaCO_3$ (carbonation) leads to an increase in mass.

A significant amount of drying occurs in the first 7 days; this was the first point at which the samples could be demoulded due to their softness (directly related to the amount of moisture in the sample). Hence, the first time the samples were weighed was upon demoulding at 7 days of curing.

According to Van Balen and Van Gemert (1994), drying of lime mortar occurs in 2 phases:

1. Drying at the surface and capillary water transport to the surface
2. Diffusion of water to the surface

Their research states that in the first drying phase, carbonation is negligible. The second phase can be described by Fick's Law (Section 2.4.2, Equation 2.4).

The measurement of mass at different curing periods gives an insight into the change in density of samples over time. Samples were weighed both on demoulding and immediately prior to being tested for flexural and compressive strength. The mass loss was then recorded in grams and expressed as a percentage in Table 3.15.

When observed graphically, there are some interesting patterns that have emerged (Figure 3.10).

Stoke Ground mortar samples with a 1:3 B/Ag ratio and 'as supplied' grading show a linear increase in mass loss over time. The equivalent Ham Hill mortar also has a linear increase, although the 90 day mass loss falls below the expected value (approximately 2% rather than 5%). On the other hand, Portland mortar samples with a 1:2 B/Ag ratio and 'as supplied' grading exhibit a linear decrease in mass loss over time, suggesting that carbonation has a greater impact on mass loss than the aforementioned samples. Standard sand samples of 1:3 B/Ag ratio actually saw a slight mass gain after both 14 and 90 days curing, although a mass loss occurred at 360 days. However, this was far smaller than the losses observed by the majority of the other samples. Ham Hill 1:2 samples have an increased mass loss up to 180 days, but this has reduced by 360 days. It would be useful to see if this mass loss continued to decrease after 360 days.

Table 3.15: Average mass loss percentage of samples between 7 days and the date of test

Aggregate type	Mix	14 days	Standard deviation	28 days	Standard deviation	90 days	Standard deviation	180 days	Standard deviation	360 days	Standard deviation
Ham Hill	1:2 'as supplied'	6.3	0.46	-	-	1.6	0.83	6.0	0.68	4.9	0.22
	1:2 'standard'	-	-	2.09	0.22	-	-	6.2	0.81	5.1	0.34
	1:3 'as supplied'	2.5	0.17	-	-	2.3	0.86	7.8	2.32	9.1	2.44
	1:3 'standard'	-	-	-	-	-	-	-	-	-	-
Portland	1:2 'as supplied'	6.5	0.95	-	-	2.1	1.07	4.04	0.66	2.1	0.14
	1:2 'standard'	-	-	6.7	0.31	-	-	2.9	0.82	-	-
	1:3 'as supplied'	-	-	-	-	0.7	0.41	7.7	0.64	3.1	0.22
	1:3 'standard'	-	-	0.6	0.10	-	-	4.36	0.43	-	-
Stoke Ground	1:2 'as supplied'	8.4	1.27	-	-	3.3	1.35	9.0	0.74	3.	0.25
	1:2 'standard'	-	-	-	-	-	-	1.44	0.68	3.16	0.54
	1:3 'as supplied'	1.7	0.22	-	-	4.2	0.97	7.9	0.91	10.2	0.34
	1:3 'standard'	-	-	-	-	-	-	-	-	-	-
Standard Sand	1:2 'standard'	-	-	3.5	0.76	-	-	-0.77	0.08	1.6	0.52
	1:3 'standard'	0.2	0.01	-	-	-0.15	0.07	-	-	1	0.14

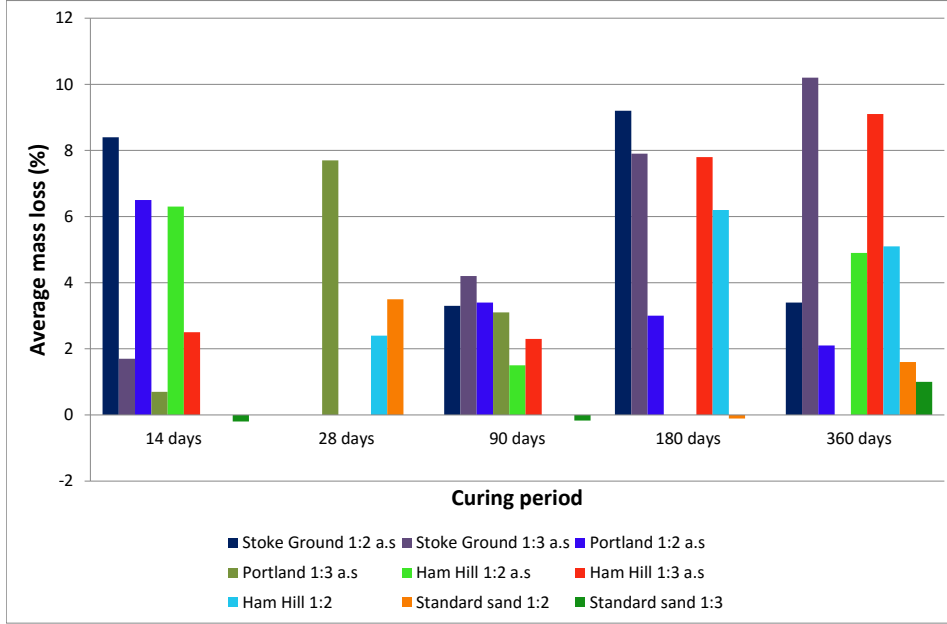


Figure 3.10: Average mass loss of samples at each curing period from the 7 day mass

3.6 Tests and procedures

3.6.1 Abrams' Law

Abrams Law shows the relationship between the strength of fully compacted concrete and the w/b ratio (Equation 3.1).

$$f_c = \frac{K_1}{K_2^{w/c}} \quad (3.1)$$

where f_c is the water/binder ratio, K_1 and K_2 are constants. Compressive strength in cementitious mortars is known to follow Abrams' Law, and is inversely proportional to water/binder ratio (Neville and Brooks, 1987). Lawrence and Walker (2008) have shown that for air lime mortars, with the exception of the lowest water/lime ratio, there is very little difference in the compressive strengths of the mortars with increasing water content.

3.6.2 Batching

BS EN 1015-11: 1999 outlines the preparation method for samples made using non-hydraulic lime. The dry materials (binder and aggregate) were combined using a paddle mixer for 2 minutes, before the required water was added. The components were then mixed for a further minute, before the bowl was scraped with a trowel to ensure all the material was combined thoroughly. The mortar was then subject to a final minute of mixing. In order to initially determine the flow required for a mortar with adequate workability, an estimated mass of water was used before flow was measured using a truncated cone. Mortar was compressed into the cone in two layers and levelled across the top of the cone, which was then removed. The mortar underwent 15 'drops' on the flow table before the average spread of mortar was measured. A trial and error process was then used to work until the required flow was achieved. The mass of the water was then noted for future mixes. The mortar was put into moulds consisting of three 40x40x160mm prisms. This was done in 2 layers, with each layer being tamped down 20 times to compact it into the corners of the mould. Samples were then cured in a conditioning chamber at 20 °C and relative humidity of 65%. For the first 7 days, the samples were cured under a plastic sheet in order to help reduce the occurrence of shrinkage cracks. Demoulding took place when the plastic sheet was removed; samples remained in the conditioning chamber for the remainder of the curing period.

3.6.3 Flexural/compressive strength

Flexural/compressive strength tests were performed in accordance with BS EN 1015-11: 1999. The flexural testing undertaken was 3 point bending; 4 point bending was considered another viable option, however 3 point bending has a simpler stress distribution and since the main purpose of the testing was comparison of different mixes, the 3 point bending was deemed satisfactory. The compressive strength results are of particular interest, since the focus of the research is to determine the reason(s) compressive strengths of air lime mortar can be higher when using limestone aggregates over silicate sand. For the flexural strength testing, the loading rate was $0.2\text{mm}/\text{min}$ while the rate for compressive strength was $0.5\text{mm}/\text{min}$. Three samples were tested for each mix in flexure, with six samples then tested in compression.

Comparisons were made between the different aggregates at curing times of 14, 28, 90, 180 and 360 days. It was hoped to also undertake testing at 7 days of curing but early research indicates that the mortars do not sufficiently harden for testing to take place at this early stage. Testing was done at these different time frames due to the importance of strength development over the first year. A comparison of carbonation over time was also of vital importance.

Figure 3.11 shows the typical test setup used in the research.

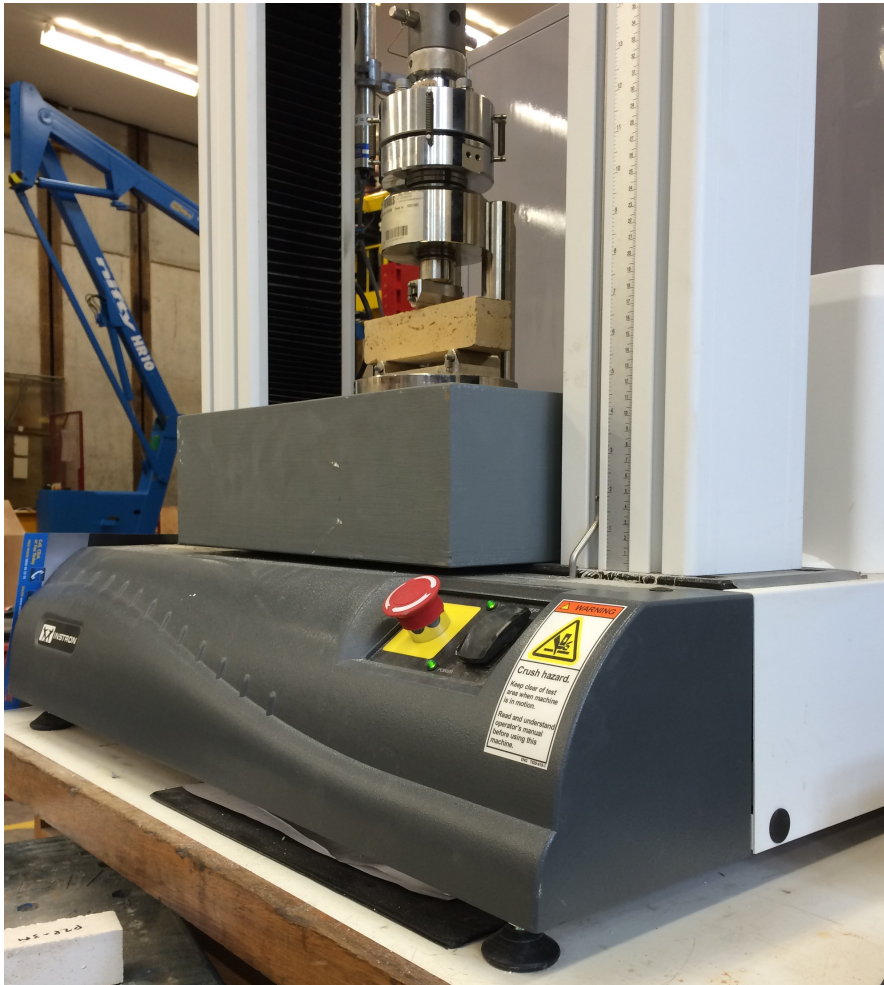


Figure 3.11: Typical setup for 3 point flexural bending

3.6.4 Phenolphthalein staining

Chemical indicators are frequently used to determine the level of pH of a substance. Phenolphthalein is most commonly used when determining the level of carbonation in a sample. Phenolphthalein has a transition range of pH 8.3-10; the colour will change gradually from clear to dark pink within this range. Calcium carbonate has a pH of 9.4, therefore when a carbonated sample is sprayed with phenolphthalein, the colour remains clear. Whereas calcium hydroxide has a pH of 12.4, meaning the sample stains pink on contact with phenolphthalein.

Phenolphthalein staining was performed on samples once flexural testing had been undertaken. The solution was sprayed onto the fractured surface of the sample, in order to determine the depth of carbonation in the sample.

Table 3.16 shows a number of chemical indicators and their colour at different levels of pH.

Table 3.16: Common chemical indicators

Indicator	Transition pH	Colour
Phenolphthalein	8.3-10	Clear - dark pink
Thymolphthalein	9.3-10.5	Clear - dark blue
Thymol blue	1.2-2.8	Red - yellow
	8-9.6	Yellow - blue
o-Cresolphthalein	8.2-9.8	Clear - red

3.6.5 Thermogravimetric analysis

Thermogravimetric analysis (TGA) was performed on a Setaram TG-92 combined with Setsoft 2000 computer software.

In order for a thorough analysis of materials to take place, it is important that their composition is known. Thermogravimetric analysis involves heating up a sample at a constant rate to a specific temperature; decomposition, break-down reactions, vapourisation and gas adsorption and desorption will occur depending on the material under investigation. The computer linked to the TGA records mass loss, which can be plotted against time/temperature. In this way, the quantity of a compound can be calculated provided the decomposition temperature is known.

The carrier gas used is argon, while the chamber gas can either be oxygen or nitrogen. When using samples containing $CaCO_3$, nitrogen is used as it does not react with the sample and

interfere with results. Rate of temperature increase can be varied but it is worth noting that a quicker rate of increase will provide fewer data points and may give a less accurate representation of temperatures at which reactions are occurring.

In addition to being able to determine the composition of the raw materials, TGA enables a comparison of the phases present at different depths of a sample as well as differences between mixes and at different curing times. This is vital in order to gain a deeper understanding of how the different aggregates are impacting carbonation, if at all. Samples were taken from the carbonated edge of the specimen in this study.

Samples were in powder form, with the ideal quantity being 12mg. The samples were placed in a crucible, with an empty crucible to balance the load. The temperature of chamber was increased from 22 °C to 1000 °C at a rate of 10 °C/min. Temperature range and rate of heating can both be altered to suit the needs of the user. A cooling rate of 30 °C/min was used in order to speed up total testing time, as this does not affect the test results.

The shield gas used in this case was argon, with the regulator set at 1 bar and the inlet pressure 0.5 bar. The carrier gas was chosen as nitrogen, based on the requirement that the gas not interfere with the sample in the chamber. Nitrogen does not react with calcium hydroxide or calcium carbonate samples used in this study so did not affect the results. The cooling water for the thermogravimetric analyser was set to 1.4L/min.

In order to perform an experiment, the machine was first first tared with an empty crucible. One crucible was left on the balance (empty), while the other was used to contain the sample and was cleaned thoroughly after each use.

Once the balance was tared, a sample of material (approximately 12mg) was placed in the crucible, which was then returned to the balance and lowered into the chamber. The mass with tare was then recorded on the software.

On the software, the rate of temperature increase was adjusted to suit individual user needs. This is a very important aspect to consider; if the rate of temperature increase is too rapid, phases of decomposition of the sample might be missed. For the current research a rate of 10 °/min was chosen as an appropriate rate. The maximum temperature was also be adjusted; for the current work 1000 ° was selected, to ensure all phases of decomposition had occurred. Cooling rate was also altered; this doesn't affect the sample/results therefore can be a higher value than the heating rate. Once these values have all been set, experimentation can begin. At the end of the experiment (once the chamber has returned to starting temperature), sample can be removed and data processing can begin. Temperature and TG can be plotted against time, and simple calculations can determine mass loss at a given time.

3.6.6 Scanning electron microscopy

A widely used analytical technique is scanning electron microscopy. Images are produced as a result of a focused beam of electrons being targeted at a sample. Primary-, secondary- and backscattered electrons bounce off the sample and the signals detect information about surface topography and, used in conjunction with EDX, chemical composition. EDX can be useful in helping identify phases within a sample, however this is not quantitative and some confusion can arise due to the software adding in elements to 'fit the curve' when they are not necessarily present in the sample. Despite this, EDX is still useful for gaining an insight into where different phases might be occurring. In the backscattered electron mode, areas of different chemical compositions can be identified from the image itself; heavy elements will appear brighter on the image i.e. $CaCO_3$ would appear brighter than $Ca(OH)_2$. It is worth noting that lighter and darker patches may also correspond to different heights on the sample, therefore care must be taken to ensure the sample surface is level.

Chamber conditions can be adjusted to suit the needs of the individual, with low vacuum and high vacuum modes; the latter can produce images at higher magnifications but the sample is required to be coated with a conductive material. Coating samples is necessary for non-conductive materials so that charging of the sample is prevented, and consequently fewer errors within images occur.

The images produced with SEM can also be used to look at crystal shapes (magnifications of up to 30,000x can be achieved) as well as the interface between binder and aggregate. This is of particular importance in the current study where the binder/aggregate interface might be contributing to the strength differences observed in mortars with different aggregate type. Specimens can also be set in resin after being stained with a dye. This is usually blue, as not many naturally occurring materials would be confused with it. Under SEM it is then possible to see the pores within the specimen so shape, size and distribution can be identified.

For the purposes of this research, specimens were taken from the carbonated edge of the sample. Specimens were analysed at a number of different curing periods, and were cut from 40x40x160mm samples as these were the ones being tested for flexural and compressive strength. The microscope used was a JEOL SEM6480LV.

The first stage of using scanning electron microscopy (SEM) to analyse a material is sample preparation. It is important to ensure that the sample is free of dust, as this has a significant effect on the image produced and the elemental analysis (if undertaken). Use of a pipette-style air blower is ideal. The sample material should preferably have at least one smooth edge, for easy attachment onto the metal stub with double-sided tape. Once samples are mounted on stubs and labelled, they are placed in a dessicator overnight to remove any excess moisture that may be in the sample.

Before analysis of the sample can begin, the electron microscope first needs to be set up. The

chamber should first be vented, after which the sample can be placed inside the chamber which is then evacuated. The sample height and horizontal position must then be adjusted, taking care not to move the platform too close to the lense; the position of the platform can be seen on a screen which enables correct positioning of the sample.

3.6.7 Mercury intrusion porosimetry

Mercury intrusion porosimetry was performed using AutoPore II 9220 porosimeter.

A mortar's pore structure can impact both strength and CO_2 access. Use of MIP can help identify pore size/distribution, pore volume and sample density, among other characteristics. As mercury is a non-wetting fluid due to its high contact angle, it will not enter the pores of a sample unless pressure is applied; rather it covers the pore. At lower pressures the larger pores are filled, while higher pressures are required for the smaller pores. At a pressure of 60,000psi, diameters as small as $0.003\mu m$ can be intruded.

The Washburn equation is used to describe the inverse relationship between pore diameter and pressure (Equation 3.2), which assumes a cylindrical pore with a circular opening of diameter, D . This is quite a simplistic representation of the pore geometry, which in reality is not uniform.

$$P = \left(\frac{2\gamma}{r} \right) \cos\theta \quad (3.2)$$

where P = Pressure, γ = surface tension of mercury, r = radius of the capillary and θ = contact angle of the mercury on the material.

There is potential for inaccuracies using MIP, but measures can be put in place to reduce these. Both the penetrometer and the mercury are compressible, which leads to a slight change in the volume of both; blank correction data is used to offset this discrepancy which could otherwise result in approximately 1% variation. The blank correction data subtracts baseline drift from the volume measurement data.

Another element of MIP that can lead to inaccuracies exists because the technique does not measure the internal pore size, but measures the largest neck from the surface of the sample to the pore. Therefore, if results from MIP analysis were compared with another method of determining pore size, such as SEM or optical microscopy, smaller pore sizes would be observed with MIP.

A further aspect that could cause errors is hysteresis. This can occur as a result of several factors. Firstly is contact angle hysteresis; the surface roughness or impurities in the sample has the ability to change the contact angle of mercury as it is intruded/extruded. However this does not account for mercury that remains in some of the pores. This is due to the effect of ink bottle pores. Where the opening of the pore is narrower than the pore (ink bottle shaped),

mercury extrudes from the neck and covers the opening, thus preventing the mercury from extruding out of the pore itself. Finally, the connectivity model is based on a network of pores and can be thought of as an extension to the idea of ink bottle pores, as it considers the effect of the pore connections, as well as the size of the pore opening.

When analysing the data output from the MIP, there are a number of elements that provide different information, depending on the individual needs of the user. The data output after the test has run includes pressure, mean pore diameter (at each pressure increment), incremental and cumulative pore volume, and incremental and cumulative pore area. Plotting cumulative intrusion volume against pore diameter can give an idea of the volume of pores at a given size increment. A sharp rise in slope on the graph indicates a high volume at that particular size. Plotting incremental intrusion volume against diameter shows two things: firstly, the pore diameter at which pore volume is most concentrated, and secondly, the distribution of the pores.

4 Preliminary testing phase

4.1 Flexural/compressive testing results

Figures 4.1 to 4.12 show how the flexural and compressive strengths of the mortar samples differ based on aggregate type and binder/aggregate ratio at both 14 and 28 days curing.

In Figure 4.1, it can be seen that Portland aggregate mortar has the lowest flexural strength at 14 days of all the 1:2 mixes, while Stoke Ground mortar exhibits the highest strength (around 3 times higher). This is despite the fact that the Stoke Ground mortar sample had a higher water content in relation to binder. Given that the B/Ag ratio and particle size distribution for each mix was the same, the differences must lie in the aggregate itself, or the binder aggregate bond. Differences in aggregate could be due to porosity, surface roughness or angularity, and these have been examined in section 4.4 using scanning electron microscopy.

The Standard sand mortar results were expected. Bath stone mortar (BS-2) had the lowest compressive strength of the limestone aggregate mortars. The flexural results were also in the lower values.

The compressive strength results for the same mixes in Figure 4.1 do not follow the same pattern, which can be seen in Figure 4.2. The Standard sand mortar (SS-2) showed the lowest compressive strength, whilst Ham Hill (H-2) had the highest, at more than double the value of SS-2. Based on the literature reviewed earlier, the Standard sand mortar result was expected. SS-2 has the highest amount of binder in relation to water content.

By 28 days, the mortars had a much smaller range of flexural strengths (Figure 4.3); the highest strength mortar (D-2) was just $0.2MPa$ stronger than the weakest. This could be due to the fact that once the majority of drying has taken place, strength stabilises; with the exception of SS-2, the mortars had a very similar w/b ratio so the main influence on the differences lies in the aggregate properties and binder/aggregate bond.

As with the 14 day compressive strengths, SS-2 was also found to have the lowest compressive strength at 28 days, which can be observed in Figure 4.4. Ham Hill mortar (H-2) was still found to have the highest compressive strength, and saw an increase of $0.2MPa$ from the 14 day value. The other mixes all saw a similar increase, leading to the assumption that carbonation of each sample must have occurred to a similar extent.

It was found that the aggregates in the 1:3 mortars had a different impact on flexural strength

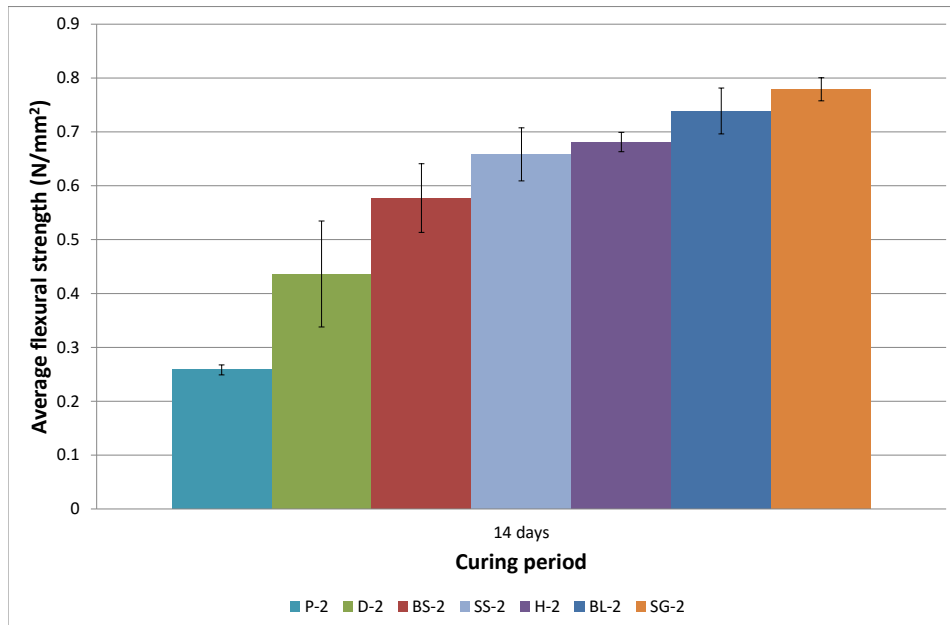


Figure 4.1: Average flexural strengths for 1:2 mixes at 14 days curing

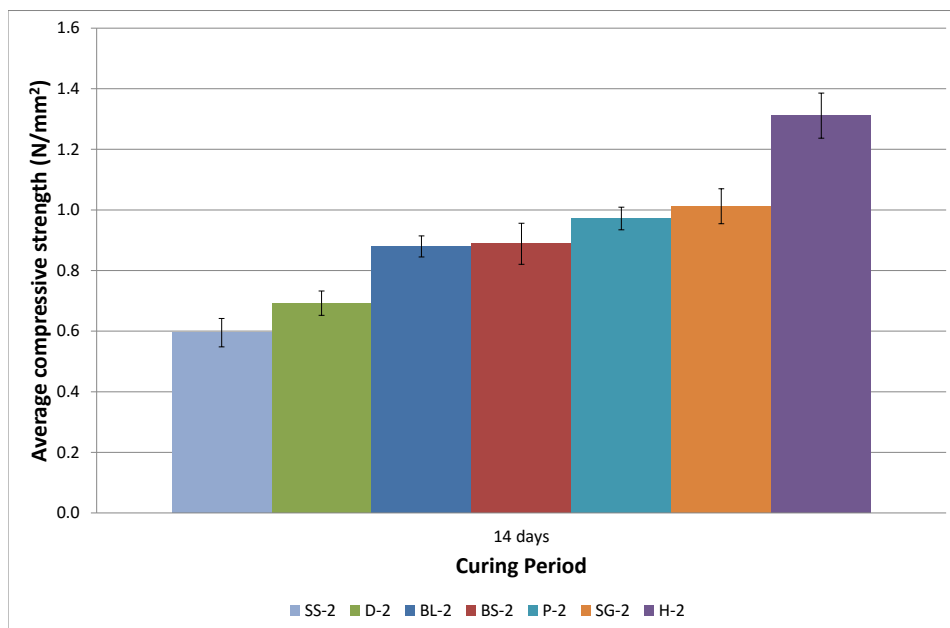


Figure 4.2: Average compressive strengths for 1:2 mixes at 14 days curing

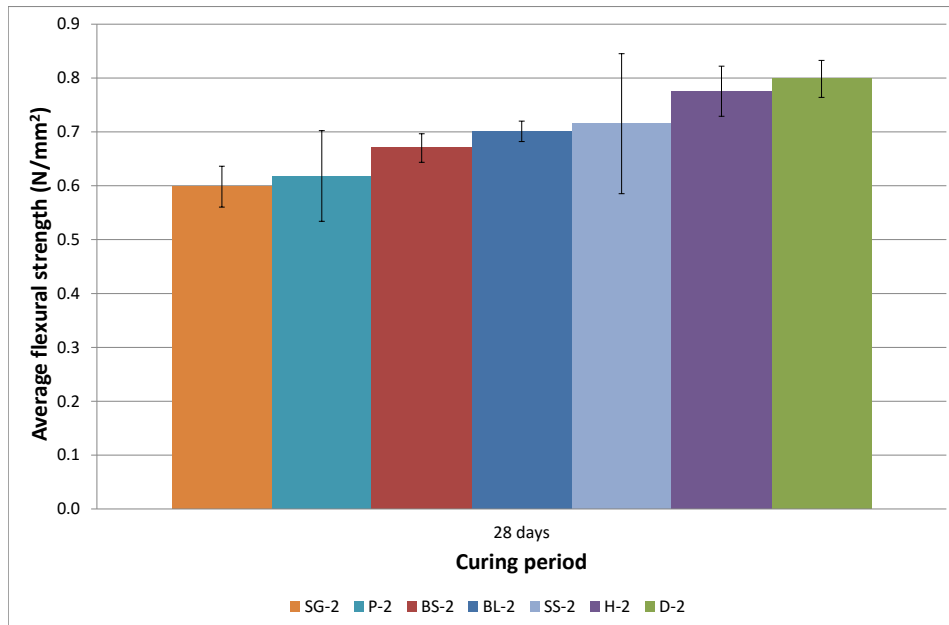


Figure 4.3: Average flexural strengths for 1:2 mixes at 28 days curing

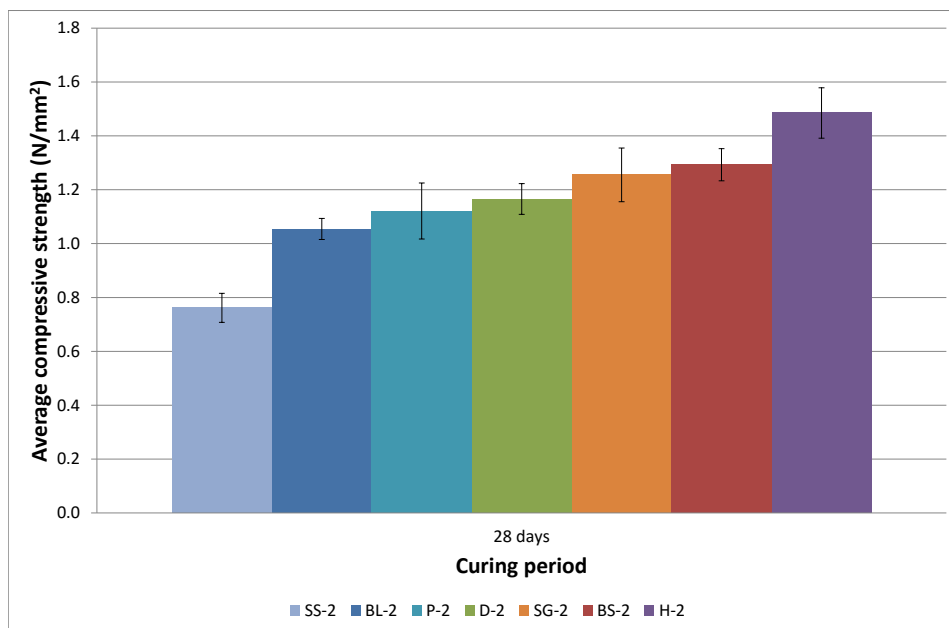


Figure 4.4: Average compressive strengths for 1:2 mixes at 28 days curing

(Figure 4.5). SG-3 was found to have the lowest flexural strength, over 3 times lower than that of D-3.

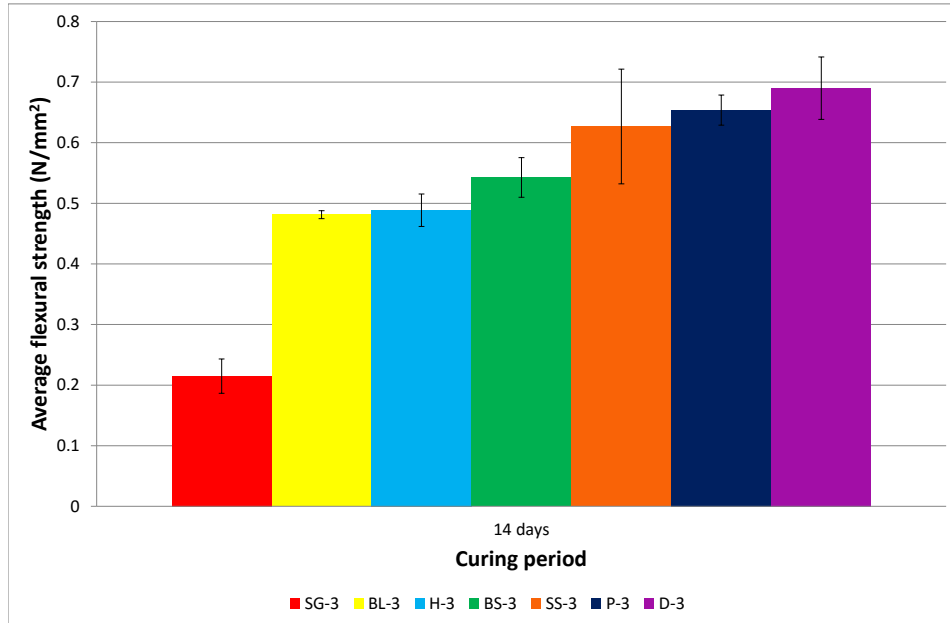


Figure 4.5: Average flexural strengths for 1:3 mixes at 14 days curing

Compressive strength results at 14 days reveal that once again, the Standard sand mix had the lowest value. Figure 4.6 reveals that many of the mixes have a very similar compressive strength (D-3, BL-3, BS-3, P-3), which could be a result of the similar properties of the aggregates. Interestingly, BL-3 shows a large error here that was not present in the flexural strength results.

After 28 days curing, it is the Bath Stone (BS-3) that displays the highest flexural strength for the 1:3 mixes (Figure 4.7). SG-3 still has the lowest strength.

BS-3 now has the highest compressive strength, as well as flexural. Figure 4.8 reveals that once again, it is the Standard sand mortar that fares worst in compression; this further supports the notion that higher strength air lime mortars can be achieved with the use of limestone aggregates over silicate.

In Figure 4.9, it can be seen that 5 out of 6 samples have flexural strengths between $0.65MPa$ and $0.75MPa$, which is a much smaller range than the 1:3 mixes.

P-4 shows the highest compressive strength after 14 days for the 1:4 mixes; Figure 4.10 illustrates this, and it can be seen that SS-4 and BL-4 perform the worst.

After 28 days, P-4 is found to have the highest strength in both flexure and compression (see Figures 4.11-4.12). This may be due to Portland aggregate having a higher compressive strength

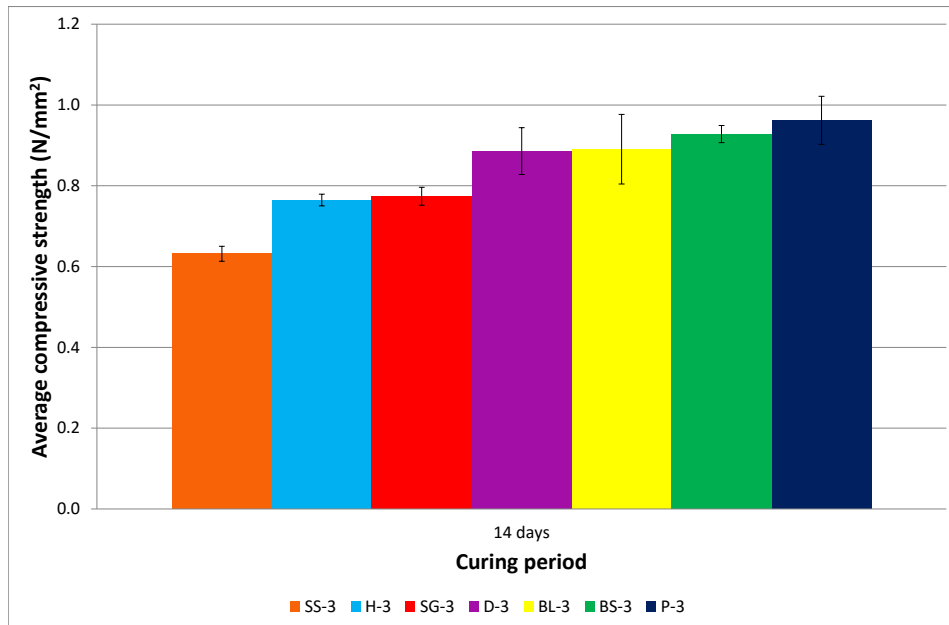


Figure 4.6: Average compressive strengths for 1:3 mixes at 14 days curing

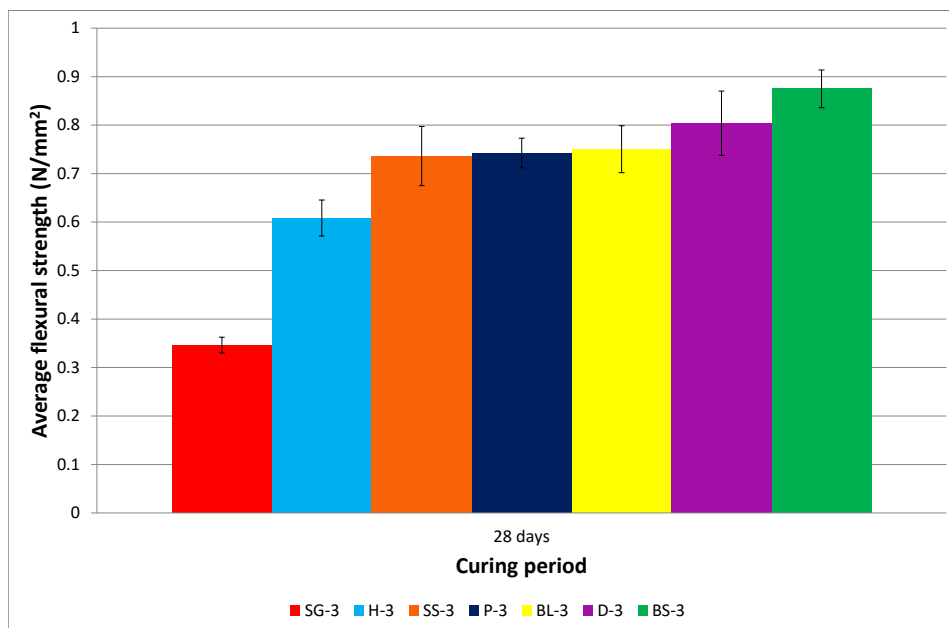


Figure 4.7: Average flexural strengths for 1:3 mixes at 28 days curing

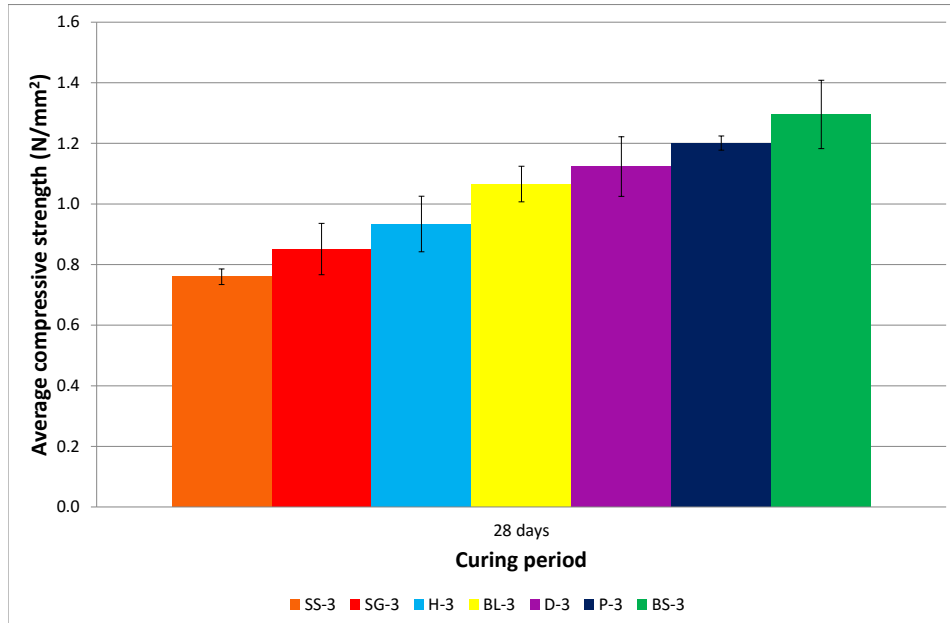


Figure 4.8: Average compressive strengths for 1:3 mixes at 28 days curing

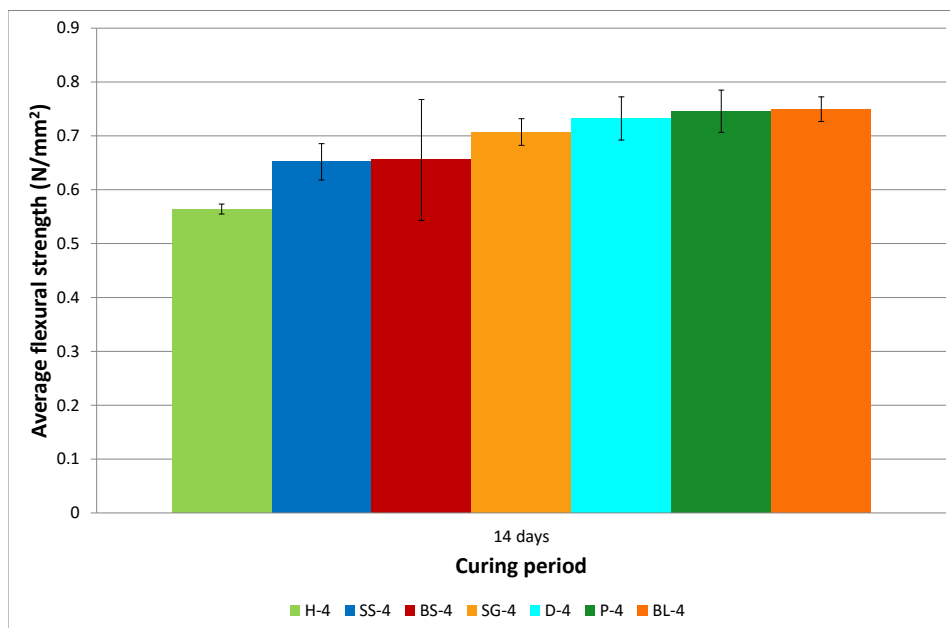


Figure 4.9: Average flexural strengths for 1:4 mixes at 14 days curing

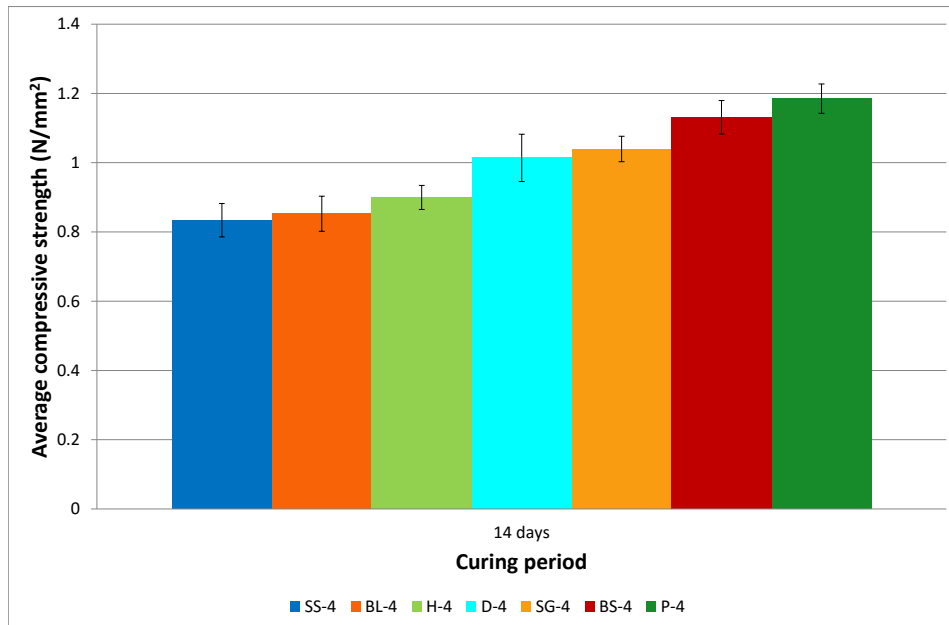


Figure 4.10: Average compressive strengths for 1:4 mixes at 14 days curing

than the other aggregates, which is noticeable with the 1:4 mix due to the higher aggregate content in relation to binder. P-4 has shown high strengths with all of the 1:4 mixes.

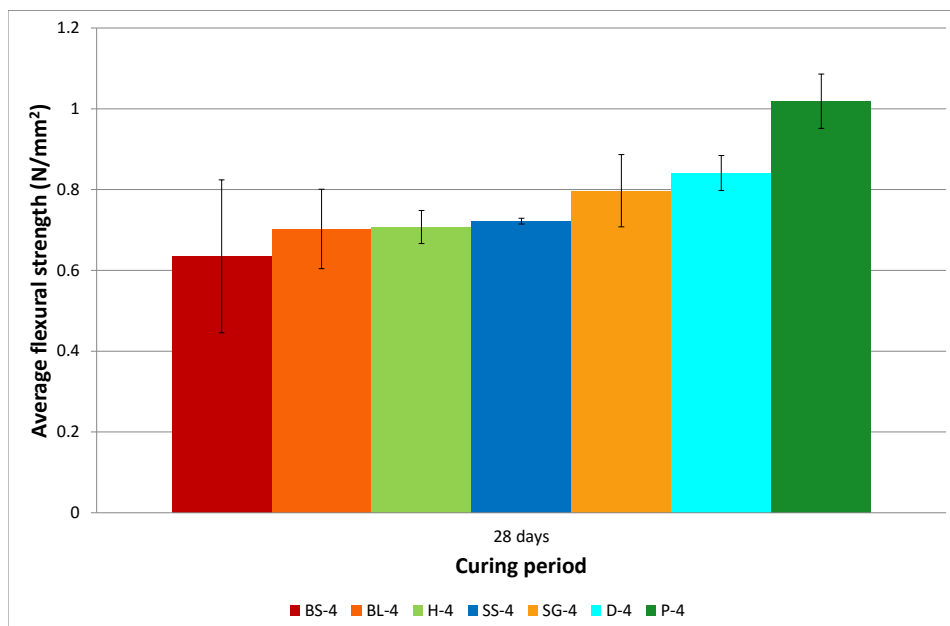


Figure 4.11: Average flexural strengths for 1:4 mixes at 28 days curing

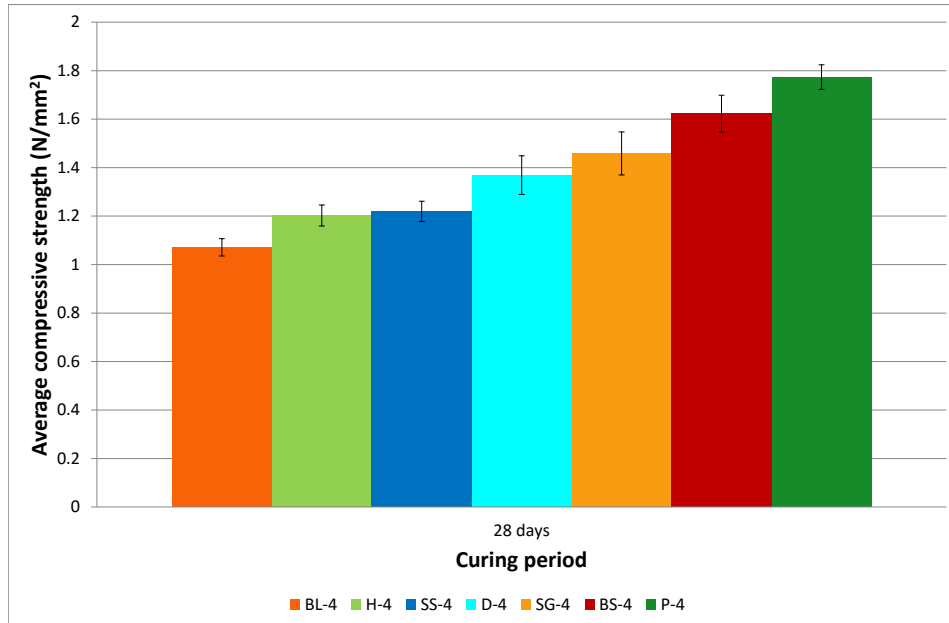


Figure 4.12: Average compressive strengths for 1:4 mixes at 28 days curing

Overall, the strongest mortars were found with the 1:2 mix, with Ham Hill and Stoke Ground limestones showing the highest compressive strengths (1.48 and 1.25MPa respectively). Standard sand mortars displayed the lowest compressive strength.

4.2 Carbonation depth using phenolphthalein indicator

Carbonation depth was measured by spraying a phenolphthalein indicator onto the fractured surface of the specimens. Once the sample had turned pink (where $Ca(OH)_2$ was still present), calipers were used to measure the distance from the edge of the sample to the edge of the pink stained area. This was done on each edge and an average taken. Figure 4.13 demonstrates the differences observed in the depth of carbonation in two mortar mixes (Ham Hill and Standard sand).

It became clear when looking at the average depth of carbonation (see Table 4.1) that the values did not relate to the compressive strength results obtained.

This suggested that since the CO_2 is not able to more deeply penetrate the limestone aggregate samples to a significant amount, the effect of carbonation on strength must be related to quality rather than quantity. Scanning electron microscopy shows a clearer image of micro-structural differences between the samples.



Figure 4.13: Phenolphthalein staining (left) Ham Hill, (right) Standard sand

Table 4.1: Average carbonation depth of samples after 28 days curing with 1:2 B/Ag, 'standard' grading

Sample	Depth (mm)	Compressive strength (N/mm^2)
Standard sand	5	0.7618
Ham Hill	6	1.4851
Bath stone	6	1.2028
Portland	6	1.1210
Stoke Ground	6	1.2553
Doulting	7	1.1656

4.3 Scanning electron microscopy

Samples were taken from the edge of specimens, where carbonation had taken place. After looking at each sample under the electron microscope, noticeable differences were observed, in particular at the binder/aggregate interface. The Standard sand sample (Figure 4.14) has some discontinuity around the edge of the aggregate.

It was found that some calcite crystals adhered to the surface of the aggregate, but the majority of the aggregate was still visible, with the surface appearing smooth. The surface texture may be preventing calcite crystals from 'sticking' to the aggregate.

All of the limestone aggregates were markedly different by comparison. Stoke ground limestone mortar (Figure 4.15) contained some cracks of $50\mu m$ or smaller, despite being the strongest mortar in compression. The higher strength could be, in part, due to the higher number of calcite crystals present on the aggregate surface; only small areas of aggregate were visible. In

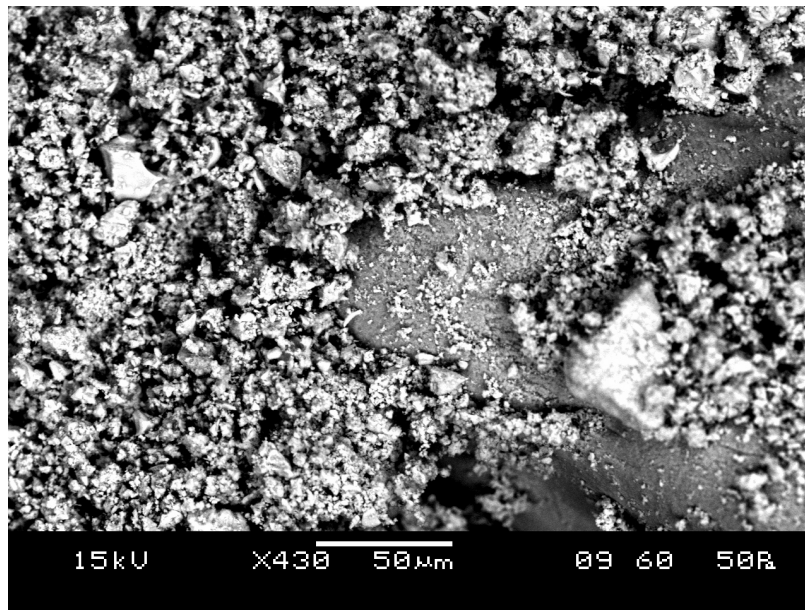


Figure 4.14: Standard sand sample at 430x magnification

the mortar made with Portland limestone aggregate (Figure 4.16), a large quantity of calcite is visible on the aggregate surface, again with just a small area of the aggregate having no calcite formation. The crystal formation surrounding the aggregate appears more uniform than that of the Stoke Ground sample.

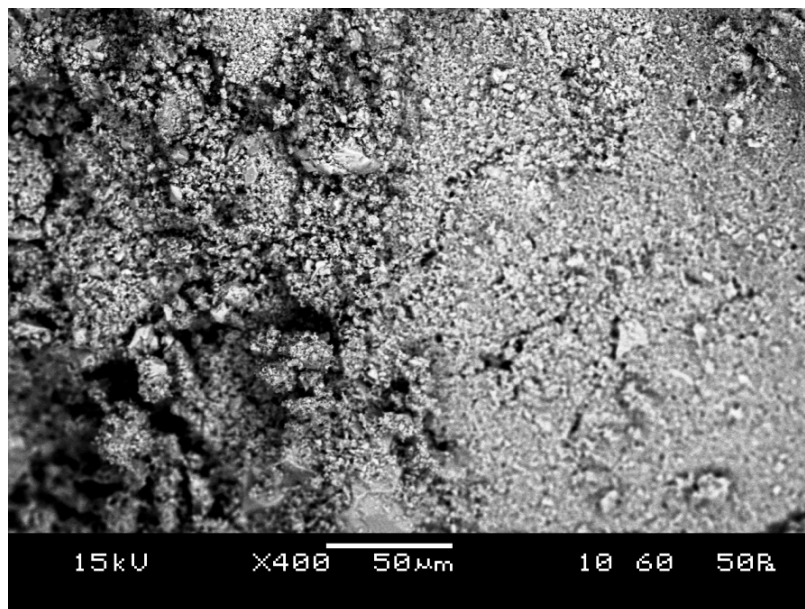


Figure 4.15: Stoke Ground sample at 400x magnification

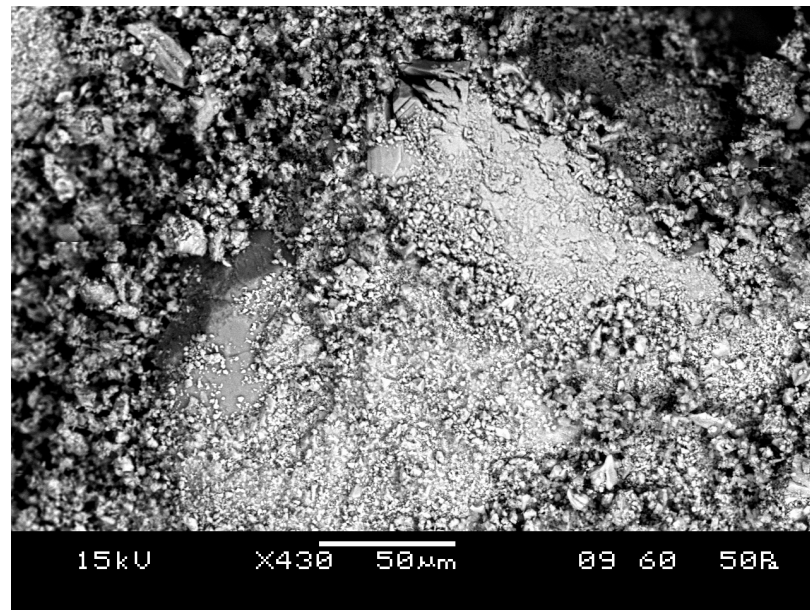


Figure 4.16: Portland sample at 430x magnification

Similar to the Portland aggregate mortar, the Bath stone mortar exhibited widespread areas of calcite crystals on the aggregate surface, which can be seen in Figure 4.17.

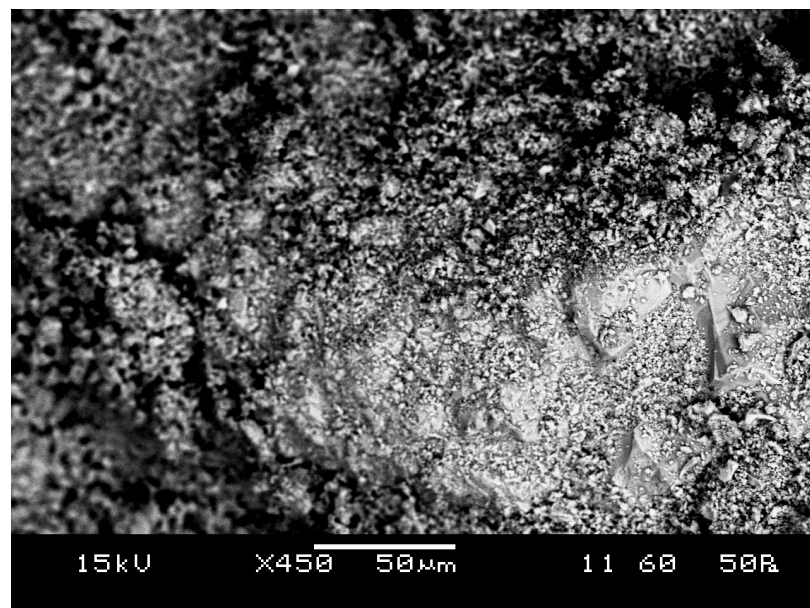


Figure 4.17: Bath stone sample at 450x magnification

4.4 Conclusions

The preliminary testing of the research showed that the relationship between aggregate type and mortar compressive strength is definitely worth exploring further. Without exception, the limestone aggregate mortars were stronger in compression than the Standard sand mortars for all of the different mixes. Preliminary SEM analysis was encouraging; there are definite differences on a micro-structural level between mortars with limestone and silicate aggregate respectively. Phase 2 will build upon these findings, looking at 14, 28, 90, 180 and 360 day flexural/compressive strength testing as well as comparing the samples using SEM, MIP and TGA at a variety of time frames.

After working with the mortar mixes for some time, it was decided that the 13cm flow was not satisfactorily workable, hence for Phase 2 the decision was made to increase the designed flow to 14cm (+/- 0.5cm).

5 Secondary testing phase

A number of changes were made after the preliminary testing phase. Two different particle size distributions were used for each mix; one was the 'Standard' grading previously used, while the other was 'as supplied' limestone dust from the quarry. The dusts used were a by-product of quarrying that would otherwise go to waste, thus reducing the carbon footprint of the mortars. Sieve analysis was undertaken on the dusts to determine particle size distribution for each aggregate. Furthermore, the aggregates were reduced to Ham Hill, Portland, Stoke Ground and Standard sand. This decision was made due to the increased number of mixes required for the 5 different curing periods and additional particle size distribution. This was also why the 1:4 mixes were left out. Aggregates were chosen due to their performance in the preliminary testing phase. Ideally, all aggregates and B/Ag ratios would have been included but there was neither the time nor resources available to achieve this. There is some missing data in this section as a result of some samples disappearing and others being damaged whilst being cured in the conditioning chamber.

5.1 Flexural/compressive strength results

5.1.1 Introduction

Compressive strength testing was a vital component in this research, due to the need to verify the strength differences observed with different aggregates, before exploring possible reasons for this variability. Flexural and compressive strength tests were undertaken on 40x40x160mm specimens.

5.1.2 Specimens with 1:2 B/Ag ratio

Flexural strength testing revealed a variety of differences between the strength profiles of the different mixes over time. Table 5.2 shows the flexural strength results for 1:2 mixes. In Figure 5.1, mixes P-2 a.s and SG-2 a.s show a similar pattern of strength change over time, whereas H-2 a.s is not only weaker, but the lowest strength occurs after 90 days of curing rather than 14. Furthermore, H-2 a.s does not see a strength increase between 14 and 360 days; it is actually almost negligible.

Table 5.1: Flexural strength for 1:2 mixes

Mix	14 days	28 days	90 days	180 days	360 days
Ham Hill (Standard)	-	0.49	-	0.65	0.59
Portland (Standard)	0.56	0.95	-	0.79	-
Stoke Ground (Standard)	0.74	0.71	-	0.76	1.04
Standard sand	0.66	0.77	-	0.69	0.81
Ham Hill (as supplied)	0.61	-	0.53	0.57	0.63
Portland (as supplied)	0.68	-	0.87	0.81	0.9
Stoke Ground (as supplied)	0.66	-	0.95	0.88	0.95

Table 5.2: Compressive strength for 1:2 mixes

Mix	14 days	28 days	90 days	180 days	360 days
Ham Hill (Standard)	1.31	1.13	-	1.7	1.21
Portland (Standard)	0.97	1.44	2.2	2.35	-
Stoke Ground (Standard)	1.01	1.46	2.09	2.71	2.19
Standard sand	0.59	0.94	1.21	2.07	1.67
Ham Hill (as supplied)	1.17	1.14	1.58	1.44	1.57
Portland (as supplied)	0.91	1.63	2.34	2.16	1.9
Stoke Ground (as supplied)	0.92	1.78	2.63	2.11	2.37

In Figure 5.2, SG-2 shows the greatest strength increase occurring between 180 and 360 days, which suggests that it is this period that has seen the greatest increase in carbonation, however evidence from the phenolphthalein indicator disagrees as the average depth does not increase at the same rate. Mix SS-2 exhibits only a small change in average flexural strength between 14 and 360 days, starting at $0.41N/mm^2$ and rising to $0.52N/mm^2$.

The compressive strength results show similar trends to the equivalent flexural strengths. In Figure 5.3, it is evident that Ham Hill mortars also exhibit the lowest average strengths at 90, 180 and 360 days, for the 1:2 'as supplied' mix. It is worth noting that H-2 had the highest water content in relation to binder, which may lead to lower strengths. Additionally, the strength gain of Ham Hill mortars after 90 days is negligible.

Both the Standard sand and Stoke Ground mortars have a linear strength increase between 14 and 180 days curing (Figure 5.4), after which the former has only a slight increase at 360 days,

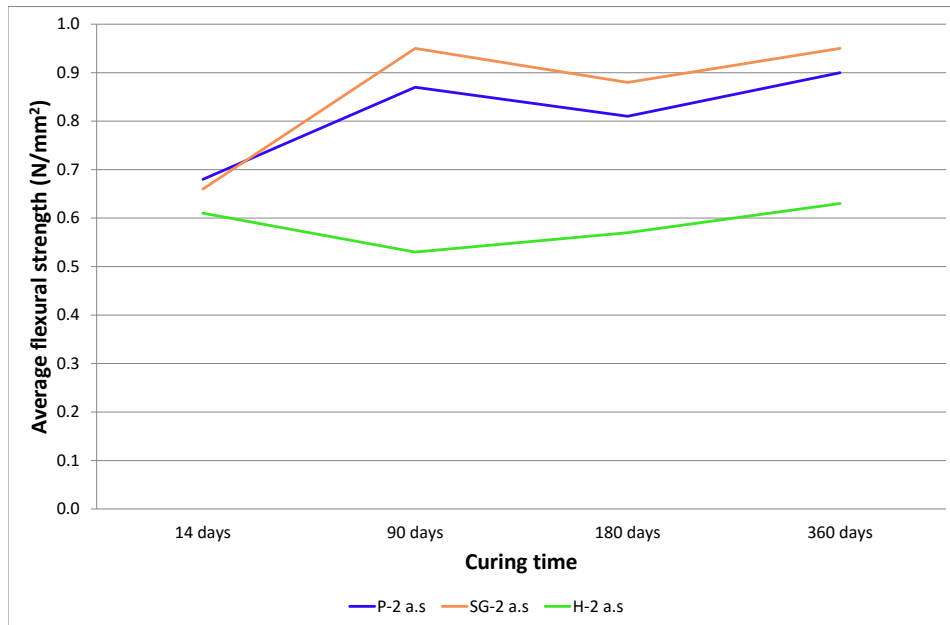


Figure 5.1: Average flexural strength for 1-2 'as supplied' samples

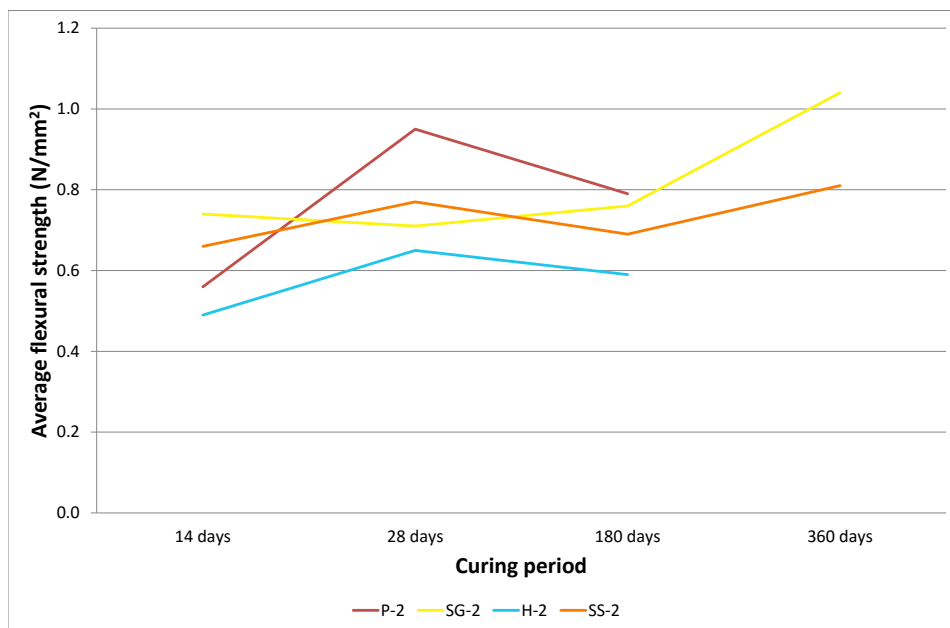


Figure 5.2: Average flexural strength for 1-2 'standard' samples

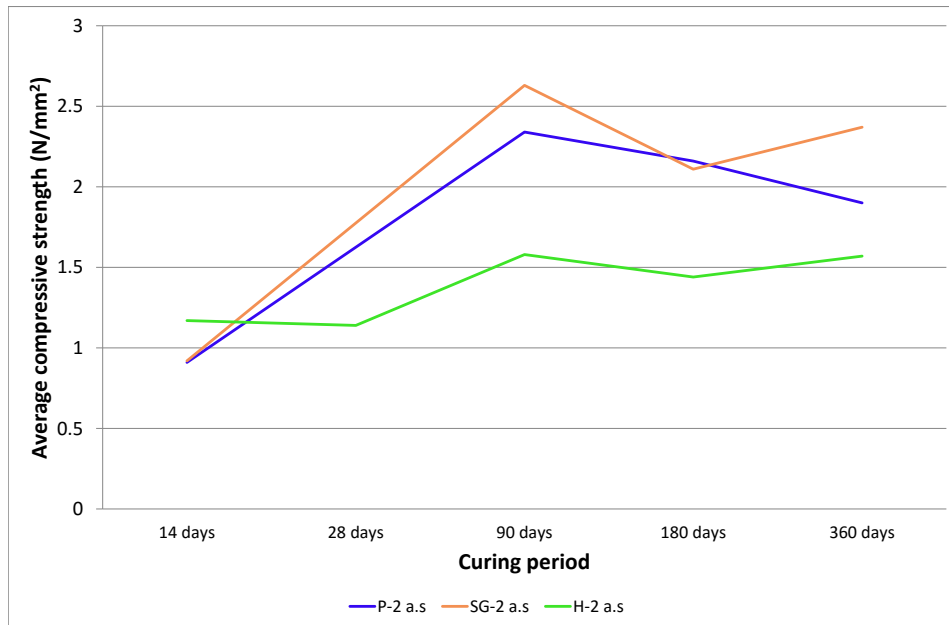


Figure 5.3: Average compressive strength for 1-2 'as supplied' samples

whereas the latter has a significant decrease in average strength (0.52MPa).

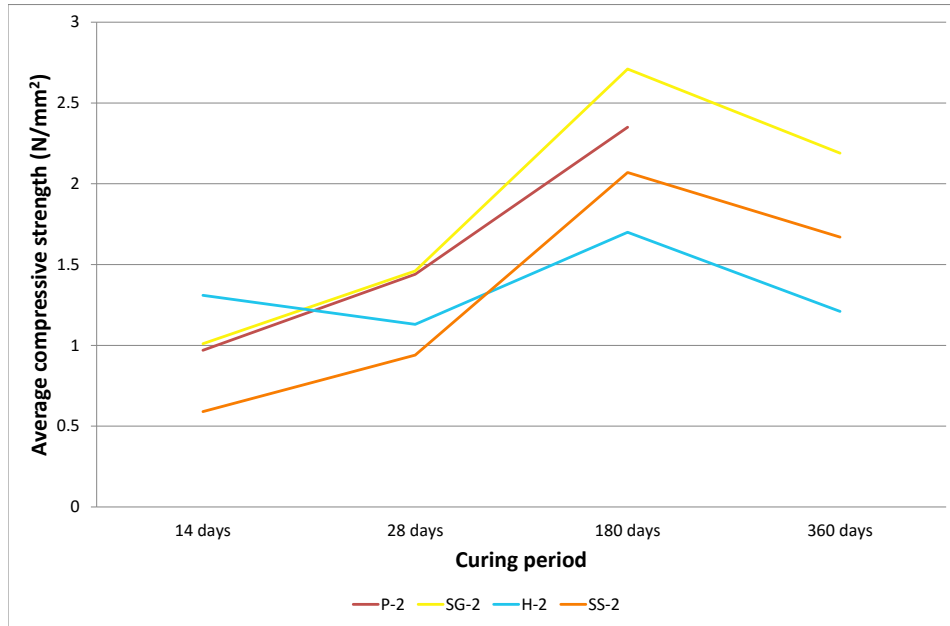


Figure 5.4: Average compressive strength for 1-2 'standard' samples

5.1.3 Specimens with 1:3 B/Ag ratio

For the 1:3 'as supplied' samples, and the 1:3 Standard sand mortar, the different mixes vary significantly in their flexural strength results. In Figure 5.5, it can be seen that Portland and Stoke Ground mortars both have a linear increase up to 180 days curing, respectively, although Stoke Ground mortar is around 0.2MPa stronger than Portland mortar at both 28 and 90 days and subsequently having the same strength at 180 days. Portland mortar has a slight increase from this at 360 days curing, while Stoke Ground mortar is slightly weaker at 360 days than its 180 day equivalent.

Ham Hill mortars have a fluctuating flexural strength between 14 and 360 days.

The Standard sand mortars only show a small variation in average strength (about 0.1MPa) between 14 and 360 days. Given that the carbonation depth increases significantly over this time, the results suggest that flexural strength does not relate to carbonation depth for Standard sand mortars with this mix design.

Without exception, the average strengths of the samples in Figure 5.6 decrease after 90 days of curing. This decrease is the least noticeable with the Standard sand mortars, with the greatest decline in strength observed with Stoke Ground between 90 and 180 days curing.

Table 5.3: Flexural strength for 1:3 mixes

Mix	14 days	28 days	90 days	180 days	360 days
Ham Hill (Standard)	-	0.44	-	-	-
Portland (Standard)	-	0.50	-	0.90	-
Stoke Ground (Standard)	-	0.61	-	-	-
Standard sand	0.41	0.46	0.45	0.48	0.52
Ham Hill (as supplied)	0.59	0.45	0.64	0.60	0.49
Portland (as supplied)	-	0.52	0.62	0.88	0.91
Stoke Ground (as supplied)	0.63	0.70	0.78	0.88	0.95

Table 5.4: Compressive strength for 1:3 mixes

Mix	14 days	28 days	90 days	180 days	360 days
Ham Hill (Standard)	0.76	0.98	-	-	-
Portland (Standard)	0.96	1.11	-	1.68	-
Stoke Ground (Standard)	0.77	1.38	-	-	-
Standard sand	0.57	0.76	1.32	1.64	1.23
Ham Hill (as supplied)	1.26	0.96	2.11	1.51	1.12
Portland (as supplied)	-	1.07	1.91	1.67	1.64
Stoke Ground (as supplied)	1.48	1.42	2.3	2.07	1.95

Analysing the strengths of different mixes at a given curing period has given an insight into the effect of different aggregates on mortar strength. In Figure 5.7 it can be seen that SG-2 has the highest flexural strength, while P-2 is the weakest. It is interesting to note that SS-2 falls in the middle of the limestone aggregate mixes; the aggregate properties are quite different.

Figure 5.8 shows 'as supplied' mixes after 14 days curing. In contrast to the 1:2 'standard' mixes, Standard sand mortar is weaker than both Ham Hill and Stoke Ground mortars.

From Figure 5.9, it can be seen that the Standard sand mix is once again not exhibiting the lowest strength. From the 14 and 28 day results of all the mixes, it appears that Standard sand mortars perform better flexurally with a 1:2 B/Ag ratio.

After 28 days, Stoke Ground is again the highest performing mortar, for both particle size distributions (Figure 5.10).

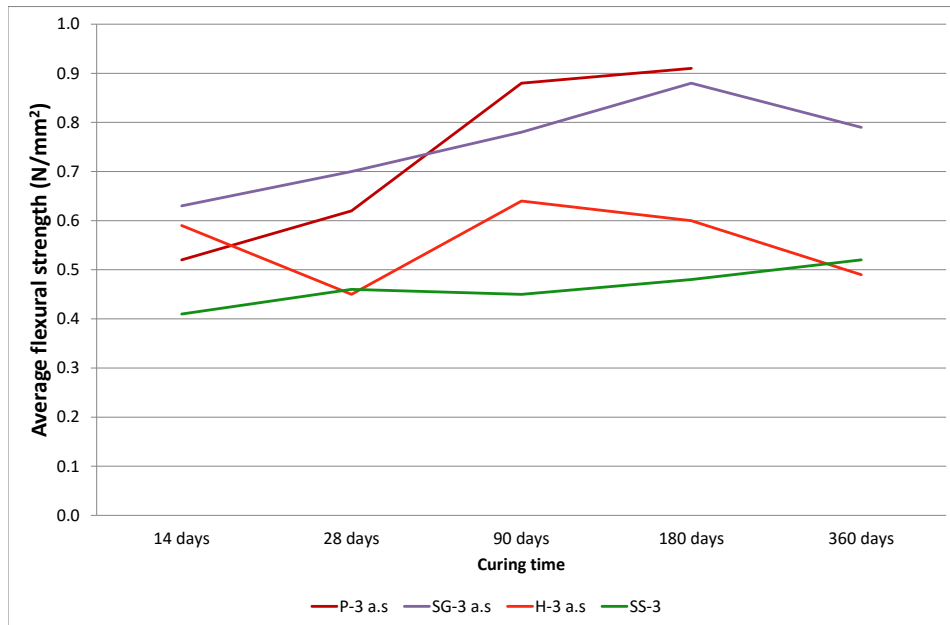


Figure 5.5: Average flexural strength for 1-3 'as supplied' samples

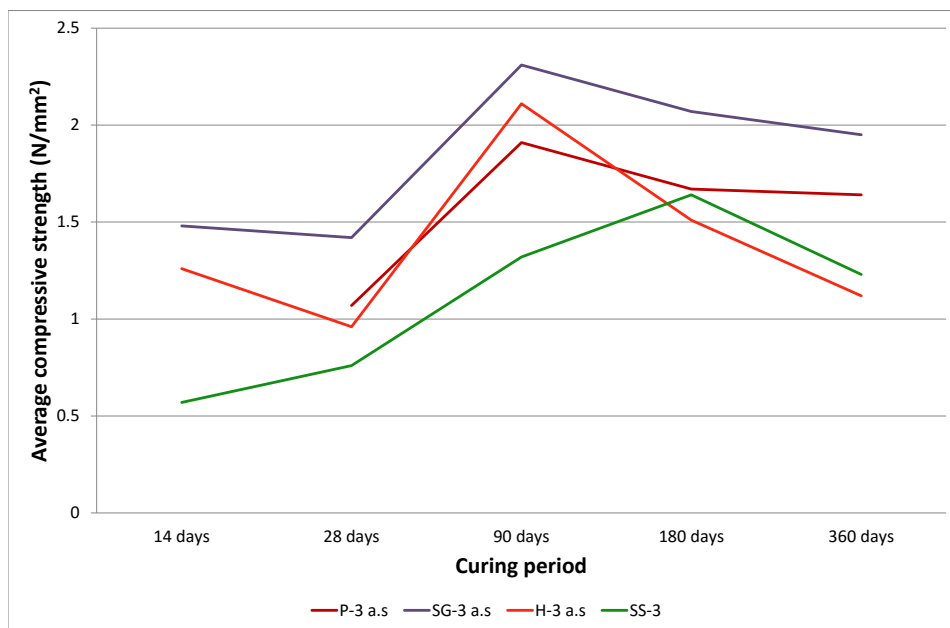


Figure 5.6: Average compressive strength for 1-3 'as supplied' samples

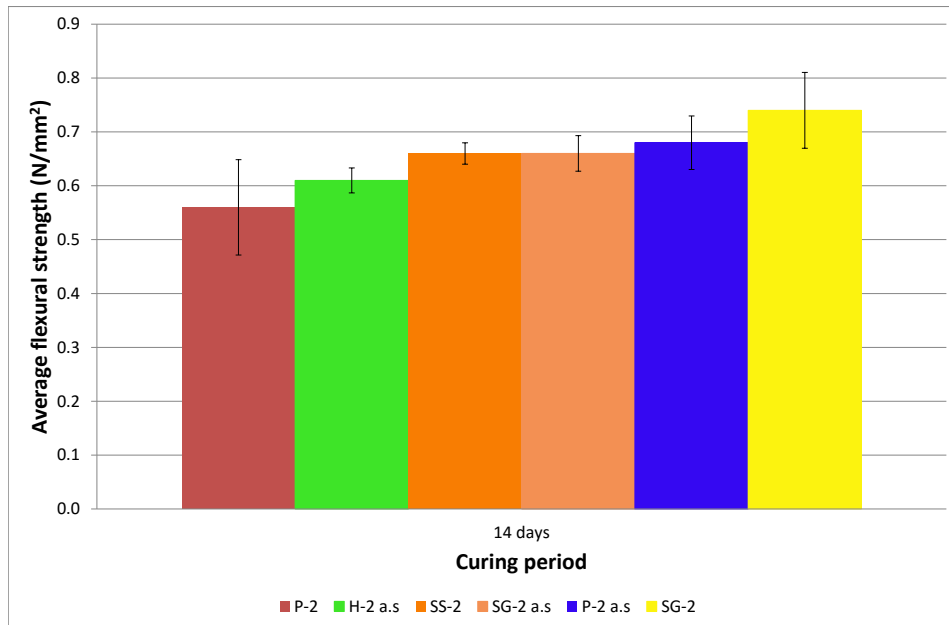


Figure 5.7: Average flexural strength at 14 days for 1:2 mixes

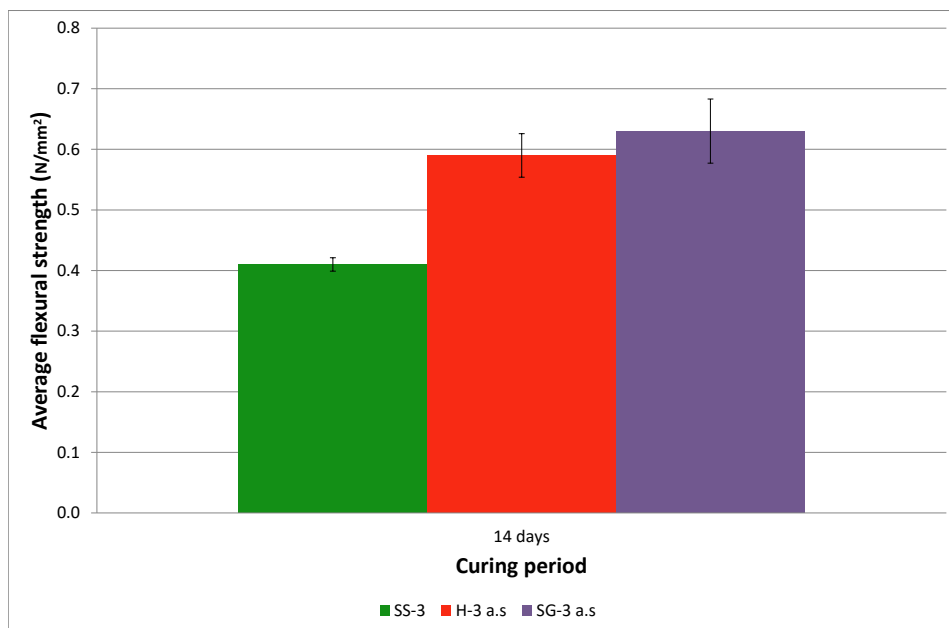


Figure 5.8: Average flexural strength at 14 days for 1:3 mixes

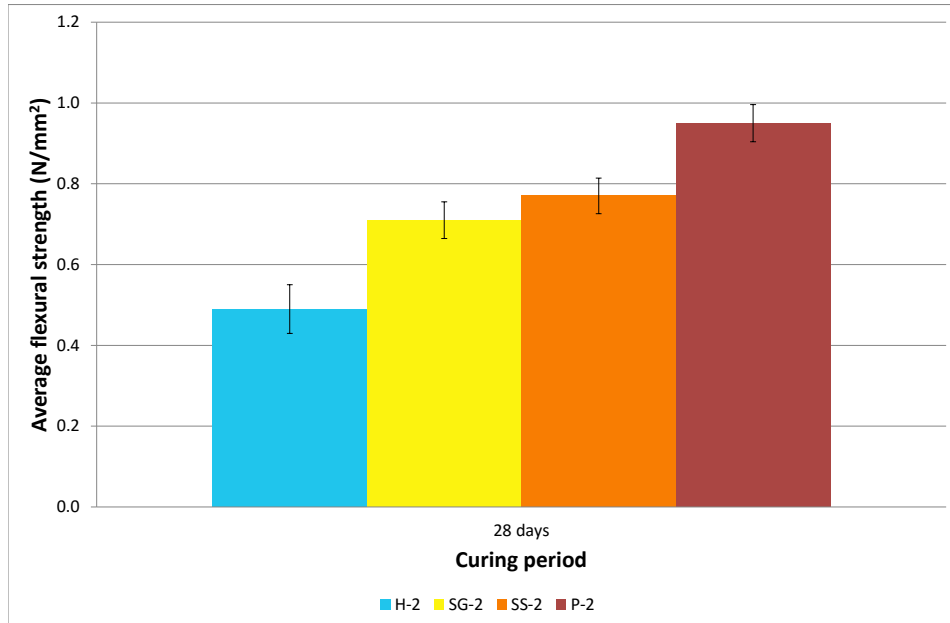


Figure 5.9: Average flexural strength at 28 days for 1:2 mixes

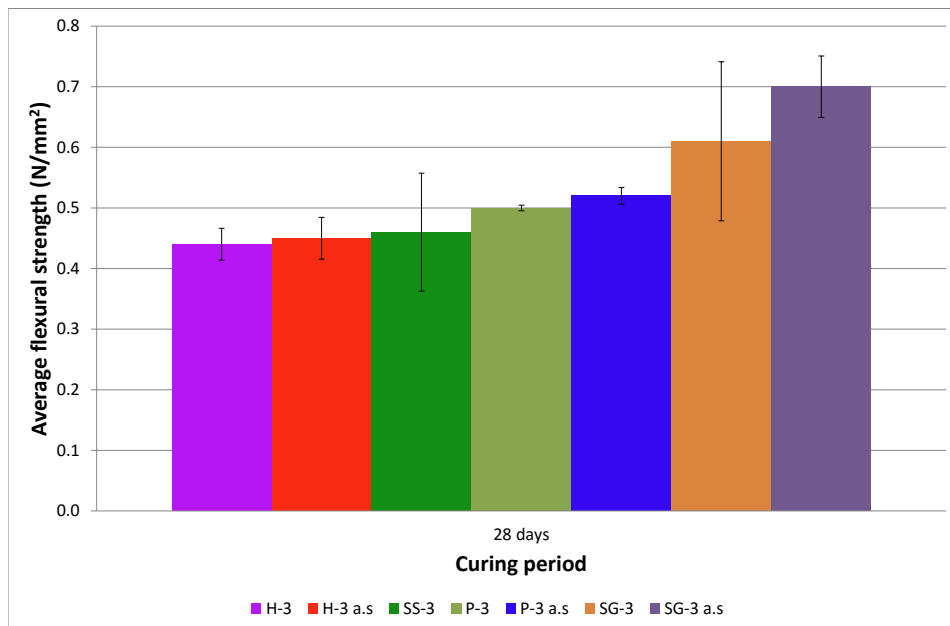


Figure 5.10: Average flexural strength at 28 days for 1:3 mixes

This trend also continues after 90 days curing (Figure 5.11), with Standard sand having the lowest flexural strength.

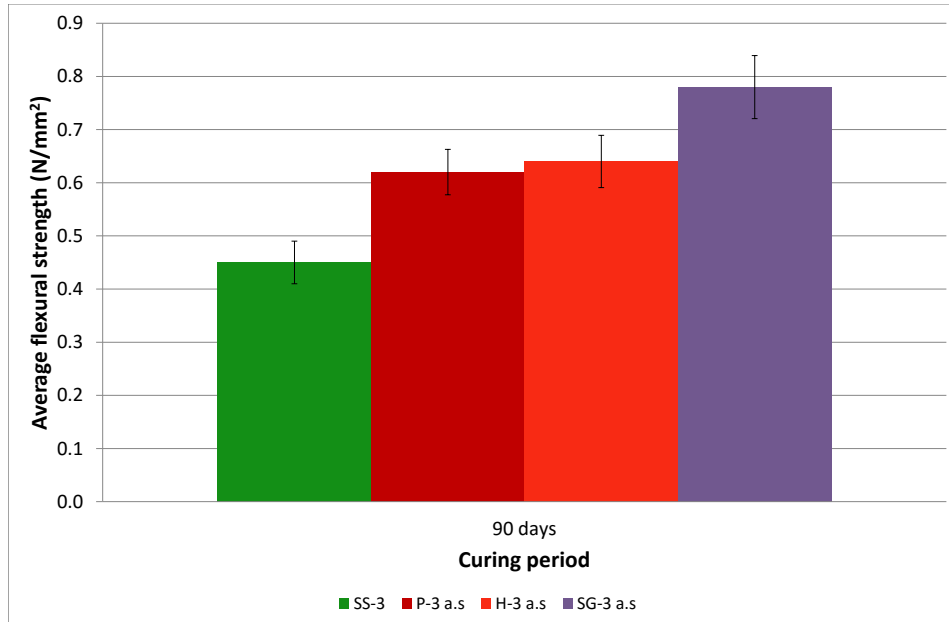


Figure 5.11: Average flexural strength at 90 days for 1:3 mixes

After 180 days Ham Hill mortars with 1:2 grading exhibited the lowest strength, followed by Standard sand. This can be seen in Figure 5.12, which also shows that the Stoke Ground with 'Standard' grading had dropped to the middle of the mixes. It is worth noting that there is not a huge difference in the average value between that and the 'as supplied' mix (around $0.15N/mm^2$).

Figure 5.13 displays the 1:3 mixes at 180 days, where it is clear that several of the mixes have equalled in strength. Ham Hill and Standard sand mortars still do not perform well, which is a common theme.

At 360 days, it is clear that Portland and Stoke Ground mortars consistently produce stronger mortars (Figures 5.14-5.15), and that Ham Hill and Standard sand produce mortars with lower flexural strength.

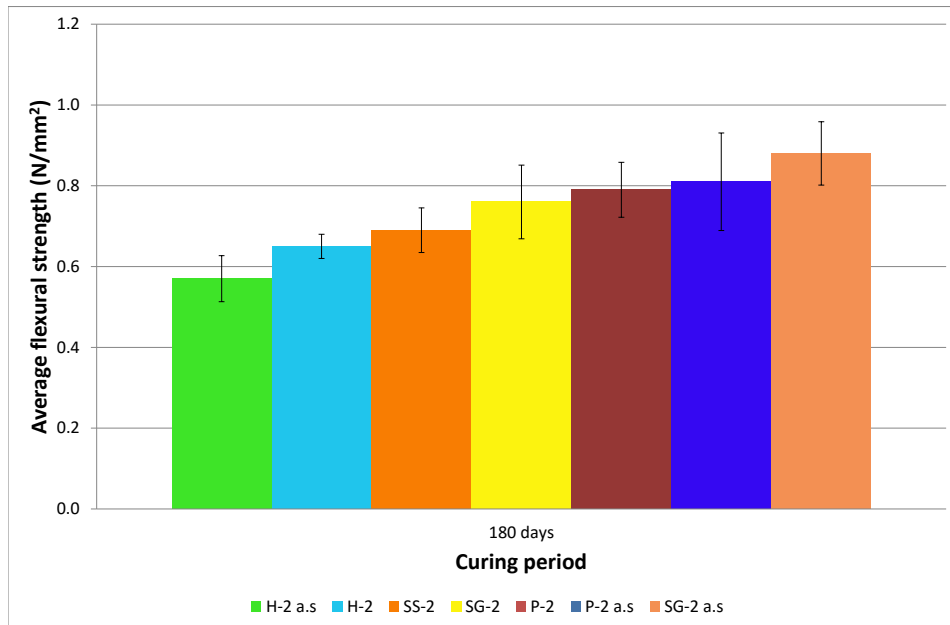


Figure 5.12: Average flexural strength at 180 days for 1:2 mixes

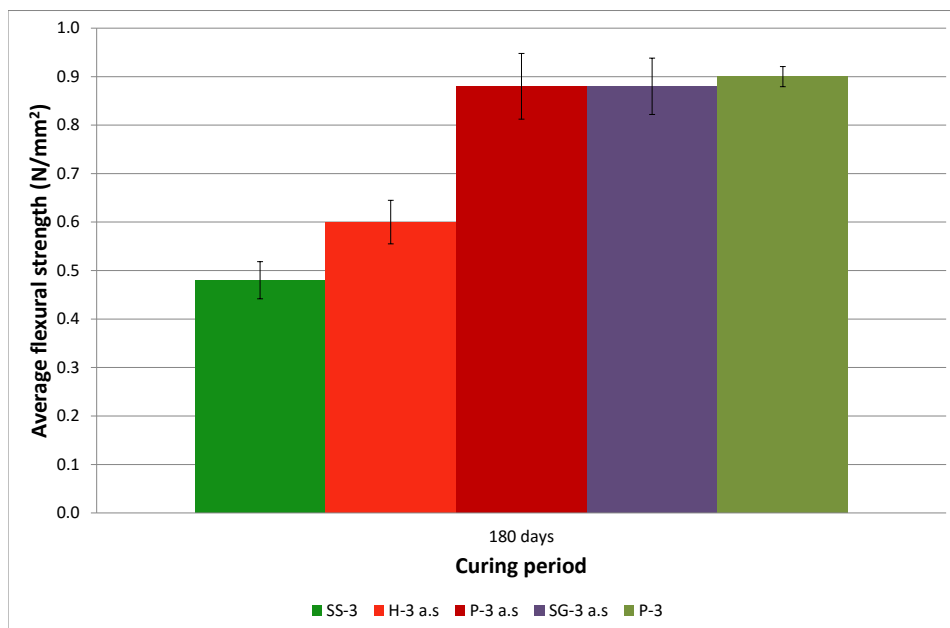


Figure 5.13: Average flexural strength at 180 days for 1:3 mixes

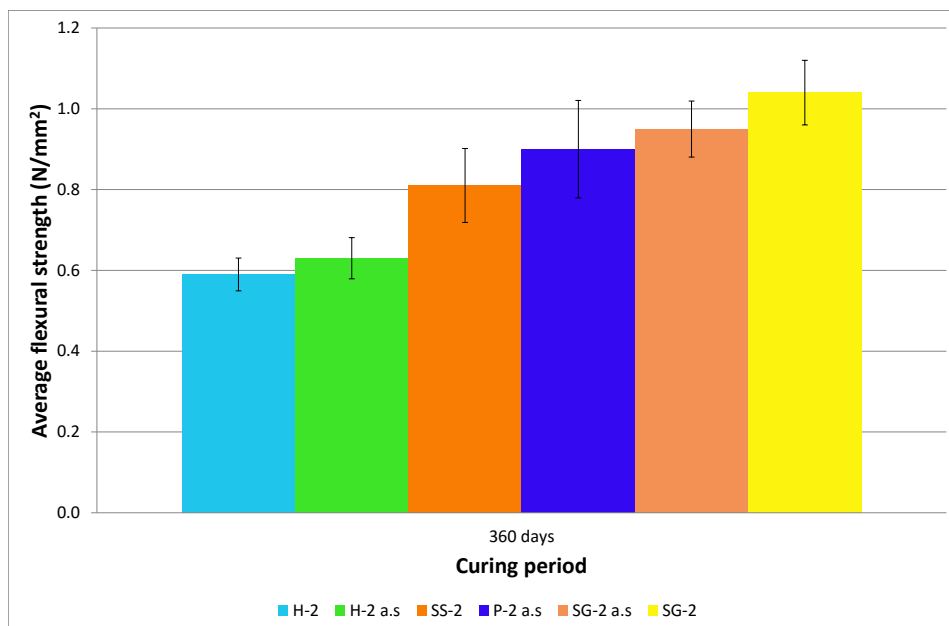


Figure 5.14: Average flexural strength at 360 days for 1:2 mixes

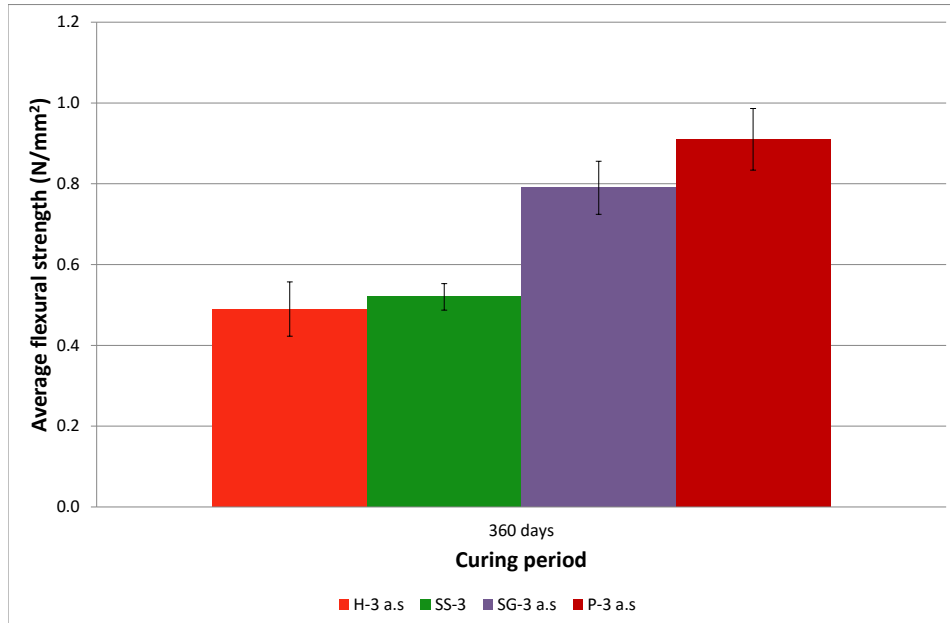


Figure 5.15: Average flexural strength at 360 days for 1:3 mixes

It is clear from Figure 5.16 that the Standard sand mortar is the weakest of all the 1:2 mixes at 14 days curing. There are a number of possible reasons, including slower rate of carbonation, possibility of internal cracking, and poor binder/aggregate bond.

Ham Hill mortar (H-2) with 'standard' grading was found to be strongest at this early stage, more than double the strength of Standard sand (SS-2), closely followed by H-2 a.s. P-2 a.s, SG-2 a.s, P-2 and SG-2 show little variation in compressive strength.

As with the 1:2 mixes, Standard sand mortar is also weaker with the 1:3 mixes, as in Figure 5.17. Interestingly, Ham Hill mortars have not shown as high strengths as with the 1:2 mixes. H-3 a.s has a high margin of error, although the original data show that there is just one anomalous value of 0.71MPa . If this were removed, the average compressive strength then increases to 1.36MPa . H-3 has significantly lower strength than all the other Ham Hill mixes at 14 days.

The results in Figure 5.17 do not agree with the notion that high water content negatively impacts strength. H-3 a.s has the highest water content and yet is the second strongest mix with 1:3 B/Ag. Additionally, SG-3 has significantly lower strength than SG-3 a.s despite having the lowest water content of the limestone aggregate mortars. SS-3 has the lowest water content of all the mixes, as well as the lowest strength.

Figure 5.18 shows 1:2 mixes at 28 days; SG-2 and P-2 again show similar compressive strengths. H-2 and H-2 a.s also have similar values but have not seen a strength increase since the 14 day

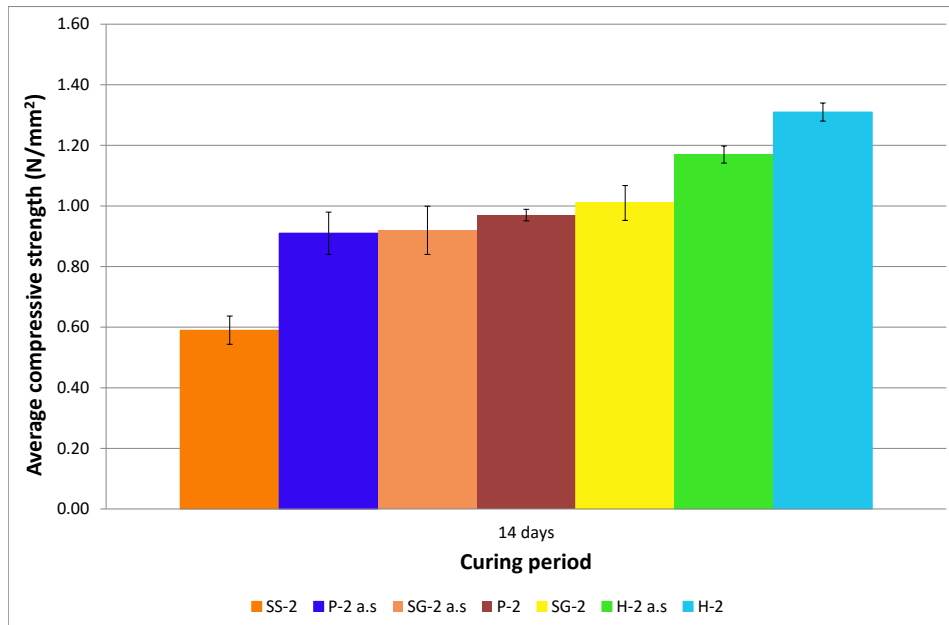


Figure 5.16: Average compressive strength at 14 days for 1:2 mixes

testing.

With the 1:3 mixes, both of the Stoke Ground samples have a greater compressive strength than the other mortars; each are around 1.4MPa. The Stoke Ground sample (SS-2) was still weakest although had a similar value to the Ham Hill samples.

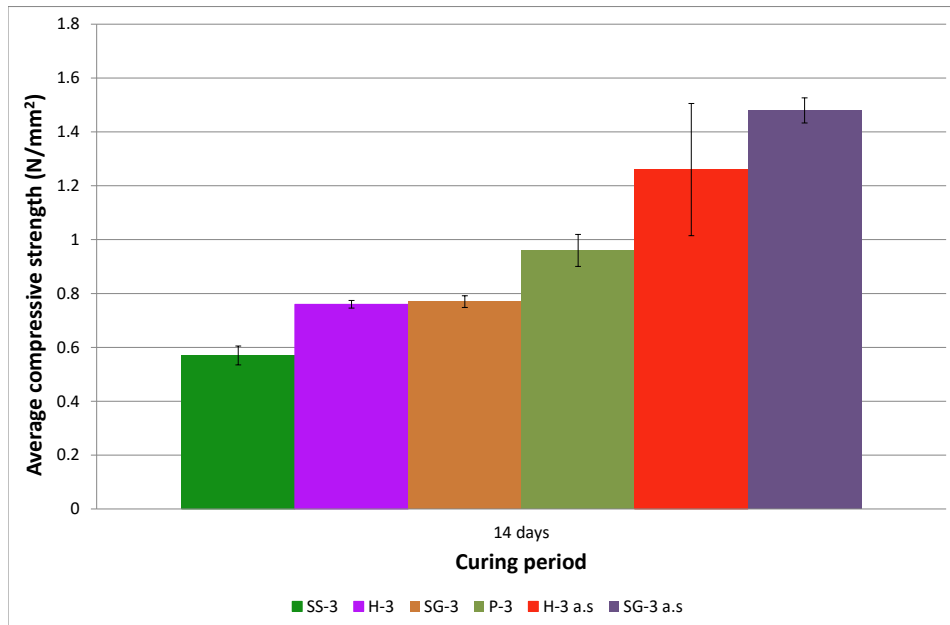


Figure 5.17: Average compressive strength at 14 days for 1:3 mixes

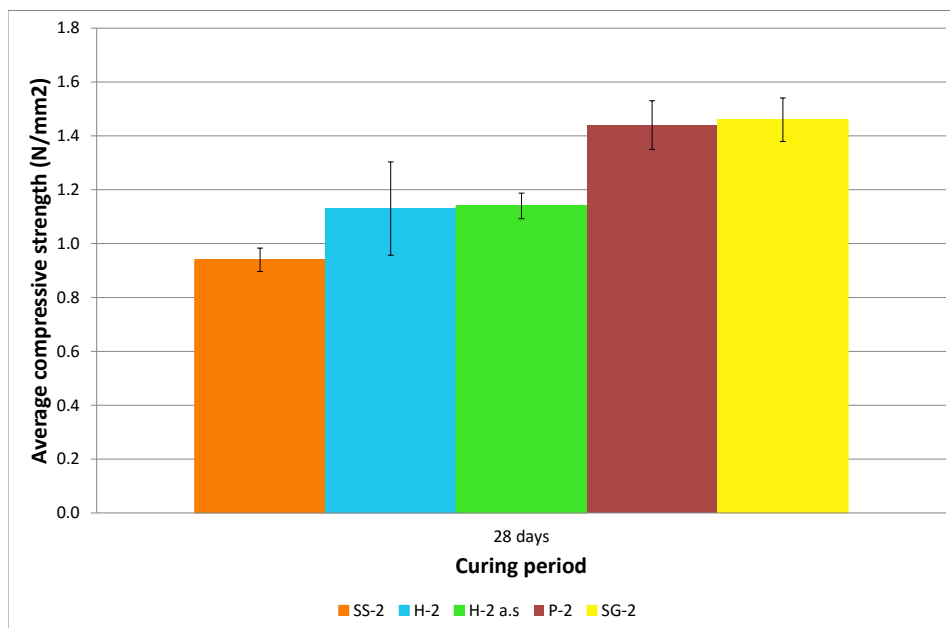


Figure 5.18: Average compressive strength at 28 days for 1:2 mixes

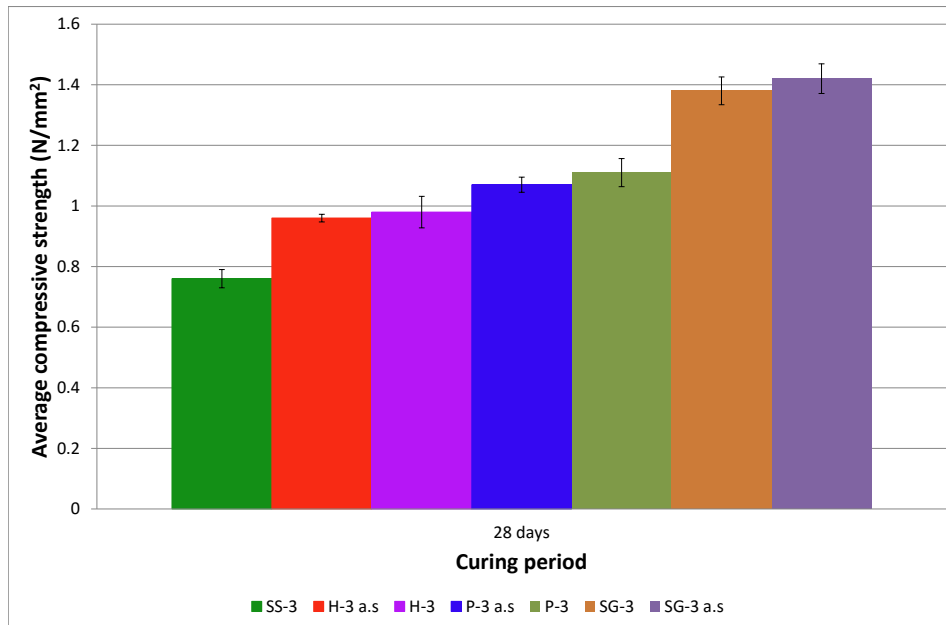


Figure 5.19: Average compressive strength at 28 days for 1:3 mixes

After 90 days of curing, it was still the Stoke Ground 'as supplied' samples that proved to have the highest compressive strengths for both 1:2 and 1:3 mixes (see Figures 5.20-5.21). Standard sand mortars were still weaker than all of the limestone aggregate mortars.

Interestingly, after 180 days curing, the Standard sand mortars were no longer the weakest for either the 1:2 or 1:3 mixes. In Figure 5.22 it can be seen that SS-2 has a compressive strength of around $2MPa$, while H-2 and H-2 a.s have strengths around $1.7MPa$ and $1.4MPa$ respectively. It is possible that the Ham Hill mortars have not seen a strength gain between 90 and 180 days due to having already fully carbonated (according to interpretation of phenolphthalein staining), although this is also true of most of the other samples. Stoke Ground and Portland samples continue to exhibit the highest compressive strength values.

For the 1:3 mixes in Figure 5.23, SG-3 a.s is once again the strongest mix. Both of the Portland aggregate mixes, the Standard sand mix and the Ham Hill mix show only a small difference in strength; all are around $1.5 - 1.6MPa$, while the Stoke Ground mix is around $2MPa$. The 1:3 mixes have lower compressive strengths than the 1:2 mixes in Figure 5.22 (aside from Ham Hill 'as supplied' which is similar).

By 360 days, Ham Hill mortars are still showing the lowest compressive strength values for the 1:2 mixes (see Figure 5.24), although H-2 a.s is only slightly weaker than SS-2. Upon analysis of the images in Figure 3.9, it is unlikely that this lower strength is down to the binder/aggregate bond, as the aggregate surface looks similar to that of the Stoke Ground aggregate. It is possible

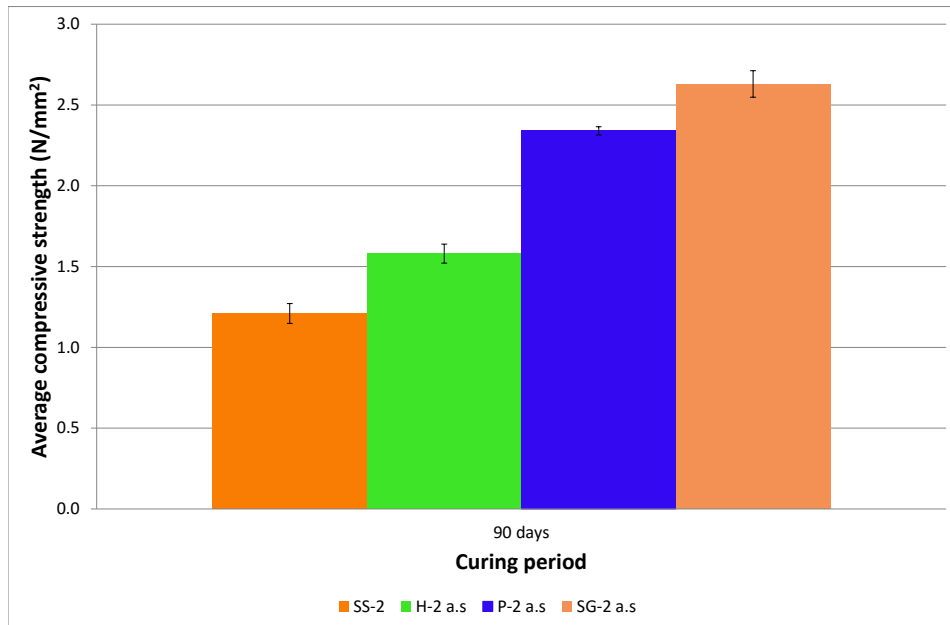


Figure 5.20: Average compressive strength at 90 days for 1:2 mixes

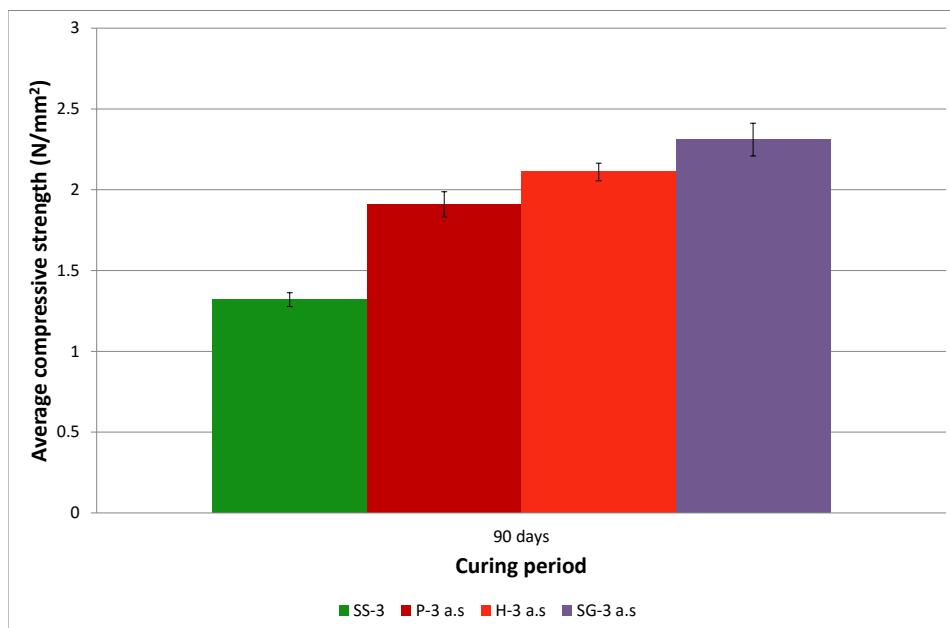


Figure 5.21: Average compressive strength at 90 days for 1:3 mixes

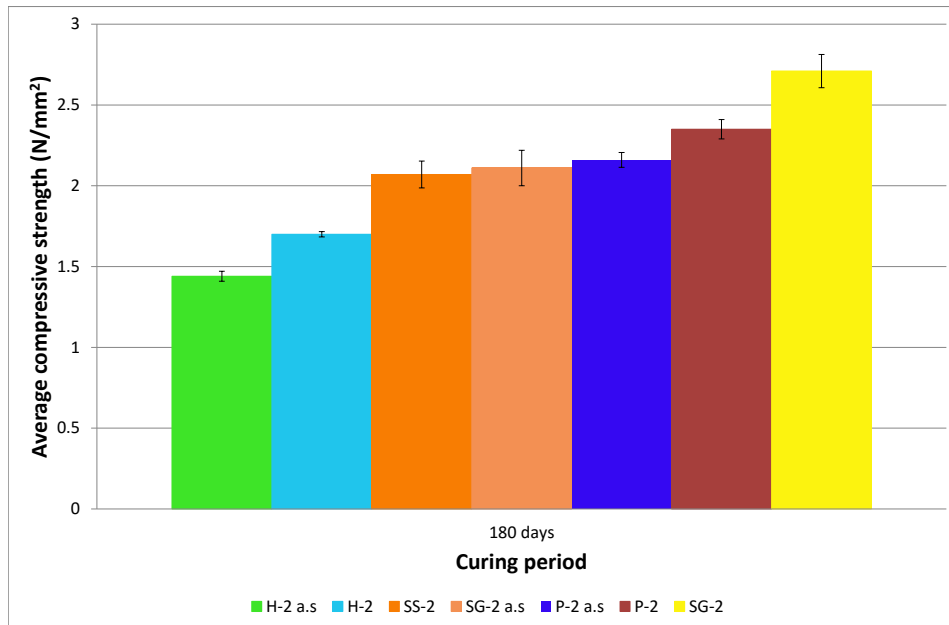


Figure 5.22: Average compressive strength at 180 days for 1:2 mixes

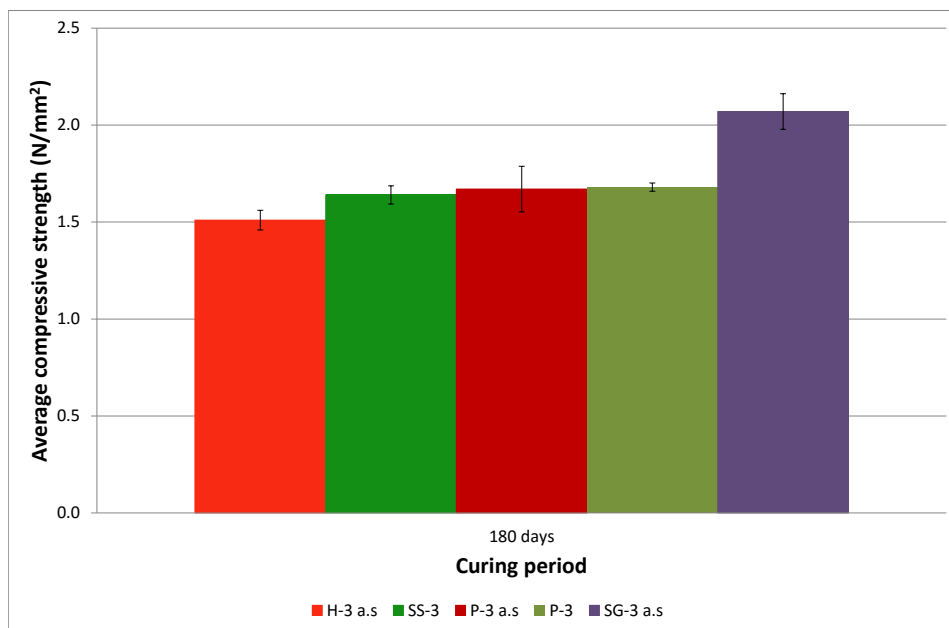


Figure 5.23: Average compressive strength at 180 days for 1:3 mixes

that the aggregate itself has a lower compressive strength than the other aggregates.

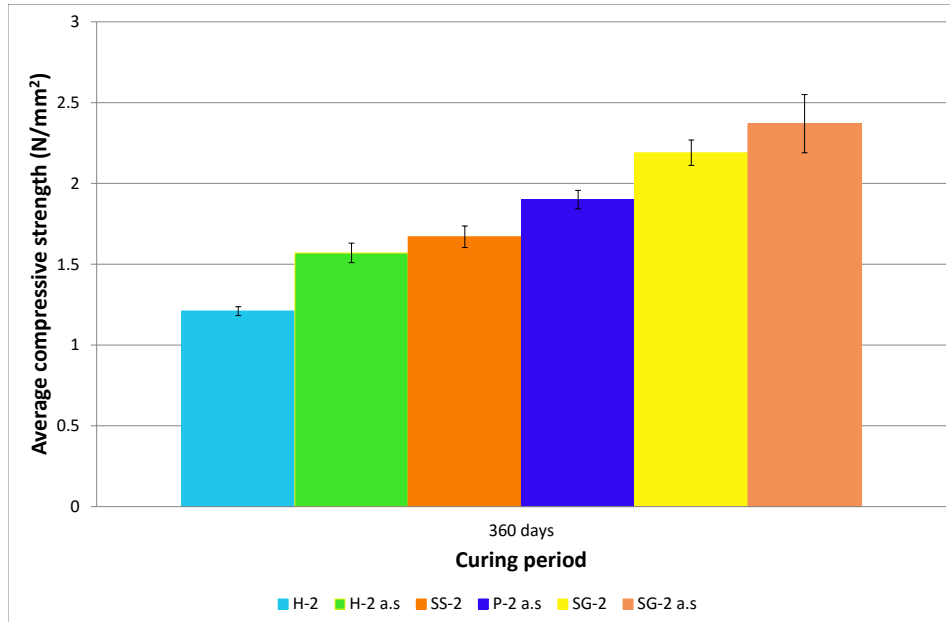


Figure 5.24: Average compressive strength at 360 days for 1:2 mixes

SG-3 a.s is still showing the highest compressive strength in Figure 5.25, although there is no strength increase from 180 days, as with other samples. H-3 a.s and SS-3 are almost half the strength of SG-3 a.s; for SS-3, the binder/aggregate bond is thought to be the most likely cause, but for H-3 a.s, it is possible that the mechanical strength of the aggregate is to blame.

5.1.4 Chemical indicators

Use of a chemical indicator is one method of establishing the depth of carbonation in a mortar sample. Once flexural strength testing has been undertaken, the fractured surface of the mortar is ideal for spraying phenolphthalein onto, in order to determine areas of $Ca(OH)_2$ and $CaCO_3$. Once the pH of a sample is above 8.3, it will become stained pink, becoming gradually darker as pH increases.

The average depth of carbonation for each of the mixes is shown in Table 5.5.

Figure 5.26 demonstrates how the depth of carbonation changes between the first test period after curing for 14 days, and the last test period after curing for 360 days. The mix is 'fully' carbonated somewhere between 90 and 360 days of curing in the climate controlled chamber. The centre image after 90 days of curing exhibits the phenomenon entitled 'Liesegang ring'.

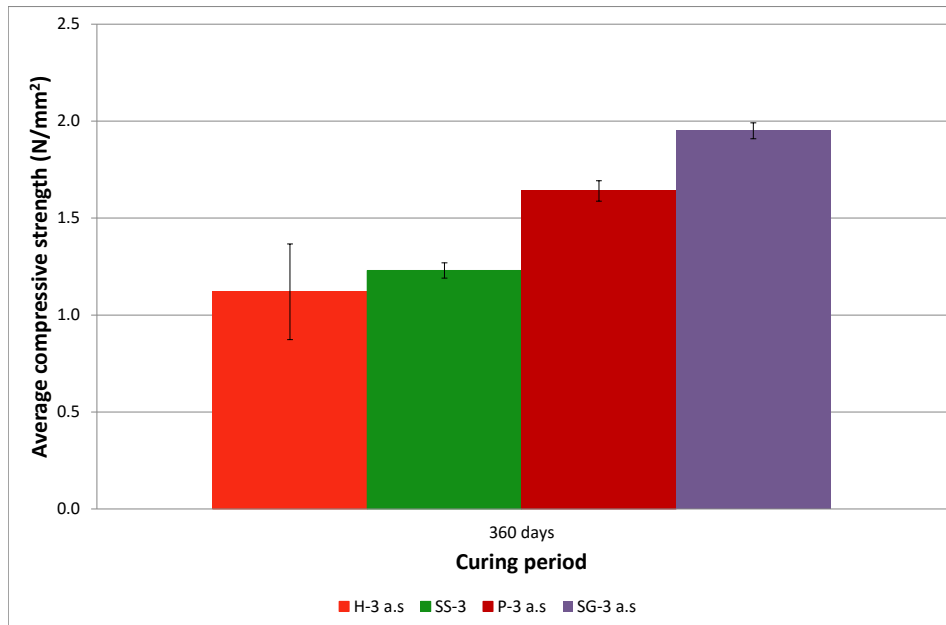


Figure 5.25: Average compressive strength at 360 days for 1:3 mixes

Table 5.5: Average depth of carbonation (mm)

Aggregate	Mix	14 days	28 days	90 days	180 days	360 days
Ham Hill	1:2 a.s	2.6	-	17.3	20	20
	1:2	-	7.2	-	20	20
	1:3 a.s	2	6.9	12.3	20	20
	1:3	-	-	-	-	-
Portland	1:2 a.s	2.2	-	20	20	-
	1:2	-	5.1	-	20	20
	1:3 a.s	-	8.3	12.8	20	20
	1:3	-	10.8	-	-	-
Stoke Ground	1:2 a.s	2.8	-	14.3 (Liesegang)	20	20
	1:2	-	6.4	-	20	20
	1:3 a.s	1.7	10.5	20 (Liesegang)	20	20
	1:3	-	7.1	-	20	20
Standard	1:2	-	5.5	-	20	20
	1:3	2.1	5.9	12.3	20	20

The centre of the sample appears to be carbonated, as there is no pink staining from the phenolphthalein indicator, however a pink ring is visible.

Carbonation in the Standard sand mortars (1:3 mix) took longer to penetrate the full depth of the sample. Figure 5.27 shows 14, 28 and 90 days of curing respectively, and it can be seen that a substantial amount of the sample remains uncarbonated after 90 days, in contrast to the Stoke Ground sample at the same time. The average depth of carbonation of SS-3 after 90 days

is 12.3mm, whereas SG-3 a.s had carbonated to the centre of the sample, but with a Liesegang ring. It is possible that the difference in porosity of the samples has led to CO_2 penetrating the sample at a different rate.



Figure 5.26: SG-3 'as supplied' mortars (left to right) 14, 28, 90, 180 and 360 days curing



Figure 5.27: SS-3 'standard' mortars (left to right) 14, 28, 90, 180 and 360 days curing

5.1.5 TGA analysis

TGA results on a selection of samples have revealed a number of things. In Figure 5.28, a comparison of mortars made with Ham Hill, Portland and Standard sand respectively can be seen, all at 28 days of curing and with a 1:3 B/Ag ratio and 'standard' grading. Whilst all of the mortars show a mass loss between $600 - 800^{\circ}C$, the quantity of $CaCO_3$ that was lost differs slightly. As expected SS28-3 has the smallest mass loss; since the aggregate used is SiO_2 rather than $CaCO_3$, only a quarter of the dry mix constituents by volume (the binder) could have been converted to $CaCO_3$. Naturally, the limestone aggregate samples have significantly more $CaCO_3$ to begin with, therefore have more to lose.

With regard to the Ham Hill and Portland mortars, the differences exhibited between the two may be as a result of either the aggregate density or initial water content of the mix.

Figure 5.29 shows 1:3 samples with 'as supplied' grading, as well as SS28-3 with 'standard' grading, all at 28 days curing. It is immediately apparent that the Ham Hill mix (H28-3 a.s) displays some differences to the 'standard' graded mix (H28-3) in Figure 5.28. It is evident in Figure 5.29 that in addition to having a mass loss between $600 - 800^{\circ}C$, there are four other 'peaks' indicating mass loss between $300 - 450^{\circ}C$. At that temperature range, mass loss occurs due to the breakdown of $Ca(OH)_2$, suggesting that despite appearing fully carbonated, the sample was in fact not. H28-3 a.s also had the smallest mass loss out of the limestone aggregate mortars; if not all of the $Ca(OH)_2$ was fully carbonated then this stands to reason.

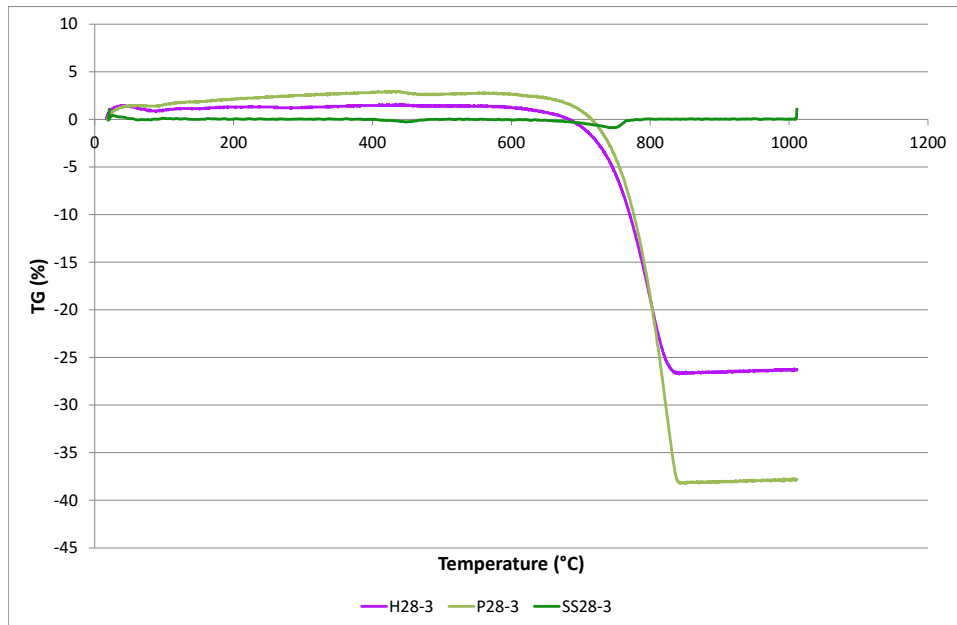


Figure 5.28: TG curve for H28-3, P28-3, SS28-3 - samples taken from the carbonated edge of the prism

P28-3 a.s ad SG28-3 a.s show very similar curve, with just a slight variation in temperature, suggesting that the aggregates have a similar impact on the mortar mix. Despite having a different particle size distribution, SS28-3 follows a very similar curve, but with a smaller mass loss, between a third and a fifth of the losses observed in the limestone aggregate mortars. This is most likely due to the lack of carbonate aggregate, meaning less $CaCO_3$ to begin with.

After 180 days of curing, Portland and Stoke Ground aggregate had an almost identical TG curve for 1:2 mixes with 'as supplied' grading (see Figure 5.30), implying that there was the same proportion of $CaCO_3$ prior to heating the samples. Again, SS180-2 follows a similar trend, despite having a different particle size distribution; however, mass loss is only a fifth of the mass loss seen in the other samples.

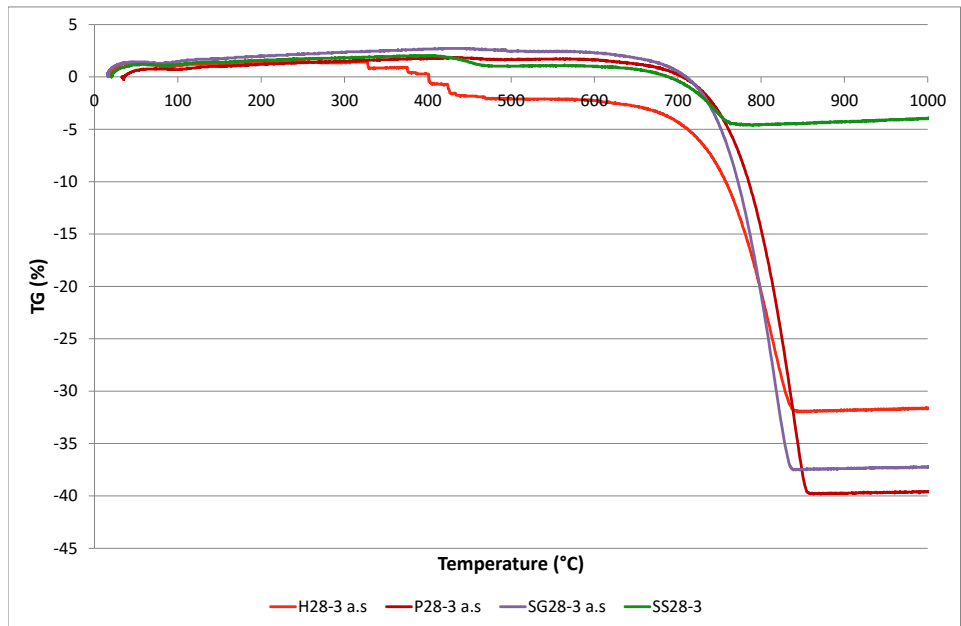


Figure 5.29: TG curve for H28-3 a.s, P28-3 a.s, SG28-3 a.s, SS28-3 - samples taken from the carbonated edge of the prism

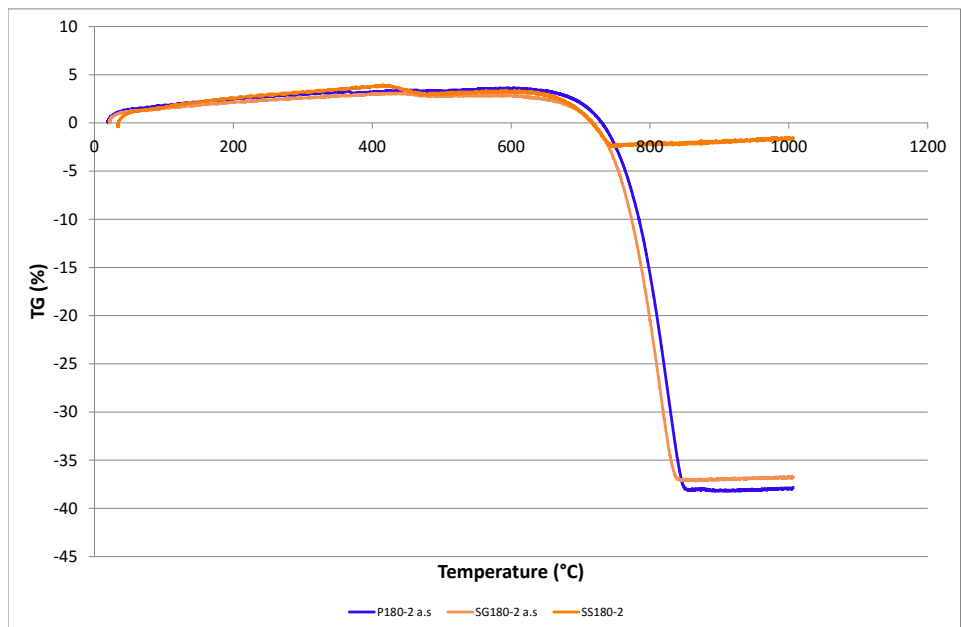


Figure 5.30: TG curve for P180-2 a.s, SG180-2 a.s, SS180-2 - samples taken from the carbonated edge of the prism

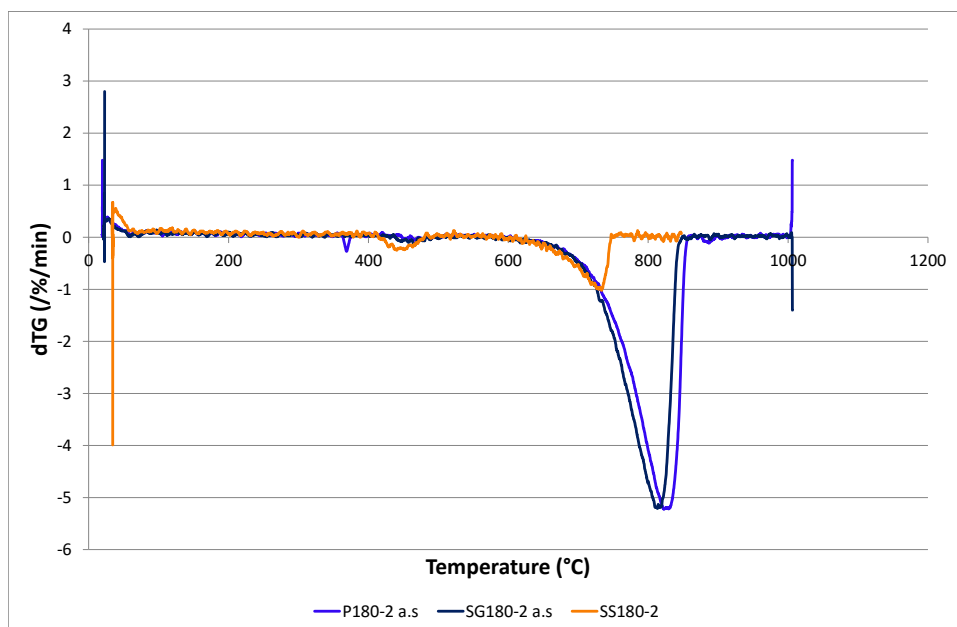


Figure 5.31: Temperature versus dTG for - samples were taken from the carbonated edge of the prism

5.2 Pore structure

5.2.1 MIP

One of the contributing factors to a mortar's strength is pore structure. Therefore, the results from the MIP analysis provide a much needed insight into the mechanisms governing strength differences due to aggregate type. Some of the samples were selected at varying stages of carbonation, in order to investigate the way in which the pore structure changes over time, and consequently, how it might affect the strength of the mortar. Limestone aggregate mortars were compared against the Standard sand mortar, in anticipation of finding distinct differences that may lead to the higher strengths observed in the limestone aggregate mortars. After phenolphthalein staining highlighted the depth of carbonation, samples were taken from the edge of the prism where carbonation had occurred.

Figure 5.32 shows the Ham Hill mortar at 1:3 B/Ag with the 'as supplied' grading, where it is evident that at both 0 days (after being mixed, the sample was placed in the oven to dry out for 24 hours before being tested) and 360 days of curing, the peak mean pore diameter is almost identical. The noticeable difference is in the volume of pores at the peak mean diameter. The total pore volume at 360 days is 0.22003 mL/g , an increase of 0.083 mL/g from 0.13657 mL/g at 0 days. The increase in pore volume is concentrated between pore sizes of $0.4 - 3\mu\text{m}$, with a negligible difference in the finer pore sizes.

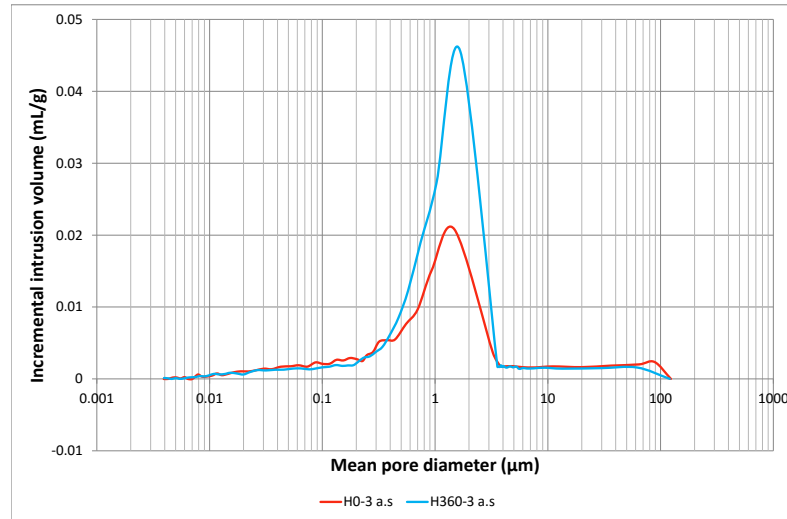


Figure 5.32: Mean pore diameter versus incremental intrusion volume for H0-3 a.s and H360-3 a.s - H360 a.s sample was taken from the carbonated edge of the prism

In Figure 5.33, it can be seen that a similar pattern to Figure 5.32 has emerged. The difference

in pore volume at $1 - 2\mu m$ is the primary change occurring over the time period.

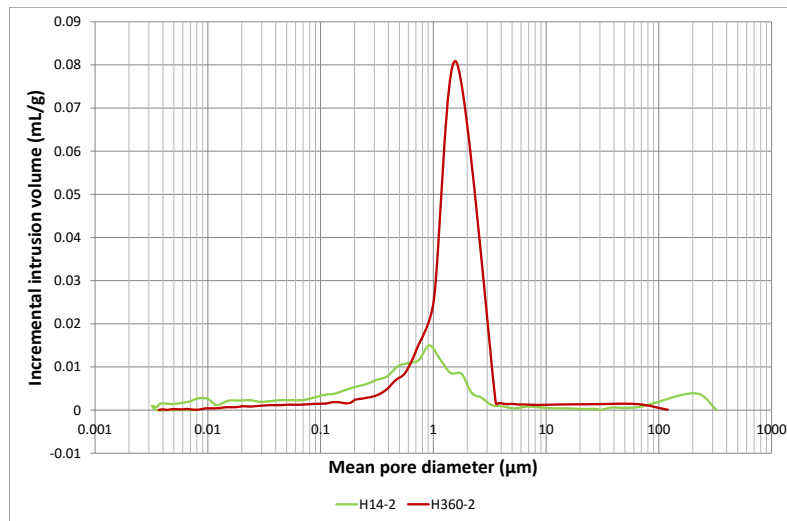


Figure 5.33: Mean pore diameter versus incremental intrusion volume for H14-2 and H360-2 - samples taken from the carbonated edge of the prism

A clear picture of the progression of the pore size distribution can be seen in Figure 5.34, which shows Stoke Ground aggregate samples with 'standard' grading, and 1:2 B/Ag at 14, 180 and 360 days of curing. As with the previous Figures, it is evident that the peaks occur at a very similar mean pore diameter. However, in contrast to the Ham Hill aggregate samples, Figure 5.34 shows a distinct change of the pore size distribution over time; both smaller pores ($< 0.4\mu m$) and larger pores ($> 4\mu m$) see a decrease in number over time. As carbonation progresses through the sample, the smaller pores become filled, while the walls of the larger pores are covered. The concentration of pores is consistently in the $1\mu m$ range.

Interestingly, the samples containing Stoke Ground aggregates with a 1:3 B/Ag and 'as supplied' grading do not have as noticeable a change over time. Figure 5.35 shows a very similar volume of pores at the smaller and larger pore diameters. Between $0.5\mu m$ and $2\mu m$, the 360 day sample was found to have a greater volume of pores, although this difference was small. The $0.018mL/g$ difference in total pore volume can be attributed to this small range of pore diameters.

The primary differences between the samples displayed in Figures 5.34 - 5.35 are the particle size distribution and the binder/aggregate ratio; despite this, the water/binder ratio does not differ significantly - 2.6 for the 1:3 mixes and 2.5 for the 1:2 mixes. Given all of the above, there are a number of possible reasons that can explain why the same trends are not evident in mortars containing the same aggregate. Firstly, the 'as supplied' particle size distribution has a greater amount of finer particles than the 'standard' grading, meaning that due to a higher packing density, the mortar sample has a higher density. The finer particles could be absorbing

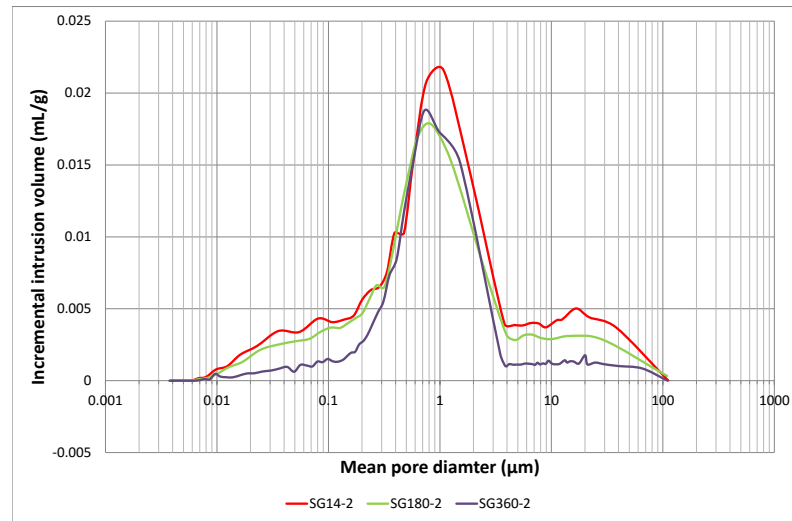


Figure 5.34: Mean pore diameter versus incremental intrusion volume for SG14-2, SG180-2 and SG360-2 - samples were taken from the carbonated edge of the prism

more of the water used in mixing thus leading to less water being available for carbonation. Consequently, the carbonation may have less impact on the pore size distribution over time.

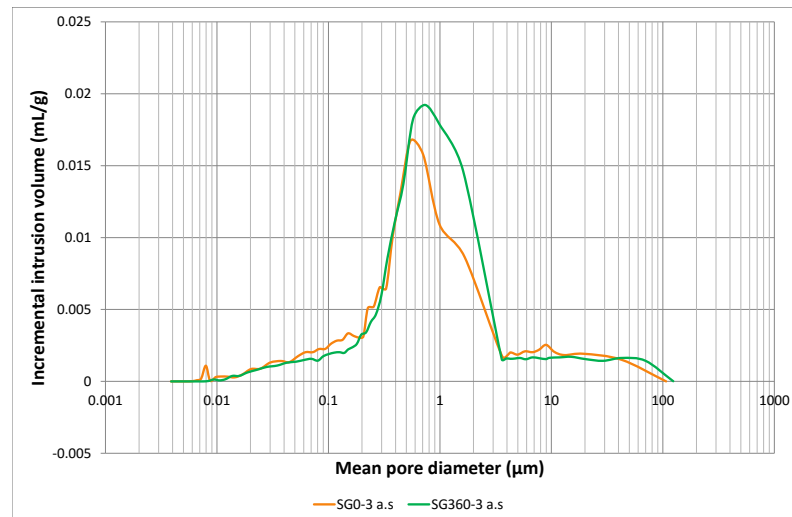


Figure 5.35: Mean pore diameter versus incremental intrusion volume for SG0-3 a.s and SG360-3 a.s - samples were taken from the carbonated edge of the prism

While the limestone aggregate mortars with 1:2 B/Ag tended to be unimodal, the 1:3 mortars were observed to be bimodal. Figure 5.36 shows how the Standard sand mortar changes over

time, but also has the Stoke Ground sample for 28 days with the same mix design. It is interesting to see that as well as having two distinct peaks where the 1:2 mixes only had one, the Standard sand and Stoke Ground mortars have a remarkably similar trend in pore size distribution. Although the Stoke Ground mortar has a greater porosity, the peaks for both samples occur at around $0.5\mu m$ and $8\mu m$ respectively. SG28-3 has a greater volume of pores at $0.5\mu m$, while SS28-3 has a greater volume of pores at $8\mu m$. Both samples also exhibit a small peak at around $200\mu m$. It is not expected that the bimodal nature is due to the aggregate itself, since Figure 3.7 in section 5.1.1.1 shows that both the Stoke Ground aggregate and the Standard sand have just one peak mean pore diameter. It is the interaction between binder and aggregate that more likely plays a role; a higher proportion of aggregate in the 1:3 mixes means there is a greater surface area that has an interface with the binder.

When looking at the progression of the pore size distribution over time for SS28-3 and SS360-3 in Figure 5.36, it is clear to see the shift in pore size distribution. Although the difference in total pore volume is very small ($0.0085mL/g$), there are a number of areas where the volume of pores at a given mean diameter varies somewhat. In general, at 360 days pore sizes are more evenly spread, whereas at just 28 days, there is a much smaller range of pores that are greater in number. While the pore size distribution is similar for both mixes in the range $0.2 - 1\mu m$, SS28-3 has a much higher volume of pores around $8\mu m$ in diameter. The reduction in larger pores between 28 and 360 days is down to the progression of the carbonation front through the sample. By 360 days, carbonation had reached the centre of the sample, meaning theoretically all the $Ca(OH)_2$ has been converted to $CaCO_3$.

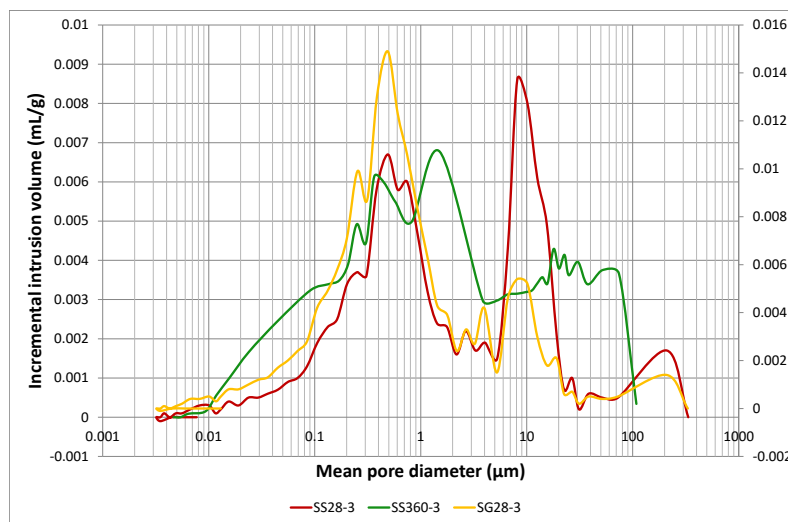


Figure 5.36: Mean pore diameter versus incremental intrusion volume for SS28-3, SS360-3 and SG28-3 - samples were taken from the carbonated edge of the prism

The curves in Figure 5.36 imply that particle size distribution and B/Ag ratio may impact pore

size distribution. SS28-3 and SG28-3 have the same B/Ag ratio and particle size distribution, with w/b ratio and aggregate type being different, and it is clear from Figure 5.36 that both follow a similar curve. The differences in the peaks (discussed above) may be attributed to the difference in porosity of the aggregates used. Stoke Ground aggregate has a porosity of approximately 25%, while Standard sand porosity was measured at around 6%. It is possible that due to the higher porosity of the Stoke Ground aggregate, calcite crystals have been able to form in the aggregate, not only forming a strong bond but also a more continuous binder matrix.

Table 5.6 shows the critical pore diameter for the samples examined using MIP. It is evident that at 360 days curing, this occurred between $3.5 - 4\mu m$, irrespective of aggregate type, binder/aggregate ratio or particle size distribution of the aggregate. This suggests that the critical pore diameter is impacted more significantly by level of carbonation of the binder. The fact that the critical pore diameters of H14-2 and SG180-2 lie outside the $3.5 - 4\mu m$ range supports this theory.

Table 5.6: Critical pore diameter

Sample	Critical diameter (μm)
H14-2	3.3
H360-2	3.8
H360-2 a.s	3.8
H360-3 a.s	3.7
P360-2 a.s	3.9
SG180-2	4.7
SG360-2 a.s	3.8
SS360-2	3.85
SS360-3	0.82 & 3.85

When looking at the accessible porosity, it can be seen in Table 5.7 that there are noticeable differences between the limestone aggregate mortars and silicate sand mortars. The two silicate sand mortars (SS360-2 and SS360-3) have a lower accessible porosity than all of the mixes made with limestone aggregate at 360 days curing; this was around 6-10% less. The standard sand mixes also had a lower porosity than the uncarbonated mixes (H0-3 a.s, P0-3 a.s, SG0-3 a.s).

It is important to take into account any hysteresis that occurs during testing. Hysteresis can result from several factors; the contact angle of the receding mercury is different to the intruding mercury, resulting in some of the mercury remaining on the sample in small quantities, as well as presence of ink bottle pores. Lawrence et al. (2007) have shown that with use of a modified Washburn equation (Equation 5.1), the presence/lack of ink bottle pores can be determined.

Table 5.7: Accessible porosity for samples subject to MIP

Sample	Accessible porosity (%)
H360-2	35.29
P360-2 a.s	31.86
SG360-2 a.s	31.51
H360-3 a.s	34.93
SS360-2	24.65
SS360-3	23.86
H0-3 a.s	24.89
P0-3 a.s	38
SG0-3 a.s	29.83

$$r = \frac{-A + \sqrt{A^2 - 2 \times P \times B}}{P} \quad (5.1)$$

Where r = pore radius, A and B are constants, and P = pressure. A and B differ based on intrusion/extrusion, as well as aggregate type used in the mortar. Table 5.8 shows the values used in this study.

Table 5.8: Constants used in modified Washburn equation

Aggregate (constant)	Intrusion	Extrusion
Limestone (A)	367.7	70
Limestone (B)	-0.739	-150
Silicate sand (A)	185	100
Silicate sand (B)	-30	-180

Figure 5.37 shows a comparison of intrusion and extrusion curves according to the Washburn equation (using a contact angle of 140° for both intrusion and extrusion), Washburn equation using 98° for extrusion contact angle, and the modified Washburn equation according to Lawrence et al. (2007). It can be seen that the modified Washburn equation maps over the Washburn equation using a different contact angle for extrusion. This shows that ink bottle pores do not exist in this instance, therefore hysteresis is caused by not taking account of a difference in the contact angle of mercury on extrusion from the sample.

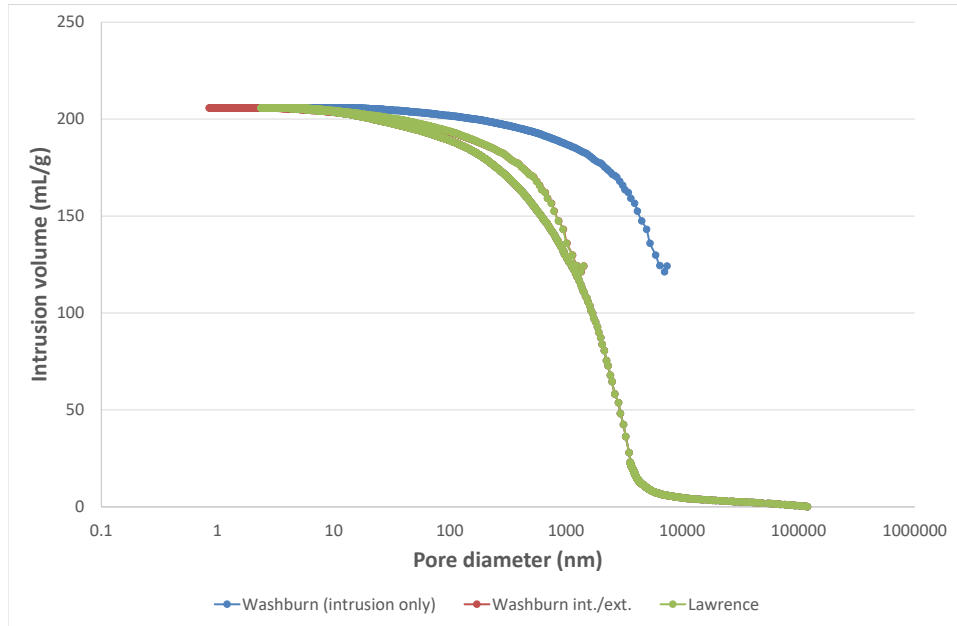


Figure 5.37: Comparison of intrusion/extrusion curves for H360-2 according to the Washburn equation, Washburn equation with modified contact angle for extrusion (98°), and modified Washburn equation (Lawrence et al., 2007)

This is by no means a rare occurrence. Figures 5.38 - 5.40 show similar results.

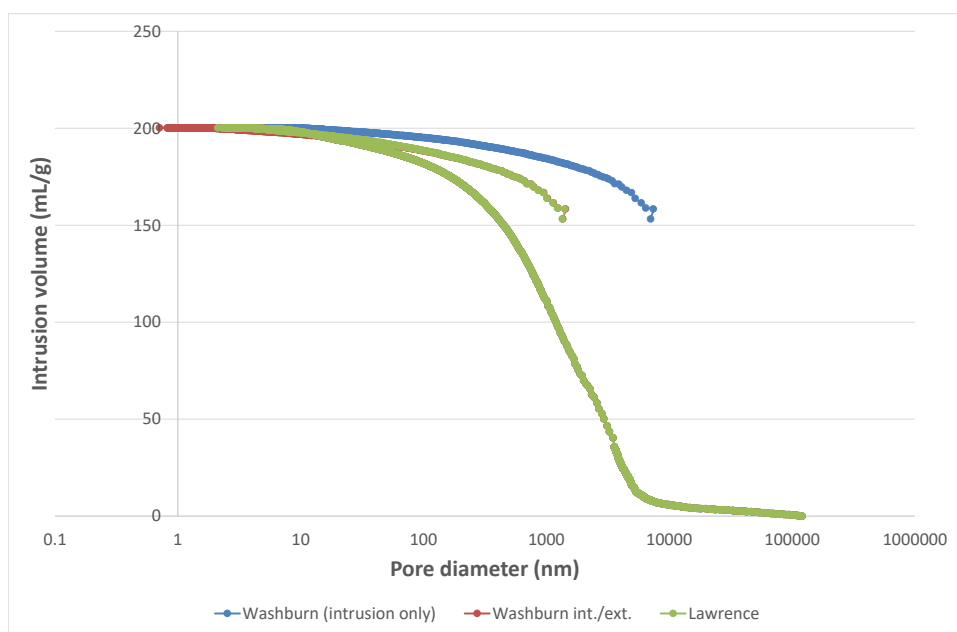


Figure 5.38: Comparison of intrusion/extrusion curves for H360-3 a.s according to the Washburn equation, Washburn equation with modified contact angle for extrusion (98°), and modified Washburn equation (Lawrence et al., 2007)

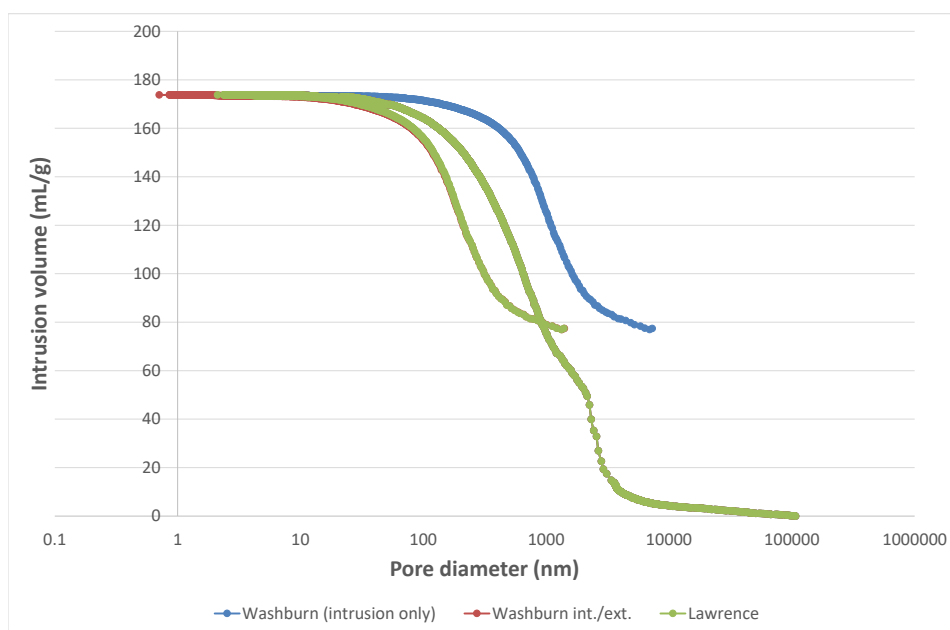


Figure 5.39: Comparison of intrusion/extrusion curves for P360-2 a.s according to the Washburn equation, Washburn equation with modified contact angle for extrusion (98°), and modified Washburn equation (Lawrence et al., 2007)

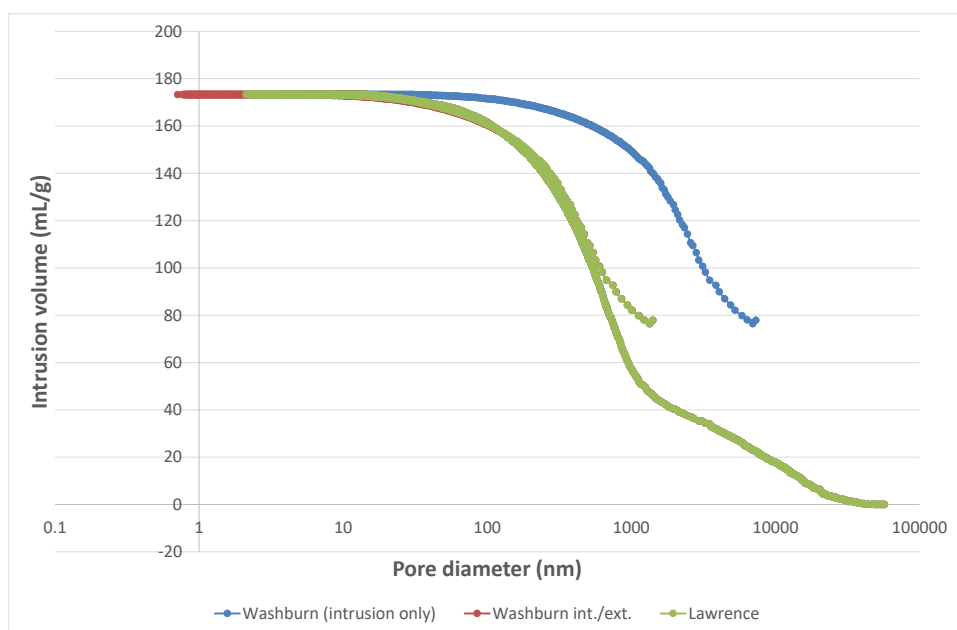


Figure 5.40: Comparison of intrusion/extrusion curves for SG360-2 a.s according to the Washburn equation, Washburn equation with modified contact angle for extrusion (98°), and modified Washburn equation (Lawrence et al., 2007)

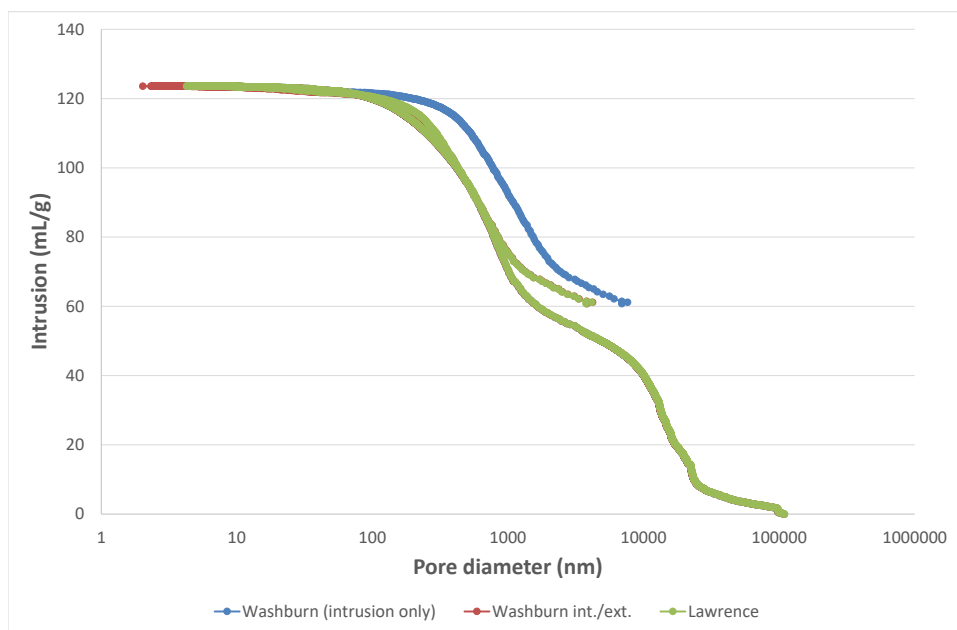


Figure 5.41: Comparison of intrusion/extrusion curves for SS360-2 according to the Washburn equation, Washburn equation with modified contact angle for extrusion (98°), and modified Washburn equation (Lawrence et al., 2007)

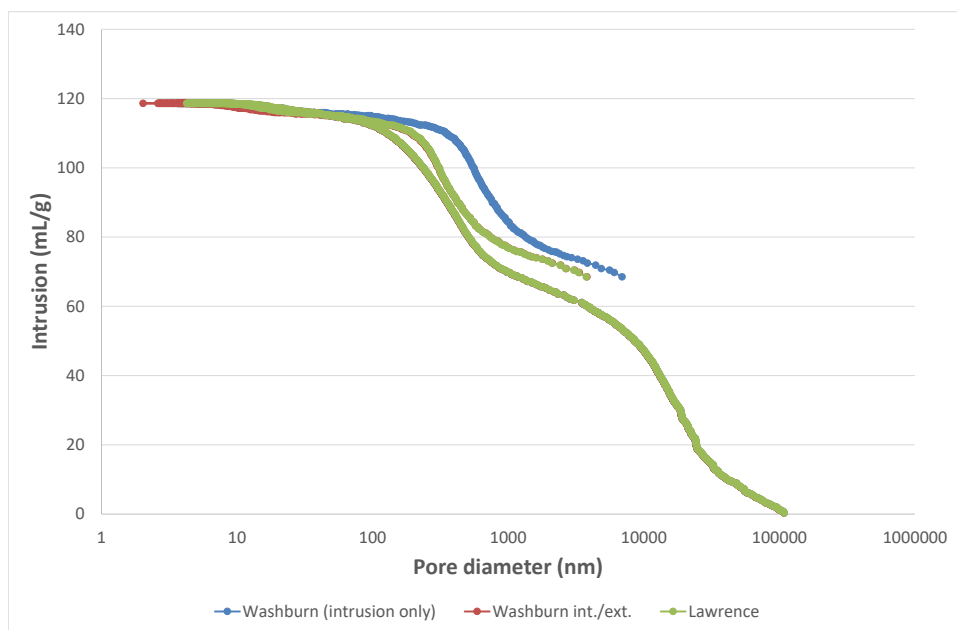


Figure 5.42: Comparison of intrusion/extrusion curves for SS360-3 according to the Washburn equation, Washburn equation with modified contact angle for extrusion (98°), and modified Washburn equation (Lawrence et al., 2007)

5.2.2 Effects of carbonation on sample density

Since carbonation affects sample density by refining the pore structure of a sample, it is worth analysing the differences that occur between the Standard sand sample and the limestone aggregate samples respectively. What we can observe in Table 5.9 is that the Standard sand mortars of the same mix specifications as the Ham Hill mortars (w/b ratio aside) have a much higher density. Usually, a higher density would lead to a higher strength due to having fewer pores; there pore walls are therefore thicker. It is clear that this is only the case in one instance.

Table 5.9: Density comparison of Ham Hill and Standard sand mortars

Sample	Density (kg/m^3)	Strength (N/mm^2)	Sample	Density (kg/m^3)	Strength (N/mm^2)
H28-2	1706	1.14	SS28-2	1991	0.97
H180-2	1736	1.72	SS180-2	1952	1.64
H360-2	1692	1.21	SS360-2	1988	1.68

Figure 5.43 makes it clear that density does not relate to strength in these samples. This finding suggests that what could be causing the strength differences is actually the quality of the interface between binder and aggregate. This is discussed further in section 5.3.

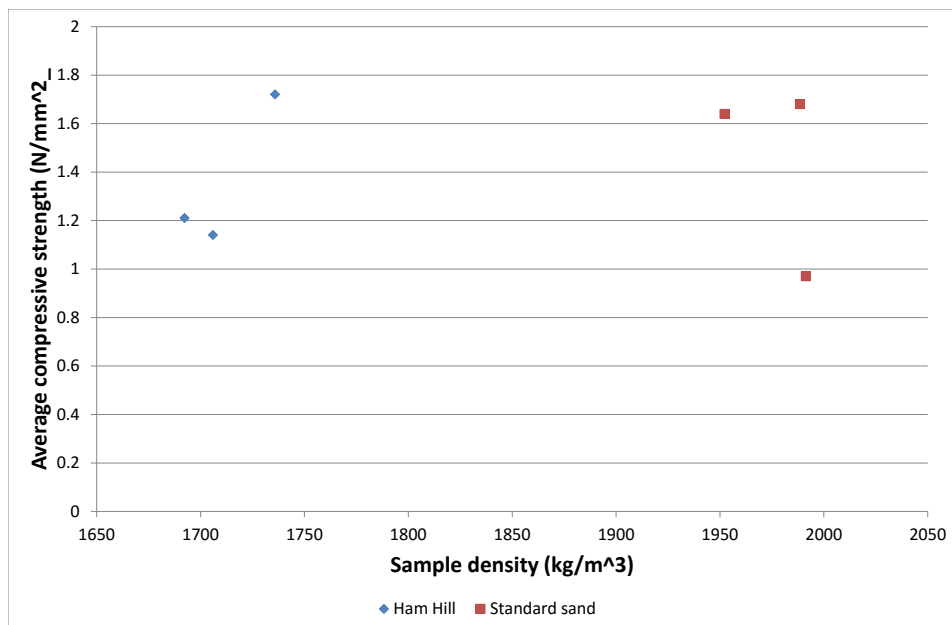


Figure 5.43: Density vs. strength for samples in Table 5.9

When looking at Stoke Ground samples, however, a relationship appears between density and compressive strength. In Figure 5.44, a clear linear relationship is seen for samples after 14 days of curing. The 14 day result may not be linear due to the quantity of water still in the sample that has not entirely dried out after mixing.

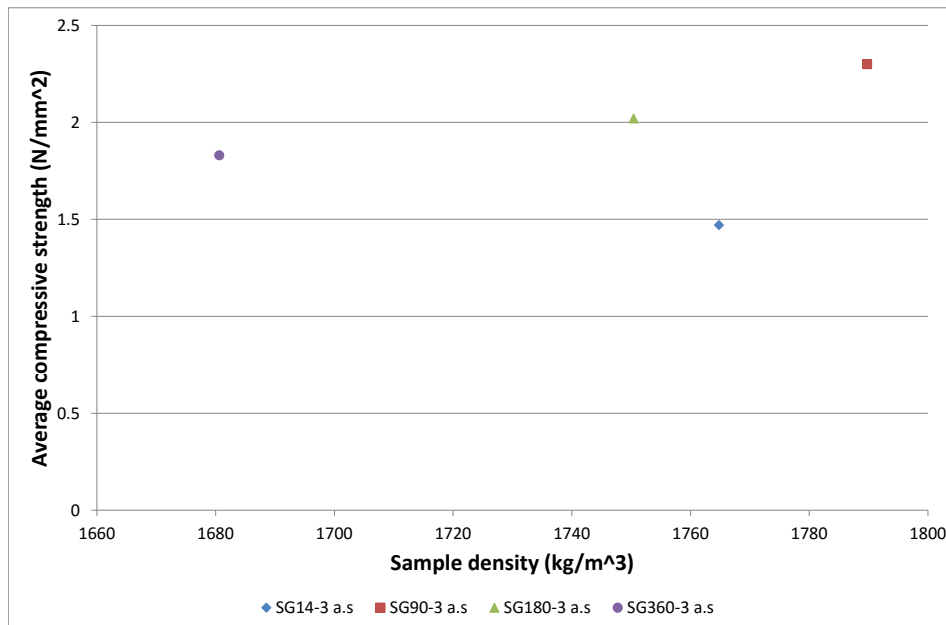


Figure 5.44: Density vs. strength for Stoke Ground samples ('as supplied')

Similar results were observed with some of the Ham Hill samples, as can be seen in Figure 5.45. The primary difference between the samples having a density/strength correlation and those that have not, is the B/Ag ratio. Although w/b ratio is also not constant, this is also true for the samples displayed in Figure 5.43 so this is not thought to be significant. The somewhat random relationship between density and strength seen in the 1:2 samples may be attributed to the higher binder amount than the 1:3 samples have. More binder leads to more carbonation

Figure 5.45 shows the relative strength of the Ham Hill samples with 'as supplied' grading and 1:2 B/Ag ratio. The highest strength per unit of density was found to occur at 180 days of curing.

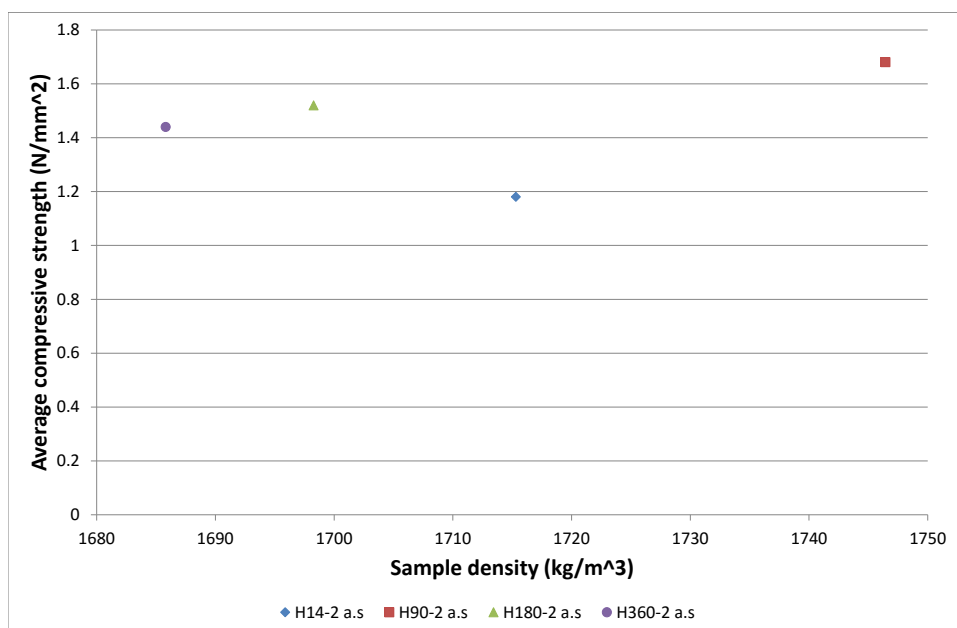


Figure 5.45: Density vs. strength for Ham Hill samples ('as supplied')

5.3 Micro-structure and binder/aggregate interface using scanning electron microscopy

The findings in Phase 1 showed that there were some interesting differences evident on the SEM images between different mixes. Further analysis of the samples used in Phase 2 was therefore undertaken. Figure 5.46 shows a carbonated mortar sample using Ham Hill aggregate, at 800x magnification. It is evident that the binder is evenly distributed throughout the image, which is assumed to be representative of the whole specimen. At the top of the image, an aggregate particle measuring approximately $60\mu m$ across, can be seen to have an intimate connection with the binder, supporting the idea that higher mortar strength relies on a continuous binder/aggregate bond.

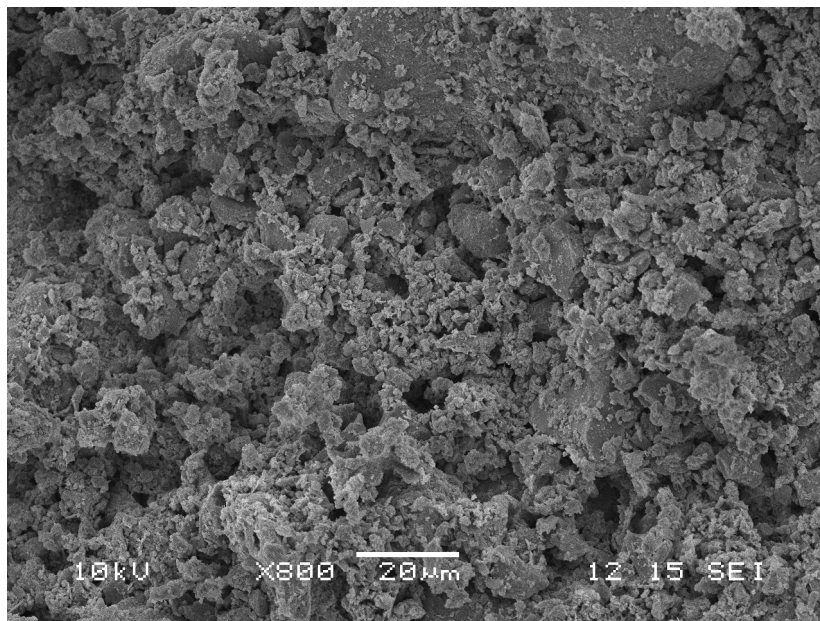


Figure 5.46: SEM image of carbonated Ham Hill aggregate mortar at 800x magnification

Similarly, Portland aggregate mortar also shows even distribution of the binder (Figure 5.47). The aggregate particle in the top left of the image is only partially visible due to the presence of binder across the aggregate; evidence of a strong binder/aggregate connection.

Figure 5.48 showing Stoke Ground aggregate mortar further supports the theory that mortar strength can be significantly impacted by binder/aggregate bond. The binder appears homogeneous and only a small area of aggregate is visible under the binder. Around the edges of the aggregate, there is only a small area where it appears the binder is not well bonded to the aggregate.

In Figure 5.49, carbonated Standard sand mortar sample is shown. A clear gap is visible between the binder and aggregate, and although some binder is apparent on the surface of the

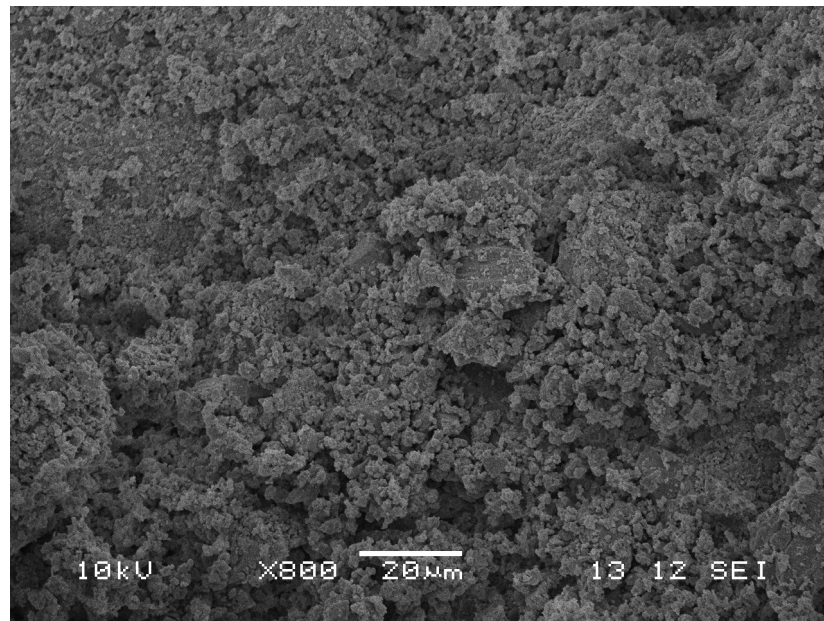


Figure 5.47: SEM image of carbonated Portland aggregate mortar at 800x magnification

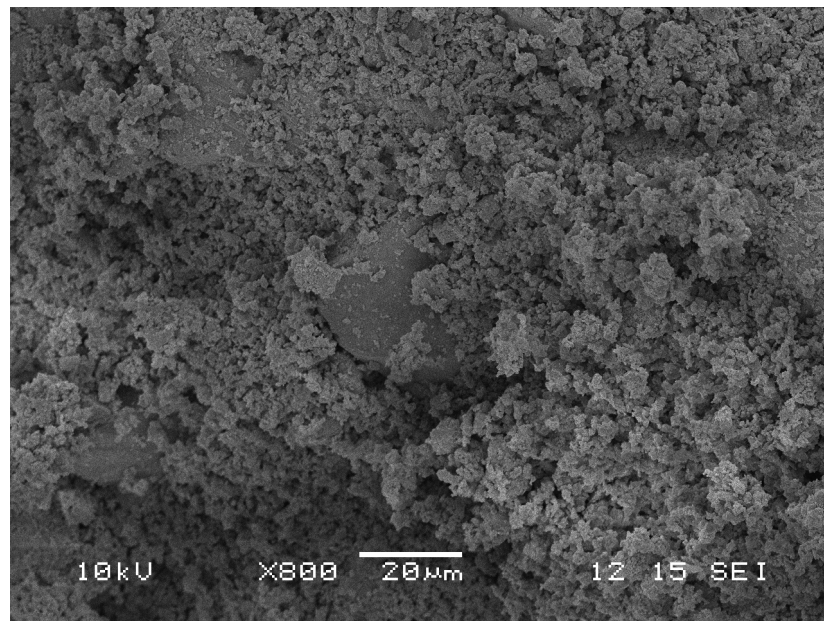


Figure 5.48: SEM image of carbonated Stoke Ground aggregate mortar at 800x magnification

aggregate, the majority of the aggregate can be seen. While there is only a small amount of binder present in this image, it appears to have a slightly uneven distribution with a 'clump' of binder to the right of the image.

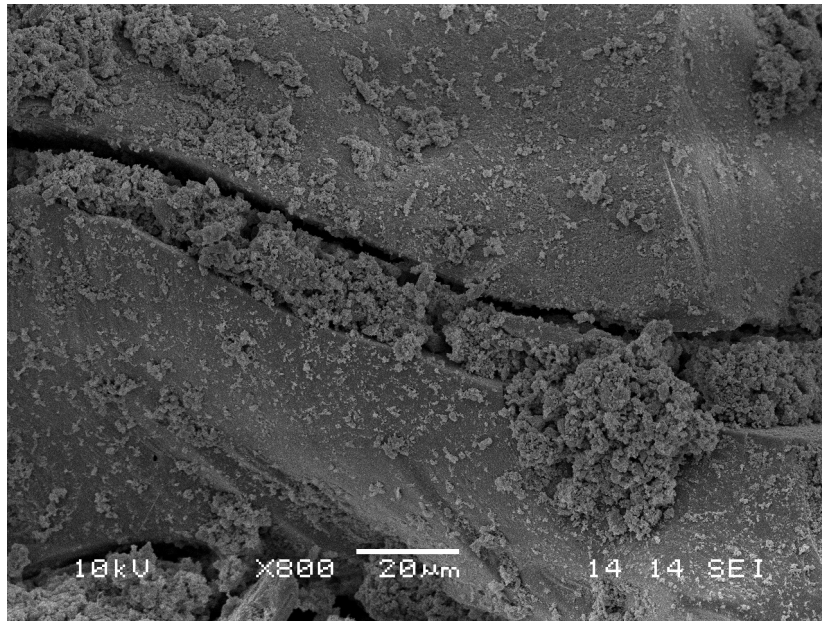


Figure 5.49: SEM image of carbonated Standard sand mortar at 800x magnification

Further evidence of the uneven binder distribution can be seen in Figure 5.50 also at 800x magnification.

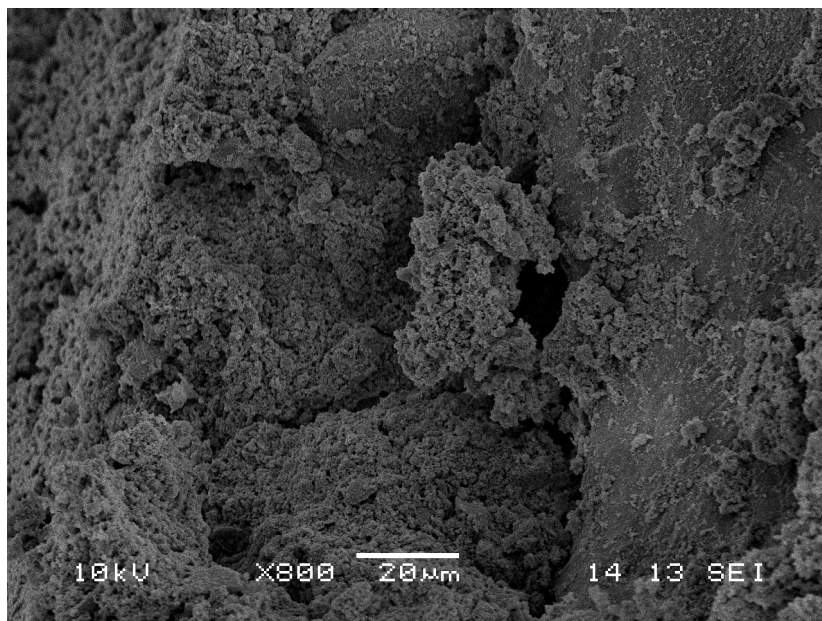


Figure 5.50: SEM image of carbonated Standard sand mortar at 800x magnification

Figures 5.51-5.54 show samples after 28 days curing. In Figure 5.52, it can be seen that there

is a micro-crack of approximately $150\mu\text{m}$ in length. While this is an interesting finding, it is not typical of the Portland aggregate mixes. However in Figure 5.53 it is evident that there are numerous micro-cracks across the entire area viewed. These cracks have not had a detrimental effect on strength, however, as SG28-3 was the strongest mortar at 28 days for 1:3 'standard' mixes. For the Standard sand sample in Figure 5.54, an aggregate particle can be clearly seen, with some evidence of calcite crystals on the surface. However, there is also a large area around the edge of the aggregate where the binder does not appear to 'stick' to the aggregate, which could result in mortar weakness.

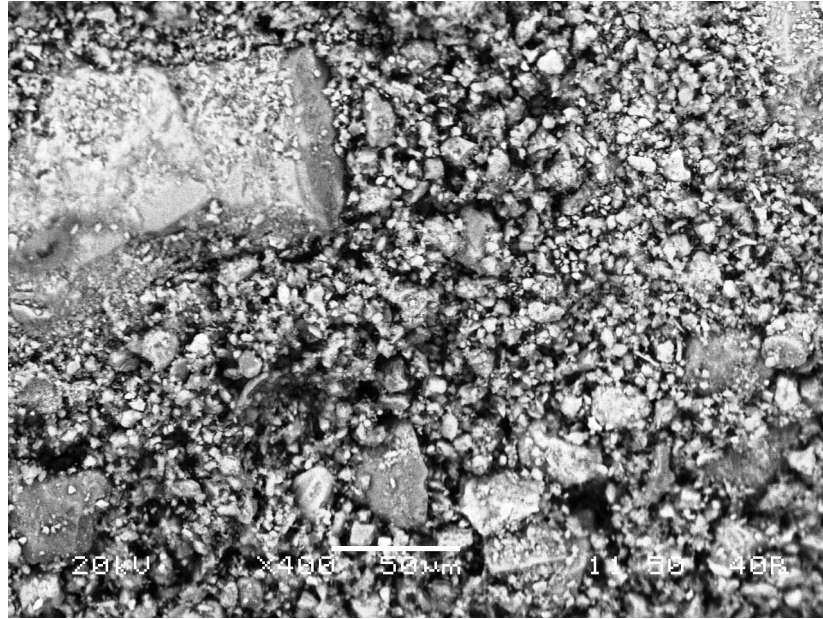


Figure 5.51: SEM image of Ham Hill aggregate mortar at 1:3 B/Ag ratio with 'standard' grading after 28 days curing - 400x magnification

The Ham Hill aggregate mortar in Figure 5.55 is unremarkable and shows no real change from the 14 day sample in Figure ???. This suggests that the carbonation at a given point does not develop further over longer curing periods.

However, in 5.56 there is a very clear cluster of calcite crystals that were not seen on 14 day samples, or in fact, in any other sample examined using SEM. This implies that there may be a greater proportion of calcite crystals (or crystals of a greater size) in this particular mix (P90-2 a.s). P90-2 a.s was also much stronger than H90-2 a.s, with SG90-2 a.s having the highest compressive strength. This is despite the fact that, as evident in 5.57, significant cracking was still present.

When looking at Figures 5.58 and 5.59 it is evident that Portland and Stoke Ground mixes still both exhibit cracking in the binder matrix. Furthermore, SS180-2 (Figure 5.60) still has a lack of continuity at the binder/aggregate interface, suggesting that this bond does not improve over a longer curing period. It is worth noting that SS180-2 uses 'standard' grading, whilst the

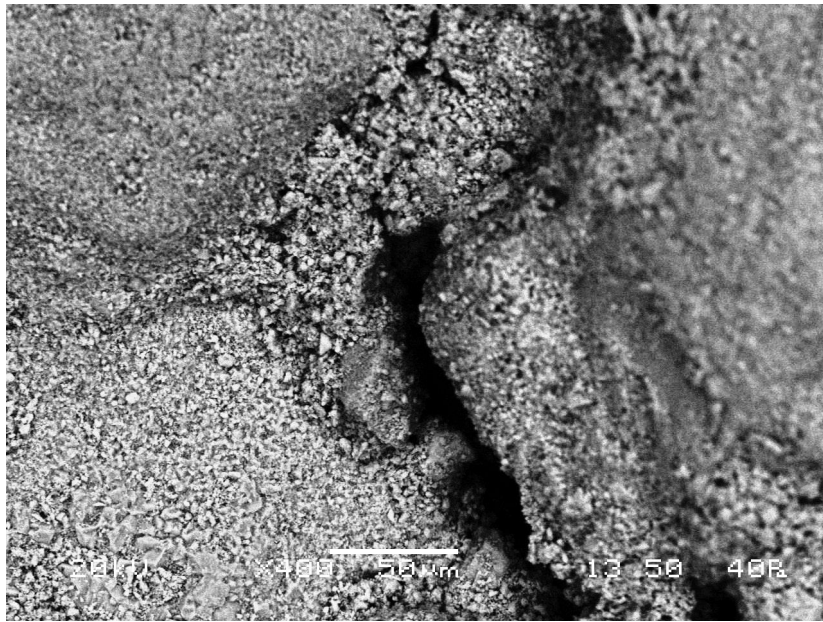


Figure 5.52: SEM image of Portland aggregate mortar at 1:3 B/Ag ratio with 'standard' grading after 28 days curing - 400x magnification

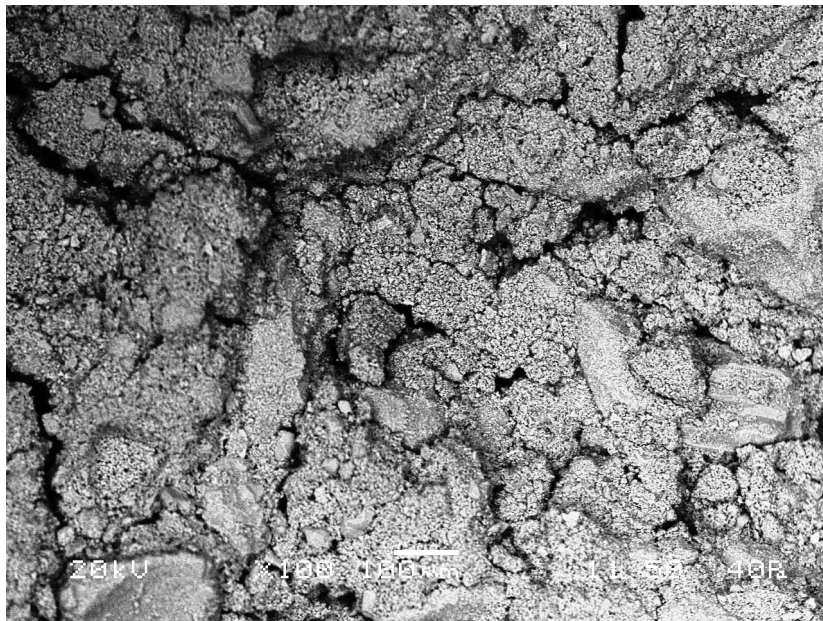


Figure 5.53: SEM image of Stoke Ground aggregate mortar at 1:3 B/Ag ratio with 'standard' grading after 28 days curing - 100x magnification

others have 'as supplied' grading, although it is not thought that the particle size distribution would impact the binder/aggregate bond.

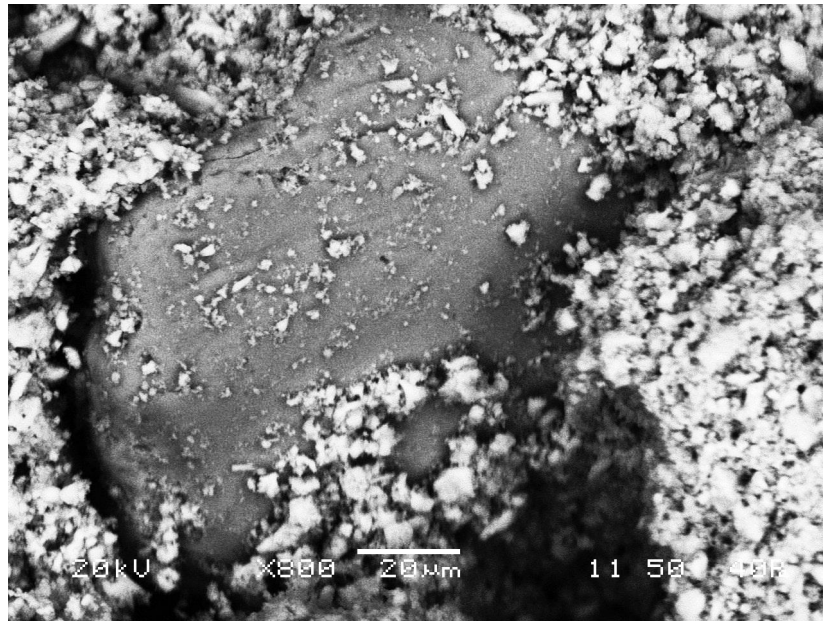


Figure 5.54: SEM image of Standard sand mortar at 1:3 B/Ag ratio with 'standard' grading after 28 days curing - 800x magnification

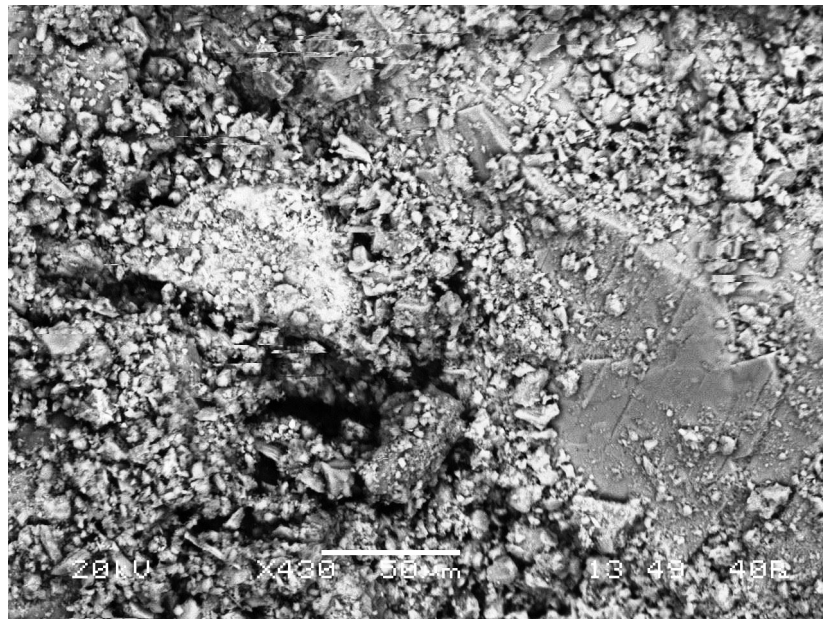


Figure 5.55: SEM image of Ham Hill aggregate mortar at 1:2 B/Ag ratio with 'as supplied' grading after 90 days curing - 430x magnification

Figures 5.61-5.64 show 1:3 mixes at 360 days curing. In Figure 5.61, it appears that there is a portlandite crystal i.e uncarbonated material, although it is not known whether more crystals would be evident throughout the rest of the sample, or indeed in samples at earlier curing

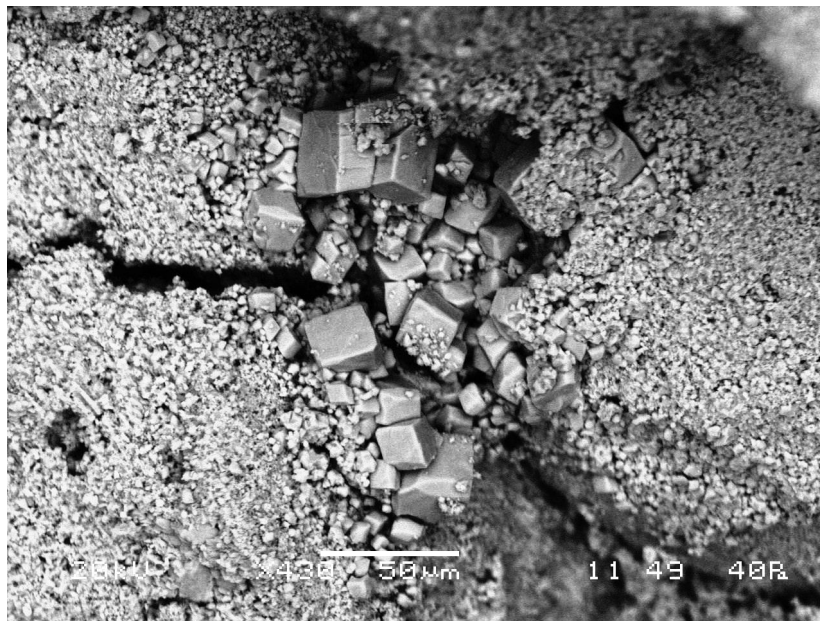


Figure 5.56: SEM image of Portland aggregate mortar at 1:2 B/Ag ratio with 'as supplied' grading after 90 days curing - 430x magnification

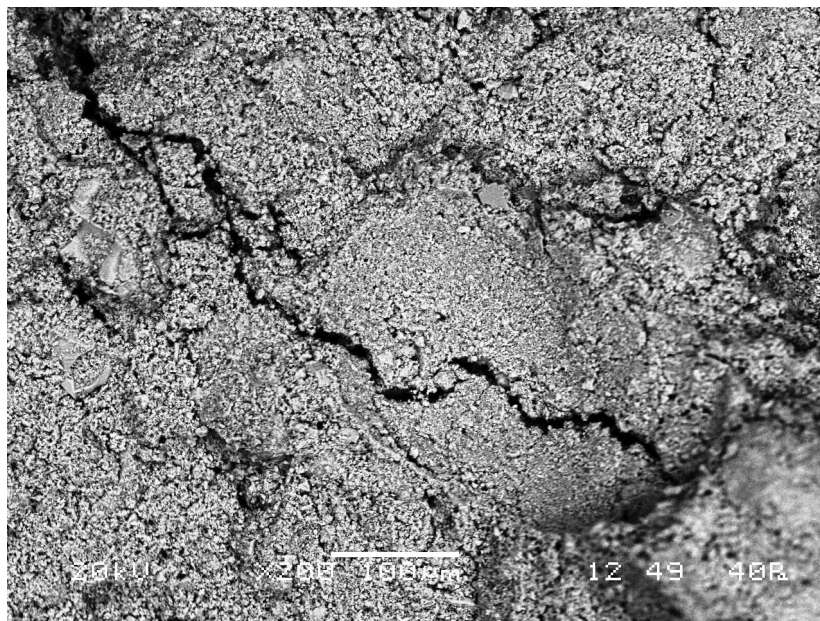


Figure 5.57: SEM image of Stoke Ground aggregate mortar at 1:2 B/Ag ratio with 'as supplied' grading after 90 days curing - 200x magnification

periods. In 5.63 there are a greater number of cracks than the other limestone aggregates; again, the Stoke Ground mix was the strongest in compression despite this cracking. 5.64

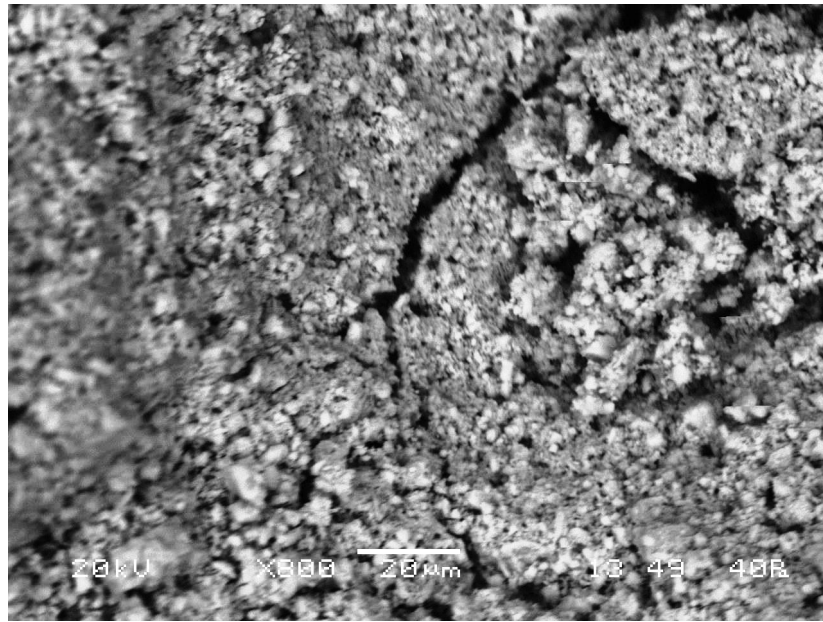


Figure 5.58: SEM image of Portland aggregate mortar at 1:2 B/Ag ratio with 'as supplied' grading after 180 days curing - 800x magnification

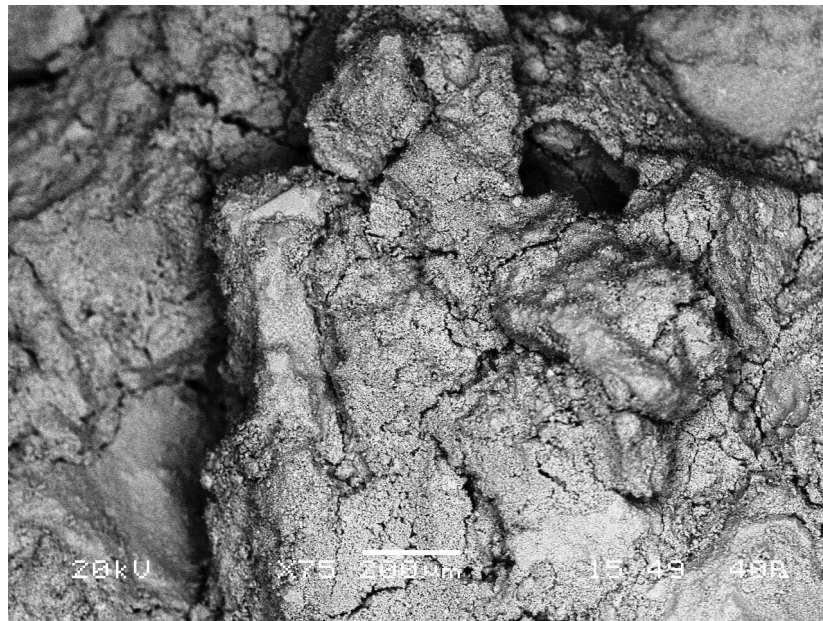


Figure 5.59: SEM image of Stoke Ground aggregate mortar at 1:2 B/Ag ratio with 'as supplied' grading after 180 days curing - 75x magnification

clearly shows that the binder is not well 'attached' to the aggregate particles.



Figure 5.60: SEM image of Standard sand mortar at 1:2 B/Ag ratio with 'standard' grading after 180 days curing - 75x magnification

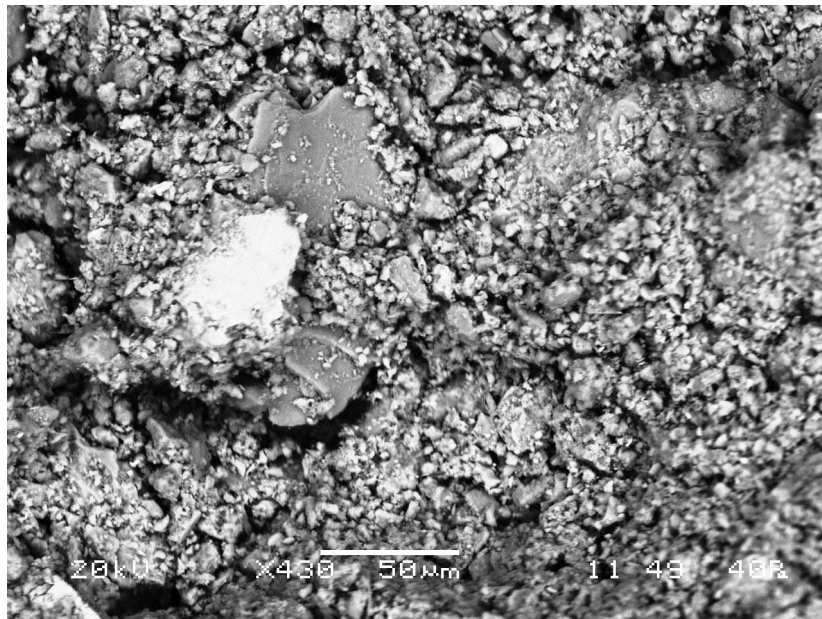


Figure 5.61: SEM image of Ham Hill aggregate mortar at 1:3 B/Ag ratio with 'as supplied' grading after 360 days curing - 430x magnification

One of the most noticeable aspects of the Portland aggregate mortars is the presence of 'craters' on the sample surface, as evidenced in Figures 5.65-5.66. It can be seen that these craters are

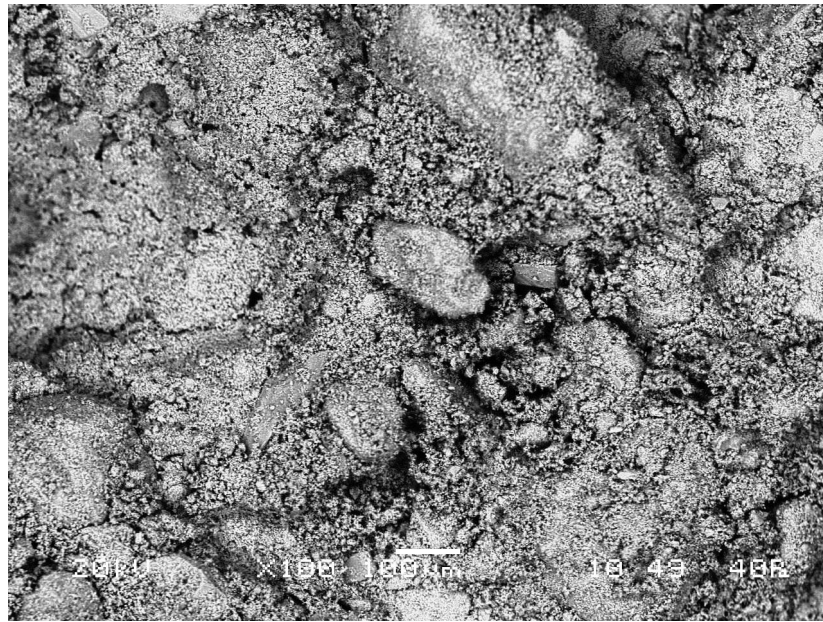


Figure 5.62: SEM image of Portland aggregate mortar at 1:3 B/Ag ratio with 'as supplied' grading after 360 days curing - 100x magnification

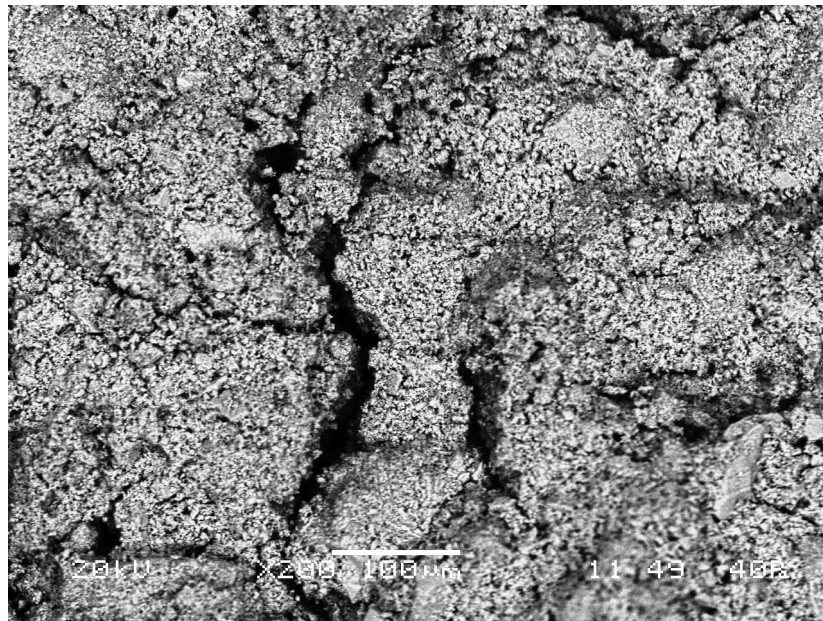


Figure 5.63: SEM image of Stoke Ground aggregate mortar at 1:3 B/Ag ratio with 'as supplied' grading after 360 days curing - 200x magnification

not smooth, with 'flecks' covering the surface, most likely calcite crystals. The craters have occurred at the fracture surface as a result of aggregate particles becoming detached from the

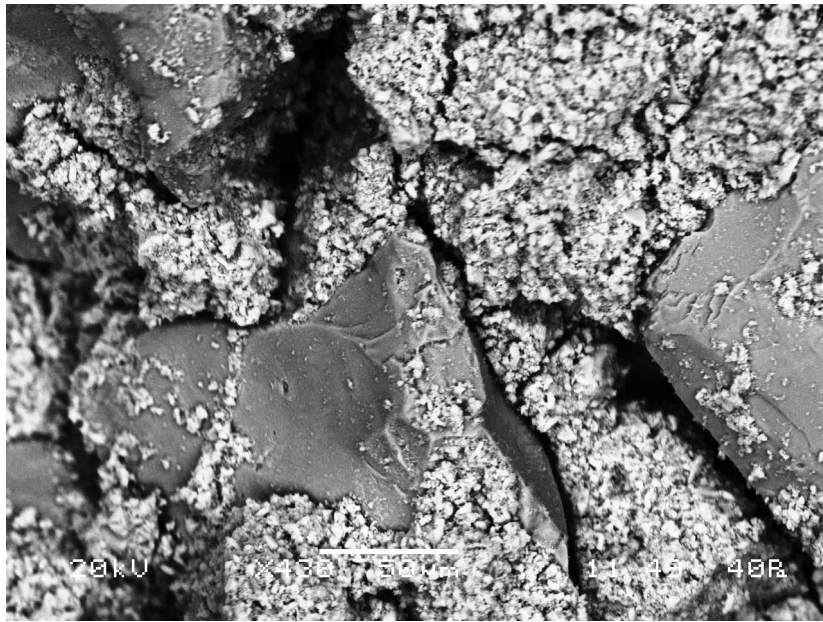


Figure 5.64: SEM image of Standard sand mortar at 1:3 B/Ag ratio with 'standard' grading after 360 days curing - 200x magnification

sample. If the specks on the craters are in fact calcite crystals, this suggests a bond with the binder, rather than the aggregate simply being surrounded by binder.

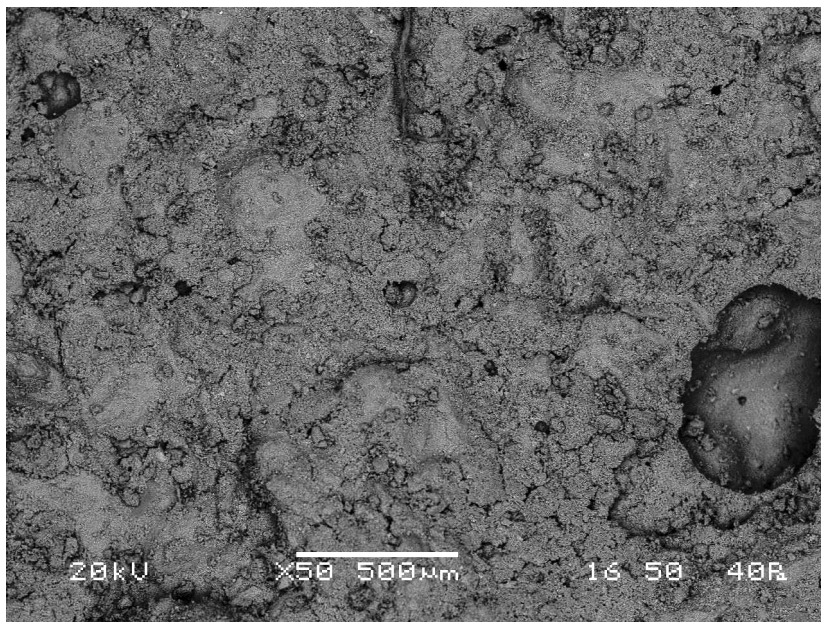


Figure 5.65: SEM image of Standard sand mortar at 1:3 B/Ag ratio with 'standard' grading after 14 days curing - 50x magnification

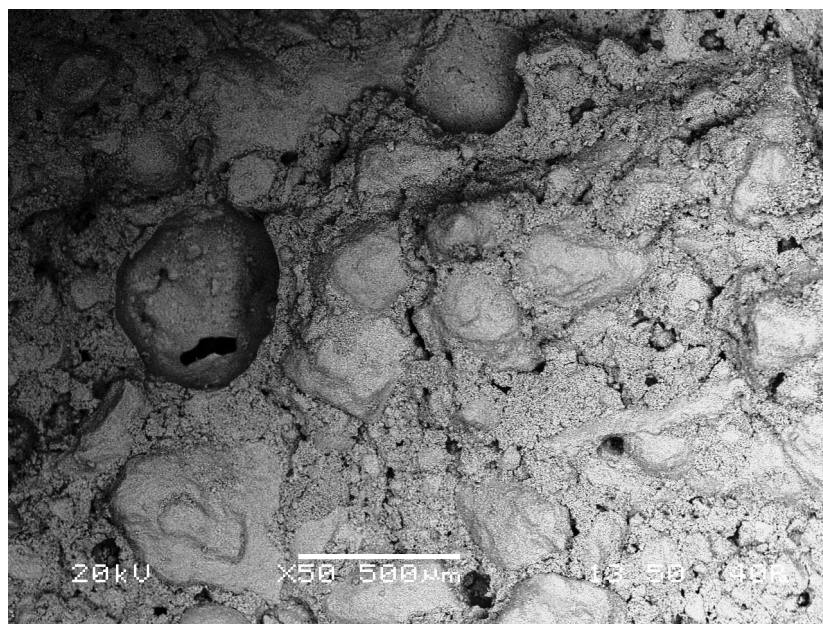


Figure 5.66: SEM image of Standard sand mortar at 1:3 B/Ag ratio with 'standard' grading after 14 days curing - 50x magnification

6 Analysis and discussion of findings

6.1 Introduction

The results presented in Chapters 4 and 5 show that clear differences exist in mortar characteristics, as result of the aggregate type used in each mix. Flexural and compressive strength results were analysed for significance using Excel's Two Sample T-test Assuming Unequal Variance.

6.2 Preliminary testing phase

This section discusses findings from the flexural and compressive strength testing, carbonation depth through use of phenolphthalein indicator, and SEM images.

6.2.1 Flexural and compressive strength testing

The compressive strength results in Chapter 4.3 suggest that Abrams' Law does not apply for these mixes. This is in agreement with the work by Lawrence and Walker (2008). The limestone aggregate mortars have a greater proportion of water and yet all have higher compressive strengths than the Standard sand mortar. A possible explanation is that the limestone aggregates form a better bond with the binder; either as a result of higher aggregate porosity or the surface texture/angularity of the limestone aggregates. A rougher surface texture would mean there is a greater surface area for the binder to adhere to.

One of the main findings from the strength testing was that the Standard sand mortars were weaker in compression than the limestone aggregate mortars, which may be a result of the quality of the binder/aggregate bond. Given that limestone aggregate is known to be more porous than the silicate (Standard sand), it is possible that some binder has entered the pores of the limestone aggregate, thus forming a more cohesive binder matrix. This could have happened during the making of the mortar specimens, when compacting the mortar into the prisms; the force of the compaction could have pushed the binder into the more porous limestone aggregate.

Of particular interest was the fact that for the 1:2 mixes (Figures 4.2 and 4.4), the increase in compressive strength between 14 and 28 days was similar for each mix. This finding is worthy

of note as the water/binder ratios were different for each mix, meaning the samples would have a different porosity and consequently it would be expected that the rate of CO_2 penetration would be different.

It was noted that with the 1:4 mixes, the range of flexural strengths across the mortars was narrower than with the 1:3 mixes. This may be due to the fact that with a higher aggregate content, the 1:4 mixes rely more on the aggregates for strength than the 1:3 mixes; different levels of carbonation in the samples may then have a different impact on sample strength. The 1:4 mixes have less binder and therefore less potential for carbonation.

The strength differences observed in the different mixes can be attributed to aggregate type, properties (surface roughness, porosity, angularity) or binder/aggregate bond.

Statistical analysis was performed on the strength results in order to determine the significance of the differences that were observed. Table 6.1 shows the 14 day strengths for 1:2 mixes, with the result at 95% confidence that a given sample is significantly different from the reference (Standard sand). Additionally, the error is shown so as to give an indication of reliability of the results obtained. It can be seen that two out of the six limestones exhibited a significant difference with the Standard sand mixes flexurally. For the compressive strengths, all the limestone aggregate mixes were significantly stronger than the Standard sand mixes. This confirmed previous research.

D14-2 exhibited a high error with the flexural strength results. Of the three specimens tested, one had a significantly lower value than the others. Ignoring this value, the error reduces to 8%. It is possible that this weaker specimen was due to inconsistencies within the mortar mix; however, the compressive strength specimens had only 8% error.

It is evident that SS-3 has a large error; this may point to inconsistencies in the mix meaning that some parts may appear stronger/weaker than they actually were.

At 14 days, with 1:3 B/Ag ratio, Stoke Ground mortar was the only mix to exhibit a significant difference than the Standard sand mix (Table 6.3), although the strength in this case was lower. Once again, all the limestone aggregate mixes were significantly stronger than the Standard sand in compression. Error values were also acceptable for all mixes so the results can be relied upon.

At 28 days, none of the limestone aggregate mixes showed a significant difference in flexural strength from the Standard sand mix (Figure 6.4). However, with compressive strength, all but SG28-3 showed a difference; again, these mixes were stronger than the Standard sand mix.

When moving onto the 1:4 mixes, it is BL14-4 that is significantly stronger than SS14-4 (see Figure 6.5). However, the compressive strength of BL14-4 is very similar to SS14-4, and is the only mix to not have a significantly higher strength than the Standard sand.

Finally, 1:4 mixes at 28 days show that the strength differences observed are not consistent over

the different mixes. It can be seen in Figure 6.6 that it is P28-4 that is significantly stronger flexurally than SS28-4. It is also clear that BS28-4 has a high error (29.93%), however the highest flexural strength value recorded was $0.8866N/mm^2$ which was significantly higher than SS28-4. H28-4 was found to have a lower compressive strength than SS28-4, although the difference was not found to be significant at 95% confidence.

6.2.2 Qualitative analysis of carbonation

Section 4.4 demonstrates the differences in carbonation depth of specimens with 1:2 B/Ag at 28 days curing. The Standard sand specimen had the lowest average depth of carbonation, which did in fact also correspond with it having the lowest compressive strength. However, four of the other specimens had the same average depth of carbonation (6mm) but with compressive strengths ranging from $1.1210N/mm^2$ – $1.4851N/mm^2$. Additionally, the Doultong specimen (which had 7mm average depth of carbonation) had a compressive strength which fell into the lower part of the range for 6mm depth ($1.1656N/mm^2$).

The Standard sand mortar result was as expected; since carbonation is primarily responsible for the strength of air lime mortars, it is logical that a sample which has carbonated to a lesser depth would have a lower strength. However, it is interesting that the sample with the greatest depth of carbonation (Doultong) does not have the corresponding higher strength that was expected, although it is $0.4N/mm^2$ stronger than the Standard sand specimen. One reason for this could be down to the aggregate itself; Doultong may have a higher compressive strength than the other aggregates. It is also possible that the higher strengths observed in the Ham Hill and Stoke Ground specimens respectively are a result of a better binder/aggregate bond rather than the level of carbonation.

6.2.3 Scanning electron microscopy images

When analysing the SEM images shown in section 4.4, discontinuity around the edge of the aggregate in the Standard sand sample could be due to the fact that the aggregate and binder are not forming a cohesive matrix, which in turn leads to lower strength values. Furthermore, the aggregates may be acting as an inert filler rather than being part of the mortar matrix. Under the compressive stresses that were applied, the binder is then more easily separated from the aggregate. The binder having lower compressive strength than the aggregate means that failure of the sample is more likely to occur through the binder rather than through the aggregate.

The smooth looking surface of the Standard sand could offer an explanation as to the lower strength of the Standard sand mortar in relation to the limestone aggregate mortars; the aggregates are acting as a filler rather than being part of the mortar matrix. Under the compressive stresses applied, the binder matrix is then more easily separated from the aggregate.

Table 6.1: Flexural and compressive strength results at 14 days with 1:2 B/Ag and 'standard' grading, confidence that results are significantly different from reference (SS14-2) at 95%, standard deviation about the mean shown as % error.

Sample	Flexural strength (N/mm^2)	Confidence at 95%	Error (%)	Compressive strength (N/mm^2)	Confidence at 95%	Error (%)
BL14-2	0.7389	No	5.76	0.8796	Yes	3.97
BS14-2	0.5772	No	11.04	0.8886	Yes	7.63
D14-2	0.4362	No	22.53	0.6926	Yes	5.80
H14-2	0.6813	No	2.63	1.3110	Yes	5.68
P14-2	0.2583	Yes	3.61	0.9719	Yes	3.84
SG14-2	0.7792	Yes	2.76	1.0122	Yes	5.68
SS14-2	06583	-	7.47	0.5949	-	7.88

Table 6.2: Flexural and compressive strength results at 28 days with 1:2 B/Ag and 'standard' grading, confidence that results are significantly different from reference (SS28-2) at 95%, standard deviation about the mean shown as % error.

Sample	Flexural strength (N/mm^2)	Confidence at 95%	Error (%)	Compressive strength (N/mm^2)	Confidence at 95%	Error (%)
BL28-2	0.7010	No	2.71	1.0543	Yes	3.7
BS28-2	0.6701	No	3.97	1.2928	Yes	4.62
D28-2	0.7984	No	4.31	1.1656	Yes	4.89
H28-2	0.7756	No	6.00	1.4851	Yes	6.31
P28-2	0.6181	No	13.61	1.1210	Yes	9.27
SG28-2	0.5984	No	6.35	1.2553	Yes	7.93
SS28-2	0.7154	-	18.16	0.7618	-	7.07

Table 6.3: Flexural and compressive strength results at 14 days with 1:3 B/Ag and 'standard' grading, confidence that results are significantly different from reference (SS14-3) at 95%, standard deviation about the mean shown as % error.

Sample	Flexural strength (N/mm^2)	Confidence at 95%	Error (%)	Compressive strength (N/mm^2)	Confidence at 95%	Error (%)
BL14-3	0.4813	No	1.35	0.8906	Yes	9.68
BS14-3	0.5427	No	6.04	0.9281	Yes	2.28
D14-3	0.6900	No	7.48	0.8860	Yes	6.54
H14-3	0.4887	No	5.48	0.7647	Yes	1.89
P14-3	0.6538	No	3.79	0.9619	Yes	6.19
SG14-3	0.2148	Yes	13.20	0.7740	Yes	2.85
SS14-3	0.6268	-	15.11	0.6317	-	2.91

Table 6.4: Flexural and compressive strength results at 28 days with 1:3 B/Ag and 'standard' grading; confidence that results are significantly different from reference (SS28-3) at 95%, standard deviation about the mean shown as % error.

Sample	Flexural strength (N/mm^2)	Confidence at 95%	Error (%)	Compressive strength (N/mm^2)	Confidence at 95%	Error (%)
BL28-3	0.7503	No	6.44	1.0658	Yes	5.50
BS28-3	0.8748	No	4.46	1.2953	Yes	8.71
D28-3	0.8038	No	8.25	1.1235	Yes	8.76
H28-3	0.6084	No	6.10	0.9337	Yes	9.82
P28-3	0.7424	No	4.11	1.2010	Yes	1.97
SG28-3	0.3463	No	4.73	0.8514	No	9.96
SS28-3	0.7362	-	8.30	0.7600	-	3.40

Table 6.5: Flexural and compressive strength results at 14 days with 1:4 B/Ag and 'standard' grading, confidence that results are significantly different from reference (SS14-4) at 95%, standard deviation about the mean shown as % error.

Sample	Flexural strength (N/mm^2)	Confidence at 95%	Error (%)	Compressive strength (N/mm^2)	Confidence at 95%	Error (%)
BL14-4	0.7495	Yes	3.06	0.8525	No	5.94
BS14-4	0.6533	No	17.14	1.1311	Yes	4.28
D14-4	0.7324	No	5.49	1.0140	Yes	6.75
H14-4	0.5642	No	1.62	0.8997	Yes	3.84
P14-4	0.7457	No	5.28	1.1850	Yes	3.59
SG14-4	0.7071	No	3.50	1.0395	Yes	3.53
SS14-4	0.6518	-	5.18	0.8339	-	5.76

Table 6.6: Flexural and compressive strength results at 28 days with 1:4 B/Ag and 'standard' grading; confidence that results are significantly different from reference (SS28-4) at 95%, standard deviation about the mean shown as % error.

Sample	Flexural strength (N/mm^2)	Confidence at 95%	Error (%)	Compressive strength (N/mm^2)	Confidence at 95%	Error (%)
BL28-4	0.7026	No	13.99	1.0713	Yes	3.33
BS28-4	0.6349	No	29.93	1.6225	Yes	4.69
D28-4	0.8411	No	5.15	1.3692	Yes	5.83
H28-4	0.7075	No	5.79	1.2024	No	3.62
P28-4	1.0188	Yes	6.59	1.7733	Yes	2.87
SG28-4	0.7972	No	11.22	1.4582	Yes	6.09
SS28-4	0.7220	-	0.99	1.2196	-	3.45

6.3 Secondary testing phase

6.3.1 Materials and mix design

Based on Table 3.9, it is clear that there are differences in the particle sizes of the different aggregates that have the potential to impact a mortar's compressive strength. Where a greater number of fines are present, such as the Ham Hill aggregate, there is the potential for a reduction in compressive strength. Kenai et al. (2008) found that with around 10% fines (less than $0.08mm$) there was no impact on compressive strength, but above this (15 and 20%) a reduction in compressive strength was observed. Consequently, it would be expected that Ham Hill mortars would have lower compressive strength than the other limestone aggregate mortars. Portland, Stoke Ground and Standard sand also have greater than 10% fines but all still amount to less than have the percentage seen in Ham Hill. It is also worth noting that Portland aggregate has a much lower proportion of the 2mm fraction, meaning that more shrinkage may occur. Whilst shrinkage was not measured in this research, it is worth keeping in mind the possible impacts.

6.3.2 Pore structure of aggregates

Differences observed in the pore structure of the different aggregates reveal a number of things. The limestone aggregates (in particular Portland and Stoke Ground), show a similar pore size distribution. This could be a result of similarities in the formation of the aggregates (and the period they are from) in addition to the fact that they are all composed of calcium carbonate. Each limestone aggregate has a peak mean pore diameter of $1 - 2\mu m$, with the main difference being the proportion of pores at this range. On the other hand, Standard sand has the majority of pores concentrated around $100\mu m$ diameter and has far fewer pores in total. This is not surprising given that silicate sand is known to have low porosity. In this study, the porosity of Standard sand (silicate) was around 5%.

6.3.3 Chemical composition of aggregates using TGA

The apparent increase in mass of Standard sand needs some explanation. It is not possible for an increase in mass to occur in the sample; the supposed increase can be attributed to a buoyant force, which occurs in all substances in a gas atmosphere in the TG machine. The buoyancy effect is dependent on the volume of material and density of the gas (in this case, Nitrogen). Due to the gas temperature increasing prior to the crucible and sample temperature, the density decrease of the gas leads to apparent mass gain of the sample (as it lowers in the chamber). One possible explanation for this being particularly evident in the Standard sand

sample is down to human error; not selecting a blank correction at the start of the test may be responsible. The chamber conditions were identical for each sample.

6.3.4 Micro-structure of aggregates using SEM

The SEM images appear to support previous research that suggested calcitic aggregates precipitate calcite growth.

Based on the images shown in section 5.1.2, it is possible that the reason smaller aggregates are 'sticking' to the larger particles ($150\mu m$) due to the presence of a greater amount of fines present in the sample analysed.

The Standard sand particle shown in Figure 3.9 is approximately $1200\mu m$ in diameter; it could be the case that further magnification would have shown a similar phenomenon to the limestone aggregates. However, based on the surrounding aggregate particles and visible space between them where the sample holder can be seen, this is thought to be unlikely.

6.3.5 Mass loss of samples due to curing

Table 6.7 shows the theoretical mass loss due to drying, and mass gain due to carbonation that air lime mortars exhibit. Based on the known initial specimen masses and quantities of $Ca(OH)_2$ and water, stoichiometry was used so that a comparison could be made between expected and observed mass change. The measured carbonated specimen masses were taken from 360 day samples, as phenolphthalein indicator showed that no $Ca(OH)_2$ remained. Since it is known that the molecular mass of $Ca(OH)_2$ is 74, and $CaCO_3$ is 100, a fully carbonated specimen would be expected to see an increase in binder mass by a factor of 1.35. Calculating the difference between the mass loss due to drying and mass gain due to carbonation means that a comparison can be made with the overall mass loss observed and recorded in Table 3.15 under the column '360 days'. Only one sample has the same value for theoretical and observed mass loss, which is Standard sand 1:3 mix. A few other samples had similar theoretical and observed values; the greatest differences occurred in the 1:2 'as supplied' mixes.

Any differences could be due to a number of things. Firstly, there is no way of knowing whether each specimen contained the same proportions of binder, aggregate and water that were initially combined, despite being thoroughly mixed. Furthermore, where the theoretical mass loss was greater than the actual mass loss, the implication is that less drying occurred than was expected. Where the actual mass loss was greater than expected, it could be that more drying occurred, or the sample was not in fact fully carbonated so mass of $CaCO_3$ was less.

Table 6.7: Initial sample mass and final sample mass, including theoretical mass gain due to carbonation and mass loss due to drying

Sample	Average initial mass (g)	Initial mass of $Ca(OH)_2$	Initial mass of water	Theoretical mass of $CaCO_3$ (g)	Theoretical mass of sample	Measured carbonated sample mass (g)	Mass gain due to carbonation (%)	Mass gain to mass of water (g)	Theoretical mass loss of water (%)
Ham Hill 1:2 'standard'	456.3	41.48	89.4	56.00	470.82	433.8	3.2	37.02	41.4
Stoke Ground 1:2 'standard'	448.4	40.76	87	55.03	462.67	436.8	3.2	25.87	29.9
Standard sand 1:2 'standard'	528.2	66.03	58.6	89.14	551.31	506.9	4.4	44.41	75.8
Ham Hill 1:2 'as supplied'	460.4	41.85	111.4	56.50	475.05	431.6	3.2	43.45	39.0
Portland 1:2 'as supplied'	479.1	36.85	80	49.75	492.00	448.1	2.7	43.90	54.9
Stoke Ground 1:2 'as supplied'	451.2	41.02	92.9	55.38	465.56	422.8	3.2	42.70	46.03
Standard sand 1:3 'standard'	512.4	46.58	41	62.88	528.7	507.2	3.2	21.5	52.4
Ham Hill 1:3 'as supplied'	485.2	30.33	94.6	40.75	495.82	430.7	2.2	65.12	68.8
Portland 1:3 'as supplied'	489.7	25.77	78.8	34.79	498.72	455.1	1.8	43.6	55.4
Stoke Ground 1:3 'as supplied'	483.1	30.19	68.6	40.76	493.67	428.1	2.2	65.57	9.59

6.3.6 Flexural and compressive strengths

Analysis of the results in Tables 6.8-6.13 go some way to explaining reasons for the strengths that were observed. It is evident in Table 6.8 that both H14-3 a.s and SG14-3 a.s had significantly higher flexural strength than SS14-3. The implication here is that since flexural bond strength is being measured, a strong bond exists at the binder/aggregate interface of H14-3 a.s and SG14-3 a.s but not SS14-3. Although the particle size distribution of the 'as supplied' mixes contained more fines than the 'standard' (SS14-3), it is not thought that this difference has a significant impact on strength, as the 1:2 'as supplied' mixes were not found to be significantly stronger than SS14-2. It is possible that since the 1:3 mixes contain a greater proportion of aggregates (and consequently a greater surface area of aggregate), the higher strengths are a result of not only a stronger binder/aggregate bond but also a larger surface area where aggregate interacts with binder.

The 1:2 a.s mixes in Table 6.8 had significantly higher compressive strengths than the Standard sand (SS14-2). This was also true of the 1:3 mixes but the difference in compressive strengths was much larger. This could again point to differences in the proportion of binder, but it is also worth considering that a higher proportion of aggregate means a smaller proportion of binder; therefore less binder available for carbonation which gives air lime mortar their strength. That being said, the influence of calcitic aggregates in air lime mortar could prove to be more influential to strength than carbonation.

Given that the particle size distribution differs (aside from P-2 and SG-2), these similarities may occur as a result of the level of carbonation in the binder, the bond between binder and aggregate, or due to similar aggregate properties. The latter is supported by the TG analysis of the aggregates, shown previously in Figure 3.8, which have a very similar TG curve, although this does not mean the other possibilities are untrue.

After 28 days, some similar trends were observed (Table 6.9). H28-2 was significantly weaker in flexure than SS28-2 (and the other mortars), leading to the conclusion that either the Ham Hill aggregate itself is weaker, or the higher proportion of water is causing lower strengths. H28-2 also saw the highest error, for both flexural and compressive strengths, although neither were unreasonably high.

SG28-2 and SS28-2 had very similar flexural strength values. Given that the only differences in the two mixes were aggregate type and proportion of water, this implies that one or both of these factors is responsible. It is possible that the higher water content in SG28-2 has offset any positive impact caused by the use of calcitic aggregate, but this would contradict findings by Lawrence and Walker (2008). It is difficult to verify this as adjusting the water content for either mix would result in mixes that are not workable.

It was found that with the 1:3 mixes (both 'standard' and 'as supplied' grading), Stoke Ground mortar was the only one to produce mortars that were significantly stronger than the Standard

sand mortar. Once again, Ham Hill mortars were not significantly stronger than Standard sand mortar in compression, in contrast with the 14 day strengths. The high error observed in the Standard sand 1:3 mix was due to one sample of the flexural tests having a higher strength than the other two; consequently two samples out of six had higher compressive strengths.

Since the 'as supplied' mortars have a higher proportion of fines, the samples with higher water content may not see reduced strength due to the water being absorbed by the finer material in the aggregate.

The 1:3 'as supplied' limestone aggregate mortars at 90 days were found to be stronger than the Standard sand mortar in both flexure and compression (Figure 6.10). Since Ham Hill and Portland mortars were not stronger than the Standard sand mortar in flexure at 28 days, it is possible that the rate of carbonation has seen an increase in the limestone mortars that was not seen in the Standard sand mortar. Alternatively, the binder/aggregate bond may now be playing a significant role in the mortar strength, with the assumption that the limestone aggregate mortars have a stronger bond. Furthermore, it is interesting to note that Ham Hill mortar is now not the weakest in compression, having overtaken Portland mortar. Two possible reasons exist. The first is that there were mix inconsistencies in the Portland mortar making it appear weaker than Ham Hill, although this is unlikely as the flexural strength was still higher than that of the Ham Hill mortar. The second possibility is that since the Ham Hill mortar had a higher proportion of water, it experienced a longer period of drying and consequently required longer to see any significant strength gains.

The negligible strength gain of Ham Hill mortar could be due to the fact that at 90 days, the sample was 'fully carbonated' as far as the phenolphthalein staining is concerned; however, the Portland and Stoke Ground mortars appear to decrease in strength after 90 days, despite also seeming fully carbonated. Phenolphthalein has the potential to be inaccurate if particles from the carbonated area spread onto the uncarbonated area; the sample could appear carbonated to a greater extent due to this contamination.

In Figure 6.11, the 1:2 'as supplied' mixes show a different trend from the 14 day results. Both Portland and Stoke Ground mortars were significantly stronger than Standard sand mortar, whereas at 14 days they were weaker. Again, this points to either an accelerated carbonation in the limestone aggregate mortars or a stronger binder/aggregate bond. Once again, Ham Hill aggregate was weakest in flexure for both 'standard' and 'as supplied' grading. The compressive strength shows that Ham Hill with 'standard' grading was significantly stronger than Standard sand mortar; conversely, Ham Hill 'as supplied' mortar was significantly weaker. This indicates that the 90 day results may have been anomalous, as they contradict the general trend of Ham Hill mortars. The lesser performance of these mortars may have been caused by the higher proportion of water ($w/b = 3.5$ for 'as supplied' mix) than was necessary in the other mixes in order to achieve the desired flow. Supporting this theory is the fact that SG180-2 had the highest compressive strength and contained one of the lowest proportions of water ($w/b = 2.49$).

The lower compressive strengths of the 1:3 mixes than the 1:2 mixes may be due to the fact that the former have a greater volume of aggregate, meaning there is more aggregate surface area to be in contact with the binder, hence more potential for failure at the binder/aggregate interface.

The 360 day strengths seen in Figure 6.12 confirm previous findings that the Ham Hill mortars generally perform the worst and often have lower flexural and compressive strength than Standard sand mortars. Whilst the Ham Hill 'as supplied' mixes have a much lower w/b ratio, the 'standard' mixes only have a slightly lower w/b. Consequently, it is unclear to what extent the water impacts strength. It is of course also possible that the Ham Hill aggregate itself does not perform well mechanically. Interestingly, the Stoke Ground 'standard' mix was also weaker in compression than the Standard sand mortar, although based on the previous results, it is likely that this was due to error in mixing.

In the final mixes (Figure 6.13, just one of the Ham Hill mixes was found to be stronger than the Standard sand; the 1:3 'standard' mix in compression. The 1:3 'as supplied' mix does have a high error (22%) although this is down to just one specimen having a much lower value than the other 2.

Water content is known to affect flexural strength in some mortars; Ham Hill mortar did require a greater amount of water than the mortars with other aggregates, in relation to binder, to achieve the desired flow of 14cm (see Table 3.11). This may be the cause of the lower strengths observed by the Ham Hill mortar (H-2 a.s), with the 14 day strength possibly being inaccurate if it failed prior to the test apparatus registering the failure.

Although the sample at 360 days has carbonated to a greater depth, if the bond at the binder/aggregate interface is weak then failure occurring here would not lead to significant strength increase over time, as the specimen would still be reliant on only bond strength not the strength of the entire mortar matrix. Therefore, if the bond does not see much improvement over time, the strength would not be expected to see a significant increase either.

Table 6.8: Flexural and compressive strength results at 14 days, confidence that results are significantly different from reference (SS14) at 95%, standard deviation about the mean shown as % error.

Sample	Flexural strength (N/mm^2)	Confidence at 95%	Error (%)	Compressive strength (N/mm^2)	Confidence at 95%	Error (%)
H14-2 a.s	0.6058	No	3.43	1.1739	Yes	3.27
P14-2 a.s	0.6298	No	7.64	0.8876	Yes	13.91
SG14-2 a.s	0.6687	No	10.49	0.9032	Yes	6.67
SS14-2	0.6583	-	7.47	0.5949	-	7.88
H14-3 a.s	0.5846	Yes	6.41	1.3757	Yes	3.16
SG14-3 a.s	0.6240	Yes	8.16	1.4716	Yes	4.71
SS14-3	0.4051	-	2.86	0.5537	-	10.33

Table 6.9: Flexural and compressive strength results at 28 days, confidence that results are significantly different from reference (SS28) at 95%, standard deviation about the mean shown as % error.

Sample	Flexural strength (N/mm^2)	Confidence at 95%	Error (%)	Compressive strength (N/mm^2)	Confidence at 95%	Error (%)
H28-2	0.4497	Yes	13.39	1.2358	Yes	11.52
P28-2	0.9548	Yes	4.15	1.4487	Yes	5.62
SG28-2	0.7105	No	6.43	1.4915	Yes	6.25
SS28-2	0.7727	-	5.54	0.9954	-	5.37
H28-3	0.4372	No	6.09	0.9847	No	4.33
P28-3	0.5046	No	0.72	1.0811	Yes	3.46
SG28-3	0.6931	Yes	5.80	1.3609	Yes	3.90
H28-3 a.s	0.4511	No	7.83	0.9625	No	2.07
P28-3 a.s	0.5166	No	2.76	1.0698	Yes	4.29
SG28-3 a.s	0.6806	Yes	9.69	1.4176	Yes	3.41
SS28-3	0.4588	-	21.39	0.8978	-	16.85

Table 6.10: Flexural and compressive strength results at 90 days, confidence that results are significantly different from reference (SS90) at 95%, standard deviation about the mean shown as % error.

Sample	Flexural (N/mm^2)	strength	Confidence at 95%	Error (%)	Compressive strength (N/mm^2)	Confidence at 95%	Error (%)
H90-3 a.s	0.6362		Yes	7.91	2.1041	Yes	2.64
P90-3 a.s	0.6693		Yes	15.03	1.9049	Yes	4.05
SG90-3 a.s	0.7781		Yes	7.76	2.3107	Yes	4.32
SS90-3	0.4494		-	8.78	1.3218	-	3.39

Table 6.11: Flexural and compressive strength results at 180 days, confidence that results are significantly different from reference (SS180) at 95%, standard deviation about the mean shown as % error.

Sample	Flexural strength (N/mm^2)	Confidence at 95%	Error (%)	Compressive strength (N/mm^2)	Confidence at 95%	Error (%)
H180-2	0.6451	No	4.77	1.7023	Yes	0.96
P180-2	0.8452	Yes	8.54	2.3496	Yes	2.53
SG180-2	0.8141	Yes	1.69	2.7195	Yes	3.82
H180-2 a.s	0.5695	Yes	10.92	1.4419	Yes	2.18
P180-2 a.s	0.8086	No	14.62	2.1557	Yes	2.16
SG180-2 a.s	0.8749	Yes	9.47	2.5051	Yes	13.09
SS180-2	0.6503	-	3.13	1.6374	-	2.93

Table 6.12: Flexural and compressive strength results at 360 days with 1: 2 B/Ag, confidence that results are significantly different from reference (SS360) at 95%, standard deviation about the mean shown as % error.

Sample	Flexural strength (N/mm^2)	Confidence at 95%	Error (%)	Compressive strength (N/mm^2)	Confidence at 95%	Error (%)
H360-2	0.6129	Yes	5.90	1.2039	Yes	2.25
SG360-2	1.0415	Yes	7.62	1.1892	Yes	3.56
H360-2 a.s	0.6136	Yes	5.94	1.5583	Yes	3.29
P360-2 a.s	0.9399	No	13.46	1.8985	Yes	2.96
SG360-2 a.s	0.9480	No	7.42	2.2568	Yes	9.48
SS360-2	0.8227	-	11.39	1.6615	-	5.00

Table 6.13: Flexural and compressive strength results at 360 days with 1:3 B/Ag; confidence that results are significantly different from reference (SS360) at 95%, standard deviation about the mean shown as % error.

Sample	Flexural strength (N/mm^2)	Confidence at 95%	Error (%)	Compressive strength (N/mm^2)	Confidence at 95%	Error (%)
H360-3	0.4393	No	9.45	1.3270	Yes	3.13
SG360-3	0.7977	Yes	9.30	1.7361	Yes	4.75
H360-3 a.s	0.4486	Yes	16.30	1.1224	No	21.87
P360-3 a.s	0.9018	Yes	5.08	1.6883	Yes	4.72
SG360-3 a.s	0.7841	Yes	7.58	1.9282	Yes	15.94
SS360-3	0.5185	-	6.52	1.1959	-	3.23

6.3.7 Carbonation measured by phenolphthalein indicator and TGA

The results from phenolphthalein staining indicate that depth of carbonation does not relate to compressive strength of mortars, leading to the conclusion that it is another factor that is contributing, such as binder/aggregate bond or aggregate strength. It is worth keeping in mind that this analysis is only qualitative and errors may have occurred when measuring carbonation depth. Furthermore, the assumption is that carbonation depth is uniform throughout the specimen, which may not be the case.

TG analysis suggests that despite the edge of the specimen appearing fully carbonated, some Ca(OH)_2 is still present. This is due to carbonation being a self-limiting process. CaCO_3 has a greater volume than Ca(OH)_2 , therefore as crystals develop, they block CO_2 access to the Ca(OH)_2 ; it is therefore unable to fully carbonate. If cracking occurs in the mortar, then CO_2 can again penetrate and lead to further carbonation.

Differences in the aggregate density may lead to changes in the way CO_2 can penetrate the sample; a more dense aggregate would see restricted access and consequently less carbonation at a given time period. However, this is not thought to be the case here, since Portland aggregate had a higher density than Ham Hill, 2926kg/m^3 and 2442kg/m^3 respectively. Furthermore, if the initial water content was higher in one mix, CO_2 penetration may also be hindered.

Table 6.14 shows the theoretical mass of CaCO_3 present in each mortar specimen. The mass is based off the samples tested using TGA, and the percentages obtained. It is important to distinguish between CaCO_3 that is present as a result of the aggregate, and that which is present due to carbonation of the sample.

It can be seen that some of the values are negative, which is of course not possible. The most probable reason for this is due to the apparent mass increase that occurred during testing, as a result of the buoyancy effect. Table 6.15 shows the corrected values.

Here, it can be seen that differences exist in the theoretical mass of CaCO_3 that is due to carbonation. For the 1:3 mixes at 28 days (both gradings), Ham Hill has the highest quantity of CaCO_3 due to carbonation. Based on the fact that only SS28-3 was weaker than H28-3 and H28-3 a.s, it is surprising to find that carbonation appears to have occurred to the greatest extent. This suggests that it is not the quantity of carbonation product that is responsible for the compressive strength results; other factors such as binder/aggregate bond and aggregate strength could therefore be responsible. Contrary to what was expected, SG28-3 a.s was found to have a lower mass of CaCO_3 than SS28-3, despite having a higher compressive strength. With 1:2 mixes at 180 days, Portland had the highest amount of CaCO_3 due to carbonation, although each of the samples were relatively close together. While a direct comparison cannot be made with the 28 day samples due to the different B/Ag ratios, the implication is that it is the early age strength that has the greatest difference in carbonation. It is worth noting that these are theoretical masses; percentages of CaCO_3 were obtained from the tested samples,

Table 6.14: Theoretical mass of $CaCO_3$ in specimens based on samples tested using TGA

Sample	Lime mass (g)	Aggregate mass (g)	Theoretical mass of $CaCO_3$ due to aggregate (g)	Theoretical mass of $CaCO_3$ from mortar specimen (g)	Theoretical mass of $CaCO_3$ due to carbonation only (g)
H28-3	150	2243	516	646	130
P28-3	150	2687	1075	1050	-25
SS28-3	150	1571	0	16	16
H28-3 a.s	150	2243	516	766	250
P28-3 a.s	150	2687	1075	1135	60
SG28-3 a.s	150	2202	881	870	-11
SS28-3	150	1571	0	86	86
P180-2 a.s	150	1791	716	776	60
SG180-2 a.s	150	1468	587	599	12
SS180-2	150	1048	0	30	30

Table 6.15: Theoretical mass of $CaCO_3$ in specimens based on samples tested using TGA

Sample	Lime mass (g)	Aggregate mass (g)	Theoretical mass of $CaCO_3$ due to aggregate (g)	Theoretical mass of $CaCO_3$ from mortar specimen (g)	Theoretical mass of $CaCO_3$ due to carbonation only (g)
H28-3	150	2243	516	694	178
P28-3	150	2687	1075	1135	60
SS28-3	150	1571	0	16	16
H28-3 a.s	150	2243	516	814	298
P28-3 a.s	150	2687	1075	1192	117
SG28-3 a.s	150	2202	881	941	60
SS28-3	150	1571	0	86	86
P180-2 a.s	150	1791	716	815	99
SG180-2 a.s	150	1468	587	663	76
SS180-2	150	1048	0	78	78

which were assumed to be representative of the entire specimen. However, it is impossible to know whether the tested samples were in fact representative of the mortar specimen.

6.3.8 Pore structure of mortars measured using MIP

Use of a modified Washburn equation to examine hysteresis in the MIP curves has shown that ink bottle pores are not present in the samples, therefore it can be assumed that the pore size distribution data are an accurate representation of pore structure; comparisons are therefore valid. The MIP analysis uncovered a number of things about the pore structure of the mortars. H0-3 a.s was the sample taken from the mortar mixture prior to it being transferred to the mortar prisms. This sample was then dried out an oven at 100° for 24 hours and placed in an air tight jar containing nitrogen up until testing. The pore size distribution was found to be very similar to that of the Ham Hill aggregate on its own. This is likely to be due to the fact that carbonation had only 24 hours to begin. By 360 days, an increase in the proportion of pores of $1 - 2\mu m$ was seen, as well as an increase in porosity. This was due to the development of the pore structure over time.

However SG-0-3 a.s and SG360-3 a.s were both found to differ from the Stoke Ground aggregate alone, with the SG360-3 a.s displaying a shift toward a higher proportion of smaller pore diameters. Since the Stoke Ground aggregate is less porous than the Ham Hill aggregate, it follows that the mortar containing Stoke Ground would show a greater porosity even after just 24 hours curing.

Mortar made with Ham Hill aggregate with a 1:2 mix exhibited an increase in peak mean pore diameter from $0.9\mu m - 1.5\mu m$ between 14 and 360 days. The proportion of pores between $0.015\mu m$ and $0.08\mu m$ was significantly higher at 360 days than at 14 days, meaning an increase in porosity over that period.

When comparing SG28-3 and SS28-3, it is interesting to see that the general shape of the curves are incredibly similar in shape. SG28-3 has a greater proportion of pores at approximately $0.5\mu m$ than SS28-3, although the latter does also see a peak at this pore size. Both samples also saw a peak at $8 - 9\mu m$ though in this instance, SS28-3 had the higher proportion.

It is interesting to see the 6-10% difference in accessible porosity of the limestone aggregate mortars and silicate sand mortars at the same 360 day curing period. This indicates that aggregate type significantly impacts the ability of CO_2 to penetrate into the sample. This could be the reason for the lack of homogeneity evidenced in the SEM images for standard sand samples. The less porous nature of the silicate aggregate is the most likely explanation for the overall lower accessible porosity in the samples; although differences in quantity of carbonated binder may also have an impact. The fact that the limestone aggregate mortars have a higher compressive strength than the silicate sand mortars, despite having a higher porosity (and subsequently, thinner pore walls), suggests that factors such as binder/aggregate

bond or quantity of $CaCO_3$ (excluding aggregate) could be responsible.

6.3.9 Mortar micro-structure using SEM

For the carbonated samples examined (Figures 5.46-5.48), which are the limestone aggregate mortars, the homogeneity of the mixture and the fact that only small areas of aggregate are visible suggests that the binder/aggregate bond is sound. Conversely, Figure 5.49 clearly has discontinuity at the binder/aggregate interface, which suggests a weakness that would lead to failure has occurring at the binder/aggregate interface rather than through the binder or through the aggregate. For the 1:2 Portland aggregate sample with 'as supplied' grading at 14 days curing (Figures 5.65, pitting was evident on the fracture surface. This suggests that the interface may have been weaker than was seen in the other mixes. Of the three limestone aggregate mortars at 14 days curing, P14-2 a.s was in fact the weakest in compression; it also had the lowest proportion of water in relation to binder, with the exception of the Standard sand mix. Portland aggregate also exhibited the highest porosity of all the aggregates (49.9%), which may be a contributing factor to lower strength. It is possible that the highly porous aggregate has absorbed some of the water used in mixing, thus creating a drier mix where the binder is less able to adhere to the aggregate and create a strong bond.

Micro-cracking observed in SG360-3 a.s (Figure 5.63) could be due to a low proportion of water in relation to binder, which is similar to that of P14-2 a.s.

It is possible that the micro-cracks prevented larger cracks from appearing, thus contributing to a good compressive strength. If the cracks were at the binder/aggregate interface, the mortar would be expected to be weaker.

One possible reason for this is that since the silicate aggregate has very low porosity, CO_2 movement can be assumed to be lower around the aggregate. Given that the sample as a whole has a higher porosity than the aggregate itself, this can be attributed to the binder, suggesting that carbonation has occurred preferentially in the binder matrix rather than around the aggregate. Due to the fact that a mortar's compressive strength is higher when when binder, water and aggregate work together as a composite, the lack of binder/aggregate bond means that the compressive stresses are effectively acting upon the binder alone, leading to lower strengths.

7 Conclusions

There are a number of conclusions that can be drawn as a result of the research undertaken. It is clear that the different aggregates used do not have the same impact on air lime mortars.

Phase 1 of the research aimed to analyse the flexural and compressive strengths of air lime mortars with a range of limestone aggregates, and a silicate aggregate for comparison. Three different B/Ag ratios were used, in order to find the optimum mix that would yield the highest strength, in particular in compression. The silicate (Standard sand) mixes were weaker in compression than the limestone aggregate mixes; this was particularly noticeable with the 1:2 and 1:3 mixes. Interestingly, Standard sand mixes were not seen to have lower flexural strengths for any of the mixes tested. SEM images show that there are differences in the mixes on a micro-structural level; most significantly, Standard sand mixes exhibit an inferior binder/aggregate bond. Phase 1 showed that there was a need to continue work into Phase 2, which narrowed down the number of aggregates and involved more in depth testing.

Phase 2 revealed a number of things as a result of flexural and compressive strength testing, phenolphthalein staining, mercury intrusion porosimetry, thermogravimetric analysis, scanning electron microscopy.

SEM images of the individual aggregates revealed that there are notable differences on the aggregate surface, with smaller particles appearing to 'stick' to the larger aggregate particles on the limestone aggregates, while the Standard sand appears smoother and more angular. It is thought that this effective roughness of the aggregate surface may contribute to a better binder/aggregate bond and consequently a higher compressive strength.

Furthermore, all aggregates were found to have a different pore size distribution and porosity, determined by MIP. The higher porosity of the limestone aggregates leads to easier access for CO_2 in the mortar samples, which could be cause for a greater amount of carbonation than the silicate sand mortar samples.

TG analysis on the aggregates shows that Portland and Stoke Ground have a very similar mass loss percentage (approx. 40%), meaning a similar $CaCO_3$ content, while Ham Hill has around half as much mass loss (22%).

Generally speaking, 1:2 mixes performed better mechanically than the 1:3 mixes, which may have been down to more aggregate surface area connecting with binder, creating more potential places for the mortar to fail.

Stoke Ground and Portland aggregate mortars were consistently strong in compression for all mixes and throughout all curing periods, while Standard sand mortars were found to be mostly the weaker mixes (with a couple of exceptions where Ham Hill mortars were weaker). The latter occurred despite mixes having a lower water content to achieve the desired flow. Ham Hill mortars were consistently weaker than Portland and Stoke Ground mortars respectively; based on the TG results of the individual aggregates, it is thought that the lower $CaCO_3$ content of the Ham Hill aggregate may have contributed to the lower compressive strengths observed in the Ham Hill mortars. Furthermore, the Ham Hill aggregate itself may have been weaker than the other aggregates or had not formed as strong a bond with the binder.

Strength increases over time did not tend to occur past 90 days curing, and sometimes the strength saw a decrease after this time. Most of the samples were 'fully' carbonated by 90 days according to the phenolphthalein indicator so a strength increase would not necessarily be expected but a decrease in strength was not expected. There are a number of possible reasons, including but not limited to, human error, increase in porosity after 90 days, or an increase in cracking in the samples (although with the Stoke Ground mortars, cracking does not appear to have had a negative impact on strength). It is important to know whether this strength decrease after 90 days would continue as the mortar continues to age; while a continual strength increase like that seen with NHL mortars is not desirable for restoration/conservation work, a strength decrease would be similarly undesirable.

Carbonation depth does not appear to relate to compressive strength; while both do increase over time, they do not increase at the same rate. However, it is worth considering that other factors might mask the true relationship between carbonation depth and compressive strength. For example, the bond between binder and aggregate.

MIP analysis indicates that carbonation of samples leads to a higher concentration of medium sized pores for many of the samples tested, for example H-2 between 14 and 360 days, and SG-3 a.s between 0 and 360 days. Over time, Stoke Ground sees a decrease in both smaller and larger pores, and between 14 and 28 days, a decrease in medium sized pores as well. Furthermore, analysis of the hysteresis of the samples does not point to presence of any ink bottle pores.

Both SG-3 a.s and H-2 a.s samples observe a linear relationship between strength and density if the 14 day values are removed; at this early stage not all drying may have taken place, leading to higher density. It is thought that mass would stabilise after the drying period.

From undertaking TG analysis on some samples, it was found that the use of different aggregates has an impact on sample mass loss (due to breakdown of components), since different losses were observed for mixes that had the same specifications apart from water content. Following a trend throughout this research, Portland and Stoke Ground again showed similar mass losses.

SEM images show differences at the binder/aggregate interface with the different aggregates, in particular between the Standard sand mixes and limestone aggregate mixes respectively. The binder/aggregate interface is a key aspect affecting mortar strength. Limestone aggregate

mortars have a more consistent bond around the aggregate particles that is not seen in the Standard sand mortars. Micro-cracks and 'pitting' were also evident in some of the samples, as well as calcite crystals.

It can be concluded that the most preferable B/Ag ratio for achieving higher compressive strengths is 1:2. Whilst there is only a slight overall difference in the performance of the mortars due to particle size distribution, it appears that 'as supplied' samples provide slightly better results. As Ham Hill aggregate generally resulted in the weakest of the limestone aggregate mortars (and sometimes overall), it is not recommended that it is used when trying to increase air lime mortar strength; Stoke Ground is arguably the most favourable option from the aggregates used in this study.

The findings of this research have shown that there are benefits to using air lime mortars with limestone aggregates for restoration and conservation work. The compressive strengths achieved can be similar to those of NHL mortars, yet they will not continue to increase in strength over time. Furthermore, porosity in the samples is sufficient to allow water egress from a building, ensuring moisture does not become problematic. Since air lime mortar re-absorbs a significant quantity of CO_2 , the mixes used here also go some way to reducing the UK's carbon footprint. Additionally, the limestone aggregates were sourced as waste from the cutting process, further enhancing the sustainable credentials.

8 Recommendations for further work

Based on the findings from this research, there are number of recommendations that would be beneficial to in order to gain a more thorough understanding of why calcitic aggregates can produce higher strength mortars than silicate aggregates.

One important finding of this research is that water content does appear to impact mortar strength, but only in some instances. Consequently, it would be advantageous to explore a number of different w/b ratios for the mixes used in this study.

Since it is possible that the aggregate strength has impacted the final mortar strength of the Ham Hill mortars, mechanical testing of the aggregates would provide some extra clarity.

Further work could focus on 1:2 mixes, due to their overall superior performance; TGA of 1:2 mixes at a wide number of curing periods would enable a deeper insight into the differences in carbonation between the limestone aggregate and Standard sand mortars respectively.

Due to the finding that strength increase seemed to drop off somewhere between 90 and 180 days curing, it would be advantageous to add a further curing period (or periods) in between, at say 120 and 150 days, in order to determine where specimens reach their highest strength.

Finally, given the importance of the microscopy images on analysing the binder/aggregate bond, it would be beneficial to set samples in resin in order to achieve better quality images.

9 References

- Abell, A.B., Willis, K.L., and Lange, D.A. Mercury Intrusion Porosimetry and Image Analysis of Cement-Based Materials. *Journal of Colloid and Interface Science*, 211:39–44, 1999.
- Abell, Anne B. and Nichols, John M. Investigation of the rheology and microstructure of hydrated lime and sand for mortars. In *ASTM Special Technical Publication*, number 1432, pages 23 – 36, 2002.
- Ambrosi, M., Dei, L., Giorgi, R., Neto, C., and Baglioni, P. Colloidal particles of $\text{Ca}(\text{OH})_2$: Properties and applications to restoration of frescoes. *Langmuir*, 17(14):4251 – 4255, 2001.
- Arandigoyen, M. and Alvarez, J.I. Blended pastes of cement and lime: Pore structure and capillary porosity. *Applied Surface Science*, 252(23):8077 – 8085, 2006.
- Arandigoyen, M. and Alvarez, J.I. Pore structure and mechanical properties of cement-lime mortars. *Cement and Concrete Research*, 37(5):767 – 775, 2007.
- Arandigoyen, M., Bernal, J.L. Perez, Lopez, M.A. Bello, and Alvarez, J.I. Lime-pastes with different kneading water: Pore structure and capillary porosity. *Applied Surface Science*, 252(5):1449 – 1459, 2005.
- Arandigoyen, M., Bicer-Simsir, B., Alvarez, J.I., and Lange, D.A. Variation of microstructure with carbonation in lime and blended pastes. *Applied Surface Sciences*, 252:7562–7571, 2006.
- Arizzi, A. and Cultrone, G. Aerial lime-based mortars blended with a pozzolanic additive and different admixtures: A mineralogical, textural and physical-mechanical study. *Construction and Building Materials*, 31:135 – 143, 2012a.
- Arizzi, A. and Cultrone, G. The difference in behaviour between calcitic and dolomitic lime mortars set under dry conditions: The relationship between textural and physical-mechanical properties. *Cement and Concrete Research*, 42:818–826, 2012b.
- Arizzi, A., Hendrickx, R., Cultrone, G., and Van Balen, K. Differences in the rheological properties of calcitic and dolomitic lime slurries: influence of particle characteristics and practical implications in lime-based mortar manufacturing. *Materials de Construcción*, 62(306):231–250, 2012a.
- Arizzi, A., Viles, H., and Cultrone, G. Experimental testing of the durability of lime-based mortars used for rendering historic buildings. *Construction and Building Materials*, 28(1): 807 – 818, 2012b.

- Ashall, G., Butlin, R.N., Teutonico, J.M., and Martin, W. Development of lime mortar formulations for use in historic buildings. In *Proceedings of the 1996 7th International Conference on Durability of Building Materials and Components, 7DBMC*, volume 1, pages 352 – 352, 1996.
- Ashurst, J. and Dimes, F.G. *Conservation of Building and Decorative Stone*. Oxford; Woburn, Mass.: Butterworth-Heinemann, 1998.
- Bauer, E., de Sousa, J.G.G., Guimaraes, E.A., and Silva, F.G.S. Study of the laboratory Vane test on mortars. *Building and Environment*, 42(1):86 – 92, 2007.
- Benachour, Y., Davy, C.A., Skoczylas, F., and Houari, H. Effect of a high calcite filler addition upon microstructural, mechanical, shrinkage and transport properties of a mortar. *Cement and Concrete Research*, 38(6):727 – 736, 2008. ISSN 00088846.
- Binici, H., Kaplan, H., and Yilmaz, S. Influence of marble and limestone dusts as additives on some mechanical properties of concrete. *Scientific Research and Essay*, 9:372–379, 2007.
- BIS, . Estimating the amount of CO2 emissions that the construction industry can influence. Technical report, Department for Business Innovation & Skills, 2010.
- Blanco-Varela, M.T, Aguilera, J, Martinez-Ramrez, S, Puertas, F, Palomo, A, Sabbioni, C, Zappia, G, Riontino, C, Balen, K Van, and Toumbakari, E.E. Thaumasite formation due to atmospheric SO₂hydraulic mortar interaction. *Cement and Concrete Composites*, 25(8):983 – 990, 2003. doi: [http://dx.doi.org/10.1016/S0958-9465\(03\)00122-7](http://dx.doi.org/10.1016/S0958-9465(03)00122-7).
- Boffey, G. and Hirst, E. The use of pozzolans in lime mortar. *Architectural Conservation*, 5(3): 34–42, 1999.
- BS EN 1015-3 *Methods of test for mortar for masonry - Part 3: Determination of consistence of fresh mortar (by flow table)*. British Standards Institution, 1999.
- Bromblet, P. Properties and durability of air lime-based mortars for limestone repairs on monuments. In Bartos, P., Groot, C., and Hughes, J.J., editors, *International RILEM Workshop on Historic Mortars: Characteristics and Tests*, 1999.
- BSI, . *Methods of test for mortar for masonry - Part 3: Determination of consistence of fresh mortar (by flow table)*, 1999.
- BSI, . *Methods of test for mortar for masonry - Part 18: Determination of water absorption coefficient due to capillary action of hardened mortar*, 2002.
- Cabrera, J. and Rojas, M.F. Mechanism of hydration of the metakaolinlime-water system. *Cement and Concrete Research*, 31(2):177 – 182, 2001.
- Carlos, A., Masumi, I., Hiroaki, M., Maki, M., and Takahisa, O. The effects of limestone aggregate on concrete properties. *Construction and Building Materials*, 24(12):2363 – 2368, 2010.

- Casadio, F., Chiari, G., and Simon, S. Evaluation of Binder/Aggregate Ratios in Archaeological Lime Mortars with Carbonate Aggregate: A Comparative Assessment of Chemical, Mechanical and Microscopic Approaches. *Archaeometry*, 47(4):671–689, 2005.
- Cazalla, O., Rodriguez-Navarro, C, Sebastian, E., Cultrone, G., and De la Torre, M.J. Aging of lime putty: effects on traditional lime mortar carbonation. *Journal of the American Ceramic Society*, 83(5):1070 – 1076, 2000.
- Cerny, R., Kunca, A., Tydlitat, V., Drchalova, J., and Rovnanikova, P. Effect of pozzolanic admixtures on mechanical, thermal and hygric properties of lime plasters. *Construction and Building Materials*, 20(10):849 – 857, 2006.
- Chelazzi, D., Poggi, G., Jaidar, Y., Toccafondi, N., Giorgi, R., and Baglioni, P. Hydroxide nanoparticles for cultural heritage: Consolidation and protection of wall paintings and carbonate materials. *Journal of Colloid and Interface Science*, 392(1):42 – 49, 2013.
- Chever, L., Pavia, S., and Howard, R. Physical properties of magnesian lime mortars. *Materials and Structures/Materiaux et Constructions*, 43(1-2):283 – 296, 2010.
- Cizer, O., Van Balen, K., Van Gemert, D., and Elsen, J. Carbonation and hydration of calcium hydroxide and calcium silicate binders with rice husk ash. In *2nd International RILEM Symposium on Advances in Concrete through Science and Engineering*, volume 2, pages 309–321, 2006.
- Cizer, O., Van Balen, K., Van Gemert, D., and Elsen, J. Blended lime-cement mortars for conservation purposes: Microstructure and strength development. In *Structural Analysis of Historic Construction: Preserving Safety and Significance - Proceedings of the 6th International Conference on Structural Analysis of Historic Construction, SAHC08*, volume 2, pages 965 – 972, 2008.
- Cultrone, G., Sebastian, E., and Huertas, M. Ortega. Forced and natural carbonation of lime-based mortars with and without additives: Mineralogical and textural changes. *Cement and Concrete Research*, 35(12):2278 – 2289, 2005a.
- Cultrone, G., Sebastian, E., and Huertas, M. Ortega. Forced and natural carbonation of lime-based mortars with and without additives: Mineralogical and textural changes. *Cement and Concrete Research*, 35(12):2278 – 2289, 2005b.
- D’Armada, P. and Hirst, E. Nano-lime for consolidation of plaster and stone. *Journal of Architectural Conservation*, 18:63–80, 1995.
- Davison, J.I. Effect of Air Content on Durability of Cement-lime Mortars. *Durability of Building Materials*, 1:23–34, 1982.
- de Vekey, B. *Building masonry with lime-based bedding mortars*. Building Research Establishment, 2005.

- Degryse, P., Elsen, J., and Waelkens, M. Study of ancient mortars from Sagalassos (Turkey) in view of their conservation. *Cement and Concrete Research*, 32(9):1457 – 1463, 2002.
- Dheilly, R.M., Tudo, J., Sebaibi, Y., and Queneudec, M. Influence of storage conditions on the carbonation of powdered $\text{Ca}(\text{OH})_2$. *Construction and Building Materials*, 16(3):155 – 161, 2002.
- Duran, A., Navarro-Blasco, I., Fernandez, J.M., and Alvarez, J.I. Long-term mechanical resistance and durability of air lime mortars with large additions of nanosilica. *Construction and Building Materials*, 58:147 – 158, 2014.
- Ellis, S., Lawrence, M., and Walker, P. A Critical Review of the Effect of Calcitic Aggregate on Air Lime Mortar. In *International Congress on Materials & Structural Stability*, 2013.
- Elsen, J. Microscopy of historic mortars: a review. *Cement and Concrete Research*, 36(8):1416 – 1424, 2006.
- Farey, M., Holmes, S., and Livesey, M. *Hydraulic lime mortar for stone, brick and block masonry: a best practice guide*. Shaftesbury: Donhead, 2003.
- Fortes-Revilla, and C. Blanco Varela, M.T. Influence of the water-repellent treatment on the properties lime and lime pozzolan mortars. *Materials de Construcción*, 1, 2001.
- Fragata, A. and Veiga, R. Air Lime Mortars: the Influence of Calcareous Aggregate and Filler Addition. In *Materials Science Forum*, 2010.
- Freedland, J.D. and Gerns, E.A. Lime mortars: Two recent case studies. In *International Building Lime Symposium*, 2005.
- Frías, M., Sánchez de Rojas, M.I., and Cabrera, J. The effect that the pozzolanic reaction of metakaolin has on the heat evolution in metakaolin-cement mortars. *Cement and Concrete Research*, 30(2):209 – 216, 2000.
- Gallucci, E. and Scrivener, K. Crystallisation of calcium hydroxide in early age model and ordinary cementitious systems. *Cement and Concrete Research*, 37(4):492 – 501, 2007.
- Gaze, M.E. and Crammond, N.J. Formation of thaumasite in a cement:lime:sand mortar exposed to cold magnesium and potassium sulfate solutions. *Cement and Concrete Composites*, 22(3):209 – 222, 2000.
- Giesche, H. Mercury porosimetry: A general (practical) overview. In *Particle and Particle Systems Characterization*, volume 23, pages 9 – 19, 2006.
- Giorgi, R., Chelazzi, D., and Baglioni, P. Nanoparticles of calcium hydroxide for wood conservation. The deacidification of the Vasa warship. *Langmuir*, 21(23):10743 – 10748, 2005.

- Gonçalves, T.D., Rodrigues, J.D., and Abreu, M.M. Evaluating the salt content of salt-contaminated samples on the basis of their hygroscopic behaviour: Part II: experiments with nine common soluble salts. *Journal of Cultural Heritage*, 7(3):193 – 200, 2006.
- Green, K.M., Carter, Margaret A., Hoff, W.D., and Wilson, M.A. Effects of lime and admixtures on the water-retaining properties of cement mortars. *Cement and Concrete Research*, 29(11): 1743 – 1747, 1999.
- Gunn, R. Listen to the mason: Portland cement-lime Type N mortar (1:1:6) provides the necessary workability and strength. In *International Building Lime Symposium*, 2005.
- Hansen, E., Tagle, A., Erder, E., Baron, S., Connell, S., Rodriguez-Navarro, C., and Van Balen, K. Effects of ageing on lime putty. In *International RILEM Workshop on Historic Mortars: Characteristics and Test*, 1999.
- Hayen, R., Van Balen, K., and Van Gemert, D. The influence of production processes and mortar compositions on the properties of historical mortars. In *9th Canadian Masonry Symposium*, 2001.
- Hendrickx, R., Minet, J., Van Balen, K., and Van Gemert, D. Workability of mortars with building lime: assessment by a panel of masons versus lab testing. In *International Brick and Block Masonry Conference*, 2008a.
- Hendrickx, R., Van Balen, K., and Van Gemert, D. Assessing workability of mortar by means of rheological parameters and desorptivity. volume 2, pages 973 – 979, 2008b.
- Hendrickx, R., Van Balen, K., and Van Gemert, D. Yield stress measurement of mortar using geotechnical techniques. In *3rd International RILEM symposium on rheology of cement suspensions such as fresh concrete*, 2009.
- Henriques, F.M.A. and Charola, A.E. Development of Lime Mortars with Improved Resistance to Sodium Chloride Crystallization. In *9th International Congress on Deterioration and Conservation of Stone*, 2000.
- Houst, Y.F. and Wittmann, F.H. Depth profiles of carbonates formed during natural carbonation. *Cement and Concrete Research*, 32(12):1923 – 1930, 2002.
- Isebaert, A., De Boever, W., Descamps, F., J. ad DumonDils, M., De Schutter, G., Van Ranst, E., Cnudde, V., and Van Parys, L. Pore-related properties of natural hydraulic lime mortars: and experimental study. *Materials and Structures*.
- Izaguirre, A., Lanas, J., and Alvarez, J.I. Ageing of lime mortars with admixtures: Durability and strength assessment. *Cement and Concrete Research*, 40(7):1081 – 1095, 2010.
- Izaguirre, A., Lanas, J., and Alvarez, J.I. Effect of a polypropylene fibre on the behaviour of aerial lime-based mortars. *Construction and Building Materials*, 25(2):992 – 1000, 2011.

- Kalagri, A., Karatasios, I., and Kilikoglou, V. The effect of aggregate size and type of binder on microstructure and mechanical properties of NHL mortars. *Construction and Building Materials*, 53:467 – 474, 2014.
- Kazmierczak, C.S., Metz, D.A., and Fröhlich, D.G. Influence of Water Absorption in the Performance of Mortars Made with Manufactured Fine Aggregates. In *Second International Conference on Sustainable Construction Materials and Technologies*, 2010.
- Kenai, S., Menadi, B., Attar, A., and Khatib, J. Effect of Crushed Limestone Fines on Strength of Mortar and Durability of Concrete. 2008.
- Khatib, J.M. and Wild, S. Sulphate resistance of metakaolin mortar. *Cement and Concrete Research*, 28(1):83 – 92, 1998.
- Lanas, J. and Alvarez, J.I. Masonry repair lime-based mortars: Factors affecting the mechanical behavior. *Cement and Concrete Research*, 33(11):1867 – 1876, 2003.
- Lanas, J., Bernal, J.L. Perez, Bello, M.A., and Galindo, J.I. Alvarez. Mechanical properties of natural hydraulic lime-based mortars. *Cement and Concrete Research*, 34(12):2191 – 2201, 2004.
- Lanas, J., Sirera, R., and Alvarez, J.I. Compositional changes in lime-based mortars exposed to different environments. *Thermochimica Acta*, 429(2):219 – 226, 2005.
- Lanas, J., Sirera, R., and Alvarez, J.I. Study of the mechanical behavior of masonry repair lime-based mortars cured and exposed under different conditions. *Cement and Concrete Research*, 36(5):961 – 970, 2006.
- Lawrence, M. *A Study of Carbonation in Non-hydraulic Lime Mortars*. PhD thesis, 2006.
- Lawrence, P., Cyr, M., and Ringot, E. Mineral admixtures in mortars effect of type, amount and fineness of fine constituents on compressive strength. *Cement and Concrete Research*, 35(6):1092 – 1105, 2005.
- Lawrence, R.M., Mays, T.J., Rigby, S.P., Walker, P., and D’Ayala, D. Effects of carbonation on the pore structure of non-hydraulic lime mortars. *Cement and Concrete Research*, 37(7): 1059 – 1069, 2007.
- Lawrence, R.M.H. and Walker, P. The impact of the water/lime ratio on the structural characteristics of air lime mortars. In *Structural Analysis of Historic Construction: Preserving Safety and Significance - Proceedings of the 6th International Conference on Structural Analysis of Historic Construction, SAHC08*, volume 2, pages 885 – 889, Bath, United kingdom, 2008.
- Lawrence, R.M.H., Mays, T.J., Walker, P., and D’Ayala, D. Determination of carbonation profiles in non-hydraulic lime mortars using thermogravimetric analysis. *Thermochimica Acta*, 444(2):179 – 189, 2006.

- Levin, E.M., Clarke, W.F., and Wells, L.S. *Plasticity and water retentivity of hydrated limes for structural purposes*. U.S Department of Commerce, National Bureau of Standards, 1956.
- Limetec, . Limetec Mortars, Plasters and Renders. <http://limetec.co.uk/wp-content/uploads/2015/12/Limetec-brochure-web-2015.pdf>, 2015.
- Lothenbach, B., Le Saout, G., Gallucci, E., and Scrivener, K. Influence of limestone on the hydration of Portland cements. *Cement and Concrete Research*, 38(6):848 – 860, 2008.
- Maravelaki-Kalaitzaki, P. Hydraulic lime mortars with siloxane for waterproofing historic masonry. *Cement and Concrete Research*, 37(2):283 – 290, 2007.
- Maravelaki-Kalaitzaki, P., Bakolas, A., Karatasios, I., and Kilikoglou, V. Hydraulic lime mortars for the restoration of historic masonry in Crete. *Cement and Concrete Research*, 35(8):1577 – 1586, 2005.
- Marie-Victoire, E. and Bromblet, P. A new generation of cement-based renderings: an alternative to traditional lime-based mortars? In *International RILEM Workshop on Historic Mortars: Characteristics and Tests*, 1999.
- Marques, S.F., Ribeiro, R.A., Silva, L.M., Ferreira, V.M., and Labrincha, J.A. Study of rehabilitation mortars: Construction of a knowledge correlation matrix. *Cement and Concrete Research*, 36(10):1894 – 1902, 2006.
- Martinez-Ramirez, S., Puertas, F., and Blanco Varela, M.T. Carbonation process and properties of a new lime mortar with added sepiolite. *Cement and Concrete Research*, 25(1):39 – 50, 1995.
- Martinez-Ramirez, S., Puertas, F., Blanco-Varela, M.T., and Thompson, G.E. Effect of dry deposition of pollutants on the degradation of lime mortars with sepiolite. *Cement and Concrete Research*, 28(1):125 – 133, 1998.
- Menadi, B., Kenai, S., Khatib, J., and Ait-Mokhtar, A. Strength and durability of concrete incorporating crushed limestone sand. *Construction and Building Materials*, 23:625–633, 2009.
- Middendorf, B., Hughes, J.J., Callebaut, K., Baronio, G., and Papayianni, I. Investigative methods for the characterisation of historic mortars - Part 1: Mineralogical characterisation. *Materials and Structures/Materiaux et Constructions*, 38(282):761 – 769, 2005a.
- Middendorf, B., Kraus, K., and Ott, C. Influence of the Fines in Natural Sands as Pozzolanic Components on the Interpretation of the Acid-Soluble Silica Content of Historic Lime Mortars. 2005b.
- Middendorf, B., Martirena, J.F., Gehrke, M., and Day, R.L. Lime Pozzolan Binders: An Alternative to OPC? In *International Building Lime Symposium*, 2005c.

- Miller, P., Rabinowitz, M., and Sembrat, J. The use and effectiveness of dispersed hydrated lime in conservation of monuments and historic structures. In *International Building Lime Symposium*, 2005.
- Moncada, A.L. and Godbey, R.J. Lime-pozzolan masonry mortar. In *International Building Lime Symposium*, 2005.
- Moorehead, D.R. Cementation by the carbonation of hydrated lime. *Cement and Concrete Research*, 16(5):700 – 708, 1986. ISSN 0008-8846.
- Moropoulou, A., Bakolas, A., and Aggelakopoulou, E. Evaluation of pozzolanic activity of natural and artificial pozzolans by thermal analysis. *Thermochimica Acta*, 420(12):135 – 140, 2004.
- Moropoulou, A., Bakolas, A., Moundoulas, P., Aggelakopoulou, E., and Anagnostopoulou, S. Strength development and lime reaction in mortars for repairing historic masonries. *Cement and Concrete Composites*, 27(2):289 – 294, 2005.
- Mosquera, M.J., Benitez, D., and Perry, S.H. Pore structure in mortars applied on restoration: Effect on properties relevant to decay of granite buildings. *Cement and Concrete Research*, 32(12):1883 – 1888, 2002.
- Mosquera, M.J., Silva, B., Prieto, B., and Ruiz-Herrera, E. Addition of cement to lime-based mortars: Effect on pore structure and vapor transport. *Cement and Concrete Research*, 36(9):1635 – 1642, 2006.
- Naik, T.R., Kraus, R.N., and Chun, Y-m. Effect of different types of aggregates on autogenous and drying shrinkage of concrete. In *1st International Conference on Advanced Construction Materials*, 2006.
- Neville, A.M. and Brooks, J.J. *Concrete Technology*. Longman Scientific & Technical, 1987.
- Nunes, C. and Slizkova, Z. Hydrophobic lime based mortars with linseed oil: Characterization and durability assessment. *Cement and Concrete Research*, 61-62:28 – 39, 2014.
- Papayianni, I. and Stefanidou, M. Strength-porosity relationships in lime-pozzolan mortars. *Construction and Building Materials*, 20(9):700 – 705, 2006.
- Pavia, S. and Hanley, R. Flexural bond strength of natural hydraulic lime mortar and clay brick. *Materials and Structures/Materiaux et Constructions*, 43(7):913 – 922, 2010.
- Pavia, S. and Toomey, B. Influence of the aggregate quality on the physical properties of natural feebly-hydraulic lime mortars. *Materials and Structures/Materiaux et Constructions*, 41(3): 559 – 569, 2008.
- Pavia, S. and Treacy, E. A comparative study of the durability and behaviour of fat lime and feebly-hydraulic lime mortars. *Materials and Structures/Materiaux et Constructions*, 39(287):391 – 398, 2006.

- Pavia, S., Fitzgerald, B., and Howard, R. Evaluation of properties of magnesian lime mortar. *Advances in Architecture Series*, 20:375 – 384, 2005.
- Philippi, P.C., Yunes, P., Rosendo, F., Fernandes, C.P., and Magnani, F.S. Microstructure of porous building materials: Study of a cement and lime mortar. *Transport in Porous Media*, 14(3): 219 – 245, 1994.
- Poitevin, P. Limestone aggregate concrete, usefulness and durability. *Cement and Concrete Composites*, 21(2):89 – 97, 1999.
- Rodriguez-Navarro, C., Ruiz-Agudo, E., Ortega-Huertas, M., and Hansen, E. Nanostructure and irreversible colloidal behavior of $\text{Ca}(\text{OH})_2$: Implications in cultural heritage conservation. *Langmuir*, 21(24):10948 – 10957, 2005.
- Rojas, M.F. and Cabrera, J. The effect of temperature on the hydration rate and stability of the hydration phases of metakaolin-lime-water systems. *Cement and Concrete Research*, 32(1):133 – 138, 2002.
- Ruiz-Alsop, R.N. and Rochelle, G.T. Effect of Deliquescent Salt Additives on the Reaction of SO_2 with $\text{Ca}(\text{OH})_2$. In *ACS Symposium Series, American Chemical Society*, volume 319, pages 208–222, 1986.
- Sabbioni, C., Zappia, G., Riontino, C., Blanco-Varela, M.T., Aguilera, J., Puertas, F., Balen, K., Van, and Toumbakari, E.E. Atmospheric deterioration of ancient and modern hydraulic mortars. *Atmospheric Environment*, 35(3):539 – 548, 2001.
- Salvadori, B. and Dei, L. Synthesis of $\text{Ca}(\text{OH})_2$ nanoparticles from diols. *Langmuir*, 17(8): 2371 – 2374, 2001.
- Sánchez-Moral, S., Luque, L., Cañaveras, J.-C., Soler, V., and Aparicio-García-Guinea, A. Limepozzolana mortars in Roman catacombs: composition, structures and restoration. *Cement and Concrete Research*, 35(8):1555 – 1565, 2005.
- Scannell, S., Lawrence, M., and Walker, P. Impact of aggregate type on air lime mortar properties. In *International Conference on Sustainability in Energy and Buildings*, 2014a.
- Scannell, S., Lawrence, M., and Walker, P. A Study of the Impacts of Calcitic Aggregates on the Properties of Air Lime Mortar. In *9th International Masonry Conference*, 2014b.
- Scannell, S., Lawrence, M., and Walker, P. Assessing the Impact of Aggregate Type on Air Lime Mortar Properties Using Scanning Electron Microscopy. *Journal of Civil Engineering and Architecture*, 10:139–147, 2016a.
- Scannell, S., Lawrence, M., and Walker, P. Analysis of the impact of calcitic aggregates on the properties of air-lime mortar. *The Journal of the Building Limes Forum*, 23:192–200, 2016b.
- Schäfer, J. and Hilsdorf, H.K. *Ancient and new lime mortars - the correlation between their composition structure and properties*. E. & F.N. Spon, 1993.

- Schuller, M.P., Van Der Hoeven, R.S.K., and Thomson, M.L. Comparative investigation of plastic properties and water permeance of cement-lime mortars and cement-lime replacement mortars. *ASTM Special Technical Publication*, (1352):145 – 158, 1999.
- Seabra, M.P., Labrincha, J.A., and Ferreira, V.M. Rheological behaviour of hydraulic lime-based mortars. *Journal of the European Ceramic Society*, 27(2-3):1735 – 1741, 2007.
- Sebaibi, Y., Dheilily, R.M., and Queneudec, M. Study of the water-retention capacity of a lime-sand mortar: Influence of the physicochemical characteristics of the lime. *Cement and Concrete Research*, 33(5):689 – 696, 2003.
- Shao, Y., Lefort, T., Moras, S., and Rodriguez, D. Studies on concrete containing ground waste glass. *Cement and Concrete Research*, 30(1):91 – 100, 2000.
- Shi, C. Studies on several factors affecting hydration and properties of lime-pozzolan cements. *Journal of Materials in Civil Engineering*, 13(6):441 – 445, 2001.
- Stefanidou, M. and Papayianni, I. The role of aggregates on the structure and properties of lime mortars. *Cement and Concrete Composites*, 27(9-10):914 – 919, 2005.
- Stewart, J., Glover, R., Houston, J., Seeley, N., and Proudfoot, T. Field and laboratory assessment of lime-based mortars. *Journal of Architectural Conservation*, 7, 2001.
- Strotmann, R.. Dispersed hydrated lime for the preservation and conservation of stone monuments. *9th International Congress on Deterioration & Conservation of Stone*, pages 1867 – 1876, 2000.
- Tasong, W.A., Lynsdale, C.J., and Cripps, J.C. Aggregate-cement paste interface: Part I. Influence of aggregate geochemistry. *Cement and Concrete Research*, 29(7):1019 – 1025, 1999.
- J.M.Teutonico, Ashall G. Garrod E. and Yates, T. A Comparative Study of Hydraulic Lime-based mortars. *Bartos et al., op. cit.*, pages 339 – 349, 2000.
- Thomson, M. Plasticity, water retention, soundness and sand carrying capacity: what a mortar needs. In *International RILEM Workshop on Historic Mortars: Characteristics and Tests*, 1999.
- Thomson, M. Properties of lime mortar. *Structure Magazine*, pages 26–29, 2005.
- Tsimas, S. and Raikos, K. Lime, an Irreplaceable Mortar Constituent. *Zement-Kalk-Gips*, 48: 1886–1893, 1995.
- Tuncoku, S.S. and Caner-Saltik, E.N. Opal-A rich additives used in ancient lime mortars. *Cement and Concrete Research*, 36(10):1886 – 1893, 2006.
- Ubbriaco, P. and Tasselli, F. Study of the hydration of lime-pozzolan binders. *Journal of Thermal Analysis and Calorimetry*, 52(3):1047 – 1054, 1998.

- Van Balen, K. Carbonation reaction of lime, kinetics at ambient temperature. *Cement and Concrete Research*, 35(4):647 – 657, 2005.
- Van Balen, K. and Sabbioni, C. Damage caused by SO_2 pollution on hydraulic mortars in ancient and modern monuments. *Luxembourg: European Communities*, pages 32–38, 2002.
- Van Balen, K. and Van Gemert, D. Modelling lime mortar carbonation. *Materiaux et constructions*, 27(171):393 – 398, 1994.
- Veiga, M. Rosario, Velosa, Ana, and Magalhaes, Ana. Experimental applications of mortars with pozzolanic additions: Characterization and performance evaluation. *Construction and Building Materials*, 23(1):318 – 327, 2009.
- Walker, D.D. The microscope and lime. In *Proceedings of the 4th International Conference on Cement Microscopy*, 1982.
- Westerholm, M., Lagerblad, B., Silfwerbrand, J., and Forssberg, E. Influence of fine aggregate characteristics on the rheological properties of mortars. *Cement and Concrete Composites*, 30(4):274 – 282, 2008.
- Winnefeld, F. and Böttger, K.G. How clayey fines in aggregates influence the properties of lime mortars. *Materials and Structures/Materiaux et Constructions*, 39(288):433 – 443, 2006.
- Ziegenbalg, G., Brummer, K., and Pianski, J. Nano-lime - a new material for the consolidation and conservation of historic mortars. In *2nd Conference on Historic Mortars*, 2010.

Appendices

A.0 Conference and journal papers

A.0.1 International Congress on Materials & Structural Stability

A Critical Review of the Effect of Calclitic Aggregate on Air Lime Mortar

S. Ellis¹, M. Lawrence² and P. Walker³

¹University of Bath, BRE Centre for Innovative Construction Materials, Architecture & Civil Engineering, Bath, UK

²University of Bath, BRE Centre for Innovative Construction Materials, Architecture & Civil Engineering, Bath, UK

³University of Bath, BRE Centre for Innovative Construction Materials, Architecture & Civil Engineering, Bath, UK

Abstract. In recent years, the importance of aggregate type on the properties of mortars has become increasingly recognised. In the context of restoration, it is particularly important to achieve the optimum properties that provide the best compatibility between the repair mortar and the existing masonry. With that in mind, the properties of the aggregate should be given priority when designing the repair mortar mix. A critical analysis of the current state of the art is presented, identifying the areas of research that have not yet been explored thoroughly. The role of calcitic aggregates in mortar is one such area, and the paper presented here examines the notion that calcitic aggregates cause an increase in the strength of lime mortar. The review establishes the limited amount of knowledge existing on the subject and seeks to determine methods that will enable validation of the claim.

1 Introduction

There are three primary constituents of mortar; binder, aggregate (usually siliceous) and water. Aggregates have been found to have an effect on the properties of mortar, which could be attributed to the mineralogy, shape, surface roughness and porosity.

In the past few years, the similarities/differences between the aggregate and mortar composition have been thought to impact the mortar's properties. Lanas and Alvarez (2003) [1] make reference to this regarding the use of calcitic aggregate in air lime mortar, stating that the similarities between binder matrix and aggregate structure could be responsible for the higher strengths observed with the calcitic aggregate.

Based on current findings from the literature, it is clear that a gap exists in the knowledge surrounding the impact of calcitic aggregates on the performance of air lime mortars. It has been found that the use of calcitic aggregate in air lime mortars exhibits a greater strength than was to be expected (Lanas and Alvarez, 2003), (Lawrence, 2006) and (Arizzi and Cultrone, 2012) [1-3], and this is worth exploring further as it may have a positive impact on the use of air lime mortars in industry.

The paper will give a brief description of the types of aggregate used in construction, namely silicate-based and limestone respectively. Further to this, the current state of the art is assessed, with a focus on what research has been done so far. Based on this, suggestions of important tests are put forward, with a justification for their usage and what is hoped to be achieved.

2 Types of aggregate

Aggregate makes up the majority of a mortar mix, by volume, and its primary role is in reducing the drying shrinkage which could otherwise lead to severe cracking.

The most commonly used aggregate in mortars is natural sand, which generally has high silica content. Since it has been found that the use of calcitic aggregates in lime mortars can result in higher mortar strengths, their use could become more commonplace, but it is expected that this would only occur when more is known about the mechanisms responsible for the higher strengths.

It is worth noting here that different types of limestone have a different composition and pore structure, and for the purpose of this study, the focus will be on the oolitic Bath Stone. Previous work by Lawrence (2006) [2] found that the use of oolitic aggregate produced mortars with superior properties when compared with the use of bioclastic aggregate (also calcitic); hence, the interest in Bath Stone.

2.1 Siliceous aggregate

Silica sand is often in the form of quartz and has the chemical composition SiO₂ (silicon dioxide). It is a hard, chemically inert material.

2.2 Calcitic aggregate

Calcitic aggregate can either compose of angular or rounded grains, and has the chemical composition CaCO_3 (calcite). There are many different forms of calcitic aggregate; for example Bath Stone is an oolitic variety. Oolitic grains are round in shape and are 0.25-2mm in diameter.

Lawrence (2006) [2] found that mortars made from crushed oolitic stone were four times as strong as those made using silicate aggregates. This could be due to the similar pore structure that exists between the aggregate and mortar respectively (Lanas and Alvarez, 2003) [1].

It is possible that if both aggregate and mortar have a similar porosity, CO_2 movement through the sample would be more constant, potentially leading to a faster and more complete carbonation.

3 Effect of aggregate type on mortar

It has been found by Lanas and Alvarez (2003) and Arizzi and Cultrone (2012) [1,3] that pure limestone aggregates yield mortars with higher strengths than those containing siliceous aggregates. This is possibly due to the limestone aggregate structure being similar to the calcitic binder matrix Lanas and Alvarez (2003) [1], which results in a more uniform mortar composition.

Conversely, Pavia and Toomey (2007) [4] suggest that the two sands containing the highest amount of calcite actually produced the weakest mortars. However, it has been suggested that the reason for this could be due to the use of chalk, where low mechanical strength is an intrinsic property. It was found that the highly siliceous aggregate produced the strongest mortar.

It was noted by Carlos et al. (2010) [5] that with an increase in the proportion of fine limestone in relation to cement and gravel content, shrinkage was reduced. This may also be the case for lime mortars.

Naik et al. (2006) [6] compared the use of crushed dolomitic limestone against crushed quartzite in concrete and found that at early ages, the limestone was weaker but at later stages, it was either a similar strength or higher than the quartzite. Dolomitic limestone was also observed to yield the lowest autogeneous shrinkage and lowest resistance to chloride ion penetration.

4 Scope for future investigation

Based on the limited amount of literature surrounding the effect of different types of aggregate (specifically limestone aggregate), and the lack of knowledge of the possible mechanisms surrounding what knowledge does exist, there is clearly a lot of scope for further investigations to be undertaken.

The following tests are thought to be the most appropriate when considering repair mortars comparing different aggregate types.

4.1 Rheology

4.1.1 Mortar flow

Mortar flow is of primary importance, particularly concerning ease of application for the mason. Measurement of flow involves looking at the mean diameter of the spread of mortar, after being subjected to vertical impacts on a flow table, as described in BS EN 1015-3: 1999 [7].

De Vekey (2005) [8] suggested that mortar should be able to flow freely, whilst still maintaining an adequate viscosity. Additionally, workability should remain for a few minutes after being applied to the stones, before starting to stiffen.

Bauer et al. (2007) [9] propose that there is a consensus suggesting that use of flow table is insufficient for defining workability, and as such, suggest also using the laboratory Vane test to measure yield stress to assist in the understanding of flow table results.

With the use of different aggregate types, it is expected that the water/binder (w/b) ratio will vary in order to keep the desired flow consistent. Porosity of the aggregate and surface roughness may contribute to this effect.

4.1.2 Setting time

The setting time of lime is considerably longer than that of cement and consequently, cement is favoured in modern construction. The more rapid setting time enables masons to be more efficient during construction.

Subsequently, if the setting time of lime could be reduced, this may promote its use in modern construction rather than primarily as a restoration mortar. It is possible that the unexplained strength increase with use of calcitic over silicate aggregate may be a result of more rapid carbonation. As a result, the setting time of the mortar may be reduced.

4.1.3 Yield stress

A common method of measuring the yield stress of mortar is the vane test (Bauer et al., 2007) and (Hendrickx et al., 2008) [9-10].

Hendrickx (2008) [11] underline the importance of yield stress in helping to understand flow table results when assessing workability.

Furthermore, research by Hendrickx et al. (2009) [12] found that air lime mortar has almost 3x higher yield stress than cement mortar.

No mention has been made, to the author's knowledge, of a relationship between yield stress and aggregate properties.

4.1.4 Drying shrinkage

It has been found that aggregate type can have an effect on drying shrinkage. Naik et al. (2006) [6] state that when using dolomitic limestone as aggregate, both autogeneous and drying shrinkage were reduced in comparison with

using river gravel or quartzite stone. It is worth bearing in mind that concrete was used in this study, however, this study can still prove useful as a comparison between different aggregate types.

In addition, Hughes et al. [13] showed that NHL 5 mortars made with silica sand observed increased shrinkage corresponding to an increase in fines content. Conversely, when carbonate (CaCO_3) sands were used, the highest shrinkage was found with the lowest fines content. Further investigations into the mechanisms would be beneficial.

4.2 Hardened mortar properties

4.2.1 Compressive/flexural strength

The primary focus of previous research on the use of limestone aggregates in mortar has involved looking at the compressive/flexural strengths of the mortars. Consequently, these tests are vital if any useful comparison is to be made, or claims are to be validated.

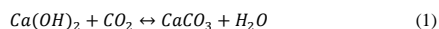
It is in general agreement that the compressive strength of air lime mortar increases more than double after the first 28 days up to a year of curing (Lanas and Alvarez, 2003) and (Moropoulou et al., 2005) [1,14].

Lanas and Alvarez (2003), Lawrence (2006) and Arizzi and Cultrone (2012) [1-3] found that pure limestone aggregates yield mortars with higher strengths than those containing siliceous aggregates. This is possibly due to the limestone aggregate structure being similar to the calcitic binder matrix (Lanas and Alvarez, 2003) [1], which results in a lack of discontinuity.

Arizzi and Cultrone (2012) [3] point out that there is a noticeable difference in the textural properties of calcareous and siliceous aggregates, with the former having more angular, rough and porous surface. It has been suggested that this impacts the degree of cohesion between aggregate surface and binder, possibly leading to the higher strengths exhibited with the use of calcareous aggregate.

4.2.2 Open porosity and pore size distribution

Carbonation is the primary chemical reaction that takes place in air lime mortars. The carbonation process describes the evolution of a mortar through chemical hardening, and for calcitic mortars it can be summarized by the following equation:



During the carbonation process, the microstructure changes, as a result of the transformation of portlandite into calcite.

Arandigoyen et al. (2006) [16] demonstrated the part carbonation plays in the porosity of mortar. Hydrated lime/cement mortars were used here, and a porosity decrease of around 10% was observed as a result of carbonation; it was found that fewer pores of $1\mu\text{m}$ can be found.

Furthermore, Lawrence et al. (2006) [17] assert that the pore size distribution is likely to have an influence on the rate of the carbonation reaction.

As a result, it is suggested that both open porosity and pore size distribution should be ascertained, in order to gain an insight into the pore structure. It is hoped that the influence of different types of aggregate on the carbonation of the mortar will be clearly evident.

With the exception of Lawrence et al. (2007) and Lanas et al. (2005) [18-19], it has been found that silicate sand is primarily used as aggregate. Consequently, a further at calcitic aggregates would be beneficial, in order to explore their effects on carbonation in more depth.

4.2.3 Elastic modulus

A mortar that has a high modulus of elasticity is not appropriate for conservation; the modulus of elasticity of cement mortar is almost 3x that of stone (Marevalaki-Kalaitzaki, 2007) [20]. On the other hand, lime mortars also have a plastic zone that is not present in cement-only mortars (Arandigoyen and Alvarez, 2007) [21]. As a result, they are much more capable of accommodating movements of ancient masonry.

Furthermore, aggregates can have an impact on the modulus of elasticity. Winnefeld and Böttger (2006) [22] note that when a higher proportion of clayey fines is incorporated, the elastic modulus is reduced by up to 50%. The authors suggest that this may be attributed to the increase in w/b ratio required.

Limestone aggregates were also found to have an impact on modulus of elasticity; a higher percentage in concrete leads to a higher elastic modulus Carlos et al. (2010) [5]. It was suggested that during the plastic stage, paste could have entered the pores of the aggregate. This could affect the elastic modulus. Although these findings were in concrete, it is possible that similar results would also be found with lime mortars, and it is therefore worth investigating further.

4.2.4 Salt crystallization

Resistance to salt crystallization is an important factor to consider when designing mortars for the repair of historic masonry, as soluble salts can be very damaging. Lime mortars have a particular tendency to suffer from salt crystallization due to their high porosity (Henriques and Charola, 2000) [23].

Again, the author has found no mention about whether the type of aggregate used has an effect on the mortar's resistance to salt crystallization. This is surprising, as it is evident that the type of lime binder was found to have an effect.

Pavia and Treacy (2006) [24] compared non-hydraulic and feebly-hydraulic lime, concluding that the former is more resistant to salt crystallization. The paper added that it wasn't possible to examine the process of decay due to the rapidity of the decay. In contrast, Stewart et al. (2001) [25] assert that hydraulic lime had a better resistance to salt crystallization.

4.2.6 Water absorption

Water absorption has been defined as the ratio of the mass of water a mortar can retain, to the dry mass of the mortar Pavia and Toomey (2007) [4].

Pavia and Toomey (2007) [4] also suggest that aggregate properties can have an impact on the water absorption of the mortar, although not a substantial effect. The highest water absorption occurred in mortars that contained coarser, more rounded aggregate, with inferior grading. In contrast, the minimum water absorption occurred in mortars with the best grading, sharpest particle size and finest average particle size. Pavia and Toomey (2007) [4] also noted that calcite content did not affect water absorption. It is worth mentioning that the limestone aggregate contained both calcite and quartz, but the proportions of these were not specified in the paper.

Therefore, it may be beneficial to take a closer look at a variety of calcitic aggregates to determine whether this is true for a wide range, or indeed just one or two types.

4.3 Analysis

In order to establish the mechanisms behind the different mortar properties due to aggregate type, it is likely that microstructural analyses will be required. There are a few techniques that could prove useful here.

4.3.1 Scanning electron microscopy (SEM)

SEM is a useful technique for determining the morphology of the microstructure in mortars (Lanas and Alvarez, 2003), (Arandigoyen and Alvarez, 2006) and (Tuncoku and Caner-Saltik, 2006) [1,25,27], in addition to phases that are present in the mortar (Lanas and Alvarez, 2003) [1].

Figure 1 shows an SEM image of the exterior of air lime mortar made with oolitic aggregate (Lawrence, 2006) [2].

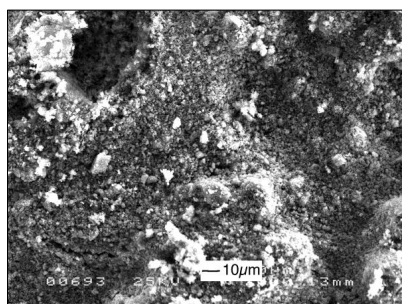


Fig. 1. SEM of exterior of oolitic mortar x500 [2]

When comparing this with Figure 2 which is air lime mortar made using sand (Lawrence, 2006) [2], there are clear differences.

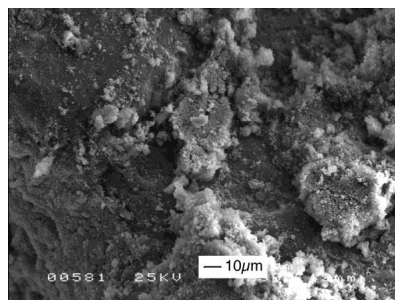


Fig. 2. SEM of exterior of sand mortar x500 [2]

Consequently, it is expected that SEM will be able to highlight differences between the use of calcitic and silicate aggregate at the B/Ag interface.

In the case of air lime mortar there are no hydraulic reactions taking place, due to the absence of silica, therefore other interactions must be taken into consideration.

As previously mentioned, a link has been suggested between the roughness and porosity of the aggregate surface, and the aggregate's cohesion with the mortar. SEM would be a good technique to use in order to examine the interface of aggregate and binder matrix, with the aim of comparing the calcitic aggregate/binder interface and the silicate aggregate/binder interface.

Use of SEM would enable verification of the extent of chemical reaction at the aggregate surface, in addition to being able to establish whether a significant amount of binder has entered the pores of the aggregate.

4.3.2 X-ray diffraction (XRD)

XRD is frequently used to determine the mineralogical phases that occur during the carbonation process (Lanas and Alvarez, 2003), (Arandigoyen and Alvarez, 2006) and (Tuncoku and Caner-Saltik, 2006) [1,26-27]. Additionally, the morphology and crystallinity can be established (Hansen et al., 2000) [28].

Lawrence et al. (2007) [18] noted that carbonation can be compared as a result of obtaining a semi-quantitative relationship between the intensity of the peaks of calcium carbonate and calcium hydroxide.

4.3.3 Phenolphthalein

Phenolphthalein staining is a useful technique in assessing the depth of carbonation in a mortar sample (Lawrence, 2006) [2]. As previously mentioned, carbonation is of utmost importance in air lime mortars.

When used together with XRD, the two techniques provide detailed information about the carbonation process, which can be used to determine the extent of the difference in carbonation between mortars with calcitic and with siliceous aggregates.

4.3.4 Thermogravimetry (TG)/differential thermal analysis (DTA)

TG is another method that can be used to establish the mineralogical composition of lime (Arandigoyen et al., 2005) [29]. Marquez et al. (2006) [30] claim that DTA/TGA is very reliable for the identification of compounds in aerial lime mortar and suggest that for hydraulic-based mortars, it is less accurate due to the increased complexity of the material.

5 Conclusions

It is clear from the existing research that there is a gap in knowledge about the effect of aggregate type on the properties of air lime mortars.

While it has been found that aggregate type can affect strength, drying shrinkage and modulus of elasticity, little is known about the mechanisms behind these findings.

The author plans further research, seeking to establish the mechanisms behind this, by firstly undertaking a number of tests on the properties of the mortar. The calcareous aggregate will be compared with a siliceous aggregate; several B/Ag ratios will be used, in addition to a number of different curing times. Subsequently, microstructural analyses will be conducted, in order to establish the differences between aggregate type (calclitic and siliceous), that may have influenced the properties of the mortar. Particular focus is on the strength of the mortar.

References

1. J. Lanas, J.I. Alvarez, *Cem. and Conc. Res. E* **33** (2003)
2. R.M.H. Lawrence, A Study of Carbonation in Non-Hydraulic Lime Mortars, Ph.D. Thesis (2006)
3. A. Arizzi, G. Cultrone, *Cem. and Conc. Res. E* **42** (2012)
4. S. Pavia, B. Toomey, *Mat. and Struct. E* **41** (2007)
5. A. Carlos, I. Masumi, M. Hiroaki, M. Maki, O. Takahisa, *Const. and Build. Mat. E* **24** (2010)
6. T.R. Naik, R.N. Kraus, Y.-M. Chun (2006)
7. British Standards Online, BS EN 1015-3: 1999
8. B. de Vekey, *Good Building Guide E* **66** (2005)
9. E. Bauer, J.G.G. de Sousa, E.A. Guimarães, F.G.S. Silva *E* **42** (2007)
10. R. Hendrickx, J. Minet, K. Van Balen, D. Van Gemert, *Int. Brick and Block Masonry Conference* (Sydney, 2008)
11. R. Hendrickx, *Int. Brick and Block Masonry Conference* (Sydney, 2008)
12. R. Hendrickx, K. Van Balen, D. Van Gemert, *RILEM Int. Symp. Rheology of Cement Suspensions Such as Fresh Concrete* (2009)
13. D.C.Hughes, V. Starinieri, R. Kozłowski, J. Weber, To be submitted to: *Const. and Build. Mat.*
14. A. Moropoulou, A. Bakolas, P. Mondoulas, E. Aggelakopoulou, S. Anagnostopoulou, *Cem. & Conc. Res. E* **27** (2005)
15. S. Pavia, R. Hanley, *Mat. and Struct. E* **43** (2009)
16. M. Arandigoyen, B. Bicer-Simsir, J.I. Alvarez, D. Lange, *Appl. Surf. Sci.* (2006)
17. R.M.H. Lawrence, T.J. Mays, P. Walker, D. D'Ayala, *Therm. Act.* (2006)
18. R.M.H. Lawrence, T.J. Mays, S.P. Rigby, P. Walker, D. D'Ayala, *Cem. and Conc. Res. E* **37** (2007)
19. J. Lanas, R. Sirera, J.I. Alvarez, *Therm. Act. E* **429** (2005)
20. P. Maravelaki-Kalaitzaki, *Cem. and Conc. Res. E* **37** (2007)
21. M. Arandigoyen, J.I. Alvarez, *Cem. and Conc. Res. E* **37** (2007)
22. F. Winnefeld, K.G. Böttger, *Mat. and Struct. E* **39** (2006)
23. F.M.A. Henriques, A.E. Charola, *9th Int. Congress on Deterioration and Conservation of Stone* (Venice, 2000)
24. S. Pavia, E. Treacy, *Mat. and Struct. E* **39** (2006)
25. J. Stewart, R. Glover, J. Houston, N. Steeley, T. Proudfoot, *J. Arch. Cons.* (2001)
26. M. Arandigoyen, J.I. Alvarez, *Appl. Surf. Sci. E* **225** (2006)
27. S.S.Tuncoku, E.N. Caner-Saltik, *Cem. and Conc. Res. E* **36** (2006)
28. E. Hansen, A. Tagle, E. Erder, S. Baron, S. Connell, C. Rodriguez-Navarro, K. Van Baelen, *Int. Workshop Historic Mortars Characteristics and Test* (2000)
29. M. Arandigoyen, J.L. Perez Bernal, M.A. Bello Lopez, J.I. Alvarez, *Appl. Surf. Sci. E* **252** (2005)
30. S.F. Marquez, R.A. Ribeiro, L.M. Silva, V.M. Ferreira, J.A. Labrincha, *Cem. and Conc. Res. E* **36** (2006)

A.0.2 International Conference on Sustainability in Energy and Buildings



Available online at www.sciencedirect.com

SciVerse ScienceDirect

Energy Procedia 00 (2014) 000–000

Energy

Procedia

www.elsevier.com/locate/procedia

International Conference on Sustainability in Energy in Buildings 2014, SEB-14

Impact of aggregate type on air lime mortar properties

Sarah Scannell*, Mike Lawrence, Pete Walker

University of Bath, Claverton Down, Bath, BA2 7AY, UK

Abstract

In recent years, the need for low energy materials has become increasingly recognised. Government targets aim to achieve a decrease in carbon emissions by 80% before 2050. With the construction industry being responsible for approximately 50% of UK carbon emissions, an increased use of low energy materials could go a long way to achieving this target. With this in mind, it is also important that materials still have adequate properties to fit their purpose. For this study, four limestone aggregates were compared with a silicate aggregate in order to assess the impact of the aggregate type on the properties of air lime mortar (CL90). The primary focus was to assess the differences in compressive strength, and investigate reasons behind the measured differences. Without exception, the mortars made with limestone aggregate have higher compressive strengths than those made with silicate sand. Phenolphthalein staining shows slight differences in carbonation levels at 28 days, which could help to explain the strength differences observed. Furthermore, SEM analysis has revealed differences at the binder/aggregate interface between limestone aggregate mortars and silicate sand mortars.

© 2014 Sarah Scannell, Mike Lawrence, Pete Walker. Published by Elsevier Ltd.
Selection and peer-review under responsibility of KES International

Keywords: limestone aggregate; silicate sand; air lime; compressive strength; scanning electron microscopy (SEM)

1. Introduction

Lime mortar has been used for centuries in masonry construction. The past few decades have seen an increase in restoration work on old structures, where the compatibility of old and new materials is of paramount importance. This means that cement-based materials are inappropriate as a repair material due to the significantly higher strengths they reach over lime-based materials; a mortar with a higher strength than the original masonry would lead to more damage due to having less ability to accommodate movement. As a result, a build-up of stresses would cause the masonry to fail (Mosquera et al. 2002) [1].

Lime mortars are inherently weak in compression, and research has shown that higher strengths can be obtained with use of limestone aggregate over silicate aggregate (Lawrence, 2006) [2]. Since low strengths are synonymous with poor durability, higher strengths could lead to longer-lasting mortars. The higher strengths obtained are still much lower than cement mortar strengths so should not have a detrimental effect on existing masonry. Aggregates are primarily used to provide structure to a mortar (Farey et al., 2003) [3] and their role in mortar strength has been largely underestimated. Despite various studies concluding that limestone aggregates can produce higher strength air lime

* Corresponding author. Tel.: +44 1225 385362
E-mail address: S.Scannell@bath.ac.uk

mortars (Lawrence, 2006; Lanas and Alvarez, 2003; Arizzi and Cultrone, 2012) [2,4,5], little is known about the reasons why. Additionally, while adequate strength is required for durability of a mortar, it is also vital to ensure other characteristics are sufficient; porosity, water retentivity and plasticity are just a few of the important properties. In the current climate, it is becoming increasingly recognized that carbon emissions need to be reduced; as the construction industry is responsible for around 50% of the UK's emissions (BIS, 2010) [6], the use of low energy materials can contribute to this reduction. Air lime is a low energy binder due to the fact that during curing, almost all of the CO_2 that was emitted during the manufacturing process is reabsorbed during carbonation (limetechnology, accessed 2013) [7]. Carbonation gives a mortar strength through the transformation of Ca(OH)_2 into CaCO_3 . It is the primary chemical reaction that occurs during setting of air lime mortar, and is a self-limiting process. This is due to the formation of calcite crystals around the calcium hydroxide particles, which block CO_2 penetration and subsequently some portlandite (Ca(OH)_2) always remains uncarbonated (Houst and Wittmann, 2002) [8].

The research originated due to lack of knowledge surrounding the effect of aggregate type on mortar properties, particularly compressive strength. Consequently, four limestone aggregates were compared against a silicate sand (CEN Standard sand) to determine firstly the compressive strengths, and secondly whether there were any differences at a microstructural level for the different mixes. Scanning electron microscopy (SEM) was used for this analysis.

Nomenclature

SEM	Scanning electron microscopy
Ca(OH)_2	Calcium hydroxide (portlandite)
CaCO_3	Calcium carbonate (calcite)
$\text{CaMg(CO}_3)_2$	Calcium magnesium carbonate (dolomite)
SiO_2	Silicon dioxide
B/Ag	Binder/aggregate

2. Effects of aggregate type

Several aspects relating to aggregates can have an impact on the strength of the mortar. The most commonly used aggregate is silicate aggregate, which is hard and chemically inert. Limestone aggregates can be calcitic or dolomitic; calcitic aggregates are in the form CaCO_3 whereas dolomitic aggregates are $\text{CaMg(CO}_3)_2$. Calcitic aggregates are used in the current study (as well as silica sand) and can either compose of angular or rounded grains. Differences in the porosity of aggregates can have an impact on overall mortar strength, due to differences in the diffusion of CO_2 through the sample. Aggregates with a higher porosity would allow a quicker rate of CO_2 diffusion, thus leading to a quicker rate of carbonation. Since carbonation is the primary strength mechanism in air lime mortar, strength would be expected to be increased.

If the aggregate has a low mechanical strength, failure of the mortar is likely to occur through the aggregate. Conversely, aggregates with high mechanical strength will result in failure at the binder/aggregate interface, assuming the aggregate is stronger than the bond.

It has been suggested in previous research (Lanas and Alvarez, 2003) [4] that a similarity between the limestone aggregate and binder matrix can also form a superior bond (over silicate aggregate) and as a result strengths are higher.

3. Materials and methods

Air lime mortar specimens (using CL90 hydrated lime) of dimensions 40x40x160mm were made in accordance with BS EN 1015-11: 1999 [9], in order for compressive/flexural strength testing to be undertaken. Samples were cured for a period of 28 days in air. Four of the samples were made with different limestone aggregates (Monks Park Bath stone, Doultling, Portland and Stoke Ground), while the fifth was made with a silicate sand. A binder/aggregate (B/Ag) ratio of 1:2 was used for all mixes. In order for the tests to be able to isolate differences in mortar properties

based on aggregate type, all limestone aggregates were made to match the silicate sand (Standard sand CEN 196-1). An additional 2mm fraction was added to all five aggregates in order to help reduce shrinkage in the mortar specimens. Table 1 shows the sieve sizes used.

Sieve size (mm)	% Passing
4	100
2	88
1.6	81.84
1	58.96
0.5	29.04
0.16	11.44
0.08	0

Table 1. Sieve sizes

Figure 1 shows the particle size distribution used in this study, compared with BS 1200: 1976 [10]. It is clear that a similar trend exists.

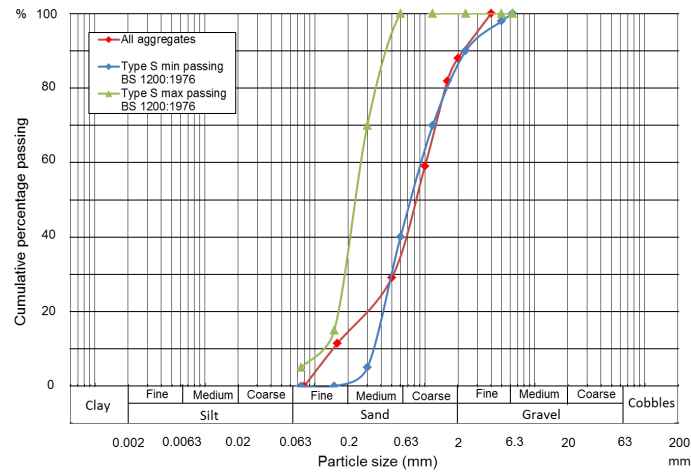


Figure 1. Particle size distribution

Due to the importance of workability of a mortar, it was decided that rather than having a constant water/binder (w/b) ratio, the flow would be kept constant at 13cm +/- 0.5cm. The main reason behind this was due to findings that if a mortar wasn't deemed workable by the mason, more water would be added to the mix, thus altering the properties (Gunn, 2005) [11].

The flow table test measures consistence of a mortar; mortar is tamped down into a truncated cone then once the cone is removed, 15 drops of the table are made at a rate of one per second. The diameter of the mortar spread is then measured. This was done in accordance with BS EN 1015-3: 1999 [12].

Table 2 shows the mix specifications used for each of the mixes in order to achieve a 13cm flow.

Sample	Lime (g)	Agg (g)	Water (g)	w/b
Bath stone	250	2050	539	2.16
Doubling	250	2238	513	2.05
Portland	250	2781	493	1.97
Stoke Ground	250	2279	535	2.14
Standard sand	250	1536	250	1.00

Table 2. Mix design

The w/b ratio is known to impact strength of cement mortars and hydraulic lime mortars. Abrams' Law shows the relationship between the strength of fully compacted concrete and the w/b ratio:

$$f_c = K_1/K_2^{w/c}$$

where f_c is the compressive strength, K_1 and K_2 are constants. Compressive strength in cementitious mortars is known to follow Abram's Law, and is inversely proportional to water/cement ratio (Neville, 2005) [13]. Lawrence and Walker (2008) [14] have shown that for air lime mortars, with the exception of the lowest water/lime ratio, there is very little difference in the compressive strengths of the mortars with increasing water content.

4. Experimental results

Results from the compressive strength testing confirmed the findings from literature that limestone aggregates (Bath stone, Doultong, Portland and Stoke Ground) can produce stronger mortars than silicate sand (Standard sand), as can be seen in Figure 2. While it is possible that the angular nature of the crushed limestone could be providing greater mortar strengths than the more rounded silicate sand, SEM testing has suggested something more complex.

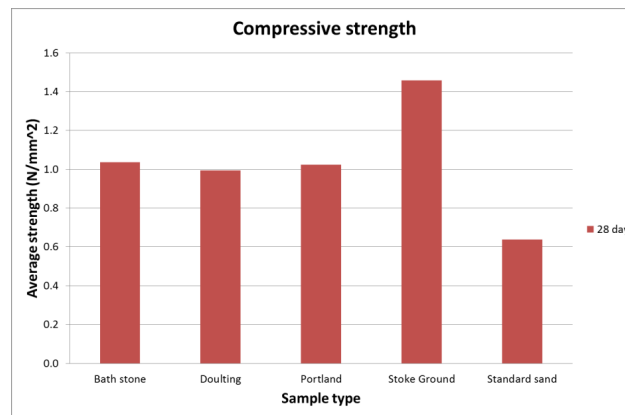


Figure 2. 28 day compressive strengths

Having confirmed previous knowledge, samples were taken from the outer edge of each of the fractured specimens in order to undertake SEM analysis to try to help understand the mechanisms behind the strength differences. The SEM used was JEOL SEM6480LV. It was used under low vacuum conditions so that the samples didn't require coating. BSE (back-scattered electron) mode was used, in combination with EDX which enables identification of the elements that make up the sample.

Figure 3 shows a sample of the specimen made with Portland aggregate. The lighter area indicates a heavier element; in this case it is expected that the lighter area contains CaCO_3 and the surrounding darker areas consist of Ca(OH)_2 . This seems to be confirmed by the EDX analysis which indicates a higher proportion of oxygen in the lighter areas. The large area of lighter material appears to be an aggregate particle that is almost entirely coated with calcium carbonate (calcite) crystals. This supports the notion that calcitic aggregate can act as a nucleation site for calcite crystals (Lanas and Alvarez, 2003) [4].

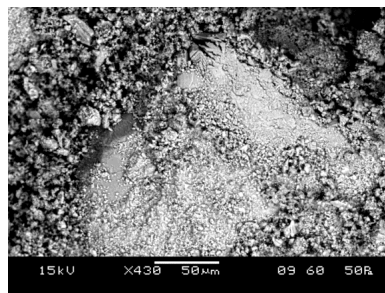


Figure 3. SEM image of sample containing Portland limestone aggregate

If more calcite crystals are forming, this suggests the carbonation is of a better quality than samples where aggregates are coated in fewer crystals. This could be contributing to the higher strengths that are being achieved with limestone aggregate mortars.

Figure 4 (below) shows a specimen containing silicate sand (Standard sand) at the same magnification as Figure 3. The aggregate particle can be seen much more easily than the Portland aggregate in Figure 3, which suggests there are less calcite crystals forming on the aggregate surface. Furthermore, the aggregate in Figure 4 appears to exhibit a larger amount of space between it and the binder. This implies that an inferior bond exists when compared with the Portland sample in Figure 3, which could be responsible for the lower strength achieved. A similarity between binder matrix and aggregate has been linked with higher mortar strengths (Lanas and Alvarez, 2003) [4] in limestone aggregate mortars; the findings shown in Figures 3 and 4 imply that this is a valid hypothesis.

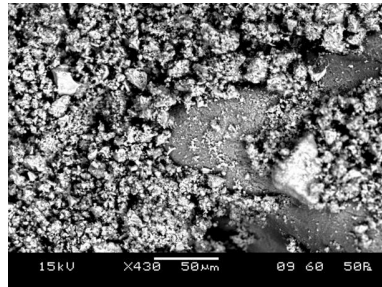


Figure 4. SEM image of sample containing Standard sand

Figure 5 shows a sample made with Douling aggregate. Again, the lighter area appears to be an aggregate particle. Cracking is evident on aggregate, as well as between the aggregate and the binder, suggesting a weaker bond than that obtained from the Portland sample. When no cracks exist at the binder/aggregate interface, cracking in the aggregate indicates that the aggregate itself is weaker than the bond that has formed at the interface. In this instance, there are cracks both within the aggregate and at the interface between binder and aggregate, which could point to similar compressive strength of aggregate and mortar respectively.

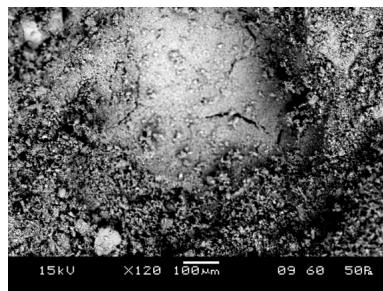


Figure 5. SEM image of sample containing Douling limestone

The Stoke Ground sample in Figure 6 (the strongest mortar) has less discontinuity than the other samples between binder and aggregate, although some cracking is evident in the aggregate itself (right hand side of Figure 6). It is possible that the Stoke Ground aggregate is causing a more thorough level of carbonation at the binder/aggregate interface. A combination of X-ray diffraction (XRD) and thermogravimetric analysis (TGA) could help to establish this.

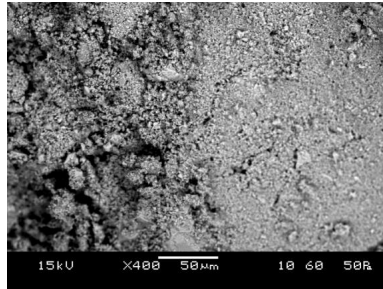


Figure 6. SEM image of sample containing Stoke Ground limestone

In Figure 7 (below), the lighter area shows a particle of Bath stone aggregate, with some calcite crystals on the surface. It is evident that there are fewer crystals than with Portland limestone, although the average compressive strengths are quite similar. Despite this, there is good continuity between the aggregate and binder, suggesting a good bond.

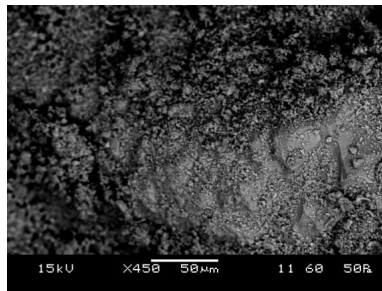


Figure 7. SEM image showing sample containing Bath stone

Phenolphthalein staining was used to determine levels of carbonation in the samples. Figure 8 below shows a Standard sand sample and a Portland sample.

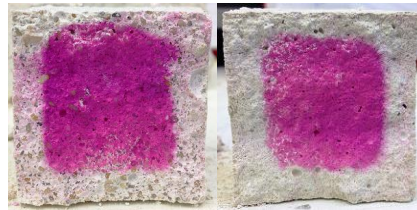


Figure 8. Left – Standard sand sample; Right – Portland sample

The dark area shows uncarbonated material in the samples; it can be seen that the sample containing Portland has a slightly smaller area of uncarbonated material, which could contribute to strength differences. It is also possible that the limestone aggregates allow quicker carbonation of the samples, due to having intrinsically higher levels of porosity.

Table 2 shows the average carbonation depth of each sample after 28 days curing. All mixes had a binder/aggregate ratio of 1:2 as well as identical partial size distribution (Figure 1).

Sample	Depth (mm)
Bath stone	6
Doulting	7
Portland	6
Stoke Ground	6
Standard sand	5

Table 2. Average carbonation depth of samples

It is evident that there is a slight variation between the different mortar mixes. However, it is clear that these differences are not directly related to the strength values that can be seen in Figure 2. While a 2mm difference in carbonation depth is evident between the Doulting sample and Standard sand sample (the value for Doulting is 1.4x higher), the Doulting sample is 1.3x stronger than Standard sand sample. Furthermore, the Stoke Ground sample was the strongest in compression but does not have the greatest depth of carbonation suggesting that while the different aggregates are causing small differences in carbonation depth of the mortar, it is unlikely that the variances have had an impact on the compressive strength. It is more feasible that the higher porosity of the limestone aggregate is causing improved binder/aggregate bond rather than higher levels of carbonation. Mercury intrusion porosimetry (MIP) will help determine whether porosity is influencing strength results.

5. Discussion

It is clear from the SEM analysis that differences exist in the microstructure between the different aggregates used in the mortar. Most noticeably, the difference between the binder/aggregate interface of the silicate sand mortar and limestone aggregate mortars respectively.

On the surface of the silicate aggregate there were far fewer calcite crystals developing after 28 days when compared with the limestone aggregate. A possible reason for this could be due to the lower porosity of the silicate aggregate, meaning binder couldn't enter the pores in the same way as it could with limestone aggregate, which has a higher porosity. Binder entering the pores would create a better bond and consequently a higher compressive strength.

Ideas have been put forward about reasons for higher strengths (Lawrence, 2006; Lanas and Alvarez, 2004) [2,4] including the notion that calcitic aggregates act as a nucleation site for calcite crystals.

6. Conclusions

The current research has shown that with the use of different aggregate types in air lime mortar, the compressive strengths can be quite different; limestone aggregates have produced higher strength mortars. SEM analysis has revealed that there are also differences on a microstructural level. An important finding is that there are more calcite crystals forming on the surface of the limestone aggregates than the silicate sand, and still some differences between those as well. Furthermore, some of the aggregates were found to exhibit cracking within themselves and some were also found to have discontinuity between binder and aggregate. Finally, it has been found that while carbonation depths have slight differences with use of different aggregates in the mortar, it is unlikely that these are related to compressive strengths.

References

- [1] Mosquera M., Benitez D, Perry S. Pore structure in mortars applied on restoration: Effect on properties relevant to decay of granite buildings, *Cem. Concr. Res.* 2002; **32**: 1883-1888.
- [2] Lawrence RMH. A Study of Carbonation in Non-hydraulic Lime Mortars, Ph.D. Thesis, University of Bath: UK, 2006.
- [3] Farey M, Holmes S, Livesey, M. *Hydraulic lime mortar for stone, brick and block masonry: a best practice guide*. Shaftesbury: Donhead; 2003.
- [4] Lanas J, Alvarez J. Masonry repair lime-based mortars: Factors affecting the mechanical behaviour, *Cem. Concr. Res.* 2003; **33**: 1867-1876.
- [5] Arizzi A, Cultrone G. The difference in behaviour between calcitic and dolomitic lime mortars set under dry conditions: The relationship between textural and physical-mechanical properties. *Cem. Concr. Res.* 2012; **42**: 818-826.
- [6] BIS (2010). Estimating the amount of CO₂ emissions that the construction industry can influence, BIS Department for Business Innovation & Skills
- [7] Houst Y. F., Wittmann F.H. Depth profiles of carbonates formed during natural carbonation, *Cem. Concr. Res.* 2002; **32**: 1923-1930.
- [8] limetechology. URL: [http://limetech.info/upload/documents/1160489618 intro to lime.pdf](http://limetech.info/upload/documents/1160489618%20intro%20to%20lime.pdf) (Accessed 2013).
- [9] BS EN 1015-11: 1999. *Methods of test for mortar for masonry*. Determination of flexural and compressive strength of hardened mortar. British Standards Institution: London 1999.
- [10] BS 1200: 1976. *Specifications for building sands from natural sources*. British Standards Institution: London 1976.
- [11] Gunn R. Listen to the mason: Portland cement-lime Type N mortar (1:1:6) provides the necessary workability and strength. In. *International Building Lime Symposium, Florida, 2005*.
- [12] BS EN 1015-3: 1999. *Methods of test for mortar for masonry*. Determination of consistence of fresh mortar (by flow table). British Standards Institution: London 1999.
- [13] Neville A.M., *Properties of Concrete*. 4th Ed. Pearson Prentice Hall: 2005.
- [14] Lawrence R.M.H, Walker P. The impact of the water/lime ratio on the structural characteristics of air lime mortars. In. *Structural Analysis of Historic Construction, London, 2008*

I have explained that carbonation provides strength to lime mortar, and that the increases wouldn't be enough to have a detrimental effect, but could improve durability, which addresses the comment asking what significance carbonation has on lime mortar, and whether the increases in strength would be significant enough to be detrimental. (2nd page)

I added that low strengths are associated with poor durability hence the need to improve. This clarifies why strengths are significant. (2nd page)

Also added are detailed mix proportions and explanation that w/b does not affect strength in air lime mortars. They don't follow Abrams' Law. This clears up the uncertainty of whether w/b would affect the mix. (4th page)

More detail to flow table test description, as requested. (4th page)

Included possibility of angular aggregate impacting strength, but have noted that there are indications of other reasons from SEM analysis. (5th page)

Fixed labelling issue with Fig. 8. (8th page)

Fixed references.

Changed "pink area" description, in case published in black and white, as pointed out. (8th page)

Added that samples were cured in air, in order to clarify that the carbonation depths were from air curing not CO₂ chamber. (2nd page)

A.0.3 9th International Masonry Conference 2014

A Study of the Impacts of Calcitic Aggregates on the Properties of Air Lime Mortar

SCANNELL, SARAH¹; LAWRENCE, MIKE²; WALKER, PETE³

ABSTRACT

Preliminary studies have been undertaken to assess the impact of limestone aggregate characteristics on the compressive/flexural strengths of air lime mortar. A number of Binder/Aggregate (B/Ag) ratios were used (1:2, 1:3, 1:4), at curing times of 14 and 28 days. It has been confirmed that different types of limestone can yield higher mortar compressive strengths when compared with the use of silicate aggregate. Some results were found to differ from previous research, despite having the same binder and aggregates, at the same B/Ag ratio and curing times. One key difference is the particle size distribution of the respective aggregates, and further studies will seek to establish the significance. Flexural strength results appear to be unaffected by aggregate type.

Keywords: compressive strength, particle size distribution, calcitic aggregate, air lime, limestone

NOTATION

H_2CO_3	carbonic acid;
$Ca(OH)_2$	calcium hydroxide;
$CaCO_3$	calcium carbonate;
B/Ag	binder/aggregate;
SEM	scanning electron microscopy;
MIP	mercury intrusion porosimetry;
TGA	thermo-gravimetric analysis

1 INTRODUCTION

The need for low energy materials has become increasingly recognised over the past decade; the construction industry accounts for around 50% of the UK's total carbon emissions so there is a demand for low energy materials that would help the government achieve their target of reducing emissions by 80% by 2050. Consequently, the current research is being undertaken at a crucial time, with one positive outcome being the wider usage of low energy materials, including lime mortar.

With that in mind, it is important to note that while low energy materials are valuable, the environmental benefits must not be at the cost of mortar properties. Air lime mortars have been found to have superior properties when compared with other binders (Lawrence, 2006) [1], and ideally the mortar properties can be optimised with careful mix design.

The research originated as a result of findings that with the use of certain types of limestone as an aggregate, stronger mortars were produced than with the most commonly used silica sand mortars

¹ Mrs, University of Bath, Architecture and Civil Engineering, S.Scannell@bath.ac.uk

² Dr., University of Bath, Architecture and Civil Engineering, M.Lawrence@bath.ac.uk

³ Prof., University of Bath, Architecture and Civil Engineering, P.Walker@bath.ac.uk

(Lawrence, 2006; Lanas and Alvarez, 2003; Arizzi and Cultrone, 2012) [1,2,3]. Since the silicate sand itself is stronger than limestone aggregate, these findings were unexpected. The primary role of aggregates in mortar and concrete is to give structure to the material (Farey, 2003) [4] and as silica sand is an inert material, there is little research that investigates the impact of aggregate properties on mortar.

Lime mortars are primarily used in restoration work due to their similarities and therefore compatibility with the original masonry being repaired/conserved. One of the key factors influencing this is the compressive strength of the lime mortar, which is much lower than that of cement mortar. If the mortar is too strong, then the original masonry can end up becoming damaged even further. This is due to higher strength mortars having less ability to accommodate movement in the masonry, therefore a build-up of stresses will cause the masonry to fail (Mosquera et al., 2002) [5].

Little is known about the higher strengths that have been observed with some limestone aggregates, which have been found to be 3x higher than silica sand mortars in some cases (Lawrence, 2006) [1], although suggestions have been made that a similarity between limestone aggregate and binder matrix may have caused a superior bond (Lanas and Alvarez, 2003) [2]. As a result, the current research is at the forefront in this field.

2 THE ROLE OF CARBONATION

Carbonation is the primary chemical reaction that occurs during setting of air lime mortar, and is influenced by a number of factors; water content of a sample, relative humidity (RH) of curing, temperature and the porosity of the material.

The carbonation process describes the evolution of a mortar through chemical hardening, and can be split into two stages. In the first stage, CO_2 reacts with moisture on the surface of the mortar or in the air to form carbonic acid. This can be summarized in the equation below.



Following this, the carbonic acid diffuses into the sample to react with the portlandite ($\text{Ca}(\text{OH})_2$), transforming it into calcite (CaCO_3). Equation 2 summarizes this.



During this process, samples see a weight gain upon transformation of calcium hydroxide to calcium carbonate. Furthermore, the pore structure changes over the carbonation period as a result of the transformation of portlandite into calcite; a decrease in total pore volume can be seen (Van Balen and Van Gemert, 1994) [6].

Van Balen and Van Gemert (1994) [6] state that upon drying, 2 different stages are present regarding water transport. The first of these stages is the shortest and relates to capillary action, where carbonation can be expected to be negligible. The second relates to water vapour diffusion, where Fick's first law can be applied.

Fick's first law of diffusion can be used to describe the process of CO_2 penetrating the pores in the mortar:

$$J = -D \frac{\delta\phi}{\delta x} \quad (3)$$

Where J = diffusion flux, D = diffusion coefficient, ϕ = concentration of substance per unit volume and x = position in length.

Arandigoyen and Alvarez (2003) [7] demonstrated the part carbonation plays in the porosity of mortar. Hydrated lime/cement mortars were used here, and a porosity decrease of 10% was observed as a result of carbonation; it was found that fewer pores of 1 μ m can be found. Cizer et al. (2006) [8] suggested that with an increase in open porosity of the mortar, a subsequent increase in carbonation depth was noticed. Lawrence et al. (2007) [9] stated that the volume of 0.1 μ m pores increases as a result of carbonation in air lime mortars. Furthermore, Lawrence et al. (2006) [10] assert that the pore size distribution is likely to have an influence on the rate of carbonation reaction.

Lawrence et al. (2006) [10] say that even when the carbonation process is thought to have ended, a substantial amount of lime remains uncarbonated. This is due to calcite crystals forming around the portlandite crystals and thus preventing further diffusion of CO₂ into the mortar.

At low temperatures, Dheilily et al. (2002) [11] revealed that the carbonation process speeds up. This is likely due to higher temperatures causing a faster drying of the mortar and thus less moisture is available for the first stage of carbonation (Equation 1). Van Balen and Van Gemert (1994) [6] suggest that 20°C provides the optimum temperature.

A high RH has been observed by Lanas et al. (2005) [12] to allow a higher level of carbonation in both air and hydraulic lime mortars. This is due to the CO₂ reaction being improved as a result of the greater amount of water that is present in the atmosphere.

With the exception of a some studies (Lawrence et al., 2007; Lanas et al., 2005) [9,12], silicate sand is primarily used as aggregate in mortars. It is therefore beneficial to look further at calcitic aggregates, in order to explore their effect on carbonation in more depth.

Since carbonation is the reason for strength gain in air lime mortar, it would follow that mortars with higher strengths might have a higher level of carbonation. This could result from use of more porous aggregates which allow improved CO₂ diffusion leading to a greater depth of penetration than mortars with less porous aggregates. Carbonation also causes a decrease in the porosity of the mortar, which could also contribute to higher strengths.

3 MATERIALS AND METHODS

For the purposes of this study, 6 different limestone aggregates were compared against Standard sand, a silicate sand.

Since the focus of investigations was to assess the effect of aggregate type, the particle size distribution was kept constant. Table 1 shows the sieve sizes that were used and the percentage passing each sieve.

Table 1. Sieve sizes

Sieve size (mm)	% Passing
4	100
2	88
1.6	81.84
1	58.96
0.5	29.04
0.16	11.44
0.08	0

The Standard sand was graded as supplied, and the limestone aggregates were crushed and graded in the lab to match, with the addition of the 2mm fraction to all aggregates in order to reduce shrinkage in the mortars. Figure 1 below shows the particle size distribution.

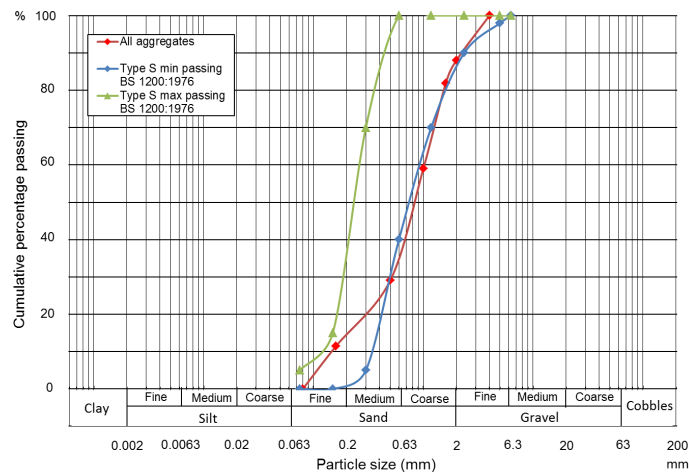


Figure 1. Particle size distribution compared with BS 1200:1976

As can be seen from Figure 1, the particle size distribution used in this study follows a similar trend to that specified in BS 1200:1976 [13].

In order to gain a wider range of results, 3 B/Ag ratios were used in this research; 1:2, 1:3 and 1:4 for each aggregate type at mortar curing times of both 14 and 28 days.

Due to the importance placed upon a mortar's workability as a result of the literature review, it was decided that rather than having a constant water/binder (w/b) ratio, a constant flow of 13cm would be used instead. This resulted from findings that if a mortar wasn't sufficiently workable, then a mason would add more water, thus altering the properties of the mortar. The flow table test was done in accordance with BS EN 1015-3:1999 [14].

Compressive/flexural testing of the samples were in accordance with BS EN 1015-11:1999 [15].

4 EXPERIMENTAL RESULTS AND DISCUSSION

Early results confirm that with use of a calcitic aggregate in air lime mortar, higher compressive strengths can be achieved than mortars with a silicate aggregate. Figure 2, below, shows the 14 and 28 day compressive strengths of all aggregates with a 1:2 B/Ag ratio.

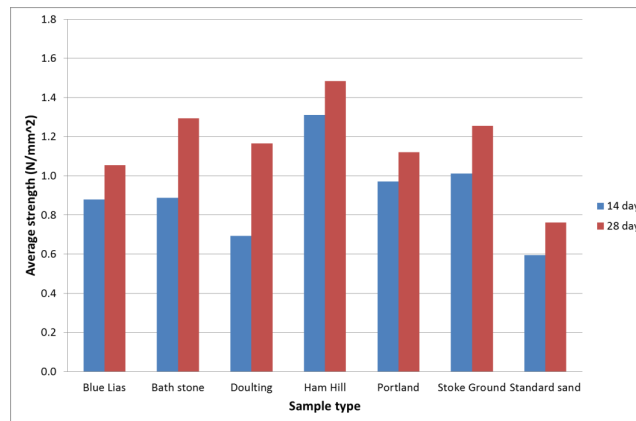


Figure 2. 14 and 28 day compressive strengths for 1:2 B/Ag

It is evident from Figure 2 that mortars made with Standard sand were the weakest when compared with the limestone aggregate mortars. This was confirmed with statistical testing at 99% confidence. Similar results were observed with the 1:3 mixes, which can be seen in Figures 3 and 4.

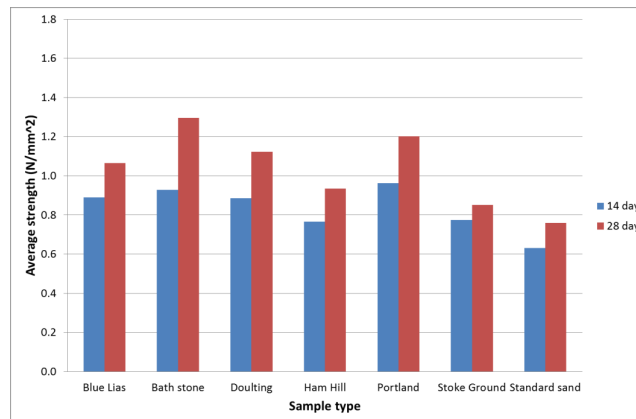


Figure 3. 14 and 28 day compressive strengths for 1:3 B/Ag

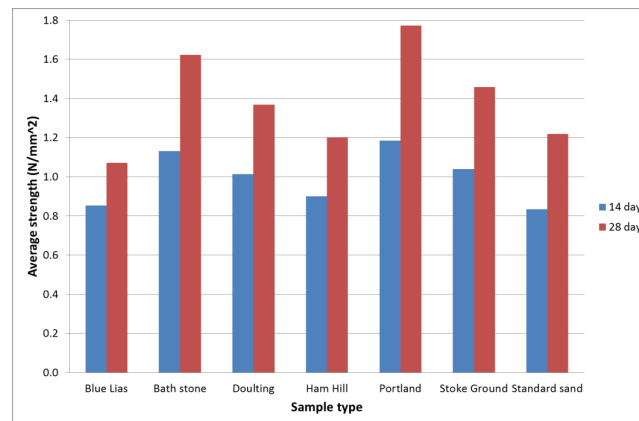


Figure 4. 14 and 28 day compressive strengths for 1:4 B/Ag

While it has been found that the majority of the limestone aggregates produce higher compressive strengths in mortars than the silicate aggregate, the differences were not as large as found by Lawrence (2006) [1]. Figure 5 shows a comparison of the data obtained in the present study and that obtained by Lawrence (2006) [1].

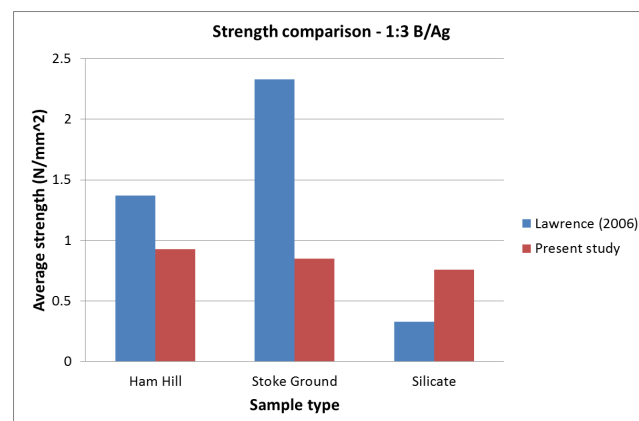


Figure 5. Comparison of strengths between current and previous work

Flexural strength testing did not show the same trends between different aggregates. There appears to be no relationship between aggregate type and flexural strength results. Figures 6-8 show flexural strength results.

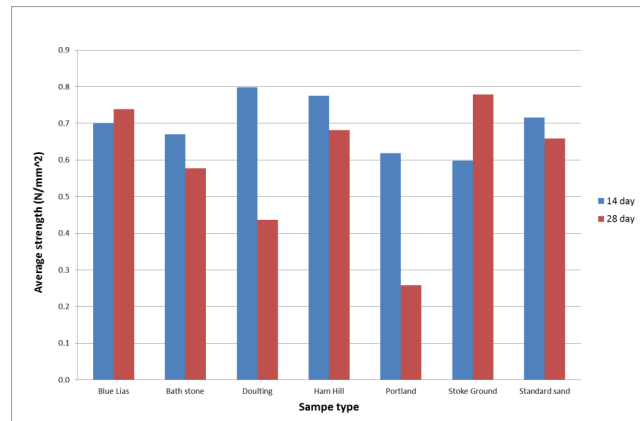


Figure 6. 14 and 28 day flexural strengths for 1:2 B/Ag

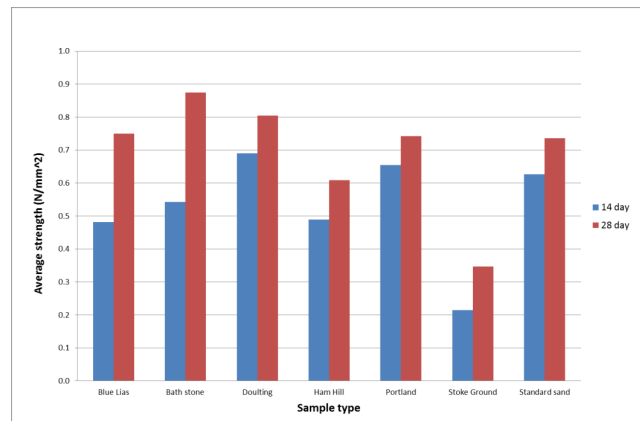


Figure 7. 14 and 28 day flexural strengths for 1:3 B/Ag

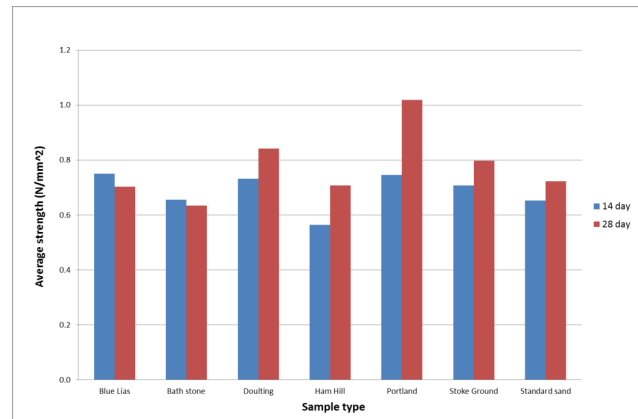


Figure 8. 14 and 28 day flexural strengths for 1:4 B/Ag

Figure 9 shows the phenolphthalein staining on two of the samples from the 1:2 mix at 28 days. The left-hand image shows the Standard sand formulation (the weakest sample) while the right-hand sample contained Ham Hill limestone (the strongest sample).



Figure 9. Phenolphthalein staining at 28 days

Small differences can be observed between the two samples, which indicate that the mix containing Ham Hill is slightly more carbonated than the mix containing Standard sand; the former has a smaller area of stained (uncarbonated) material. It is possible that this difference would be more noticeable over a longer curing period.

It is clear from the compressive strength results that despite using the same aggregate type and binder type at the same B/Ag ratio, Lawrence (2006) [1] obtained stronger mortars with both of the limestone aggregates. Conversely, the present study achieved stronger mortars with the silicate aggregate.

It has been identified that two differences exist in the mixes. Firstly, the water/binder ratio is different; however, the effect on strength has been assumed negligible due to work by Lawrence and Walker (2008) [16] that showed a minor effect of the water/binder ratio on compressive strength when using air lime binder. Secondly, the particle size distribution is noticeably different between the two pieces of research. Lawrence (2006) [1] used a higher proportion of finer aggregate (for the limestones) than the current research, which could have led to the higher strengths observed. This

would be in agreement with Fragata and Veiga (2010) [17] who also used calcitic aggregates compared against silicate aggregates, and found that the addition of fines led to an increase in both flexural and compressive strength of mortars.

There are several ways in which properties relating to aggregate type could have impacted the strength of the mortar. Failure in a mortar could occur as a result of low mechanical strength of the aggregate, where the aggregate would fail preferentially to the mortar, or due to poor binder/aggregate bond which would cause failure to occur at the interface of binder and aggregate. The latter would occur if the aggregate strength was higher than binder strength. Since it has been suggested that calcitic aggregates form a stronger bond with the binder (Lanas and Alvarez, 2003) [2], failure in these mortars may be occurring in the aggregate. It is possible that some of the paste is entering the pores of the aggregate so failure would be expected where no paste is in contact with the aggregate. Conversely, the silicate aggregate could be failing at the interface of binder and aggregate, if the bond wasn't as strong. SEM will be utilised to investigate further into the failure modes of the samples.

Furthermore, calcitic aggregates could have a better connected porosity (ie. improved gas and liquid diffusion) than silicate aggregates. This would allow better flow of CO₂ through the mortar, leading to a deeper level of carbonation and the potential for higher strengths. Figure 6 could be evidence of this and Mercury Intrusion Porosimetry (MIP) will give a better insight into the pore structure.

5 CONCLUSIONS AND FURTHER WORK

The research originally set out to verify whether use of calcitic aggregates in air lime mortars led to improved compressive strength over silicate sand mortars. It has been found that there was a significant difference between limestone mortar and silicate sand strengths. The majority of results showed higher strengths of limestone aggregate mortars at 95% significance or more. The exceptions were Stoke Ground at 1:3 B/Ag and Bath stone and Ham Hill, both at 1:4 B/Ag; these mixes were not found to be significantly stronger than the respective Standard sand mortars.

Additionally, some differences have been observed between the level of carbonation of the strongest and weakest mortars respectively. These differences appear to correlate with strength; higher strengths have higher levels of carbonation.

Since the current research found strength increases to a lesser degree than Lawrence (2006) [1], further work is now seeking to establish reasons for this. Additional research will look in more detail at the effect the granulometry of the aggregate has on the mortar strength, as well as microstructural investigations using SEM, TGA and MIP.

REFERENCES

- [1] Lawrence, R.M.H.: *A Study of Carbonation in Non-hydraulic Lime Mortars*. PhD-Thesis, University of Bath, 2006.
- [2] Lanas, J. & Alvarez, J.: Masonry repair lime-based mortars: Factors affecting the mechanical behaviour. *Cement and Concrete Research*, **33** (2003) 12, 1867-1876.
- [3] Arizzi, A. & Cultrone, G.: The difference behaviour between calcitic and dolomitic lime mortars set under dry conditions: The relationship between textural and physical-mechanical properties. *Cement and Concrete Research*, **42** (2012) 6, 818-826.
- [4] Farey, M.: *Hydraulic lime mortar for stone, brick and block masonry: a best practice guide*, Shaftesbury: Donhead 2003.
- [5] Mosquera, M.; Benitez, D. & Perry, S.: Pore structure in mortars applied on restoration: Effect on properties relevant to decay of granite buildings, *Cement and Concrete Research*, **32** (2002) 12, 1883-1888.
- [6] Van Balen, K. & Van Gemert, D.: Modelling lime mortar carbonation, *Materials and Structures*, **27** (1994), 393-398.
- [7] Arandigoyen, M. & Alvarez, J.: Blended pastes of cement and lime: Pore structure and capillary porosity. *Applied Surface Science*, **252** (2006) 23, 8077-8085.
- [8] Cizer, O.; Van Balen, K.; Van Gemert, D. & Elsen, J.: Carbonation and hydration of calcium hydroxide and calcium silicate binders with rice husk ash. In: *International Conference on Sustainable Construction Materials and Technologies*, Taylor & Francis: Coventry 2007, 611-621.
- [9] Lawrence, R.M.; Mays, T.J.; Rigby, S.P.; Walker, P. & D'Ayala, D.: Effects of carbonation on the pore structure of non-hydraulic lime mortars. *Cement and Concrete Research*, **37** (2007) 7, 1059-1069.
- [10] Lawrence, R.; Mays, T.; Walker, P. & D'Ayala, D.: Determination of carbonation profiles in non-hydraulic lime mortars using thermogravimetric analysis. *Thermochimica Acta*, **444** (2006) 2, 179-189.
- [11] Dheilly, R.; Tudo, J.; Sebaibi, Y. & Queneudec, M.: Influence of storage conditions on the carbonation of powdered Ca(OH)₂. *Construction and Building Materials*, **16** (2002) 3, 155-161.
- [12] Lanas, J.; Sirera, R. & Alvarez, J.: Compositional changes in lime-based mortars exposed to different environments. *Thermochimica Acta*, **429** (2005) 2, 219-226.
- [13] BS 1200: 1976: *Specifications for building sands from natural sources*. British Standards Institution: London 1976.
- [14] BS EN 1015-3: 1999: *Methods of test for mortar for masonry*. Determination of consistence of fresh mortar (by flow table). British Standards Institution: London 1999.
- [15] BS EN 1015-11: 1999: *Methods of test for mortar for masonry*. Determination of flexural and compressive strength of hardened mortar. British Standards Institution: London 1999.
- [16] Lawrence, R.M.H. & Walker, P.: The impact of the water/lime ratio on the structural characteristics of air lime mortars. In: *6th International Conference on Structural Analysis of Historic Construction: Preserving Safety and Significance*, Taylor & Francis Group: Bath 2008, 885-889.
- [17] Fragata, A. & Veiga, R.: Air lime mortars: Influence of calcareous aggregate and filler addition. In: *5th International Materials Symposium*, Trans Tech Publications: Lisbon 2010, 1280-1285.

A.0.4 Journal of Civil Engineering and Architecture



Assessing the Impact of Aggregate Type on Air Lime Mortar Properties Using Scanning Electron Microscopy

Sarah Scannell, Mike Lawrence and Pete Walker

Building Research Establishment Centre for Innovative Construction Materials, Department of Architecture and Civil Engineering, University of Bath, Bath BA2 7AY, UK

Abstract: In recent years, the need for low energy materials has become increasingly important. With government targets aiming to reduce carbon emissions by 80% by 2050, and the construction industry being responsible for 50% of the UK's carbon emissions, it is of vital importance that positive changes are made. One of these changes is to reduce the carbon footprint of the materials used in construction. Lime mortar has been used for centuries, but since the arrival of cement, its use in modern construction has diminished, in part due to having lower compressive strengths than cement mortar. Air lime mortar, in particular, can be categorised as low energy due to the reabsorption of a significant amount of CO₂ during the setting process: carbonation. The current study focuses on the impact of different types of aggregate (limestone and silicate) on air lime mortar strength. Previous research has found that higher strengths can be achieved with the use of limestone aggregate, but little is known about the reasons why. The research presented here looks at a microstructural analysis through use of SEM (scanning electron microscopy) in order to determine reasons behind the strength differences. At early stages of curing, there are clear differences at the interface of binder and aggregate.

Key words: Air lime, limestone, silicate aggregate, scanning electron microscopy, carbonation.

1. Introduction

1.1 Background

Lime mortar has been used for centuries in masonry construction, and the past few decades have seen an increase in restoration of old buildings, where the compatibility of old and new materials is particularly important. Use of cement mortar is inappropriate for a number of reasons. The high compressive strengths reduce the amount of movement that can occur in the structure and consequently, a build-up of stresses would cause the masonry to fail [1]. Additionally, soluble salts can leech out of the cement, causing damaging salt crystallization.

Lime mortars are inherently weak, and research has been shown that higher strengths can be obtained with use of limestone aggregate over silicate aggregate [2]. Since low strengths are synonymous with poor durability, higher strengths could lead to longer

lasting mortars. The obtained higher strengths are still much lower than cement mortar strengths so would not have a detrimental effect on existing masonry. Aggregates are primarily used to provide structure to a mortar [3] and their role in mortar strength has been largely underestimated. Despite various studies concluding that limestone aggregates can produce higher strength air lime mortars [2, 4, 5], little is known about the reasons why.

In the current climate, there is a huge demand for the reduction of carbon emissions; Government targets aim to reduce emissions in the UK by 80% by 2050. The construction industry is responsible for around 50% of the UK's carbon emissions [6], therefore, it has a responsibility to work towards a reduction. The use of low energy materials, such as the air lime mortar used in this study, can make a significant contribution. Air lime is a low energy binder due to the fact that during the curing process, almost all of the CO₂ that was emitted during the manufacturing process is reabsorbed during

Corresponding author: Sarah Scannell, Ph.D., research fields: limestone aggregate and non-hydraulic lime.

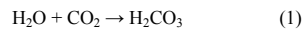
carbonation [7].

The research originated due to lack of knowledge surrounding the effect of aggregate type on mortar properties, particularly compressive strength. Consequently, three limestone aggregates were compared against a silicate sand—CEN (Comité Européen de Normalisation) standard sand to determine firstly the compressive strengths, and secondly whether there were any differences at a microstructural level for the different mixes. SEM (scanning electron microscopy) was used for this analysis.

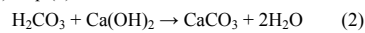
1.2 The Role of Carbonation

Carbonation is the primary chemical reaction that occurs during the setting of air lime mortar, and it is influenced by several factors: water content of a sample, relative humidity of curing, temperature and the porosity of the material.

The carbonation process describes the evolution of a mortar through chemical hardening, and it can be split into two stages. In the first stage, CO₂ diffuses into the pores of the mortar reacts with moisture on the surface of the pores or in the air to form carbonic acid. This can be summarized in the equation below:



Following this, the carbonic acid reacts with the portlandite (Ca(OH)₂), transforming it into calcite (CaCO₃). Eq. (2) summarizes this:



During this process, samples see a weight gain upon transformation of calcium hydroxide to calcium carbonate. Furthermore, the pore structure changes over the carbonation period as a result of the chemical changes; A decrease in total pore volume can be seen [8].

Fick's first law of diffusion can be used to describe the process of CO₂ penetrating the pores in mortar:

$$J = -D (\delta\phi/\delta x) \quad (3)$$

where, J = diffusion flux, D = diffusion coefficient, ϕ = concentration of substance per unit volume and

x = position in length.

The carbonation of lime mortar samples can be measured and assessed in a variety of ways, including but not limited to: phenolphthalein staining; thermogravimetric analysis; scanning electron microscopy; X-ray diffraction; elemental analysis.

2. Impact of Aggregate Type

2.1 Compressive Strength

Aggregate is largely considered to be an inert filler material, but previous research has shown that the use of different aggregate types in air lime mortar can have an impact on the compressive strength of the mortar [2, 4, 5]. The use of limestone aggregate can yield strengths up to three times higher than mortar made with silicate aggregate [2].

2.2 Carbonation

The use of different aggregate types in mortar has an impact on the carbonation of samples. Limestone aggregate in mortars leads to a greater depth of carbonation over the same curing period as silicate aggregate mortars. This is likely to be due to the higher porosity of limestone over silicate aggregate, which in turn leads to a higher overall porosity of the entire sample; CO₂ can penetrate the sample much more readily. Skoulidakis et al. [9] looked at the properties of hydrated lime in the use of consolidation of the surface of stones in monuments, and it found that when 6% calcite was added to the calcium hydroxide, the rate of carbonation increased. It was suggested that Ca(CO)₃ is a seed for crystallization, agreeing that a deeper carbonation can consequently occur.

3. Materials and Methods

Air lime mortar specimens (using calcium lime CL90 hydrated lime) of dimensions 40 mm × 40 mm × 160 mm were manufactured in accordance with BS EN 1015-11: 1999 [10], in order for compressive strength testing to be undertaken. Samples were cured in air and tested for flexural and

compressive strength at 28 days. Three of the mixes were made with different limestone aggregates (Portland, Ham Hill and Stoke Ground Bath Stone), while the fourth was made with a silicate sand. A binder/aggregate (B/Ag) ratio of 1:3 by volume was used for all mixes. In order for the tests to be able to isolate differences in mortar properties based on aggregate type, the grain size distribution of all limestone aggregates were made to match that of the silicate sand (standard sand CEN 196-1) for one set of mixes. The other set used the limestone aggregates “as supplied” from the quarry but with no particles larger than 4 mm.

An additional 2~4-mm fraction was added to all five aggregates in order to help reducing shrinkage in

the mortar specimens. Table 1 shows the sieve sizes used for the “standard” grading, while Table 2 shows the “as supplied” grading of the limestone aggregates. The particle size distribution can be seen in Fig. 1.

Due to the importance of workability of a mortar, it was decided that rather than having a constant water/binder (w/b) ratio, the flow would be kept constant

Table 1 Sieve sizes for “standard” grading.

Sieve size (mm)	Percentage of passing (%)
4	100
2	88
1.6	81.84
1	58.96
0.5	29.04
0.16	11.44
0.08	0

Table 2 Sieve sizes for “as supplied” grading.

Sieve size (mm)	Percentage of passing (%)		
	Ham Hill	Portland	Stoke Ground
4	90.10	99.70	92.90
2	75.30	97.40	78.80
1	59.40	87.70	61.70
0.5	55.30	68.80	43.40
0.25	42.30	30.30	25.70
0.125	31.40	13.40	14.10
0.063	15.20	3.5	4.30

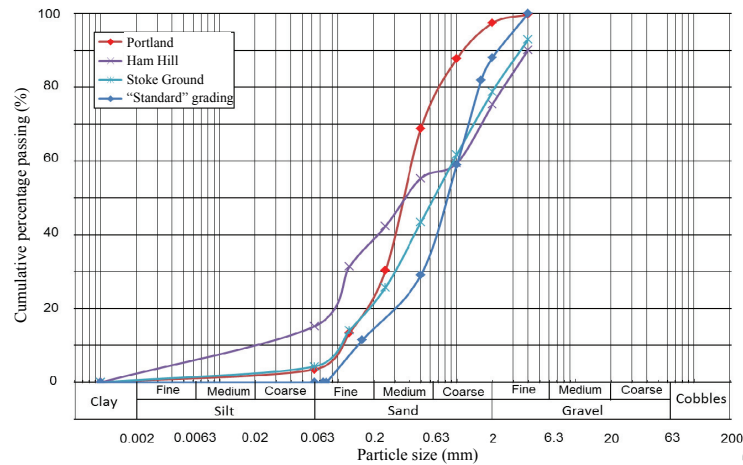


Fig. 1 Particle size distribution of all aggregates.

at $14 \text{ cm} \pm 0.5 \text{ cm}$. The rationale for this approach was that, since the compressive strength of air lime mortars is insensitive to the w/b ratio within a normal range of workability, a flow representative of that which a mason would use would be more representative. As can be seen from Table 3, significantly more water is required for the stone aggregate mortars due to the greater porosity of the aggregate, which competes with the lime for the available water.

The flow table test measures consistency of a mortar. Mortar is tamped down into a truncated cone, then once the cone is removed, 15 drops of the table are made at a rate of 1 s^{-1} . The diameter of the mortar spread is then measured. This was done in accordance with BS EN 1015-3: 1999 [11].

Tables 3 and 4 shows the mix specifications used for each of the mixes in order to achieve a flow of $14 \text{ cm} \pm 0.5 \text{ cm}$.

The w/b ratio is known to impact strength of cement mortars and hydraulic lime mortars. Abrams' Law shows the relationship between the strength of fully compacted concrete and the w/b ratio (Eq. (4)):

$$f_c = K_1/K_2^{w/c} \quad (4)$$

where, f_c is the water/cement ratio, w/c is the water/cement ratio by volume, K_1 and K_2 are constants. Although compressive strength in cementitious mortars is known to follow Abram's Law, being inversely proportional to water/cement ratio [12, 13] have shown that for air lime mortars, with the

exception of the lowest water/lime ratio, there is very little difference in the compressive strengths of the mortars with increasing water content.

4. Experimental Results

4.1 Compressive Strength

Results from the compressive strength testing confirmed the findings in the literature that limestone aggregates can produce higher strength mortars than silicate aggregates. Fig. 2 shows the average compressive strengths of the samples at 28 days curing at 55% RH (relative humidity), where it is clear to see that the standard sand mortar was the weakest in compression.

While there is a possibility that the higher strengths are in part due to the difference in angularity of the aggregates (the limestone aggregates are more angular), SEM analysis suggests that something more complex is occurring.

4.2. SEM (Scanning Electron Microscopy)

Samples were taken from the outer edge of each sample immediately after compressive strength testing, and placed in glass jars filled with nitrogen so as to prevent further carbonation occurring, thus effectively freezing the samples at 28 days curing. The used microscope was JEOL SEM6480LV. It was used under low vacuum conditions.

Fig. 3 shows a Ham Hill aggregate mortar after

Table 3 Mix design for 1:3 "standard" samples.

Sample	Lime (g)	Aggregate (g)	Water (g)	w/b
Ham Hill	150	2,243	458	3.05
Portland	150	2,687	455	3.03
Stoke Ground	150	2,202	351	2.34
Standard sand	150	1,571	150	1.00

Table 4 Mix design for 1:3 "as supplied" samples.

Sample	Lime (g)	Aggregate (g)	Water (g)	w/b
Ham Hill	150	2,243	579	3.86
Portland	150	2,687	542	3.61
Stoke Ground	150	2,202	390	2.60

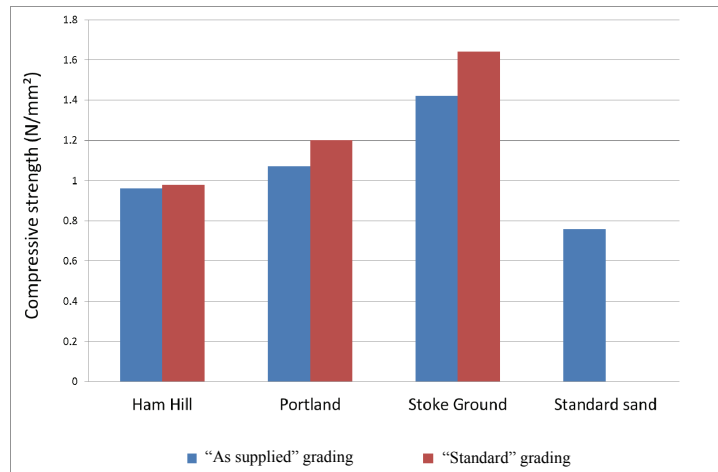


Fig. 2 Average compressive strength at 28 and 360 days.

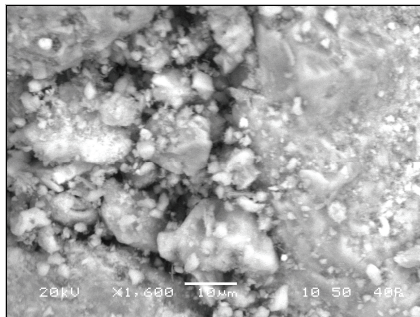


Fig. 3 Ham Hill mortar “standard” grading.

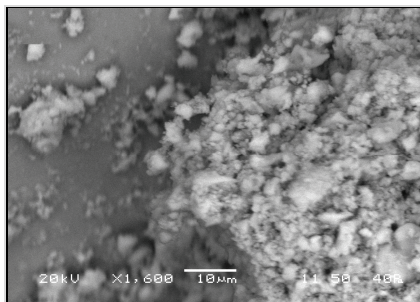


Fig. 4 Standard sand mortar.

28 days curing at 1,600× magnification. The right-hand third of the image is a section of aggregate, which has some calcite crystals on the surface. To the left of the image, calcite crystals can be seen adhering to the aggregate. Similarly, Fig. 4 shows the standard sand aggregate mortar at the same magnification.

The calcite crystals that are on the surface of the aggregate appear to be in larger clusters than in Fig. 3. Moreover, the aggregate that can be seen in Fig. 4 has a smoother surface than the Ham Hill in Fig. 3.

Despite having the highest compressive strength, the sample containing Stoke Ground aggregate with the “standard” grading contained more micro-cracking than the other samples, which can be seen in Fig. 5, which was taken at 800× magnification. The crack measures around 75 µm in length, and appears to be at the binder/aggregate interface.

It is clear from the image of the Portland aggregate mortar with “standard” grading (Fig. 6) that some portlandite still exists in the sample. This can be seen in the center of the bottom of the image. Furthermore, calcite crystals appear small and are continuous over the sample.

In the Ham Hill “as supplied” sample in Fig. 7,

some portlandite still exists, with crystals of around $7\text{ }\mu\text{m}$.

Cracking was also found with the “as supplied” Stoke Ground samples, seen in Fig. 8, although many of these are around $250\text{ }\mu\text{m}$, much larger than in the

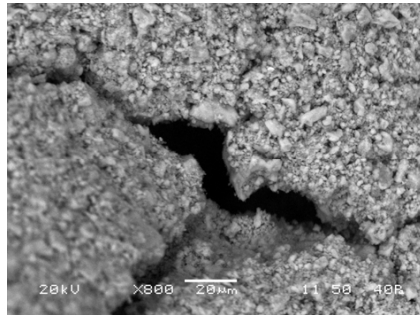


Fig. 5 Stoke Ground mortar “standard” grading.

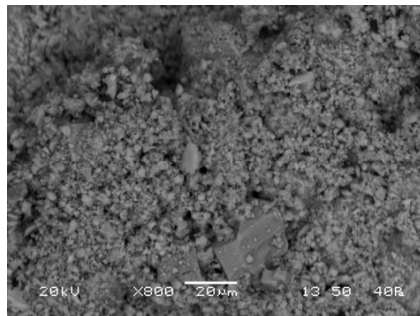


Fig. 6 Portland mortar “standard” grading.

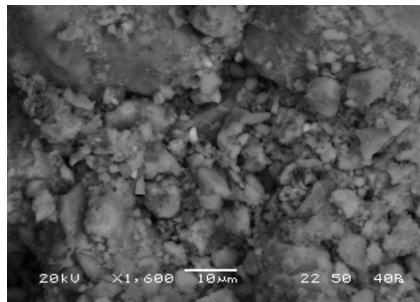


Fig. 7 Ham Hill mortar “as supplied” grading.

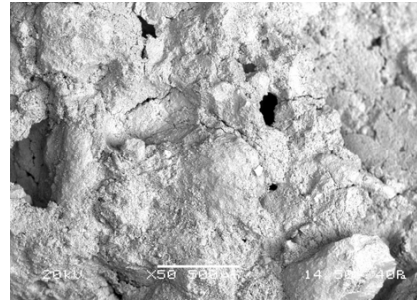


Fig. 8 Stoke Ground mortar “as supplied” grading.

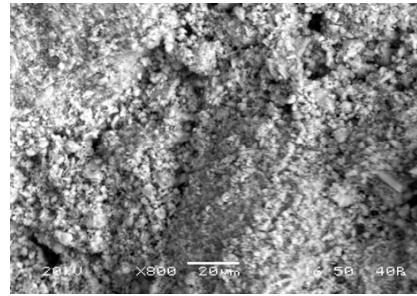


Fig. 9 Portland mortar “as supplied” grading.

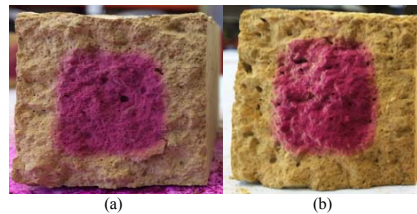


Fig. 10 Ham Hill grading: (a) “standard”; (b) “as supplied”.

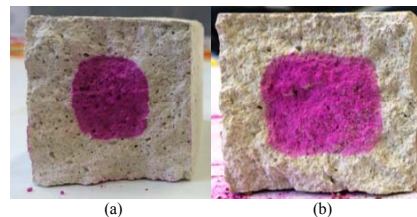


Fig. 11 Portland grading: (a) “standard”; (b) “as supplied”.

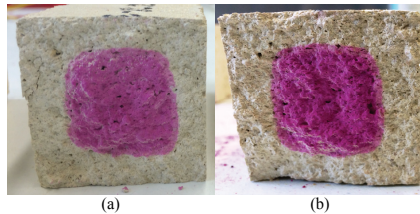


Fig. 12 Stoke Ground: (a) 28 days; (b) 360 days.

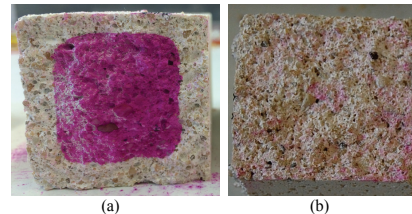


Fig. 13 Standard sand: (a) 28 days; (b) 360 days.

Table 5 Average carbonation depths.

Sample type	Average depth of carbonation (mm)	
	"Standard"	"As supplied"
Ham Hill	7.6	7.5
Portland	10.5	8.0
Stoke Ground	7.5	7.3
Standard sand	6	-

"standard" Stoke Ground sample in Fig. 5.

The Portland aggregate mortar with "as supplied" grading in Fig. 9 has fewer visible portlandite crystals, with similar size calcite crystals.

4.3 Phenolphthalein Staining

Since the primary setting mechanism of air lime mortar is carbonation, the depth of carbonation was measured using phenolphthalein staining. In this way, it is easy to see how much of the $\text{Ca}(\text{OH})_2$ has converted into CaCO_3 . $\text{Ca}(\text{OH})_2$ is alkaline, therefore will turn pink once sprayed with phenolphthalein. CaCO_3 is neutral on the pH scale, meaning areas of the sample that have been carbonated will remain colourless once sprayed.

Figs. 10-13 show the carbonation depths for Ham Hill, Portland, Stoke Ground and Standard sand, respectively. Table 5 summarizes the average depths.

5. Discussion

5.1 Strength Results

The compressive strength results showed what was expected as a result of the literature search; Limestone aggregate in mortar can produce higher compressive strengths than use of silicate aggregate.

There are a number of possible reasons for this that

relate to aggregate type. Firstly, there is a difference in the aggregates themselves. The silicate aggregate has rounded grains, whereas the limestone aggregates are angular. This can impact the bond between the binder and aggregate, since the binder would be expected to adhere better to the angular aggregate.

Secondly, the porosity of the aggregates could be impacting the mortar strength. Limestone is more porous than silica; Consequently, it is possible that some of the binder has entered the pores of the limestone aggregate and as a result formed a stronger interface. It is also possible that due to the higher porosity of the limestone, more CO_2 is able to penetrate the sample and lead to a more thorough carbonation at a given point.

Thirdly, the surface texture of the aggregate may impact the adhesion of the binder to the surface, thus resulting in stronger/weaker bond.

The "standard" graded mortars were found to be stronger than the "as supplied" mortars. This difference was greater for Stoke Ground limestone mortars, which also had the least difference in w/b between the "standard" and "as supplied" mixes.

5.2 SEM (Scanning Electron Microscopy) Analysis

The SEM analysis has given a deeper insight into

possible reasons for the strength differences, which is something that has been missing from literature. SEM images indicate that there are differences at the binder/aggregate interface; the development of calcite crystals is a key finding. Since binder/aggregate ratio, and particle size distribution were the same for the “standard” mixes, it is likely that aggregate type is responsible. Despite the mixes having a different water/binder ratio in order to achieve the same flow, it is not thought to influence calcite crystal growth, particularly due to the fact that Stoke Ground aggregate mortar has a significantly different w/b than the other two limestones, yet it does not appear to have fewer crystals on the aggregate surface, as can be seen with the silicate aggregate.

It is currently unclear as to why the Stoke Ground aggregate mortar suffers from the highest proportion of cracks, yet it has the highest compressive strength, but could be due to the lower w/b ratio that was required in order to achieve the desired flow. This is true for both the “standard” and “as supplied” mixes.

Both of the Portland mortar samples appear quite homogeneous, with the exception of one or two portlandite crystals.

6. Conclusions and Ongoing Research

6.1 Conclusions

Based on the compressive strength results and the SEM analysis, it is clear that aggregate type influences air lime mortar strength. Whilst there is currently no conclusive explanation, ongoing research is expected to clarify this.

6.2 Ongoing Research

Compressive strength testing and SEM analysis are also being undertaken at 14, 90, 180 and 360 days. Alongside the compressive strength testing and SEM analysis, further tests are being carried out. Thermogravimetric analysis seeks to establish differences in carbonation between the samples and at different curing periods. In this way, it will be

possible to determine whether the mortars containing limestone aggregate have achieved a higher level of carbonation at a given time. Mercury intrusion porosimetry is being used to look at differences in porosity between not only the mortar samples but also the individual aggregates. To date, it has been found that key differences exist.

Acknowledgments

This work was supported by Lhoist (UK). The HIVE research building is funded by the Engineering and Physical Sciences Research Council (Grant Numbers EP/L005689/1 and EP/K040391/1).

References

- [1] Mosquera, M., Benitez, D., and Perry, S. 2002. “Pore Structure in Mortars Applied on Restoration: Effect on Properties Relevant to Decay of Granite Buildings.” *Cement and Concrete Research* 32: 1883-8.
- [2] Lawrence, R. M. H. 2006. “A Study of Carbonation in Non-hydraulic Lime Mortars.” Ph.D. thesis, University of Bath.
- [3] Farey, M., Holmes, S., and Livesy, M. 2003. *Hydraulic Lime Mortar for Stone, Brick and Block Masonry: A Best Practice Guide*. Shaftesbury: Donhead.
- [4] Lanas, J., and Alvarez, J. 2002. “Masonry Repair Lime-Based Mortars: Factors Affecting the Mechanical Behaviour.” *Cement and Concrete Research* 32: 1867-76.
- [5] Arizzi, A., and Cultrone, G. 2012. “The Difference in Behaviour between Calcitic and Dolomitic Lime Mortars Set under Dry Conditions: The Relationship between Textural and Physical-Mechanical Properties.” *Cement and Concrete Research* 42: 818-26.
- [6] BIS (Department for Business Innovation & Skills). 2010. *Estimating the Amount of CO₂ Emissions that the Construction Industry Can Influence*. London: BIS.
- [7] Lime Technology. 2013. “Limetec Mortars, Plasters and Renders.” Lime Technology. Accessed May 6, 2013. <http://limetech.info/upload/documents/1160489618introto lime.pdf>.
- [8] Van Balen, K., and Van Gemert, D. 1994. “Modelling Lime Mortar Carbonation.” *Materials and Structures* 27: 393-8.
- [9] Skoulidakis, T. H., Charalambous, D., and Tsakona, K. 1996. “Amelioration of the Properties of Hydrated Lime for the Consolidation of the Surface or/and the Mass of Building Materials of Monuments or New Buildings or

- Statues and Ornaments.” Presented at the 8th International Congress on Deterioration and Conservation of Stone, Berlin, Germany.
- [10] British Standards Institution. 1999. *BS EN 1015-11: 1999. Methods of Test for Mortar for Masonry. Determination of Flexural and Compressive Strength of Hardened Mortar*. London: British Standards Institution.
- [11] British Standards Institution. 1999. *BS EN 1015-3: 1999. Methods of Test for Mortar for Masonry. Determination of Consistence of Fresh Mortar (by flow Table)*. London: British Standards Institution.
- [12] Neville, A. M. 2005. *Properties of Concrete*. New Jersey: Pearson Prentice Hall.
- [13] Lawrence, R. M. H., and Walker, P. 2008. “The Impact of the Water/Lime Ratio on the Structural Characteristics of Air Lime Mortar.” In *Proceedings of the 6th International Conference on Structural Analysis of Historic Construction*, 885-9.

A.0.5 The Journal of the Building Limes Forum

Analysis of the impact of calcitic aggregates on the properties of air-lime mortar

Sarah Scannel, Mike Lawrence, Pete Walker

Sarah Scannel studied civil and structural engineering at the University of Bradford, where she undertook a project on lime-based paint systems. Subsequently, she moved to Bath to study for her PhD titled 'Understanding the impact of calcitic aggregates on the properties of air-lime mortar'.

Mike Lawrence is a lecturer in low-carbon design at the University of Bath. He is also director of the Building Research Park, which hosts research programmes aimed at reducing the environmental impact of construction. Sarah's PhD is an extension of Mike's PhD on carbonation of air-lime mortars, which first identified the unexpected performance differences found when using calcitic aggregates.

Pete Walker is director of the BRE Centre for Innovative Construction Materials. He is currently head of the Department of Architecture and Civil Engineering at the University of Bath, and his research is in the field of natural building materials, particularly earth and bio-based materials. Pete was Mike's supervisor for his PhD.

Abstract

This paper reports on research conducted on air-lime mortars made using calcitic aggregates. Three different calcitic aggregates were compared with a mortar made from a standard silicate sand (BS EN 196-1:2016,¹ with an additional 2-mm fraction). The results show that calcitic aggregate/air-lime mortars can be designed to have compressive strengths of a similar order to weak NHL 2 mortars – 2 to 2.5 mega Pascals (MPa) – without running the risk of the strength increasing excessively over time, as is seen in many natural hydraulic lime (NHL) mortars. Early compressive strengths of the order of 1.5 MPa mean that these

mortars also contribute to 'buildability'. The analysis suggests that the reasons for this higher strength are partly due to more rapid and complete carbonation, and partly due to better interfacial bond between binder and aggregate.

Introduction

Over the past few decades, there has been an increase in the amount of restoration work being undertaken on historic structures. One of the main factors influencing the repair and conservation of buildings is the compatibility of new and existing materials; the repair mortar should be appropriate in terms of both strength and porosity not only to allow moisture transport out

of the original structure but also to prevent damage to the structure as a result of high strength. If a mortar is too strong, less movement can be accommodated, which leads to stresses building up in the structure and subsequent cracking.²

Lime mortars are inherently weak in compression, and research has shown that higher strengths can be obtained with the use of limestone aggregate compared to silicate aggregate.³

In the current climate, it is of vital importance to take steps to reduce the amount of carbon dioxide (CO₂) emissions. This is particularly important in the construction industry, which is responsible for around 50 per cent of the UK's carbon emissions. Government targets aim to reduce emissions by 80 per cent by 2050. The use of air-lime (non-hydraulic lime) mortar would help to reach this target because a significant amount of CO₂ is reabsorbed during the curing process, which takes place by the process of carbonation.

Types of lime

Hydraulic lime

Hydraulic lime can harden in both air and water. Clay-bearing limestone is burnt at 950°C to 1200°C before being slaked. Natural hydraulic lime is defined in terms of its compressive strength at 28 days according to BS EN 459-1:2015;⁴ NHL 2 has a compressive strength range of 2 to 7 MPa, NHL 3.5 from 3.5 to 10 MPa, and NHL 5 from 5 to 15 MPa.

Non-hydraulic lime

In order to produce non-hydraulic lime, limestone is burnt at around 900°C to form calcium oxide (CaO), also known as quicklime, which is subsequently slaked with water to form calcium hydroxide (portlandite – Ca(OH)₂). Also known as air lime, non-hydraulic lime will only set in the presence of CO₂ through the carbonation process (see below).

Lime putty

Lime putty is the saturated form of non-hydraulic lime. The difference here is that during slaking, an excess of water is used. Putty should be stored as a suspension in water for a minimum of three months. (No upper time limit has been suggested in previous research.) A longer storage time has been found to produce a faster and higher degree of carbonation, primarily because the Ca(OH)₂ crystals reduce in size with age, resulting in a higher surface area that is therefore more reactive.

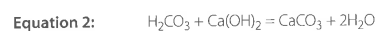
Carbonation

Air-lime mortars only set through carbonation, which requires moisture in the sample and CO₂ in the air. The carbonation reaction can be split into two distinct

parts. Firstly, CO₂ diffuses into the pores of the mortar and reacts with moisture on the surface of the pores or in the air (at the surface) to form carbonic acid, as seen in Equation 1,



Following this, the carbonic acid reacts with the Ca(OH)₂, transforming it into calcite (CaCO₃), as seen in Equation 2.



The pore structure of a mortar changes as a result of carbonation; Van Balen and Van Gemert (1994)⁵ found a decrease in total pore volume was evident.

Types of aggregate

Silicate sand

Silicate sand is a naturally occurring granular material, often in the form of quartz (a silica mineral), and it has the chemical composition SiO₂ (silicon dioxide). It is a hard, chemically inert material that is resistant to weathering, in part due to its very low porosity. Silicate sand contains low levels of impurities, such as clay and iron oxide.

Calclitic aggregate

Calclitic aggregate can comprise angular or rounded grains, and it is composed of CaCO₃. There are many different forms of calclitic aggregate: for example, Bath stone is a Jurassic oolitic stone. Oolitic grains are round in shape and are 0.25 to 2 mm in diameter. Limestone can have other characteristics, such as being crystalline, shelly, or fossiliferous. Jurassic limestones can also be bioclastic, consisting of broken seashells bound with a calclitic cement.

Methodology

Materials and mix design

The binder used in this research was powdered hydrated air lime, designated CL90 in BS EN 459-1.

Four different aggregates were used: three limestone aggregates and a silicate sand (CEN standard sand with an additional 2-mm fraction to reduce the risk of shrinkage). The limestone aggregates used in this study were all sourced from the south-west of the UK and were produced as sawing waste from stone processing. Stoke Ground Bath stone is an oolitic Jurassic limestone from the Great Oolite Group; Portland stone is an Upper Jurassic stone that is ooidal and bioclastic; and Ham Hill stone is a Lower Jurassic stone that is bioclastic and ferruginous, which gives it its characteristic honey-gold colour.

Aggregate characterisation

The aggregates used were characterised using mercury intrusion porosimetry and scanning electron microscopy in order to determine initial properties, such as porosity and chemical composition, which could be compared later against values obtained from mortar samples containing each aggregate.

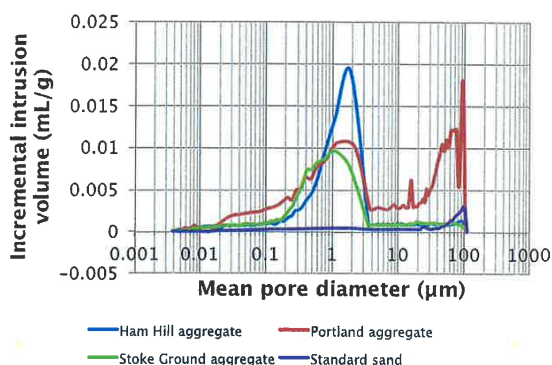
A comparison of the aggregates in Figure 1 shows a marked difference between the limestone aggregates and the silicate sand, but also similarities and differences between the limestone aggregates. Ham Hill aggregate has a much greater volume of pores at around $2\mu\text{m}$ than the other aggregates. Ham Hill aggregate and Stoke Ground aggregate both have their greatest mean pore diameter between 1 and $2\mu\text{m}$. With the standard sand and Portland aggregate the greatest mean pore diameter is around $100\mu\text{m}$, although Portland aggregate also has a peak between 1 and $2\mu\text{m}$. Total porosity of the standard sand is far lower than the limestone aggregates (see Table 1).

It can be seen clearly from Figure 2 that there are significant differences in the aggregates. The surface of the standard sand particles is much cleaner than that of the limestone aggregates; Ham Hill, Stoke Ground, and Portland all have finer particles of aggregate adhering to the surface of the larger particles. This could lead to a greater proportion of finer particles being present in a given mix than is determined by sieve analysis, as they are 'sticking' to larger particles.

Aggregate type	Total porosity (%)
Ham Hill	28.33
Portland	49.90
Stoke Ground	24.84
Standard sand	5.81

Table 1 Total porosity of all aggregates.

Fig. 1 (Below) Mercury intrusion porosimetry data for all aggregates.



Each of the limestone aggregates was used 'as supplied' and in a modified form, in which the grading was adjusted to match the modified particle size distribution of the standard sand (i.e., with an additional

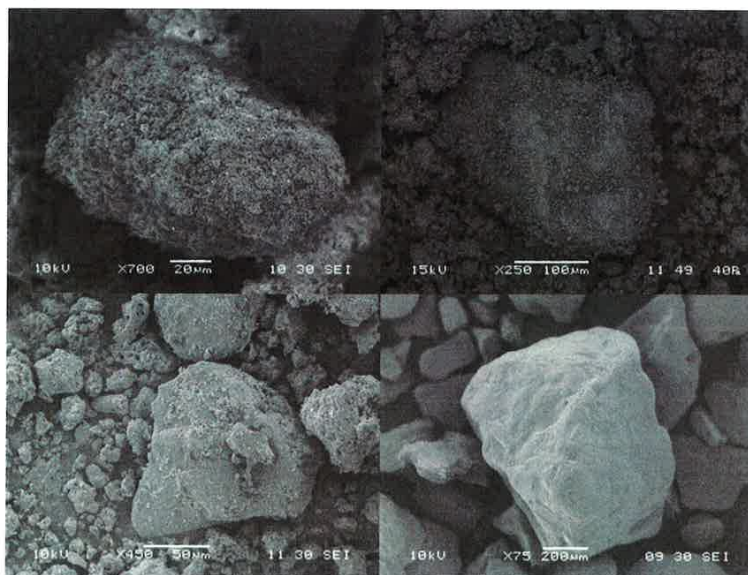
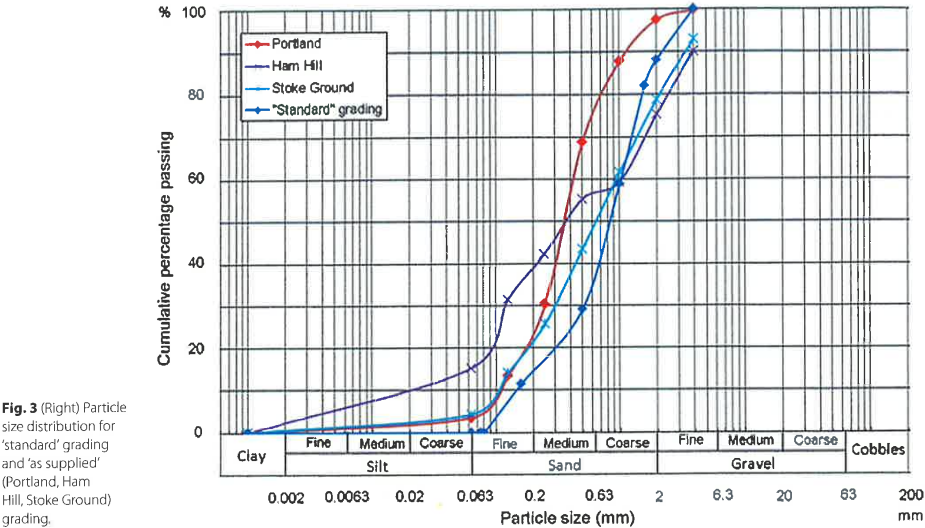


Fig. 2 (Left) Scanning electron microscopy images of the aggregates; clockwise from top left: Ham Hill, Stoke Ground, Standard sand, Portland.



2-mm fraction to reduce shrinkage). Figure 3 shows the particle size distributions of both the 'standard' grading and 'as supplied' (Portland, Ham Hill, and Stoke Ground) grading. It can be seen that the aggregates with 'as supplied' grading have a higher proportion of fines.

and the other one part lime binder to three parts aggregate (by volume). Tables 2 to 5 show the mix specifications for all the mortar samples. Samples were made to a flow of 14 centimetres, based on the feel of the material, so the water/binder (w/b) ratio differs for each mix.

Mortar mixes

For each of the two grades of limestone aggregates ('as supplied' and 'standard') and the silicate sand, two types of mortar mixes were made: one comprising one part lime binder to two parts aggregate (by volume),

Preparation of mortar prisms

The dry mix constituents (according to Tables 2 to 5) were combined for two minutes prior to water being added. A further two minutes of mixing was then

Table 2 Mortar mixes 1:2 by volume, aggregate 'as supplied' particle size distribution.

	Lime (g)	Aggregate (g)	Water (g)	water/binder ratio
Ham Hill (H-2 a.s.)	150	1495	525	3.50
Portland (P-2 a.s.)	150	1791	389	2.59
Stoke Ground (SG-2 a.s.)	150	1468	405	2.70

Table 3 Mortar mixes 1:2 by volume, aggregate "Standard" particle size distribution.

	Lime (g)	Aggregate (g)	Water (g)	water/binder ratio
Ham Hill (H-2)	150	1495	400	2.67
Portland (P-2)	150	1791	358	2.39
Stoke Ground (SG-2)	150	1468	374	2.49
Standard sand (SS-2)	150	1048	150	1.00

	Lime (g)	Aggregate (g)	Water (g)	water/binder ratio
Ham Hill (H-3 a.s.)	150	2243	579	3.86
Portland (P-3 a.s.)	150	2687	542	3.61
Stoke Ground (SG-3 a.s.)	150	2202	390	2.60

Table 4 Mortar mixes 1:3 by volume, aggregate 'as supplied' particle size distribution.

	Lime (g)	Aggregate (g)	Water (g)	water/binder ratio
Ham Hill (H-3)	150	2243	458	3.05
Portland (P-3)	150	2687	455	3.03
Stoke Ground (SG-3)	150	2202	351	2.34
Standard sand (SS-3)	150	1571	150	1.00

Table 5 Mortar mixes 1:3 by volume, aggregate 'standard' particle size distribution.

undertaken. The mortars were cast into prisms. These prisms were cured in air at 20°C and a relative humidity of 55 per cent; curing times were 14, 28, 90, 180, and 360 days. The mass of the prisms was measured upon demoulding after curing for 7 days and prior to testing, so that mass loss and density change could be calculated.

Flexural and compressive strength testing

Flexural and compressive strength tests according to BS EN 1015-11:1999⁶ were undertaken on air-lime mortar (CL90) prisms measuring 40 x 40 x 160 mm.

Mercury intrusion porosimetry

The main purpose of mercury intrusion porosimetry was to determine pore size distribution and total pore volume of the mortar samples. Mercury is intruded into the sample under pressure; at low pressures the largest pores are filled, whereas at progressively higher pressures smaller pores are filled. The Washburn equation (below) is used to describe the inverse relationship between pore diameter and pressure, which assumes a cylindrical pore with a circular opening of diameter, D . This is a simplistic representation of the pore geometry, which in reality is not uniform.

$$P = \left(\frac{2\gamma}{r} \right) \cos \theta$$

Where P = pressure, γ = surface tension of mercury, r = radius of the capillary, and θ = contact angle of the mercury on the material.

Prisms were selected after various periods of curing, and samples were taken from the carbonated edge of the prisms. Limestone aggregate mortars were

compared with the standard silicate sand mortar, in anticipation of finding distinct differences that may explain the higher strengths observed in the former during previous research.

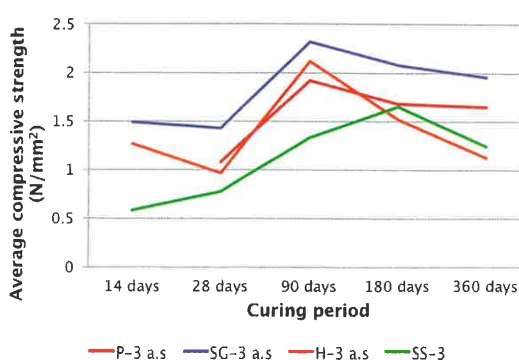
Results and discussion

Flexural and compressive strength testing

Previous research had shown that calcitic aggregates can produce stronger air-lime mortars than silicate aggregates, so the compressive strength results were of particular interest.

The average strengths of the limestone 'as supplied' aggregate prisms in Figure 4 (P-3 a.s., SG-3 a.s., and H-3 a.s.) decreased after a curing period of 90 days. Standard sand prisms (SS-3) continued to increase in strength up to 180 days curing, but strength had decreased by 360 days. The decreases in strength

Fig. 4 (Below) Average compressive strength for 1:3 'as supplied' samples and 1:3 'standard' sand (SS-3).



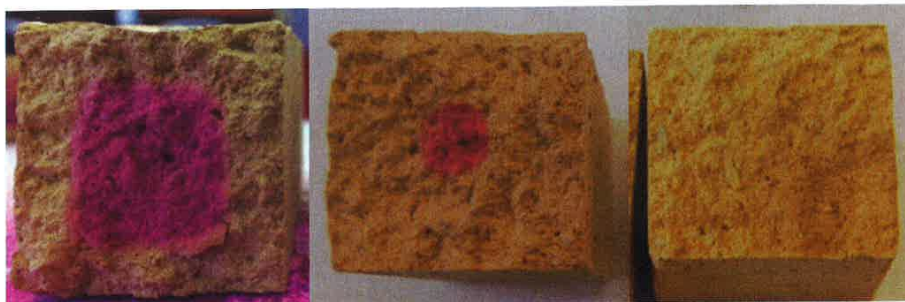


Fig. 5 (Above) Depth of carbonation in Ham Hill stone 1:3 'as supplied' mortar, revealed by phenolphthalein staining at 28, 90, and 180 days.

correspond to a decrease in density of the samples. It appears that the increase in density due to carbonation causes an increase in strength up to 90 days for the limestone aggregate samples. Further research is required to understand why there is a reduction in strength beyond 90 days.

The carbonation depth of Ham Hill 1:3 'as supplied' samples can be seen in Figure 5. A phenolphthalein indicator was used in order to determine the presence of $\text{Ca}(\text{OH})_2$. Where the indicator turns pink, $\text{Ca}(\text{OH})_2$ is present and therefore the sample is not fully carbonated at that point. Where there is no colour change, no $\text{Ca}(\text{OH})_2$ is detected, and it is assumed that carbonation is complete. It is clear from Figure 5 that carbonation has reached the centre of the sample before 180 days, which explains why strength does not continue to increase between 180 and 360 days. The same phenomenon was observed in nearly all the mortars tested, regardless of aggregate grading, mineralogy, or binder/aggregate ratio.

Mercury intrusion porosimetry

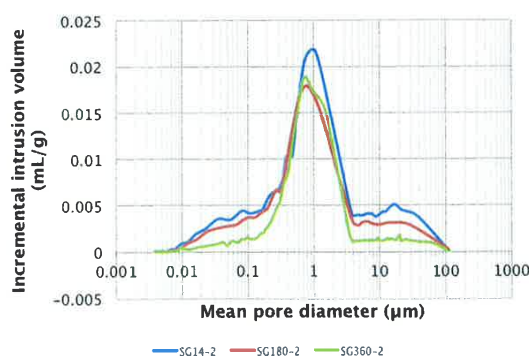
One of the most interesting results can be seen with the Stoke Ground samples with 1:2 binder/aggregate ratio

and 'standard' grading, shown in Figure 6. The results indicate that while the peak mean pore diameter occurs at around $1\mu\text{m}$ for each of the curing periods, there is a change in pore size distribution over time: there is a decrease in the number of both smaller pores ($<0.4\mu\text{m}$) and larger pores ($>4\mu\text{m}$). As carbonation progresses through the sample, the smaller pores become completely filled with precipitated CaCO_3 , while the walls of the larger pores become covered with CaCO_3 crystals. The concentration of pores is consistently in the $1\mu\text{m}$ range.

When looking at the progression of the pore size distribution over time for the 1:3 standard sand mortars at 28 and 360 days (SS28-3 and SS360-3 in Figure 7), it is clear to see the shift in pore size distribution. Although the difference in total pore volume is very small (0.0085 mL/g), there are a number of areas in which the volume of pores at a given mean diameter varies somewhat. In general, at 360 days pore sizes are more evenly spread, whereas at 28 days, the distribution of pore sizes is more concentrated in two size ranges. Although the pore size distribution is similar for both mixes in the 0.2 to $1\mu\text{m}$ range, SS28-3 has a much higher volume of pores that are around $8\mu\text{m}$ in diameter than is seen in SS360-3. The reduction in larger pores between 28 and 360 days is caused by the progression of the carbonation front through the sample. By 360 days, carbonation has reached the centre of the sample, meaning that theoretically all the $\text{Ca}(\text{OH})_2$ has been converted to CaCO_3 .

Figure 7 also compares the standard sand and Stoke Ground 1:3 samples at 28 days (SS28-3 and SG28-3). Overall, the curves for both mortars have a similar pattern and range of pore size distribution, with a concentration of pores in the 3 to $4\mu\text{m}$ and 8 to $10\mu\text{m}$ ranges. However, the magnitudes of these peaks are different. SG28-3 has a much higher proportion of pores in the 3 to $4\mu\text{m}$ range, whereas the greatest concentration of pores in SS28-3 is at 8 to $10\mu\text{m}$. Given that both mortars are made with aggregates

Fig. 6 (Below) Pore size distribution of Stoke Ground mortar samples with 1:2 binder/aggregate ratio and 'standard' grading, at 14, 180, and 360 days.



that have a similar particle size distribution and the same binder/aggregate ratio, the difference in magnitude of the two peaks may be due to the nature, and in particular the porosity, of the aggregates used. Stoke Ground aggregate has a porosity of approximately 25 per cent, whereas standard sand porosity was measured at around 6 per cent. It is possible that the higher porosity of the Stoke Ground aggregate has allowed CaCO_3 crystals to partly penetrate into the individual aggregate particles, as well as between them, and that there is therefore a larger amount of CaCO_3 filling up the pores. In turn, this would make the pores smaller and would lead to fewer pores being greater than 3 to 4 μm than in the equivalent standard sand sample (SS28-3). It would not only form a strong binder/aggregate bond but also a more continuous binder matrix. SG28-3 has a porosity of 32 per cent; this is much higher than SS28-3, which has a porosity of approximately 22 per cent.

Thermogravimetric analysis

The use of thermogravimetric analysis enables an insight into the chemical composition of the cured mortar prisms. Samples were taken from the edge of the mortar prisms, where phenolphthalein had indicated that full carbonation had occurred, and it was therefore expected that all $\text{Ca}(\text{OH})_2$ had been converted to CaCO_3 . Samples were heated to 1000°C at a rate of 10°C per minute.

Figure 8 shows how the apparently fully carbonated surface of Ham Hill, standard sand, and Portland 1:3 mortars compare after a curing period of 28 days. Clear differences can be observed. SS28-3 and P28-3 show a very small mass loss in the carbonated sample at around 450°C, which is a result of dehydroxylation (breakdown of $\text{Ca}(\text{OH})_2$). However, this is only about 0.5 per cent. It can also be seen that there are different mass losses at around 800°C due to decarboxylation (breakdown of CaCO_3). Taking into account the losses that occur due to the limestone aggregate, this still leaves differences between the mixes, as shown in Table 6. Specimens under test contained varying proportions of CaCO_3 within the aggregate, so in order to establish the extent of carbonation, it is necessary

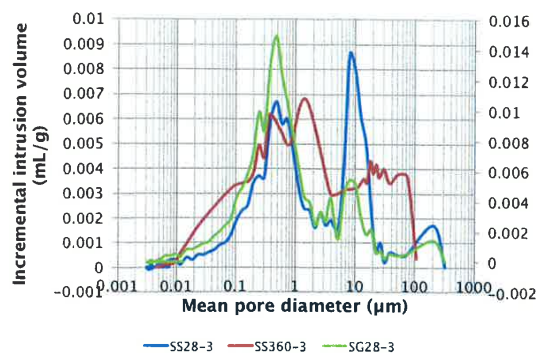


Fig. 7 (Above) Pore size distribution for standard sand mortar samples, with 1:3 binder/aggregate ratio, at 28 (SS28-3) and 360 (SS30-3) days, and Stoke Ground 1:3 mortar at 28 days (SG28-3).

to separate out the impact of the thermal decomposition of the aggregate from that of the binder.

Table 6 shows the results of measured mass loss due to decarboxylation for the outer surface of three 28-day-old specimens made with different aggregates, which all appeared to be fully carbonated when tested with phenolphthalein solution. Whereas the measured mass loss of the calcitic aggregate mortars is at, or

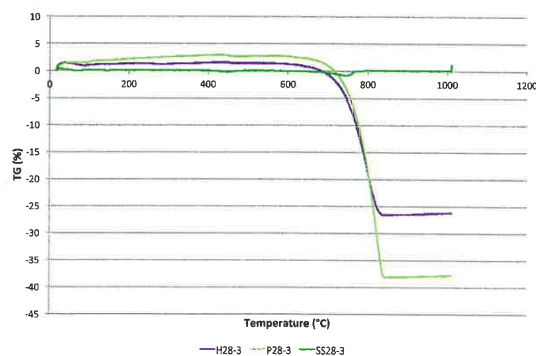


Fig. 8 (Above) Thermogravimetric analysis data for H28-3, SS28-3, and P28-3 – samples taken from the edge of the mortar prism.

Sample	Aggregate content (g)	Carbonate content of aggregate (g)	Binder content (g)	Dry mass of fresh sample	Theoretical dry mass of fully carbonated sample	Theoretical mass loss %	Measured mass loss %
H28-3	2243	548	150	2393	2452	26.0	26
P28-3	2687	1075	150	2837	2896	40.1	38
SS28-3	1571	0	150	1721	1780	5.0	1

Table 6 Comparison of theoretical mass loss of mortar sample due to decarboxylation (after adjusting for the carbonate content of the aggregate) and actual (measured) mass loss observed in the specimen.

almost at, the theoretical value for a fully carbonated sample (indicating that the binder in the samples was almost fully carbonated), the standard sand mortar has lost only 20 per cent of the mass that it would lose had it been fully carbonated.

This shows that, despite the results of the phenolphthalein testing, the standard sand sample was not fully carbonated, which therefore demonstrates that mortars made from carbonate-based aggregate appear to carbonate more effectively than mortars made from silicate aggregate. One possible reason why phenolphthalein staining does not reveal uncarbonated binder in the standard sand specimens is because $\text{Ca}(\text{OH})_2$ crystals can be encapsulated by CaCO_3 crystals, limiting the accessibility of dissolved CO_2 and therefore the crystals remain uncarbonated. This coating also hides them from access to the phenolphthalein, and they can only be detected by thermal analysis.⁷

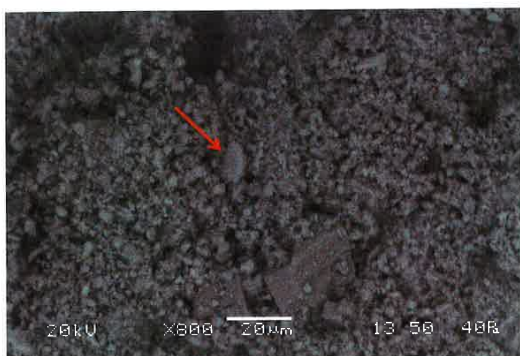


Fig. 9 (Above) Portland 1:3 mortar sample (28 days) at 800x magnification.

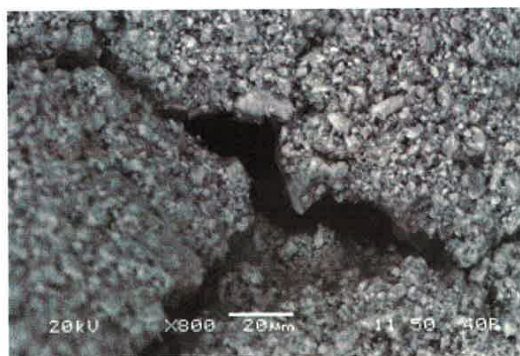


Fig. 10 (Above) Stoke Ground Bath stone 1:3 mortar sample (28 days) at 800x magnification.

Scanning electron microscopy

Scanning electron microscopy has enabled a close look at the binder/aggregate interface, as well as the analysis of porosity. In Figure 9, we can see a $\text{Ca}(\text{OH})_2$ crystal in the 'standard' graded P28-3 sample at 800x magnification, although the majority of the sample comprises small newly carbonated crystals of CaCO_3 .

Stoke Ground 'standard' samples exhibited micro-cracking throughout, shown in Figure 10, approximately 80µm in length, although this did not appear to have a detrimental effect on compressive strength (in fact, only SG28-3 a.s had higher compressive strength at 28 days). This was not evident in any of the other samples analysed at 28 days curing.

For the limestone aggregate mortars, it was not easy to see individual aggregate particles due to the quantity of new CaCO_3 crystals growing on their surface; however, individual particles of the standard sand were clearly evident in SS28-3 (see Figure 11). Some small CaCO_3 crystals can be seen on the surface of the aggregate particles but the rest of the surface is visible. Figure 12 shows Ham Hill aggregate mortar at 28 days curing. To the right of the image is a piece of aggregate covered in CaCO_3 , very different from the standard sand in Figure 11.

Figures 11 and 12 indicate a possible reason for the strength differences observed between the limestone aggregate mortars and the silicate sand mortar. It is clear from Figure 12 that there is a more continuous matrix of CaCO_3 crystals across the surface of the aggregate, which is not present in Figure 11. This suggests a better bond between the limestone aggregate and binder than between the silicate sand and binder, which would naturally lead to higher strength mortars. Compressive stresses would be more evenly distributed through a sample with a stronger binder/aggregate bond, whereas with a weaker bond stresses would cause failure at the binder/aggregate interface. In the case of the latter, the compressive strength reflects only binder strength rather than the strength of the mortar as a whole.

Conclusions

Several things have come to light as a result of this research. Mercury intrusion porosimetry analysis has shown that differences exist in a mortar's pore size distribution irrespective of binder/aggregate ratio and particle size distribution of the aggregate. Consequently, it is highly likely that these differences exist as a result of aggregate type or water/binder ratio.

Furthermore, after adjusting for the type of aggregate used, the mass loss of samples due to decarboxylation is greater for calcitic aggregates; consequently, it can be inferred that the use of limestone aggregate increases the amount of carbonation for the samples studied.

Fig. 11 (Right) Silicate sand 1:3 mortar sample (28 days) at 400x magnification.

Clear differences can also be seen at the binder/aggregate interface, leading to the conclusion that limestone aggregates produce air-lime mortars that have a stronger binder/aggregate bond and are therefore stronger in compression. Since it is known that the water/binder ratio has limited impact on mechanical performance,⁸ the key controlling factor in a mortar's mechanical performance is evidently the aggregate's mineralogy.

There are a number of elements that make the use of limestone aggregates in air-lime mortar an attractive option for conservation and restoration work. Since low strength is synonymous with poor durability, improving the strength will increase durability; however, the strength increases are not high enough to cause damage to existing masonry. Additionally, the limestone aggregate mortars have a higher porosity, which facilitates water transport through a structure. This plays a vital role in preventing the build-up of soluble salts in the masonry, as well as increasing moisture dissipation that in turn reduces the risk of mortar remaining saturated for long periods and suffering frost damage. It is evident that the use of limestone aggregates with air lime can produce mortars of equivalent compressive strength to weak NHL 2 mortars (2 to 2.5 MPa) made with silicate sand, but with higher porosity. Furthermore, without the risk of ongoing strength gain that has been seen in some natural hydraulic lime mortars, these mortars may be more suitable for certain conservation applications.

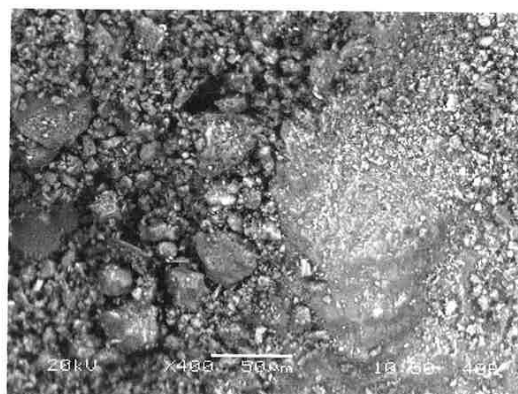
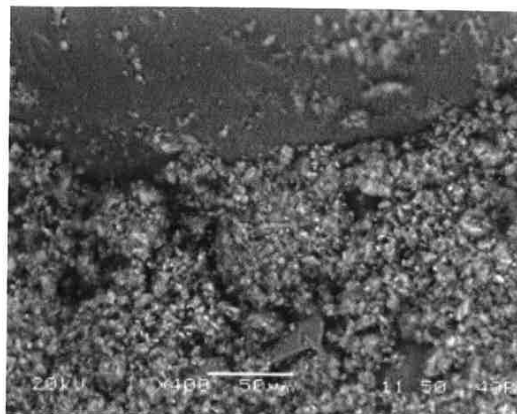


Fig. 12 (Right) Ham Hill 1:3 mortar sample (28 days) at 400x magnification.

References

- 1 BS EN 196-1. Methods of testing cement – Part 1: Determination of strength. British Standards Institution, London, 2016.
- 2 M. J. Mosquera, D. Benítez and S. H. Perry, 'Pore structure in mortars applied on restoration: effect on properties relevant to decay of granite buildings', *Cement and Concrete Research*, 32(12), 2002, pp. 1883–1888.
- 3 R. M. H. Lawrence, *A study of carbonation in non-hydraulic lime mortars*, PhD thesis, 2006; J. Lanas and J. I. Alvarez, 'Masonry repair lime-based mortars: factors affecting the mechanical behaviour', *Cement and Concrete Research*, 33(11), 2003, pp. 1867–1876; A. Arizzi and G. Cultrone, 'Aerial lime-based mortars blended with a pozzolanic additive and different admixtures: a mineralogical, textural and physical-mechanical study', *Construction and Building Materials*, 31, 2012, pp. 135–143.
- 4 BS EN 459-1. Building lime. Definitions, specifications and conformity criteria. British Standards Institution, London, 2015.
- 5 K. Van Balen and D. Van Gemert, 'Modelling lime mortar carbonation', *Materials and Structures*, 27, 1994, pp. 393–398.
- 6 BS EN 1015-11. Methods of test for mortar for masonry – Part 11: Determination of flexural and compressive strength of hardened mortar. British Standards Institution, London, 1999.
- 7 Lawrence, 2006, see 3 above.
- 8 R. M. H. Lawrence and P. Walker, 'The impact of the water/lime ratio on the structural characteristics of air-lime mortars', in D. F. D'Ayala and E. Fodde (eds.), *Structural analysis of historic construction: preserving safety and significance*, 2008, pp. 885–889. Proceedings of the VI International Conference on Structural Analysis of Historic Construction, SAHC08, 2–4 July 2008, Bath, UK.